USING CHEMICALLY MODIFIED OLIGONUCLEOTIDES TO MODULATE GENE EXPRESSION, TREAT GENETIC DISEASES, AND PROBE NOVEL MECHANISMS OF RNA INTERFERENCE

APPROVED BY SUPERVISORY COMMITTEE

David R. Corey, Ph.D (Mentor)

Hongtao Yu, Ph.D (Chairman)

Nicholas K. Conrad, Ph.D

Qinghua Liu, Ph.D

DEDICATIONS

To my parents, Liyan and Rongmin, who gave me life, confidence, love, and courage;

To my Grandparents and all my dear family, who loved and prayed for me since day one;

To Ping Z, Andy T, Vida GM, Monica S, Brian E, Robin K, Jon W, Keith G, and David C, who mentored me in science and in humanity;

To Yueyin S, Ming L, Liang X, Olena B, Vijay Y, Alex S, Rui T, Véronique W, Corinne B, Danny W, Hannah P, and Ming C, whose friendships defined and inspired my twenty-eight years of journey thus far;

In remembrance of Hui W,
who taught me to treasure every second of life …

USING CHEMICALLY MODIFIED OLIGONUCLEOTIDES TO MODULATE GENE EXPRESSION, TREAT GENETIC DISEASES, AND PROBE NOVEL MECHANISMS OF RNA INTERFERENCE

by

Dongbo Yu

DISSERTATION

Presented to the Faculty of the Graduate School of Biomedical Sciences

The University of Texas Southwestern Medical Center at Dallas

In Partial Fulfillment of the Requirements

For the Degree of

DOCTOR OF PHILOSOPHY

The University of Texas Southwestern Medical Center at Dallas

Dallas, Texas

August, 2012

USING CHEMICALLY MODIFIED OLIGONUCLEOTIDES TO MODULATE GENE EXPRESSION, TREAT GENETIC DISEASES, AND PROBE NOVEL MECHANISMS OF RNA INTERFERENCE

Dongbo Yu, Ph.D.

The University of Texas Southwestern Medical Center at Dallas, 2012

Supervising Professor: David R. Corey, Ph.D

A number of inherited neurological disorders remain incurable despite having well-defined monogenic etiologies. One example is Huntington's disease (HD), which is caused by CAG trinucleotide expansion in the gene *HUNTINGTIN* (*HTT*) and production of toxic glutamine-expanded protein. Targeting HTT with siRNAs could be a powerful approach, but allele-selectivity is a major challenge: nearly all HD patients are heterozygous at the *HTT* locus, and expression of wild-type HTT may need to be preserved. One way to achieve allele-selectivity is by exploiting the fact that the mutant *HTT* allele contains more CAG repeats. Previous work with double-stranded siRNAs (dsRNA) and chemically modified antisense oligonucleotides (ASO) that target the poly-CAG sequence both showed promise but each had significant limitations. To

combine the simplicity of ASO and high selectivity of dsRNA, we tested chemically modified, single-stranded small-interfering RNA (ss-siRNA) of sequences targeting CAG repeats in collaboration with ISIS Pharmaceutical, and showed them to have high potency (IC_{50} ~2 nM) and allele-selectivity (>30-fold) against mutant HTT in HD-patient-derived cell-lines. Mechanistically, CAG-targeting ss-siRNA functions through endogenous RNAi by recruiting Ago2 and GW182 to *HTT* mRNA in the absence of a passenger strand and reducing mutant HTT protein level without affecting its mRNA level. Selectivity is likely achieved through preferential cooperative binding of multiple RISC units to the longer poly-CAG tract on the mutant *HTT* mRNA versus that of the wild-type. Structural-activity relationship (SAR) studies showed that several ss-siRNAs tolerated significant structural modifications and still retained high potency and selectivity. Furthermore, intraventricular infusion of a candidate ss-siRNA in a HD knock-in mouse model yielded selective inhibition of mutant HTT in a wide range of brain regions. Finally, we showed that a subset of ss-siRNAs were also potent, allele-selective inhibitors of *ATAXIN-3*, the mutated gene in spinocerebellar ataxia type 3 (SCA3). Taken together, we have identified and characterized a novel class of mechanistically interesting and therapeutically promising nucleic-acid-based compounds that could open new doors to finding a cure for genetic diseases such as HD.

PRIOR PUBLICATIONS

1. **Yu, D.**, Pendergraff, H., Liu, J., Kordasiewicz, H., Cleveland, D.W., Swayze, E.E., Lima, W.F., Crooke, S.T., Prakash, T.P., and Corey, D.R. (2012) Single-Stranded RNAs Use RNAi to Potently and Allele-Selectively Inhibit Mutant Huntingtin Expression. Cell, *150,* 895-908

2. **Yu, D.**, Sakurai, F., and Corey, D.R. (2011) Clonal Rett Syndrome cell lines to test compounds for activation of wild-type MeCP2 expression. Bioorg Med Chem Lett. *21*, 5202-5

3. Hu, J.‡, Liu, J.‡, **Yu, D.**, Chu, Y., and Corey D.R. (2012) Mechanism of Allele-Selective Inhibition of Huntingtin Expression by Duplex RNAs that Target CAG Repeats. Nucleic Acids Res. *40,* 11270-80

4. Watts, J.K., **Yu, D.**, Charisse, K., Montaillier, C., Potier, P., Manoharan, M., and Corey, D.R. (2010) Effect of chemical modifications on modulation of gene expression by duplex antigene RNAs that are complementary to non-coding transcripts at gene promoters. Nucleic Acids Res. *38*, 5242-59

TABLE OF CONTENTS

LIST OF FIGURES

LIST OF TABLES

LIST OF DEFINITIONS

5-aza – 5-aza-2'-deoxycytidine

AGO – Argonaute

agRNA – antigene RNA

ASO – antisense oligonucleotide

ATXN-3 – ataxin-3

BLK – blank

C3PO – component 3 promoter of RISC

ChIP – chromosome immunoprecipitation

CNS – central nervous system

CSF – cerebrospinal fluid

co-IP – co-immunoprecipitation

DMSO – dimethylsulfoxide

DNA – deoxyribonucleic acid

DNMT – DNA methyltransferase

dsRNA – double-stranded RNA

HD – Huntington's Disease

HDAC – histone deacetylase

HTT – huntingtin

IgG – immunoglobulin G

IP – immunoprecipitation

lincRNA – long non-coding RNA

LNA – locked nucleic acid

MeCP2 – methyl CpG binding protein 2

miRNA – microRNA

MJD – Machado-Joseph Disease (see also SCA3)

MM – mismatch(ed)

mRNA – messenger RNA

MUT – mutant

NT – no treatment

ORF – open reading frame

PCR – polymerase chain reaction

PNA – peptide nucleic acid

PR – progesterone receptor

q-PCR – quantitative polymerase chain reaction

RIP – RNA immunoprecipitation

RISC – RNA induced silencing complex

RNA – ribonucleic acid

RNAi – RNA interference

RNAPII – RNA polymerase II

RNP – ribonucleoparticle

RTT – Rett syndrome

SAHA – suberoylanilide hydroxamic acid (vorinostat)

SAR – structure-activity relationship

SCA3 – spinocerebellar ataxia 3

siRNA – small interfering RNA

SNP – single-nucleotide polymorphism

ssRNA – single-stranded RNA

ss-si-RNA – single-stranded silencing RNA

TNRC6 – trinucleotide-repeat-containing 6

TSN – translin

UTR – untranslated region

WT – wild-type

CHAPTER ONE

Potent and Allele-selective Inhibition of Huntingtin by Chemically Modified Single-stranded RNAs That Target CAG Repeats

ABSTRACT

CAG-expansion in the huntingtin (HTT) gene causes Huntington's disease (HD), an incurable neurological disorder. Silencing mutant HTT using nucleic acids would eliminate the root cause of HD. Developing nucleic acid drugs is challenging, and an ideal clinical approach to gene silencing would combine the simplicity of single-stranded antisense oligonucleotides (ASO) with the efficiency of RNAi. Here we describe RNAi by single-stranded silencing RNAs (ss-siRNAs). ss-siRNAs are potent (>100-fold more than unmodified RNA) and allele-selective (>30-fold) inhibitors of mutant HTT expression in cells derived from HD patients. Strategic placement of mismatched bases mimics micro-RNA recognition and optimizes discrimination between mutant and wild-type alleles. ss-siRNAs require the RNAi factor Ago2 and function through the endogenous RNAi pathway. Intraventricular infusion of ss-siRNA produced selective silencing of the mutant *HTT* allele throughout the brain in a mouse HD model. These data demonstrate that chemically modified ss-siRNAs function through the RNAi pathway, and provide both allele-selective lead compounds for clinical development and novel insight into the mechanism of RNAi.

Note: The following chapter is substantially made up of a research article published by Dongbo Yu under the guidance of Dr. David R. Corey (Yu et al, 2012).

INTRODUCTION

Huntington's disease (HD), traditionally also known as Huntington's chorea, is an incurable neurological disorder that afflicts at least 1:100,000 people worldwide (Walker, 2007; Finkbeiner 2011). The disease itself is characterized by a spectrum of cognitive and behavioral abnormalities, including involuntary muscle movement, loss of motor control, regression in cognitive abilities, memory loss, and psychiatric disturbances. Histologically, HD is characterized by degeneration of the striatum and enlargement of the ventricles. Patients present symptoms around 40 years of age and progress towards death over 10-15 years.

Genetically, HD is caused by a dominant heterozygous expansion of CAG trinucleotide repeats within exon 1 of the *Huntingtin* (*HTT*) gene. The mutated *HTT* allele leads to production glutamine-expanded, neurotoxic peptide products that form intracellular aggregates. The average mutant *HTT* allele in patients contains 45 consecutive CAG trinucleotides (MacDonald et al., 1993; Duyao et al., 1993; Kremer et al., 1994), and patients with very long CAG-expansion alleles (>120 copies in extreme cases) develop juvenile HD in which symptoms may develop as early as teenage years.

While the genetic origin of HD has been known for almost twenty years, curative drugs have not been identified. Effective agents that will benefit HD patients are urgently needed. With a molecular weight over 350 kD, HTT is a large and difficult target for traditional small molecule drugs as it interacts with many other proteins. Certain classes of chemicals such as phosphodiesterase (PDE) inhibitors (Giampa et al., 2010; Schmidt and Beaumont, Pfizer and CHDI, 2012) may provide symptomatic relief but none have been shown to slow disease progression.

Because the genetic origin of HD is localized to just one gene, inhibiting expression of HTT is a promising therapeutic option by aiming directly at the very root cause of the disease. Importantly, work using conditional HD mouse models has shown that genetic inactivation of CAG-expanded *HTT* allele can reverse the HD symptoms (Yamamoto et al, 2000). As a result, much effort has been devoted to testing different strategies of specifically eliminating mutant HTT expression. RNA-based approaches of gene knockdown offer the distinct advantage of target specificity and inhibitory potency, and several examples of inhibiting HTT with RNA include the use of single-stranded antisense oligonucleotides (ASOs) and duplex RNAs (dsRNAs) that target *HTT* mRNA (Sah and Aronin, 2011; Matsui and Corey, 2012). ASOs and dsRNAs that inhibit expression of HTT have been shown to reduce HTT expression in cell-lines as well as alleviate symptoms and prolong survival in mouse HD models when reliably introduced (Harper et al. 2005; DiFiglia et al., 2007; Boudreau et al., 2009; Drouet et al., 2009). Even a transient lowering of HTT was shown to result in sustained phenotypic improvement (Kordasiewicz et al, 2012). These successes suggest that silencing HTT expression can be a productive strategy for developing drugs to treat HD.

HD is dominantly inherited, with almost all the patients expressing both mutant and wild-type *HTT* alleles. While simultaneously inhibiting both alleles may prove to be a successful clinical strategy, it carries the risk of depleting wild-type HTT that may have important functions. Multiple studies have suggested that reducing wild-type HTT levels may have deleterious effects, with the most striking example being that *HTT* knockout mice are embryonically lethal (Nasir et al., 1995; Zeitlin et al., 1995; White et al., 1997; Godin et al. 2010; Omi et al., 2005; Huang et al., 2011). Allele-selective inhibitors that maximize reduction of mutant HTT and minimize loss of wild-type HTT would be ideal. One approach to achieving this goal exploits the existence of single nucleotide polymorphisms (SNPs) that allow dsRNAs to distinguish the mutant and wild-

type alleles (Miller et al., 2003; Schwarz et al., 2006; van Bilsen et al., 2008; Carroll et al., 2011). The identity of SNPs varies between patients, but some SNPs are common and a few SNPs may be sufficient to cover a majority of HD patients in certain populations (Pfister et al., 2009; Lombardi et al., 2009; Carroll et al., 2011: Warby et al., 2009).

An alternative strategy for allele-selective inhibition exploits a universal difference between the mutant and wild-type alleles – the mutant allele has more trinucleotide repeats. The longer poly-CAG tract in mutant *HTT* mRNA offers more binding sites for complementary oligomers (Gagnon et al, 2010). In addition, trinucleotide repeats can form hairpin self-structures (Michlewski and Krzyzosiak, 2004; de Mezer et al., 2011; Krzyzosiak et al., 2011), and the expanded mutant repeats will likely form structures that differ from wild-type. These mutant structures may be more susceptible to recognition and selective binding by oligonucleotides and allow preferential inhibition of the mutant allele. We initially used single-stranded ASOs to test the hypothesis that oligomers complementary to CAG repeats could be allele-selective inhibitors (Hu et al., 2009; Gagnon et al., 2010; Hu et al. 2011; Gagnon et al., 2011). We identified several allele-selective ASOs, but did not achieve selectivity greater than 4-8 fold.

The mechanism of RNAi differs from that of ASOs (Watts and Corey, 2012), and we reasoned that changing our silencing strategy to RNAi might improve selectivity. Our initial tests with fully complementary siRNAs generated potent inhibition but little selectivity (Hu et al., 2009). Fully complementary duplexes function through an siRNA pathway that involves cleavage of target mRNAs, while mismatch-containing duplexes can act through a microRNA (miRNA)-like pathway that suppresses translation (Filipowicz et al., 2008). To test whether duplexes that resemble miRNAs might afford greater selectivity, we altered the mechanism of gene silencing by generating duplexes that mimicked miRNAs by introducing mismatches into the central region of the dsRNA. The mismatches were at positions predicted to disrupt cleavage

of the target by Argonaute 2 (Ago2) (Wang et al., 2008), an essential protein for substrate recognition and degradation during RNAi (Liu et al., 2004). Using this strategy, we identified mismatch-containing RNAs that were potent and selective inhibitors (Hu et al., 2010). Krzyzosiak and colleagues also reported allele-selectivity using RNA duplexes with mismatches at positions 13 and 16 (Fiszer et al., 2011).

Compounds that combine the favorable biodistribution and simpler synthesis of single-stranded oligonucleotides with the potency of duplex RNAs would offer an ideal strategy for silencing gene expression. Single-stranded RNAs (ssRNA) has been reported to enter the RNA induced silencing complex (RISC) under specific conditions and inhibit gene expression (Martinez et al., 2002; Schwarz et al. 2002; Holen et al., 2003). Unlike duplex RNA, which is stable in serum, the half-life of ssRNA in serum is measured in seconds to minutes (Braasch et al., 2003). Most ssRNAs would likely be degraded by nucleases before entering cells and inhibiting gene expression. Chemical modifications can stabilize RNA, and one study has reported that boranophosphate-modified RNA single strands could be active inside cells (Hall et al., 2006). There was no experimental follow-up and little exploration of mechanism, leaving it unclear whether the approach could have practical application. Very recently, another report of gene silencing by chemically modified ssRNAs has appeared (Haringsma et al., 2012), but their robustness and mechanism of action remains unclear.

Recently, the action of ssRNAs that function through the RNAi pathway has been revisited (Lima et al., 2012). Systematic chemical modifications and iterative design improvements led to stabilized single-strand silencing RNAs (ss-siRNAs) (Figure 1-1A) that efficiently enter the RNA pathway and silencing gene expression. Here, we describe potent and allele-selective inhibition of mutant HTT expression in HD patient-derived cells and HD model mice by ss-siRNAs targeting CAG repeats.

RESULTS

ss-siRNAs Are Potent and Allele-Selective Inhibitors of Mutant HTT Expression

The ss-siRNAs used in these studies contain a mixture of 2'-fluoro (2'-F), 2'-*O*-methyl (2'-*O*-Me), and 2'-methoxyethyl (2'-MOE) ribose modifications (Figure 1-1B; Lima et al., 2012). The ss-siRNAs possess both phosphodiester and phosphorothioate internucleotide linkages. The 5' terminus was capped with either a phosphate or a 5'-*(E)*-vinylphosphonate. We initially tested ss-siRNA 537787 (fully complementary to the CAG repeat) and ss-siRNAs 537775 and 537786 (containing mismatch bases at positions 9 (P9) or 10 (P10) respectively).

These ss-siRNAs were introduced into HD-patient-derived fibroblast cell line GM04281 (69 CAG repeats/mutant allele, 17 CAG repeats/wild-type allele) by standard transfection methods. From our previous studies, oligomers with centrally located mismatches relative to their mRNA targets are predicted to inhibit expression of HTT protein but have little effect on *HTT* mRNA (Hu et al., 2010), leading us to focus on measuring protein levels. HTT is a large protein, 347 kDa in molecular weight and the expanded repeat leads to only a few thousand Dalton increase. The small molecular weight difference makes discrimination between alleles challenging, but mutant and wild-type alleles can be efficiently resolved using temperature-controlled SDS-PAGE (Hu et al., 2009).

ss-siRNAs 537787, 537775, and 537786 inhibited HTT expression with varying potencies and selectivities (Figure 1-2 and Table 1-1). Fully complementary ss-siRNA 537787 possessed an IC_{50} value of 8 nM and a selectivity of >13 fold (Figure 1-2A; see Methods for calculations on allele-selectivity). This selectivity is better than the selectivity of the analogous unmodified duplex RNA (2-fold) (Hu et al. 2009). ss-siRNA 537775 (single mismatch at position 9) possessed an IC_{50} value of 3.5 nM and a selectivity of >29 fold (Figure 1-2B). ss-

siRNA 537775 was the best inhibitor with potency and selectivity values similar to the most selective dsRNAs identified (Hu et al., 2010). ss-siRNA 537786 (single mismatch to P10, one base shift relative to 537775) possessed an IC_{50} value of 22.3 nM and a selectivity of >4 fold , making it less effective than the analogous mismatch-containing dsRNA (Hu et al., 2010).

These results suggest that chemical modifications and the precise positioning of mismatched bases affect allele-selective recognition and silencing. In one case, selectivity was better relative to the analogous dsRNA, in another selectivity was similar, and in the third example selectivity and potency were worse. While ss-siRNAs appear to function similarly to dsRNAs, the exact outcome of recognition depends on sequence.

We examined inhibition of HTT by ss-siRNA 537775 over time. ss-siRNA was added only once, at the beginning of the experiment. During this period, cells were allowed to grow, undergoing 3-4 population doublings and diluting out the ss-siRNA available to silencing HTT. We observed >80% inhibition of mutant HTT expression for up to 8 days before population doublings gradually diluted out the drug-induced inhibition (Figure 1-2C), returning to original levels after two weeks.

To provide a comparison with a silencing strategy that is non-allele selective and does not involve RNAi, we tested a gapmer ASO complementary to a region outside the CAG tract. The "gapmer" ASO contains a central DNA "gap" to recruit RNase H that is flanked by chemically modified bases to improve binding (Watts et al., 2012). The gapmer inhibited HTT expression with an IC_{50} value of 7.4 nM and a selectivity of 1.7-fold (Figure 1-2D and Table 1-1). These data suggest that ss-siRNAs targeted to the CAG repeat can achieve potencies that are similar to those achieved using ASOs, a gene silencing approach broadly used in clinical testing (Watts and Corey, 2012) while having the added benefit of being allele-selective.

As a further comparison, we examined silencing by anti-CAG ssRNAs that lacked chemical modifications. These unmodified ssRNAs were not active when tested at concentrations up to 400 nM (Figure 1-2E). These results contrast with reports that unmodified ssRNAs possessed silencing activity in mammalian cells (Martinez et al., 2002; Schwarz et al., 2002), possibly due to differences in the cell lines, transfection techniques, the mRNA target, or the sequence of the silencing RNA.

Optimizing ss-siRNA Design

ss-siRNAs 537787, 537775, and 537786 contain 5'-*(E)*-vinylphosphonate moieties designed to improve stability and potency *in vivo*. This modification is not needed for testing in cell culture (Lima et al., 2012), and substitution with a phosphate moiety facilitates the synthesis of the large number of compounds needed to identify improved inhibitors and investigate mechanism. To determine whether potent and allele selective inhibition could be achieved with 5'-phosphate ss-siRNAs, we tested analogous compounds 553819, 553822, and 553821. These ss-siRNAs possessed potencies and selectivities similar to their 5'-*(E)*-vinylphosphonate analogues (Figure 1-3A and 1-4, Table 1-1).

We chose the 5'-phosphate design for large-scale tests and synthesized compounds that varied in the number and placement of mismatched bases (Table 1-1). Several compounds possessed good potencies and selectivities, with the best combination of potency and selectivity achieved by ss-siRNA 557426. ss-siRNA 557426 contained three centrally located mismatched bases and combined an IC_{50} value of 3.3 nM with >30 fold selectivity (Figure 1-3B).

We had previously observed that a mismatched base at position P6 within a dsRNA abolished RNA-mediated inhibition of HTT. P6 is within the seed sequence (bases 2-8), a region

critical for efficient RNAi (Lim et al., 2005). ss-siRNA 556888, an ss-siRNA that contained a mismatched base at P6, was the only single-mismatch compound not to inhibit HTT (Figure 1-3C, Table 1-1). This result suggests that ss-siRNAs and duplex RNAs share critical recognition elements and supports the hypothesis that ss-siRNAs act through the RNAi pathway.

Most HD patients have mutant HTT alleles containing 40-50 repeats (Duyao et al., 1993; MacDonald et al. 1993). To determine whether ss-siRNAs might also be an effective strategy for allele-selective inhibition in this patient cohort, we tested inhibition in GM04719 HD-patient-derived fibroblast cells (44 mutant repeats/15 wild-type repeats) (Figure 1-3D). We found that phosphate ss-siRNA 553822 inhibited expression of mutant HTT with an IC_{50} value of 0.9 nM and an allele-selectivity >100-fold, demonstrating the potential to achieve allele-selectivity in cell lines with the median range of CAG repeat copy numbers.

Another challenge for agents that target trinucleotide repeats is the existence of other genes that contain repetitive regions (Kozlowski et al., 2010). We observed no inhibition of TATA-box binding protein (TBP; 19 CAG repeats), androgen receptor (AR; ~20 CAG repeats), AP2-associated kinase-1 (AAK-1, 6 CAG repeats), POU3F2 (6 CAG repeats), or forkhead box protein P2 (FOXP2, 40 glutamines encoded by a mixture of CAG/CAA trinucleotides) (Figure 1-3E) at concentrations well above those needed to achieve selective inhibition of mutant HTT.

Involvement of Ago2 Protein

Ago2 is a key protein involved in RNAi (Liu et al., 2004; Meister et al., 2004). There are four Ago genes in human cells. Ago2 is the best characterized and the only variant with endonucleolytic activity. Ago1, Ago3, and Ago4 are also expressed, but their functions are less well defined. To determine which Ago variant is involved in gene silencing by ss-siRNAs, we

used siRNAs targeting mRNAs encoding Ago1-4 to reduce their expression (Figure 1-6). We observed that reducing Ago2 levels reversed silencing by 537775, consistent with involvement of Ago2 (Figure 1-7A). By contrast, silencing Ago1, Ago3, or Ago4 had little effect on allele-selective inhibition of mutant HTT.

To further investigate involvement of Ago, we used RNA immunoprecipitation (RIP) to examine the ability of ss-siRNA 537775 (P9 mismatch with 5'-*(E)*-vinylphosphonate chemistry) to promote association of Ago2 with *HTT* mRNA. We transfected ss-siRNA 537775 into cells, harvested extracts, immunoprecipitated Ago-bound material using an anti-Ago2 antibody, and assayed the abundance of *HTT* mRNA. We observed that *HTT* mRNA could be recovered upon transfection of ss-siRNA 537775 and immunoprecipitation with anti-Ago2 antibody, but not when we used a noncomplementary ss-siRNA (Figure 1-7B). A locked nucleic acid (LNA) ASO that targets the CAG repeat and inhibits mutant HTT expression with an allele-selectivity >6 fold (Hu et al., 2009; Gagnon et al., 2010) did not recruit Ago2 to *HTT* mRNA. The difference between the ss-siRNA and the LNA ASO underlines a fundamental difference in the mechanisms of action: ss-siRNAs rely on Ago2 while ASOs do not. Taken together, results from double-transfection and RNA immunoprecipitation assays support the conclusion that Ago2 is required for the action of ss-siRNA and that silencing proceeds through the endogenous RNAi pathway.

Ago is typically thought to mediate recognition of mRNA inside cells by dsRNA consisting of a guide strand hybridized to a passenger strand. To determine the functional necessity of passenger strand, we created a duplex by annealing ss-siRNA 537775 to an unmodified RNA passenger strand. This heteroduplex inhibited HTT expression with an IC_{50} of 5.4 nM and a selectivity of >15-fold (Figure 1-7C), similar to the ss-siRNA alone (IC_{50}: 3.7 nM; selectivity: >29-fold). This result demonstrates that introduction of chemically modified bases into the guide strand does not interfere with strand loading and that ss-siRNA can function

through RNAi pathways that were once thought to require a passenger strand. This finding is significant because it shows that ss-siRNA is the only active species during gene silencing and the passenger strand is not necessary. During standard dsRNA-mediated RNAi using unmodified RNA, the main role of the passenger strand is likely to protect the guide strand from digestion by nucleases, ensuring that it survives long enough to reach its target mRNA.

Inhibitory ss-siRNAs Do Not Reduce *HTT* mRNA Levels

siRNAs that are fully complementary to their target mRNAs are usually thought to cause Ago2-mediated mRNA cleavage and reduction of mRNA levels. The introduction of centrally located mismatches is predicted to interfere with strand cleavage without affecting binding (Wang et al., 2008). To test this hypothesis, we measured RNA levels by quantitative PCR (q-PCR) (Figure 1-7D). A duplex siRNA that targets a sequence outside of the CAG repeat reduces *HTT* mRNA levels by >80%. By contrast, 5'-phosphonate ss-siRNA 537775 and 5'-phosphate ss-siRNA 553822 that contain mismatches at position P9 do not reduce *HTT* mRNA levels. This result is consistent with a mechanism that involves blocking protein translation rather than degradation of mRNA.

We also examined the potential for cleavage using an *in vitro* assay combining purified human Ago2 or RNase H, different ss-siRNAs, and an *in vitro*-transcribed *HTT* RNA transcript containing 17 CAG repeats. ss-siRNAs 537775, 556887, 553822, and 553819, all potent and selective inhibitors inside cells, did not lead to transcript cleavage (Figure 1-7E). By contrast, a control duplex RNA targeting a non-CAG sequence yielded cleavage products of the expected size. A control DNA oligonucleotide yielded cleavage upon addition of RNase H. These data

demonstrate that ss-siRNAs targeting the CAG repeat do not cause RNA cleavage through the RNAi or RNase H pathways.

Inhibition by ss-siRNAs Is Cooperative

The repetitive region within a mutant *HTT* mRNA with 69 repeats is predicted to bind up to 9 to 10 twenty-nucleotide-long oligomers. A wild-type mRNA with 17 repeats, by contrast, could bind no more than 2. It is possible that binding of multiple oligomers at adjacent sites can lead to cooperative inhibition and contribute to allele-selective recognition of expanded mutant repeat regions. To determine whether inhibition is cooperative, we examined inhibition of mutant HTT by ss-siRNA 553822 over a wide range of concentrations (Figure 1-7F). After fitting the data to the Hill equation, we calculated Hill coefficients (n^h) of 2.2 and 1.2 for inhibition of mutant and wild-type HTT expression, respectively. These data are consistent with cooperative inhibition and suggest that association of the ss-siRNA with the expanded mutant repeat is likely to involve multiple binding events.

An ss-siRNA Is an Allele-Selective Inhibitor in HD Model Mice

To test ss-siRNAs in animals, we used *Hdh*$^{Q150/Q7}$ heterozygous knock-in HD-model mice (Lin et al., 2001). The *Hdh*$^{Q150/Q7}$ heterozygous mice carry one mouse *HTT* allele with 150 CAG repeats knocked into exon 1 (Q150) and a second allele with a wild-type mouse *HTT* gene (Q7). The two *HTT* alleles in the HdhQ150/Q7 animals differ only in the length of the glutamine repeats, making them ideal for determining whether an ss-siRNA can discriminate between the expanded and unexpanded *HTT* transcripts *in vivo*.

To best mimic the human treatment paradigm, 5'-*(E)*-vinylphosphonate ss-siRNA 537775 was introduced into the cerebral spinal fluid of the right lateral ventricle to achieve distribution throughout the CNS, including brain regions implicated in HD pathology. ss-siRNA 537775 was continuously infused into the right lateral ventricle for twenty-eight days (300 μg/day). Due to the long *in vivo* half-life of the HTT protein and the need to monitor levels of protein rather than RNA, animals were treated for four weeks to ensure that reduced HTT synthesis could be detected in the total accumulated protein levels.

We analyzed brain tissue for HTT expression by western analysis and q-PCR. As a positive control, we used a non-allele-selective gapmer ASO complementary to a region outside the CAG repeat (administered at 75 μg/day for fourteen days). We observed allele-selective inhibition of HTT protein expression in the frontal cortex of all five mice in the experimental cohort relative to animals treated with saline (Figure 1-8A and B). q-PCR showed no decrease in *HTT* mRNA levels in animals treated with ss-siRNA (Figure 1-8C), consistent with results in cultured cells showing inhibition does not result from cleavage of mRNA.

We then assayed inhibition in other tissues, including contralateral cortex, thalamus, ipsilateral striatum, contralateral striatum, cerebellum, and brainstem, all of which displayed a reduction in levels of the mutant HTT protein when treated with ss-siRNA 537775 (Figure 1-8D, E). Consistent with our results in cultured cells, injection of ss-siRNA 537775 did not reduce expression of other proteins containing trinucleotide repeats (Figure 1-9). These experiments demonstrate that ss-siRNAs can distribute broadly within the central nervous system and inhibit mutant HTT expression.

DISCUSSION

Therapeutics that slow or reverse progression of HD are a major unmet medical need. Trinucleotide expansions cause numerous other hereditary diseases (Orr and Zoghbi, 2007), and anti-CAG agents that treat HD might also advance treatments for these conditions. ss-siRNAs combine strengths of dsRNAs and ASOs, and our objective for this study was to determine whether they would provide a novel starting point for HD drug development. Substantial challenges confront the application of gene silencing strategies to neurological disorders (Sah and Aronin, 2011; Davidson and McCray, 2011), and optimizing the chemical properties of inhibitory molecules for maximal biological effect is a central goal. Our results demonstrate that ss-siRNAs can mimic miRNAs to allele-selectively suppress translation and inhibit mutant HTT expression with potencies and allele-selectivities that are at least equal to those possessed by duplex RNAs and ASOs.

More broadly, gene silencing strategies that use synthetic nucleic acids have the potential to provide a new class of clinical agents for treating diseases that are currently incurable or where current therapies are inadequate (Watts and Corey, 2012). ss-siRNAs provide a new starting point for drug development and an additional option for overcoming roadblocks to successful clinical application. For basic research, ss-siRNAs provide a fresh perspective on the mechanism of RNAi.

ss-siRNAs Function Through RNAi

We provide several lines of evidence that anti-CAG ss-siRNAs also act through RNAi: i) the maximum selectivity of inhibition by ss-siRNAs (> 30 fold) (Table 1-1) is much closer to that produced by duplex RNA (> 30 fold) (Hu et al., 2010) than that yielded by the non-RNAi-

mediated ASOs (4- to 8-fold) (Hu et al., 2009; Gagnon et al., 2010); ii) reduction of Ago2, a key RNAi factor, leads to less efficient silencing of mutant HTT (Figure 1-7A); iii) addition of ss-siRNA, but not an allele-selective ASO, leads to robust recruitment of Ago2 to *HTT* mRNA (Figure 1-7B); iv) adding an unmodified RNA guide strand to the ss-siRNA does not affect its activity (Figure 1-7C); and v) same as what was observed for dsRNA (Hu et al., 2010), introduction of a mismatch at position 6 within the putative seed sequence for recognition by ss-siRNA largely abolishes inhibition of HTT (Figure 1-3C).

Action through the RNAi pathway is accompanied by potent inhibition of HTT expression. Several compounds possess IC_{50} values less than 10 nM, and the best ss-siRNAs have potencies that are almost identical to those observed for duplex RNAs (Hu et al., 2010). Easy identification of multiple potent and selective compounds that function through RNAi also has implications for therapeutic development. It is likely that many other compounds, with different mismatch positions or patterns of chemical modifications, will also be active. This large design-space is compatible with allele-selective inhibition and provides many options for optimization of drug-like characteristics of ss-siRNAs and their subsequent theraoeutic development. If one compound has a toxic effect related to its sequence or chemical composition, numerous other compounds can be developed instead.

While all data indicate that ss-siRNAs function through the RNAi pathway, knowing how a dsRNA functions will not always fully predict the properties of an analogous ss-siRNA. For example, fully complementary ss-siRNAs were allele-selective inhibitors of HTT expression (Figure 1-2A) while the analogous fully complementary dsRNA was not selective (Hu et al., 2009). In another example, we had previously observed that duplex RNAs with mutations at positions 9 or 10 are equally potent and selective inhibitors (Hu et al., 2010). ss-siRNAs with mutations at positions 9 or 10, by contrast, are quite different in potency (Table 1-1).

The origin of functional differences between dsRNAs and ss-siRNAs lies in the chemical differences between modified and unmodified RNA. ss-siRNAs have 2'-F and 2'-*O*-methyl sugar modifications, as well as phosphorothioate internucleotide linkages. The 2' modifications tend to increase affinity, while phosphorothioate linkages tend to decrease affinity. The countervailing and sometimes unpredictable effects of these modifications are apparent from our data. Compared to analogous unmodified RNAs, some ss-siRNAs have lower melting temperature (T_m) values for association with complementary sequences, while others have higher values. In addition, the extensive chemical modifications may affect RNA recognition, Ago loading, and subsequent inhibition of gene expression. Understanding the intrinsic properties and potential of ss-siRNA will be an important goal for future research. Many chemically modified bases exist that can be substituted within ss-siRNAs, and it is likely that chemical optimization of recognition, potency, and selectivity will prove a productive area of investigation.

Mechanism of Allele-Selective Inhibition

We have shown that our anti-CAG ss-siRNAs bind Ago2, suggesting that the first steps of allele-selective inhibition by ss-siRNAs involve recognition of Ago2 and subsequent association with *HTT* mRNA. Mutant and wild-type *HTT* mRNAs both contain CAG sequences but the lengths of the repeat regions differ. In our most extreme case, selectivity is achieved even though the difference in the number of repeats in GM04719 cells (44 mutant repeats versus 15 wild-type repeats) is only 29. One explanation is that the mutant allele provides more binding sites for the ss-siRNA. For example, a wild-type allele with 20 repeats would have space for no more than three ss-siRNAs, while a mutant allele with 40 repeats would have space for as many six ss-siRNAs. Our observation of cooperative effects on inhibition of HTT expression support

the conclusion that multiple ss-siRNAs bind to the expanded repeat target and lead to a preference for the mutant over the wild-type repeat. Indeed, the potential for multiple binding of small RNAs to adjacent sites to lead to cooperative gene silencing has been noted previously using expression constructs containing 3'-untranslated regions with varying numbers of target sequences (Broderick et al., 2011).

Once bound, inhibition leads to potent reduction of mutant HTT protein expression but no change in mRNA levels. Inhibition by ss-siRNAs is much more efficient than by analogous unmodified ssRNAs (Figure 1-2D) and is as efficient as analogous duplex RNAs (Hu et al., 2010). The guide strand, therefore, appears to be the only strand necessary for efficient RNAi (Figure 1-7A). For experiments with conventional duplex RNAs, the passenger strand likely serves as a delivery agent protecting the critical guide strand.

For mismatch-containing ss-siRNAs, the observed reduction in protein but not mRNA is consistent with our initial design assumptions that mismatches would disrupt Ago-mediated cleavage of mRNA. After multiple ss-siRNAs bind in complex with Ago to the repeat, they likely act as a roadblock to ribosome progress and prevent protein translation (Figure 1-10). This "steric blocking mechanism" is similar to that used by ASOs that lack the ability to recruit RNase H and cannot cause cleavage of mRNA except that, in this case, the ss-siRNA is delivered by the endogenous RNAi machinery that has greater potential to facilitate efficient gene silencing. Multiple binding sites within expanded repeats permit cooperative binding and discrimination relative to shorter wild-type repeats.

Implications for Therapeutic Gene Silencing

Advances in nucleic acid chemistry, a better understanding of nucleic acid pharmacology, and a more mature appreciation of the basic science underlying diseases have led to substantial

recent clinical progress for nucleic acid therapeutics (Watts and Corey, 2012). It is now possible to cite several examples of nucleic acid drugs that have potent effects on target gene expression in humans. For example, Mipomersen, a drug designed to treat familial hypercholesterolemia, has been shown to benefit patients in multiple Phase III trials and is now awaiting FDA review. Even brain disorders are becoming more amenable to nucleic acid silencing. ASOs have been shown to inhibit superoxidase dismutase (SOD) in the spinal cord of primates, and a Phase I trial designed to test treatment of patients with familial amyotrophic lateral sclerosis (ALS) is ongoing.

Our results introduce ss-siRNAs as a novel strategy for treating neurodegenerative disease that provides an alternative to ASOs or dsRNAs. Chemically, ss-siRNAs are similar to ASOs because they both consist of a single chemically modified antisense strand. Mechanistically, they resemble duplex RNAs that function through RNAi. ss-siRNAs combine strengths of the two existing approaches, possess unique advantages, and provide a distinctive new strategy for silencing gene expression.

Here, we demonstrate that the first generations of anti-CAG ss-siRNAs achieve potencies and selectivities for inhibiting HTT that are similar to those achieved by well-established gene silencing technologies. By further optimizing the type of chemical modification, placement of mismatched bases, or other design features, it is likely that subsequent generations of inhibitory ss-siRNAs will possess even more favorable properties. The availability of a gene silencing strategy that combines the strengths of siRNAs and ASOs will provide an important option for transforming the potential benefits from nucleic-acid-based silencing into practical benefits for patients.

MATERIALS AND METHODS

ss-siRNAs

ss-siRNAs were synthesized by Isis Pharmaceuticals Inc. (Carlsbad, CA, USA) (Lima et al., 2012) and reconstituted in nuclease-free water. 100 μM stocks were maintained for long-term storage and 20 μM stocks are used for transfections. All concentrations were verified by UV spectrometry.

Antibodies

Mouse monoclonal anti-huntingtin antibody MAB2166 (clone 1HU-4C8) was purchased from Millipore and diluted 1:10,000 for western blot analysis. Rabbit polyclonal anti-androgen receptor (AR) antibody SC-816 (clone N20) was purchased from Santa Cruz and diluted 1:1000 for western analysis. Rabbit polyclonal anti-FoxP2 antibody AB16046 was purchased from Abcam and diluted 1:1000 for western analysis. Rabbit polyclonal anti-AAK-1 antibody AB59740 was purchased from Abcam and diluted 1:1000 for western analysis. Rabbit polyclonal anti-POU3F2 antibody ab94977 was purchased from Abcam and diluted 1:1000 for western analysis. Mouse monoclonal anti-ataxin-3 antibody MAB5360 (clone 1H9) was purchased from Millipore and diluted 1:10,000 for western analysis. Mouse monoclonal anti-polyglutamine/TATA-box binding protein (TBP) antibody MAB1574 (clone 5TF1-1C2) was purchased from Millipore and diluted 1:10,000 for western analysis. Mouse monoclonal anti-Ago2/eIF2C2 antibody AB57113 was purchased from Abcam and used for RIP-pulldown assay, and another rat monoclonal anti-Ago2 antibody (clone 11A9) was purchased from Helmholtz Zentrum München and diluted 1:2000 for western analysis. Mouse monoclonal anti-Ago1 antibodies 015-22411 (clone 2A7) and 04-083 (clone 6D8.2) were purchased from Wako

Chemicals and Millipore, respectively, and diluted 1:1000 for western analysis. Normal mouse IgG 12-371 was purchased from Millipore and used as background control in RNA immunoprecipitation assays.

Thermal Denaturing by UV Melt Analysis

Thermal denaturation analysis of ss-siRNA was carried out using a CARY Varian model 3 UV-Vis spectrophotometer (Agilent Tech, Santa Clara, CA, USA). Absorbance was monitored at 260 nm in a 1-cm quartz cuvette. ss-siRNAs (2 μM) were annealed in the presence of equimolar complementary RNA strand (5'-CAGCAGCAGCAGCAGCAGCAGC-3') in 1 x Dulbecco's phosphate buffered saline (Sigma Aldrich, St. Louis, MO, USA) and melted three times from 18°C to 99°C at a ramp rate of 1°C/min.

Cell Culture and Transfection

Patient-derived fibroblast cell lines GM04719 (44 CAG repeat) and GM04281 (69 CAG repeat) were obtained from the Coriell Institute (Camden, NJ, USA). Cells were maintained at 37°C and 5% CO_2 in MEM Eagle Media (Sigma Aldrich, M4655) supplemented with 10% heat inactivated fetal bovine serum (Sigma Aldrich) and 0.5% MEM nonessential amino acids (Sigma Aldrich). Cells were plated in 6-well plates at 60 000 cells/well in supplemented MEM media 2 days prior to transfection. 6-well plates were used because they provide the number of cells necessary for western analysis of protein levels. Cells were transfected using lipid RNAiMAX (Invitrogen) per manufacturer instructions, Optimem (Invitrogen), and 0.2, 0.6, 1.8, 5.6, 16.7, 50, and 100 nM concentrations of ss-siRNAs. Optimem containing RNA and lipid were mixed and allowed to sit for 20 minutes for complex formation, and lower doses were obtained by serial dilution at 1:2 or 1:3-fold. The final volume of mixture added to cell was 1.25 mL. After 24 h,

the media were removed and replaced by fresh supplemented MEM media. Cells were harvested 4 days after transfection for protein analysis and 3 days after transfection for RNA analysis.

Analysis of HTT Expression

Cells were washed with Dulbecco's phosphate buffered saline (PBS) (Sigma Aldrich) then harvested with trypsin-EDTA solution (Invitrogen). The protein concentration was quantified with BCA assay (Thermo Scientific, Waltham, MA, USA). SDS-PAGE (separating gel: 5% acrylamide-bisacrylamide [50:1], 450mM Tris-acetate pH 8.8; stacking gel 4% acrylamide-bisacrylamide [50:1], 150mM Tris-acetate pH 6.8) was used to separate wild-type and mutant HTT proteins. Gels were run at 30 – 35mA per gel for 5-7 h in either XT-tricine (Bio-Rad, Hercules, CA, USA) for 69 repeat or Novex Tris-acetate SDS running buffer (Invitrogen) for 44 repeat. The electrophoresis chamber was placed in a 15°C ice water bath to prevent overheating. Protein samples were analyzed for β-actin expression by SDS-PAGE (7.5% acrylamide precast gels; Bio-Rad). B-actin gels were run for 20 min at 80V followed by 1h at 100V in TGS buffer (Bio-Rad).

Proteins were transferred to membrane (Hybond-C Extra; GE Healthcare Bio-Sciences) after electrophoresis. For HTT expression, membranes were blocked in Blotting-Grade Blocker (Bio-Rad) for 1h prior to addition of primary antibody. Primary antibodies specific for HTT (MAB2166, Chemicon) and β-actin (Sigma) were diluted in a 1:10 000 ratio in Blotting-Grade Blocker (Bio-Rad). The membranes were in primary antibody for 75 min (HTT) or 30 min (β-actin) followed by a 3 x 5 min wash with Dulbecco's PBS (Sigma). HRP conjugate antimouse secondary antibody (Jackson ImmunoResearch Laboratories) was diluted 1:10 000 in Blotting-Grade Blocker (Bio-Rad). Membranes were in secondary antibody for 45 min (HTT) or 30 min

(β-actin) followed by a 3 x 15 min PBS wash. SuperSignal West Pico Chemiluminescent Substrate (Thermo Fisher) was used to visualize protein expression.

IC_{50}, Selectivity, and Cooperativity Calculations

Protein bands were quantified from autoradiographs using ImageJ software. The percentage of inhibition was calculated as a relative value to a no-treatment control sample. The program GraphPad Prism 4 was used to draw the fitting curves for dose response experiments for inhibition of HTT. Hill Equation was used for fitting in the following form: $Y=100[(1-X^n/(K^n+X^n)]$, where Y is percentage of inhibition and X is the ss-siRNA concentration, K is the IC_{50} value, and n is the Hill coefficient. At least three experiment data sets were used for fitting the curves. The error of IC_{50} is standard deviation, which is calculated from each individual dose curve. Selectivity was calculated by taking the ratio of the IC_{50} for inhibition of the mutant HTT protein over that of the wild-type protein and rounded to the closest integral value. Cooperativity was measured by obtaining the Hill's coefficient that best fits the plotted curve, which corresponds to the value n in the equation.

Quantitative PCR (qPCR)

Total RNA was extracted using TRI® Reagent (Sigma) 3 days after transfection. RNA concentration was measured by UV Diode array spectrophotometer (Hewlett Packard). Two micrograms of RNA was treated with 2 units of DNase I (Worthington Biochemical Corp.) for 10 min at 25°C followed by 15 min at 75°C. RNA was reverse-transcribed using High Capacity cDNA Reverse Transcription Kit (Applied Biosystems) according to the manufacturer's protocol. Quantitative PCR was performed on a BioRad CFX96 real time system using iTaq SYBR Green Supermix with ROX (Bio-Rad). Data were normalized to *GAPDH* mRNA levels. Primers

specific to GAPDH were purchased from Applied Biosystems. Primers specific for *HTT* 64-65 exon boundary were used: forward primer, 5'CGACAGCGAGTCAGTGAATG-3'; reverse, 5'-ACCACTCTGGCTTCACAAGG-3'. Experiments were performed in biological triplicate and error reported as standard deviation. The Q-PCR cycles are as follows: 50°C for 2 min; 95°C for 5min; (95°C for 15s; 60°C for 1min) × 40 cycles.

Double-transfection Experiment

Patient-derived fibroblasts GM04281 (69 CAG repeat) were seeded in 6-well plates at 60,000 cells/well in supplemented MEM media. Two days later (Day 0), the first round of transfection was performed to individually knock down Ago1-4 expressions by siRNAs at 25-50nM, with sequences given in our previous AGO-activity publication (Chu et al., 2010) and with the same transfection procedure as described earlier in the section. After 24 h (Day 1), the media were removed and replaced by fresh supplemented MEM media. After another 48 h (Day 3), cells were split 1:3 into new plates, and 24 hr after that (Day 4), a second round of transfection was carried out with HTT-targeting ss-siRNAs or control oligomers. Cells were harvested 4 days after the second transfection (Day 8) for protein analysis. Extra wells were seeded and harvested on Day 3 (for RNA) or Day 4 (for protein) to check for efficiencies of AGO knock-down.

RNA Immunoprecipitation (RIP)

HD-patient derived GM04281 (69 CAG repeat) fibroblasts were grown in 150 cm^2 dishes and transfected with chemically modified ss-siRNAs at 15-25nM using lipid RNAiMAX (Invitrogen) and Optimem (Invitrogen). Media were changed 24 and 72 hr after transfection, and

cells ($\sim 4 \times 10^7$) were harvested by trypsin 96 hr after transfection. Typically, six dishes of cells were seeded and harvested per treatment.

A small quantity of cells are saved and harvested for protein to check knockdown efficiency by western blot. Cells were pelleted by gentle centrifugation at 500g and resuspended in cold PBS washing solution. After a second round centrifugation at 500g and aspirating off PBS, total cell lysate was isolated by adding to the cell pellet 1mL/dish of lysis buffer of the following formula: 150 mM NaCl, 20 mM Tris–HCl pH 4, 2 mM $MgCl_2$, 0.5% NP-40, with 1 × Roche protease inhibitors cocktail and RNAse in (50 U/ml final) supplemented just prior to usage (Note: no formaldehyde cross-linking is used in this protocol). The mixture was left on ice for 10 min, and insoluble material was removed by centrifugation at maximum speed for 15 min at 4°C. Materials may be stored at -80°C at this point until immunoprecipitation.

60 μL of protein A/G agarose Plus beads were washed with phosphate-buffered saline (1 × PBS, pH 7.4) and incubated with 200 μL of cell lysate and 4 μg anti-AGO2 (4G8, 011-22033, Wako) antibody, or 4 μg normal mouse IgG (12-371, Millipore, for IP) antibody in 0.75mL of IP buffer at 4°C on rotator for 3-4 h. 10 μL of lysate was set aside for input control. At the end of incubation, the immuno-complexed beads were sedimented at 1000 g for 2 min and the supernatant was removed. Four washes were performed by adding 500 μL of IP wash buffer (500 mM NaCl, 50 mM Tris-HCl, 2 mM $MgCl_2$, 0.05% NP-40) and consisting of 3-min-long rotation and 2-min-long centrifugation at 1000 g and 4°C. Complexes were then eluted twice with 250 μL freshly made elution buffer (1% SDS, 0.1M $NaHCO_3$ and RNase inhibitor) and the two eluates were combined. At this step the 10 μL input sample was diluted in 50 0μL elution buffer and included for all subsequent treatments. Following proteinase K treatment (42°C for 45 min), RNA extraction (by phenol:chloroform:isoamyl alcohol mixture) and precipitation (3 M

sodium acetate, Glycoblue, and 100% ethanol), samples were treated with recombinant DNase I followed by reverse transcription. Corresponding cDNA was amplified using reverse primer targeting HTT exons 3/5 (forward: 5'- CAGAAACTTCTGGGCATCGCTATGG-3', reverse: 5'-CCTCCACAGGGCAGCACGCAAACTC-3') and GAPDH mRNA (Applied Biosystems).

Results were normalized by the two following parameters: (i) ratios of *HTT* mRNA to *GAPDH* mRNA (a housekeeping control) to eliminate small variations of total RNA across all samples; (ii) binding of *HTT* mRNA to anti-Ago2 antibodies over that of IgG to measure fold-enrichment of *HTT* mRNA in Ago2 IP relative to the non-specific IgG background binding.

***In Vitro* RNase-H and Ago2 Activity Assay**

HTT 17-CAG RNA substrate was obtained via cloning and *in vitro* transcription as described in our previous publication (Gagnon et al., 2010; Gagnon et al., 2011). 5'-phosphorylation of RNA substrate and RNase H assays were done with methods described in the same publication. AGO2 activity assay was performed with methods analogous to those described by Liu et al., 2011 with minor changes. The final reaction mixture contained 3µL of recombinant hAgo2 protein, 3µL of ss-siRNA (250nM stock), 0.5µL of tRNA (10mg/mL), 0.5µL of NTP mix (25mM), 0.25µL of Superase-IN (Ambion, 10,000U), and 1µL of 10X reaction buffer (0.5M Tris at pH7.4, 20mM $MgCl_2$, 5mM DTT, 2.5mM ATP, 1M KCl, 0.5M NaCl). The mixture was allowed 1.5 h at room temperature for pre-loading of ss-siRNAs, after which 50,000 cpm of radio-labeled RNA substrate was added to each reaction. AGO2-cleavage reactions were allowed to proceed for 2 - 2.5 hr at 37°C and then quenched with $LiClO_4$ in acetone. RNA was precipitated by centrifugation and washed once with acetone. The air-dried pellet was then reconstituted in 90% formaldehyde and 1XTBE with dye, boiled at 90-95°C for 2 min, and

loaded onto 10-14% sequencing gel, which was visualized on phosho-imager after overnight exposure in the dark.

Animals

Hdh$^{Q150/Q7}$ (CHL2) animals (Lin et al., 2001) were obtained from Jackson laboratories and maintained on the congenic C57BL/6 background. Mice were maintained on a 12-hr light/dark cycle with food and water available *ad libitum*. Five- to six-month-old *Hdh*$^{Q150/Q7}$ heterozygous mice of both genders were used. All procedures were accomplished using a protocol approved by the Institutional Animal Care and Use Committee (Department of Health and Human Services, NIH Publication 86–23). The animals are not reported to be symptomatic at the age of treatment.

Dosing and Surgical Procedure

To continuously deliver compounds, osmotic pumps delivering 0.25 μL/hr (Model 2004) were used to deliver 300 μg/day of ss-siRNA or phosphate buffered saline (PBS) (Sigma Aldrich) for 28 days and pumps designed to deliver 0.5 μL/hr (Model 2002) were used to deliver 75 μg/day of the positive control MOE ASO for 14 days. Pumps were assembled according to manufacturer's instructions (Durect Corporation) and were filled with ss-siRNA or MOE diluted in sterile PBS and then incubated at 37ºC for 24 (2002) or 48 (2004) hours prior to implantation. Mice were anesthetized with 2.5 % Isofluorane and a midline incision was made at the base of the skull. Through the use of stereotaxic guides a cannula was implanted into the right lateral ventricle and secured with Loctite adhesive. A catheter attached to an Alzet osmotic mini pump was attached to the cannula and the pump was placed subcutaneously in the midscapular area. The incision was closed with 5.0 nylon sutures.

Tissue Collection

Animals were sacrificed 4 weeks after initiation of treatment. Brains were sectioned into 1-2mm coronal sections and frozen on dry ice and stored at -80. Brain regions were harvested for RNA and biochemical analysis using 2 mm punches.

REFERENCES

The Huntington's Disease Collaborative Research Group. (1993). A novel gene containing a trinucleotide repeat that is expanded and unstable on Huntington's disease chromosomes. Cell. *72*, 971-83.

Boudreau, R.L., McBride, J.L., Martins, I., Shen, S., Xing, Y., Carter, B.J., and Davidson, B.L. (2009). Nonallele-specific silencing of mutant and wild-type huntingtin demonstrates therapeutic efficacy in Huntington's disease mice. Mol. Ther. *17*, 1053-1063.

Braasch, D.A., Jensen, S., Liu, Y., Arar, K., White, M. A., and Corey, D.R. RNA interference in mammalian cells by chemically modified RNA. (2003) Biochemistry *42*, 7967-7975

Broderick, J.A., Salomon, W.E., Ryder, S. P., Aronin, N., and Zamore, P.D. (2011). Argonaute protein identity and pairing geometry determine cooperativity in mammalian RNA silencing. RNA *17*, 1858-1869

Carroll, J.B., Warby, S.C., Southwell, A.L., Doty, C.N., Greenlee, S., Skotte, N., Hung, G., Bennett, C.F.,Freier, S.M., and Hayden, M.R. (2011). Potent and selective antisense oligonucleotides targeting single-nucleotide polymorphisms in the Huntington disease gene / allele-specific silencing of mutant huntingtin. Mol Ther. *19*, 2178-85.

Chu Y, Yue X, Younger S.T., Janowski B.A., Corey D.R. (2010) Involvement of argonaute proteins in gene silencing and activation by RNAs complementary to a non-coding transcript at the progesterone receptor promoter. Nucleic Acids Res. *38*, 7736-48

Davidson, B.L., and McCray, P.B (2011). Current prospects for RNA interference based therapies. Nature Rev. Genetics *12*, 329-340.

DiFiglia, M., Sena-Esteves, M., Chase, K., Sapp, E., Pfister, E., Sass, M., Yoder, J., Reeves, P., Pandey, R.K., Rajeev, K.G., et al. (2007). Therapeutic silencing of mutant huntingtin with siRNA attenuates striatal and cortical neuropathology and behavioral deficits. Proc. Natl. Acad. Sci. USA *104*, 17204-17209.

de Mezer, M., Wajciechowska, M., Naperala, M., Sobczak, K., and Kryzosiak, W. J. (2011). Mutant CAG repeats of Huntingtin transcript fold into hairpins, form nuclear foci and are targets for RNA interference. Nucleic Acid Res. *39*, 3852-3863

Drouet, V., Perrin, V., Hassig, R., Dufour, N. Auregan, G., Alves, S., Bonvento, G., Brouillet, E., Luthi-Carter, R., Hantraye, P. and Deglon, N. (2009). Sustained effects of nonallele-specific Huntingtin silencing. Ann. Neurol. *65*, 276-285.

Duyao, M., Ambrose, C., Myers, R., Novelletto, A., Persichetti, F., Frontali, M., Folstein, S., Ross, C., Franz, M., Abbott, M., et al. (1993). Trinucleotide repeat length instability and age of onset in Huntington's disease. Nat. Genet. *4*, 387-392.

Fiszer, A., Mykowska, A., and Krzyzosiak, W.J. (2011). Inhibition of mutant huntingtin expression by RNA duplex targeting expanded CAG repeats. Nucleic Acids Res. *39*, 5578-5585

Filipowicz, W., Bhattacharyya, S.N., and Sonenberg, N. (2008). Mechanisms of post-transcriptional regulation by microRNAs: are the answers in sight? Nat. Rev. Genet. *9*, 102-114.

Finkbeiner, S. (2011). Huntington's Disease. Cold Spring Harb. Perspect. Biol. *3*, a007476

Gagnon, K.T., Pendergraff, H.M., Deleavey, G., Swayze, E., Potier, P., Randolph, J., Roesch, E., Chattopadhyaya, J., Damha, M., Bennett, F., Chrisophe, M., Lemaitre, M., and Corey, D.R. (2010). Allele-selective silencing of mutant huntingtin expression with antisense oligonucleotides targeting the expanded CAG repeat. Biochemistry *49*, 10166-10178

Gagnon, K.T., Watts, J. K., Pendergraff, H. M., Montaillier, C., Thi, D., Potier, P. and Corey D. R. (2011). Antisense and antigene inhibition of gene expression by cell-permeable oligonucleotide-oligospermine conjugates. J. Am. Chem. Soc. *133*, 8404-8407

Giampà C, Laurenti D, Anzilotti S, Bernardi G, Menniti FS, Fusco FR. (2010) Inhibition of the striatal specific phosphodiesterase PDE10A ameliorates striatal and cortical pathology in R6/2 mouse model of Huntington's disease. PLoS One. *5*, e13417

Godin, J.D., Colombo, K., Molina—Calavita, M., Keryer, G., Zala, D., Charrin, B.C., Dietrich, P., Vovert, M-L., Guillemot, F., Dragatsis, I. *et al.* (2010). Huntingtin is required for Mitotic Spindle Orientation and Mammalian Neurogenesis. Neuron *67*, 392-406

Hall, A. H. S., Wan, J., Spesock, A., Sergueeva, Z., Ramsay Shaw, B, and Alexander, K.A. (2006). High potency silencing by single-stranded boranophosphate siRNA. Nucleic Acids Res. *34*, 2773-2781.

Harigsma, H.J., Li, J.J., Soriano, F., Kenski, D.M., Flanagan, W.M., and Willingham, A.T. (2012). mRNA knockdown by single-stranded RNA is improved by chemical modifications. Nucleic Acids Res. *40*, 4125-36.

Harper, S.Q., Staber, P.D., He, X., Eliason, S.L., Martins, I.H., Mao, Q., Yang, L., Kotin, R.M., Paulson, H.L., and Davidson, B.L. (2005). RNA interference improves motor and neuropathological abnormalities in a Huntington's disease mouse model. Proc. Natl. Acad. Sci. USA *102*, 5820-5825.

Hayden, Michael M. R. (2012). Changing prevalence of HD: altered demographics and its implications. Talk at HD Therapeutics Conference.

Holen, T., Amarzguioui, M., Babaie, E., and Prydz, H. (2003). Similar behavious of single and double strand siRNAs suggests they act through a common RNAi pathway. Nucleic Acids Res. *31*, 2401-2407.

Hu, J., Matsui, M., Gagnon, K.T., Schwartz, J.C., Gabillet, S., Arar, K., Wu, J., Bezprozvanny, I., and Corey, D.R. (2009). Allele-specific silencing of mutant huntingtin and ataxin-3 genes by targeting expanded CAG repeats in mRNAs. Nat. Biotechnol. *27*, 478-484.

Hu, J., Gagnon, K.T., Liu, J., Watts, J.K., Syeda-Nawaz, J., Bennett, C.F., Swayze, E.E., Randolph, J., Chattopadhyaya, J., and Corey D. R. (2011). Allele-selective inhibition of ataxin-3 (ATX3) expression by antisense oligomers and duplex RNAs. Biol. Chem. *392*, 315-325

Hu, J., Liu, J., and Corey, D.R. (2010). Allele-selective inhibition of huntingtin expression by switching to an miRNA-like RNAi mechanism. Chem. Biol. *17*, 1183-1188

Hu, J.‡, Liu, J.‡, Yu, D., Chu, Y., and David R. Corey (2012) Mechanism of allele-selective inhibition of huntingtin expression by duplex RNAs that target CAG repeats. Nucleic Acids Res. *40,* 11270-80

Huang, K., Sanders, S. S., Kang, R., Carroll, J. B., Sutton, L., Wan, J., Roshini, S., Young, F. B., Liu, L., El-Hesseini, A. *et al.* (2011). Wild-type HTT modulates the enzymatic activity of the neuronal palmitoyl transferase HIP14. Hum. Mol. Genet. *20*, 3356-3365

Kordasiewicz HB, Stanek LM, Wancewicz EV, Mazur C, McAlonis MM, Pytel KA, Artates JW, Weiss A, Cheng SH, Shihabuddin LS, Hung G, Bennett CF, Cleveland DW. (2012) Sustained Therapeutic Reversal of Huntington's Disease by Transient Repression of Huntingtin Synthesis. Neuron. *74*, 1031-44.

Kozlowski, P., de Mezer, and Krzyzosiak, W.J. (2010). Trinucleotide repeats in the human genome and exome. *Nucleic Acids Res.* 38, 4027-4039

Kremer, B., Goldberg, P., Andrew, S.E., Theilmann, J., Telenius, H., Zeisler, J., Squitieri, F., Lin, B., Bassett, A., Almqvist, E., et al. (1994). A worldwide study of the Huntington's disease mutation. The sensitivity and specificity of measuring CAG repeats. N. Engl. J. Med. *330*, 1401-1406.

Lim, L.P., Lau, N.C., Garrett-Engele, P., Grimson, A., Schelter, J. M., Castle, J., Bartel, D.P., Linsley, P.S., and Johnson, J.M. (2005). Microarray analysis shows that some microRNAs downregulate large numbers of target mRNAs. Nature *433*, 769-773.

Lima, W.F., Prakash, T.P., Murray, H.M., Kinberger, G.A., Li, W., Chappell, A.E., Li C.S., Murray, S.F., Gaus, H., Seth, P.P., Swayze, E.E., and Crooke, S.T. (2012) Single-stranded siRNAs Activate RNAi in Animals. Cell, *150,* 883-94

Lin, C.H., Tallaksen-Greene, S., Chien, W.M., Cearley, J.A., Jackson, W.S., Crouse, A.B., Ren, S., Li, X.J., Albin, R.L., and Detloff, P.J. (2001). Neurological abnormalities in a knock-in mouse model of Huntington's disease. Hum Mol Genet *10*, 137-144.

Liu, J., Carmell, M.A., Rivas, F.V., Marsden, C.G., Thomson, J.M., Song, J.J., Hammond, S.M., Joshua-Tor, L., and Hannon, G.J. (2004). Argonaute2 is the catalytic engine of mammalian RNAi. Science *305*, 1437-1441.

Lombardi, M.S., Jaspers, L., Spronkmans, C., Gellera, C., Taroni, F., Di Maria, E., Donato, S.D., and Kaemmerer, W.F. (2009). A majority of Huntington's disease patients may be treatable by individualized allele-specific RNA interference. Exp. Neurol. *217*, 312-319.

MacDonald, M.E., Ambrose, C.M., Duyao, M.P., Myers, R.H., Lin, C., Srinidhi, L., Barnes, G., Taylor, S.A., James, M., Groot, N., *et al*. (1993). A novel gene containing a trinucleotide repeat that is expanded and unstable on Huntington's disease chromosomes. The Huntington's Disease Collaborative Research Group. Cell *72*, 971-983.

Martinez, J., Patkaniowska, A., Urlaub, H., Luhrmann, R., and Tuschl, T. (2002). Single-stranded antisense RNA cleavage in RNAi. Cell *110*, 563-574.

Matsui, M. and Corey D.R. (2012). Drug Discov. Today. *17,* 443-50.

Meister, G., Landthaler, M., Patkaniowska, A., Dorsett, Y, Teng, G., Tuschl, T. (2004). Human argonaute2 mediates RNA cleavage targeted by miRNAs and siRNAs. Mol. Cell *15*, 185-197.

Michlewski, G. and Krzyzosiak, W.J. (2004). Molecular architecture of CAG repeats in human disease related transcripts. J. Mol. Biol*. 340*, 665-679

Miller, V.M., Xia, H., Marrs, G.L., Gouvion, C.M., Lee, G., Davidson, B.L., and Paulson, H.L. (2003). Allele-specific silencing of dominant disease genes. Proc. Natl. Acad. Sci. USA *100*, 7195-7200.

Nasir, J., Floresco, S.B., O'Kusky, J.R., Diewert, V.M., Richman, J.M., Zeisler, J., Borowski, A., Marth, J.D., Phillips, A.G., and Hayden, M.R. (1995). Targeted disruption of the Huntington's disease gene results in embryonic lethality and behavioral and morphological changes in heterozygotes. Cell *81*, 811-823.

Omi, K., Hachiya, N.S., Tokunaga, K., and Kaneko, K. (2005). siRNA-mediated inhibition of endogenous Huntington disease gene expression induces an aberrant configuration of the ER network in vitro. Biochem. Biophys. Res. Commun. *338*, 1229-1235.

Orr, H. T. and Zoghbi, H.Y. (2007). Trinucleotide repeat disorders. Annu. Rev. Neurosci. *30*, 575-621.

Pfister, E.L., Kennington, L., Straubhaar, J., Wagh, S., Liu, W., DiFiglia, M., Landwehrmeyer, B., Vonsattel, J.P., Zamore, P.D., and Aronin, N. (2009). Five siRNAs targeting three SNPs may provide therapy for three-quarters of Huntington's disease patients. Curr. Biol. *19*, 774-778.

Sah, D.W.Y. and Aronin, N. (2011). Oligonucleotide therapeutic approaches for Huntingtin Disease. J. Clin. Invest. *121*, 500-507

Schwarz, D.S., Ding, H., Kennington, L., Moore, J.T., Schelter, J., Burchard, J., Linsley, P.S., Aronin, N., Xu, Z., and Zamore, P.D. (2006). Designing siRNA that distinguish between genes that differ by a single nucleotide. PLoS Genet. *2*, e140.

van Bilsen, P.H., Jaspers, L., Lombardi, M.S., Odekerken, J.C., Burright, E.N., and Kaemmerer, W.F. (2008). Identification and allele-specific silencing of the mutant huntingtin allele in Huntington's disease patient-derived fibroblasts. Hum. Gene Ther. *19*, 710-719.

Walker, F.O. (2007). Huntington's disease. Lancet *369*, 218-228.

Wang, Y., Juranek, S., Li, H., Sheng, G., Tuschl, T., and Patel, D.J. (2008). Structure of an argonaute silencing complex with a seed-containing guide DNA and target RNA duplex. Nature *456*, 921-926.

Warby, S.C., Montpetit, A., Hayden, A. R., Carroll, J. B., Butland, S. L., Visscher, H., Collins, J. A., Semaka, A., Hudson, T.J., and Hayden, M.R. (2009). CAG expansion in the Huntington disease gene is associated with a specific and targetable predisposing haplogroup. Am. J. Hum. Genet. *84*, 351-366.

Watts, J.K. and Corey, D.R. (2012). Silencing disease genes in the laboratory and the clinic. J. Pathol. *226*, 365-379.

White, J.K., Auerbach, W., Duyao, M.P., Vonsattel, J.P., Gusella, J.F., Joyner, A.L., and MacDonald, M.E. (1997). Huntingtin is required for neurogenesis and is not impaired by the Huntington's disease CAG expansion. Nat. Genet. *17*, 404-410.

Yamamoto A, Lucas JJ, Hen R. (2000) Reversal of neuropathology and motor dysfunction in a conditional model of Huntington's disease. Cell. *101*,57-66.

Yu, D., Pendergraff, H., Liu, J., Kordasiewicz, H., Cleveland, D.W., Swayze, E.E., Lima, W.F., Crooke, S.T., Prakash, T.P., and Corey, D.R. (2012) Single-Stranded RNAs Use RNAi to Potently and Allele-Selectively Inhibit Mutant Huntingtin Expression. Cell, *150,* 895-908

Zeitlin, S., Liu, J-P., Chapman, D.L., Papaioannnou, V.E., and Estratiadis, A (1995). Increased apoptosis and early embryonic lethality in mice nullizygous for the Huntington's disease gene homologue. Nat. Genet*. 11*, 155-163.

Figure 1-1

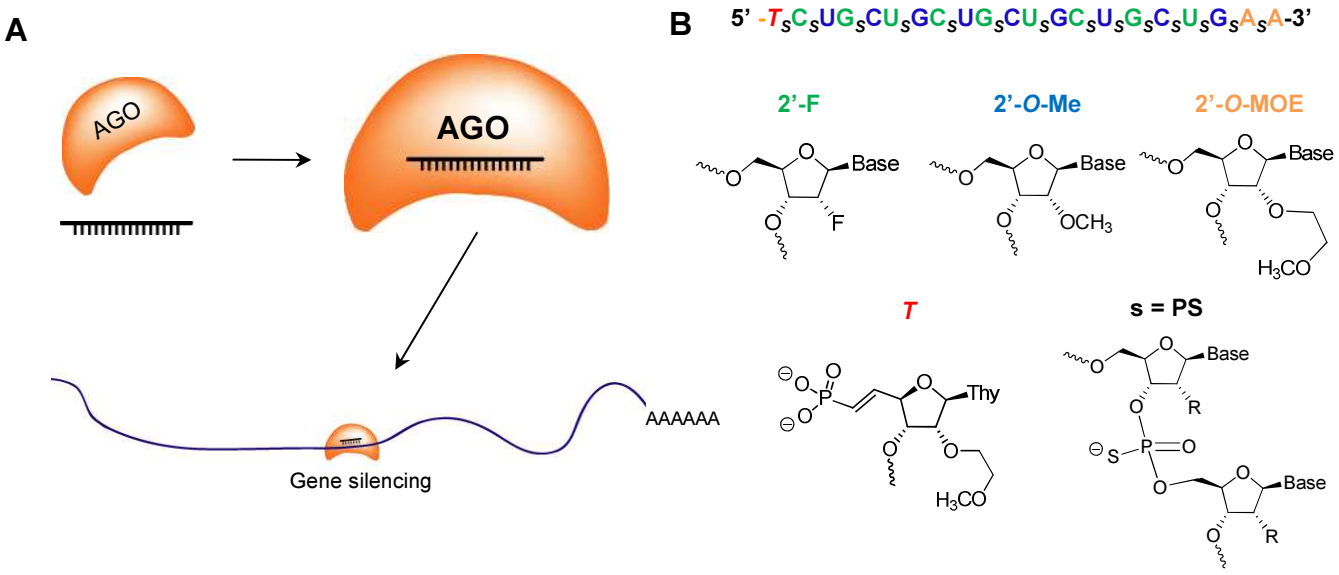

Figure 1-1. **AGO-modulated gene silencing and chemically modified ss-siRNAs**
(A) Recognition of mRNA by ss-siRNA. Argonaute (Ago) protein binds an ss-siRNA and the complex recognizes a complementary sequence within an mRNA target.
(B) Sequence and chemical modifications of a typical ss-siRNA.

Figure 1-2

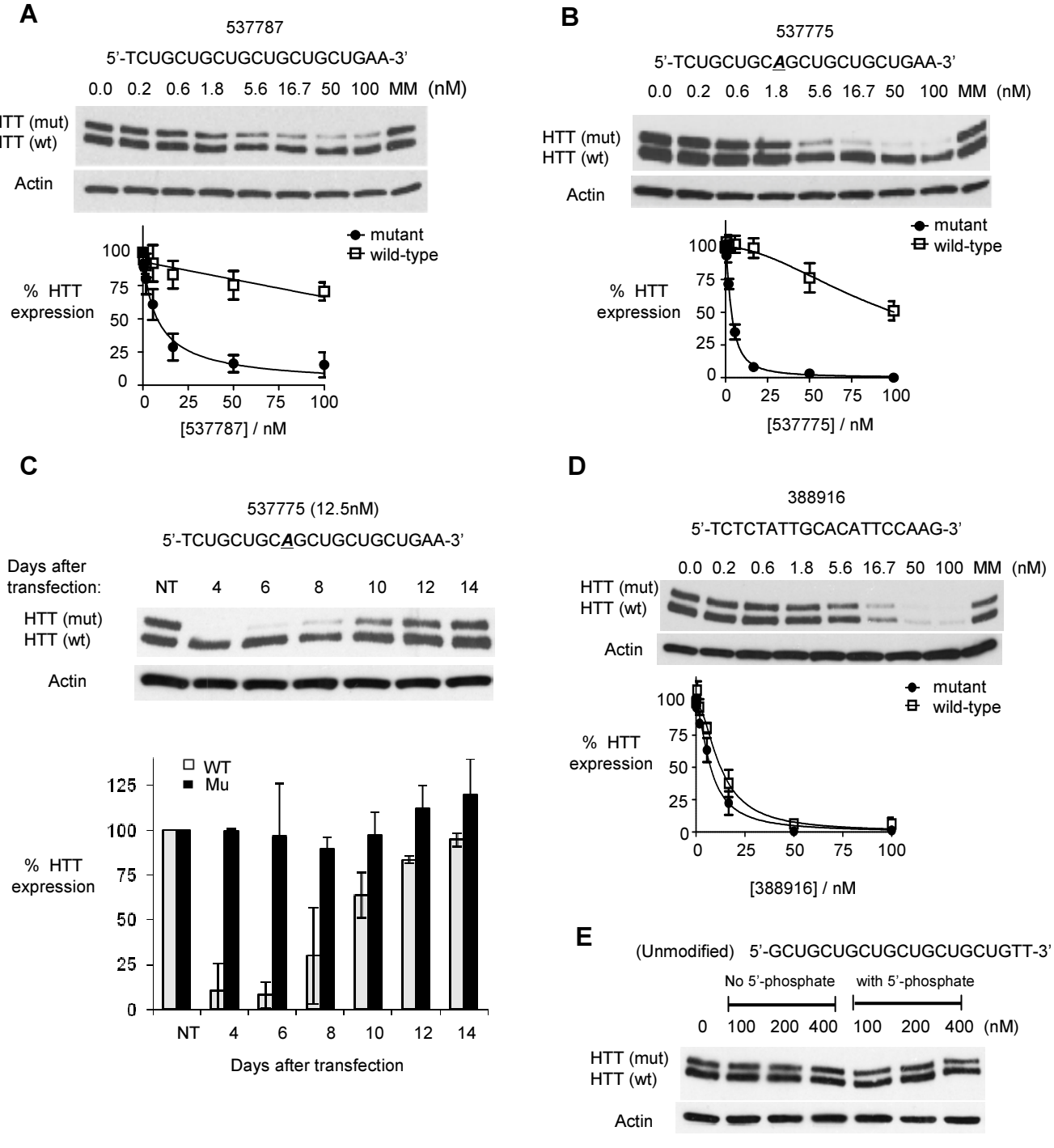
A
537787
5'-TCUGCUGCUGCUGCUGCUGAA-3'
0.0 0.2 0.6 1.8 5.6 16.7 50 100 MM (nM)
HTT (mut)
HTT (wt)
Actin
mutant
wild-type
% HTT expression
[537787] / nM
B
537775
5'-TCUGCUGCAGCUGCUGCUGAA-3'
0.0 0.2 0.6 1.8 5.6 16.7 50 100 MM (nM)
HTT (mut)
HTT (wt)
Actin
mutant
wild-type
% HTT expression
[537775] / nM
C
537775 (12.5nM)
5'-TCUGCUGCAGCUGCUGCUGAA-3'
Days after transfection:
NT 4 6 8 10 12 14
HTT (mut)
HTT (wt)
Actin
WT
Mu
% HTT expression
Days after transfection
D
388916
5'-TCTCTATTGCACATTCCAAG-3'
0.0 0.2 0.6 1.8 5.6 16.7 50 100 MM (nM)
HTT (mut)
HTT (wt)
Actin
mutant
wild-type
% HTT expression
[388916] / nM
E
(Unmodified) 5'-GCUGCUGCUGCUGCUGCUGTT-3'
No 5'-phosphate
with 5'-phosphate
0 100 200 400 100 200 400 (nM)
HTT (mut)
HTT (wt)
Actin

Figure 1-2. **ss-siRNAs inhibit HTT expression.**

Western analysis of inhibition of HTT expression by:

(A) ss-siRNA 537787 (no mismatches);

(B) ss-siRNA 537775 (one mismatch at P9);

(C) ss-siRNA 537775 over fourteen days with quantitation.

(D) a methoxyethyl antisense oligonucleotide that targets a non-repeat region of *HTT* mRNA.

(E) a fully complementary single-stranded RNA lacking any chemical modifications with and without a 5' terminal phosphate.

MM: an RNA containing multiple mismatches. Error bars are standard error of the mean (SEM).

Figure 1-3

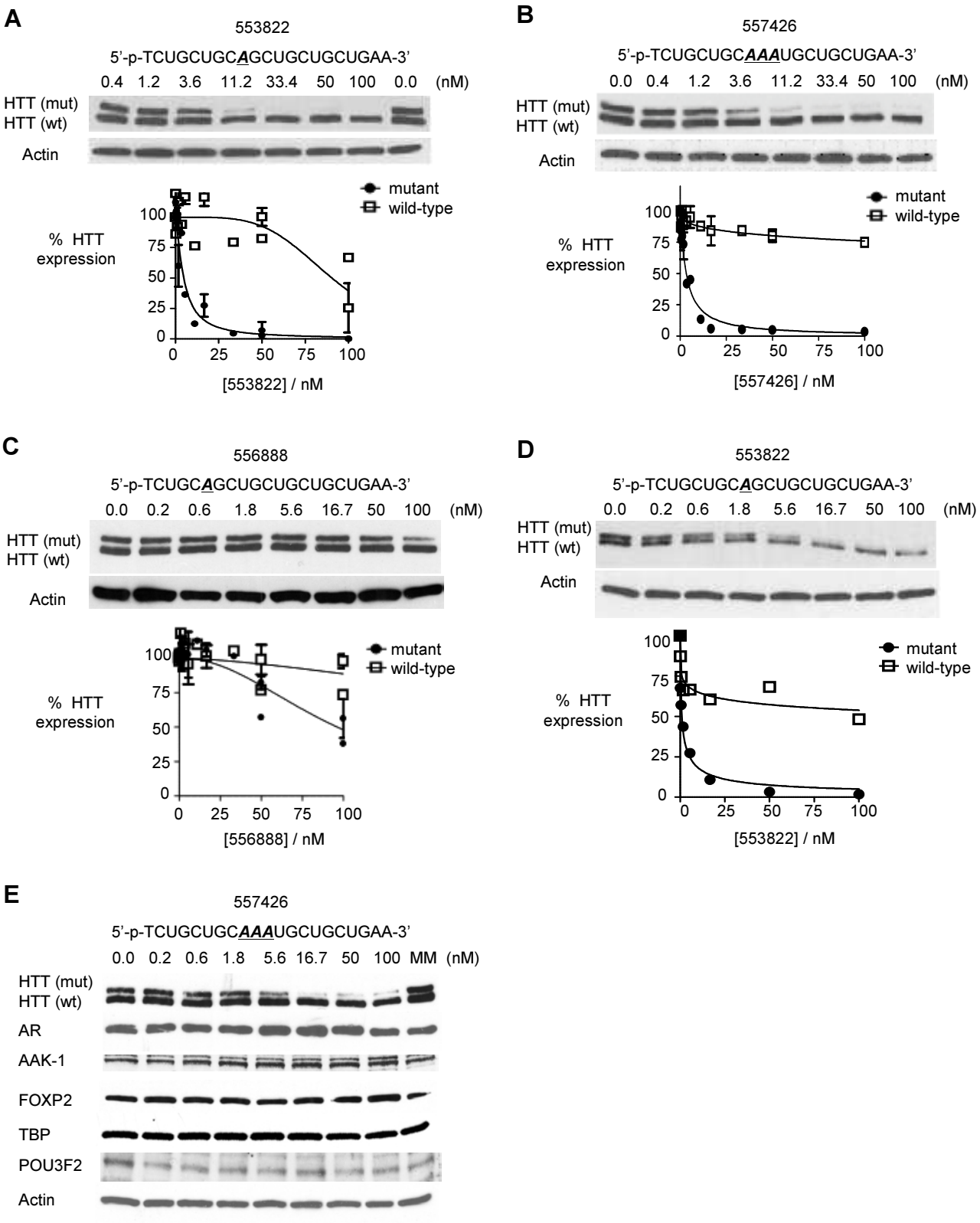
A
553822
5'-p-TCUGCUGCAGCUGCUGCUGAA-3'
0.4 1.2 3.6 11.2 33.4 50 100 0.0 (nM)
HTT (mut)
HTT (wt)
Actin
mutant
wild-type
% HTT expression
[553822] / nM
B
557426
5'-p-TCUGCUGCAAAUGCUGCUGAA-3'
0.0 0.4 1.2 3.6 11.2 33.4 50 100 (nM)
HTT (mut)
HTT (wt)
Actin
mutant
wild-type
% HTT expression
[557426] / nM
C
556888
5'-p-TCUGCAGCUGCUGCUGCUGAA-3'
0.0 0.2 0.6 1.8 5.6 16.7 50 100 (nM)
HTT (mut)
HTT (wt)
Actin
mutant
wild-type
% HTT expression
[556888] / nM
D
553822
5'-p-TCUGCUGCAGCUGCUGCUGAA-3'
0.0 0.2 0.6 1.8 5.6 16.7 50 100 (nM)
HTT (mut)
HTT (wt)
Actin
mutant
wild-type
% HTT expression
[553822] / nM
E
557426
5'-p-TCUGCUGCAAAUGCUGCUGAA-3'
0.0 0.2 0.6 1.8 5.6 16.7 50 100 MM (nM)
HTT (mut)
HTT (wt)
AR
AAK-1
FOXP2
TBP
POU3F2
Actin

Figure 1-3. Characterization of inhibition by modified ss-siRNAs.

Inhibition of HTT expression by:

(A) ss-siRNA 553822 (mutation at P9) containing a 5'phosphate;

(B) ss-siRNA 557426 containing three central mismatches;

(C) ss-siRNA 556888 containing a mismatch at P6; and

(D) ss-siRNA 553822 in 44-CAG-repeat GM04719 cells.

(E) Effect of ss-siRNA 537775 on other genes containing trinucleotide repeats.

MM: an RNA containing multiple mismatches. Error bars are standard error of the mean (SEM).

Table 1-1: ss-siRNAs and other oligonucleotides used in these studies

No.	Abbr. Name	Sequence	Position of Mismatch	Tm, °C	mut IC_{50} (nM)	wt IC_{50} (nM)	Selectivity (fold)
ssRNAs with 5'-*(E)*-vinyl phosphonate chemistry:							
537787	REP	**5' -*T*$_s$C$_s$UG$_s$CU$_s$GC$_s$UG$_s$CU$_s$GC$_s$U$_s$G$_s$C$_s$U$_s$G$_s$A$_s$A-3'**	None	90-91	8.0 ± 1.7	> 100	>13
537775	P9	**5' -*T*$_s$C$_s$UG$_s$CU$_s$GC$_s$*A*G$_s$CU$_s$GC$_s$U$_s$G$_s$C$_s$U$_s$G$_s$A$_s$A-3'**	9	84-85	3.5 ± 0.3	> 100	>29
537786	P10	**5' -*T*$_s$C$_s$UG$_s$CU$_s$GC$_s$U*A*$_s$CU$_s$GC$_s$U$_s$G$_s$C$_s$U$_s$G$_s$A$_s$A-3'**	10	84-85	22.3 ± 2.6	> 100	>4
ssRNAs with 5'-phosphate chemistry:							
553819	REP	**5'-P -T$_s$C$_s$UG$_s$CU$_s$GC$_s$UG$_s$CU$_s$GC$_s$U$_s$G$_s$C$_s$U$_s$G$_s$A$_s$A-3'**	None	> 95	5.7 ± 1.4	71.8 ± 15.6	13
556886	P4	**5'- P-T$_s$C$_s$U*A*$_s$CU$_s$GC$_s$UG$_s$CU$_s$GC$_s$U$_s$G$_s$C$_s$U$_s$G$_s$A$_s$A-3'**	4	85	8.8	61.1	7
556887	P5	**5' - P-T$_s$C$_s$UG$_s$*A*U$_s$GC$_s$UG$_s$CU$_s$GC$_s$U$_s$G$_s$C$_s$U$_s$G$_s$A$_s$A-3'**	5	82-89	17.2 ± 2.6	>100	>6
556888	P6	**5' - P-T$_s$C$_s$UG$_s$C*A*$_s$GC$_s$UG$_s$CU$_s$GC$_s$U$_s$G$_s$C$_s$U$_s$G$_s$A$_s$A-3'**	6	81-85	N.I.	N.I.	N/A
556889	P7	**5' - P-T$_s$C$_s$UG$_s$CU$_s$*A*C$_s$UG$_s$CU$_s$GC$_s$U$_s$G$_s$C$_s$U$_s$G$_s$A$_s$A-3'**	7	83-85	11.2 ± 1.7	51.1 ± 8.5	5
556890	P8	**5' - P-T$_s$C$_s$UG$_s$CU$_s$G*A*$_s$UG$_s$CU$_s$GC$_s$U$_s$G$_s$C$_s$U$_s$G$_s$A$_s$A-3'**	8	83-85	4.1 ± 0.7	29.5 ± 4.3	7
553822	P9	**5' - P-T$_s$C$_s$UG$_s$CU$_s$GC$_s$*A*G$_s$CU$_s$GC$_s$U$_s$G$_s$C$_s$U$_s$G$_s$A$_s$A-3'**	9	85	4.9 ± 0.8	90.4 ± 9.7	18
553821	P10	**5' - P-T$_s$C$_s$UG$_s$CU$_s$GC$_s$U*A*$_s$CU$_s$GC$_s$U$_s$G$_s$C$_s$U$_s$G$_s$A$_s$A-3'**	10	82-86	17.8 ± 3.5	>100	>6
557407	P10R	**5' - P-T$_s$C$_s$UG$_s$CU$_s$GC$_s$U*U*$_s$CU$_s$GC$_s$U$_s$G$_s$C$_s$U$_s$G$_s$A$_s$A-3'**	10	77-80	15.3 ± 2.4	>100	>7
556891	P11	**5' - P-T$_s$C$_s$UG$_s$CU$_s$GC$_s$UG$_s$*A*U$_s$GC$_s$U$_s$G$_s$C$_s$U$_s$G$_s$A$_s$A-3'**	11	78-81	12.8 ± 1.7	>100	>8
556892	P12	**5' - P-T$_s$C$_s$UG$_s$CU$_s$GC$_s$UG$_s$C*A*$_s$GC$_s$U$_s$G$_s$C$_s$U$_s$G$_s$A$_s$A-3'**	12	81-84	3.4 ± 0.6	72.0 ± 12.3	21
557406	P13	**5' - P-T$_s$C$_s$UG$_s$CU$_s$GC$_s$UG$_s$CU$_s$*A*C$_s$U$_s$G$_s$C$_s$U$_s$G$_s$A$_s$A-3'**	13	78-82	4.2 ± 0.6	>100	>24
557408	P16	**5' - P-T$_s$C$_s$UG$_s$CU$_s$GC$_s$UG$_s$CU$_s$GC$_s$U$_s$*A*C$_s$U$_s$G$_s$A$_s$A-3'**	16	81-84	8.1	27.3	3
557409	P910	**5' - P-T$_s$C$_s$UG$_s$CU$_s$GC$_s$*AA*$_s$CU$_s$GC$_s$U$_s$G$_s$C$_s$U$_s$G$_s$A$_s$A-3'**	9, 10	78-81	6.3 ± 0.5	>100	>16
557426	PM3	**5' - P-T$_s$C$_s$UG$_s$CU$_s$GC$_s$*AA*$_s$*A*U$_s$GC$_s$U$_s$G$_s$C$_s$U$_s$G$_s$A$_s$A-3'**	9, 10, 11	74	3.3 ± 0.5	>100	>30
557427	PM4	**5' - P-T$_s$C$_s$UG$_s$CU$_s$G*A*$_s$*AA*$_s$*A*U$_s$GC$_s$U$_s$G$_s$C$_s$U$_s$G$_s$A$_s$A-3'**	8, 9, 10, 11	65-66	11.8 ± 1.9	>100	>8
557428	RM3	**5' - P-T$_s$C$_s$U*A*$_s$CU$_s$GC$_s$U*A*$_s$CU$_s$GC$_s$U$_s$*A*C$_s$U$_s$G$_s$A$_s$A-3'**	4, 10, 16	65	22.3	>100	>4
557429	RM4	**5' - P-T$_s$C$_s$*A*G$_s$CU$_s$G*U*$_s$UG$_s$CU$_s$*A*C$_s$U$_s$G$_s$*U*$_s$U$_s$G$_s$A$_s$A-3'**	3, 8, 13, 17	65-66	N.I.	N.I.	N/A
557430	REPU	**5' - P-T$_s$G$_s$CU$_s$GC$_s$UG$_s$CU$_s$GC$_s$UG$_s$C$_s$U$_s$G$_s$C$_s$U$_s$A$_s$A-3'**	None	>95	19.4 ± 4.7	>100	>5
Control oligomers:							
388916	Gapmer	**5'-TCTCTA$_d$T$_d$T$_d$G$_d$C$_d$A$_d$C$_d$A$_d$T$_d$T$_d$CCAAG-3'**	N/A	N/A	7.4 ± 0.7	12.6 ± 1.3	1.7
387898	Gapmer	**5'-CTCGAC$_d$T$_d$A$_d$A$_d$A$_d$G$_d$C$_d$A$_d$G$_d$G$_d$ATTTC-3'**	N/A	N/A	5.8	7.1	1.2
522247	Neg.Ctrl	**5' - T$_s$U$_s$AU$_s$CU$_s$AU$_s$AA$_s$UG$_s$AU$_s$C$_s$A$_s$G$_s$G$_s$U$_s$A$_s$A-3'**	N/A	N/A	N.I.	N.I.	N/A
N/A	LNAT	**5'-GCTGCTGCTGCTGCTGCTG-3'**	None	97	40 ± 7	>100	>2.5
N/A	CM	**5'-GCUAUACCAGCGUCGUCAUAA-3' 3'-TTCGA UAUGGUCGCAGCAGUA-5'**	N/A	N/A	N.I.	N.I.	N/A

Color schemes represent different chemical modifications as follows:

U: 2'-fluoro; A: 2'-*O*-methyl; A: 2'-methoxyethyl (2'-MOE); T:locked nucleic acid (LNA); *T:* phosphonate; s: phosphorothioate; d: deoxyribose. All other sugars are riboses unless specifiied otherwise.

N.I.: no inhibition; N/A: not available.

Except for CM (a dsRNA species), all Tm's are measured using ss-siRNAs duplexed with equi-molar of unmodified ssRNA of the sequence 5'-CAGCAGCAGCAGCAGCAGCAGC-3'.

Gapmers are entirely of phosphorothioate backbone, with 10 central bases having deoxy-ribose and each 5 flanking bases being 2'-MOE chemistry.

Figure 1-4

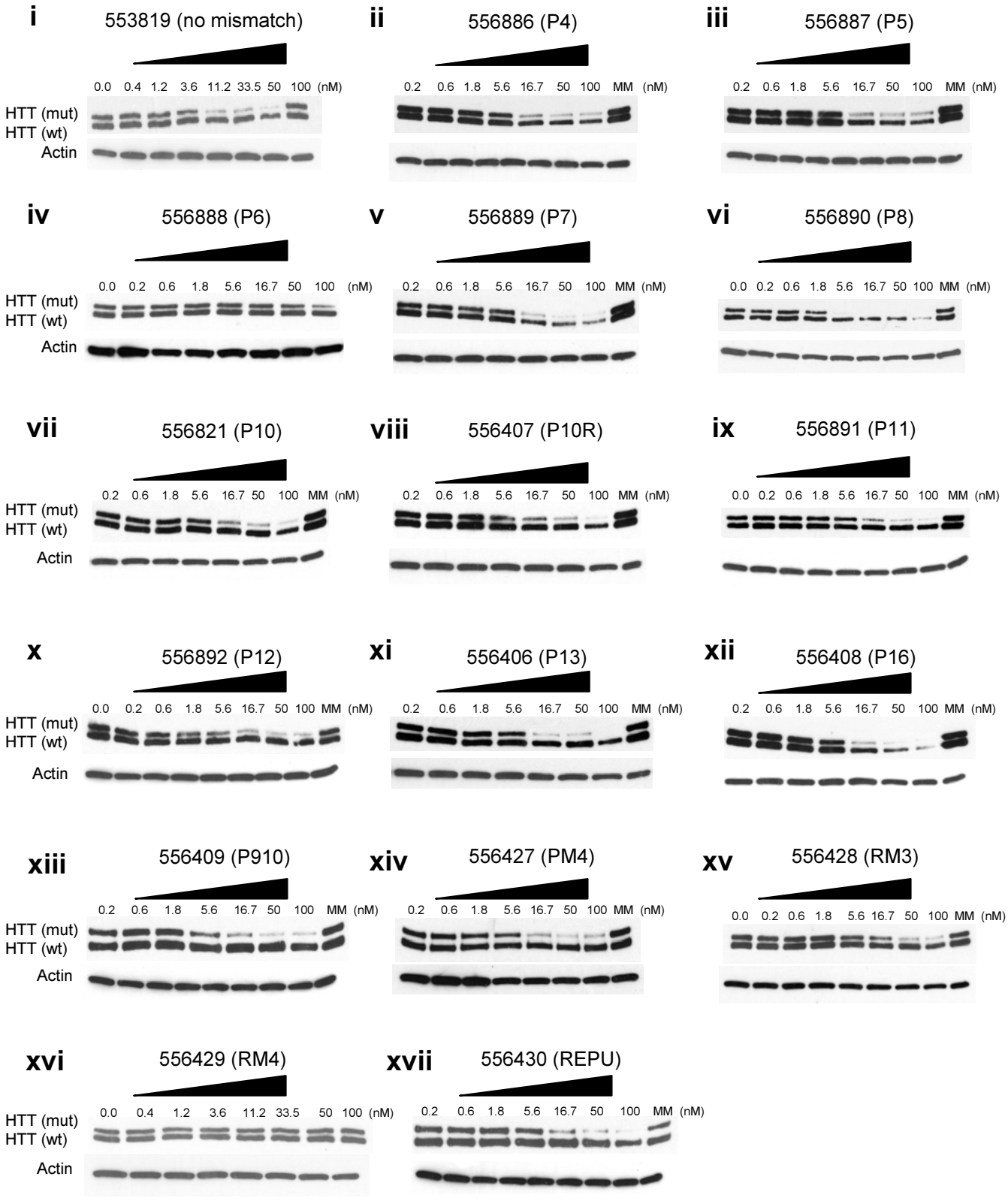
i
553819 (no mismatch)
0.0 0.4 1.2 3.6 11.2 33.5 50 100 (nM)
ii
556886 (P4)
0.2 0.6 1.8 5.6 16.7 50 100 MM (nM)
iii
556887 (P5)
0.2 0.6 1.8 5.6 16.7 50 100 MM (nM)
iv
556888 (P6)
0.0 0.2 0.6 1.8 5.6 16.7 50 100 (nM)
v
556889 (P7)
0.2 0.6 1.8 5.6 16.7 50 100 MM (nM)
vi
556890 (P8)
0.0 0.2 0.6 1.8 5.6 16.7 50 100 MM (nM)
vii
556821 (P10)
0.2 0.6 1.8 5.6 16.7 50 100 MM (nM)
viii
556407 (P10R)
0.2 0.6 1.8 5.6 16.7 50 100 MM (nM)
ix
556891 (P11)
0.0 0.2 0.6 1.8 5.6 16.7 50 100 MM (nM)
x
556892 (P12)
0.0 0.2 0.6 1.8 5.6 16.7 50 100 MM (nM)
xi
556406 (P13)
0.2 0.6 1.8 5.6 16.7 50 100 MM (nM)
xii
556408 (P16)
0.2 0.6 1.8 5.6 16.7 50 100 MM (nM)
xiii
556409 (P910)
0.2 0.6 1.8 5.6 16.7 50 100 MM (nM)
xiv
556427 (PM4)
0.2 0.6 1.8 5.6 16.7 50 100 MM (nM)
xv
556428 (RM3)
0.0 0.2 0.6 1.8 5.6 16.7 50 100 MM (nM)
xvi
556429 (RM4)
0.0 0.4 1.2 3.6 11.2 33.5 50 100 (nM)
xvii
556430 (REPU)
0.2 0.6 1.8 5.6 16.7 50 100 MM (nM)
HTT (mut)
HTT (wt)
Actin

Figure 1-4. **Western analysis of the effects on HTT expression of ss-siRNAs with mismatched bases at different positions.**

Inhibition of HTT expression by ss-si-RNAs with mismatched bases at: (**i**) none, (**ii**) P4, (**iii**) P5, (**iv**) P6, (**v**) P7, (**vi**) P8, (**vii**) P10, (**viii**) P10R, (**ix**) P11, (**x**) P12, (**xi**) P13, (**xii**) P16, (**xiii**) P9,10, (**xiv**) P9,10,11, (**xv**) P4,10,16, (**xvi**) P3,8,13,17, (**xvii**) none (different registry)**.**

Representative western blot images are presented. MM: an RNA duplex containing multiple mismatches at 50 nM.

Figure 1-5

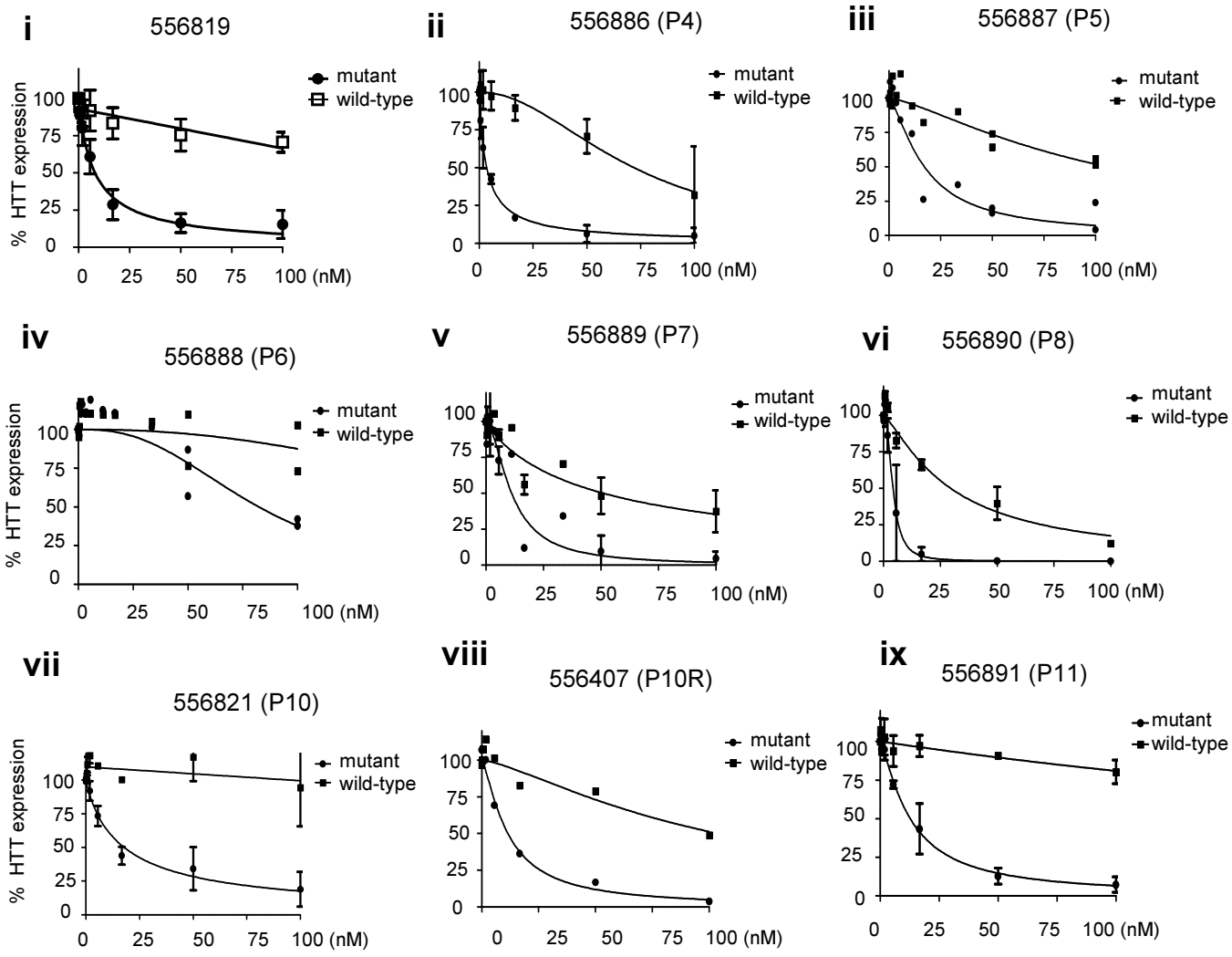
i
556819
ii
556886 (P4)
iii
556887 (P5)
iv
556888 (P6)
v
556889 (P7)
vi
556890 (P8)
vii
556821 (P10)
viii
556407 (P10R)
ix
556891 (P11)
% HTT expression
mutant
wild-type
0
25
50
75
100
100 (nM)

Figure 1-5 (cont'd)

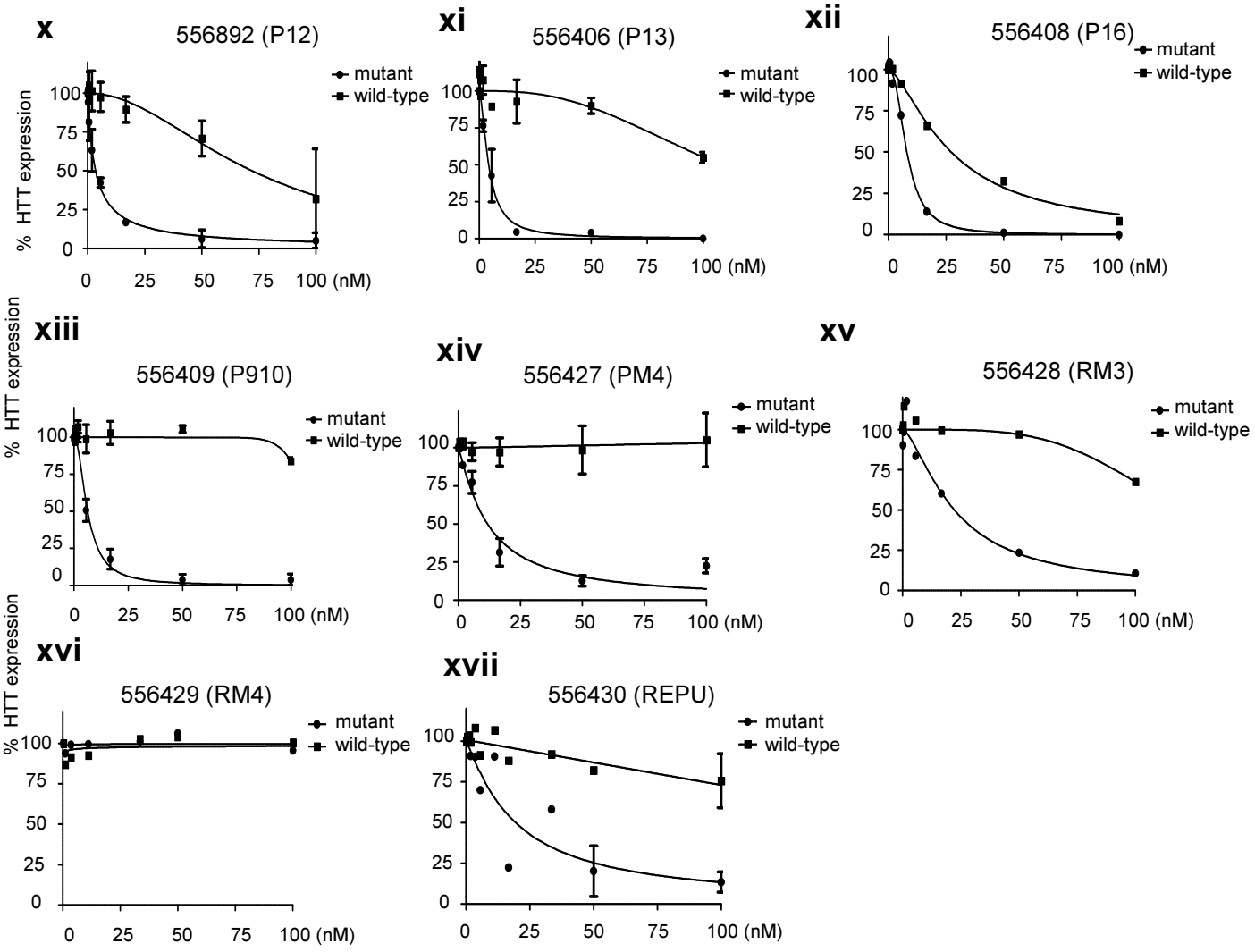

Figure 1-5. **Western analysis of the effects on HTT expression of ss-siRNAs with mismatched bases at different positions (graphic plots).**

Inhibition of HTT expression by ss-si-RNAs with mismatched bases at: (**i**) none, (**ii**) P4, (**iii**) P5, (**iv**) P6, (**v**) P7, (**vi**) P8, (**vii**) P10, (**viii**) P10R, (**ix**) P11, (**x**) P12, (**xi**) P13, (**xii**) P16, (**xiii**) P9,10, (**xiv**) P9,10,11, (**xv**) P4,10,16, (**xvi**) P3,8,13,17, (**xvii**) none (different registry)**.**

MM: an RNA duplex containing multiple mismatches at 50 nM. Error bars are standard error of the mean (SEM) from biological replicates.

Figure 1-6

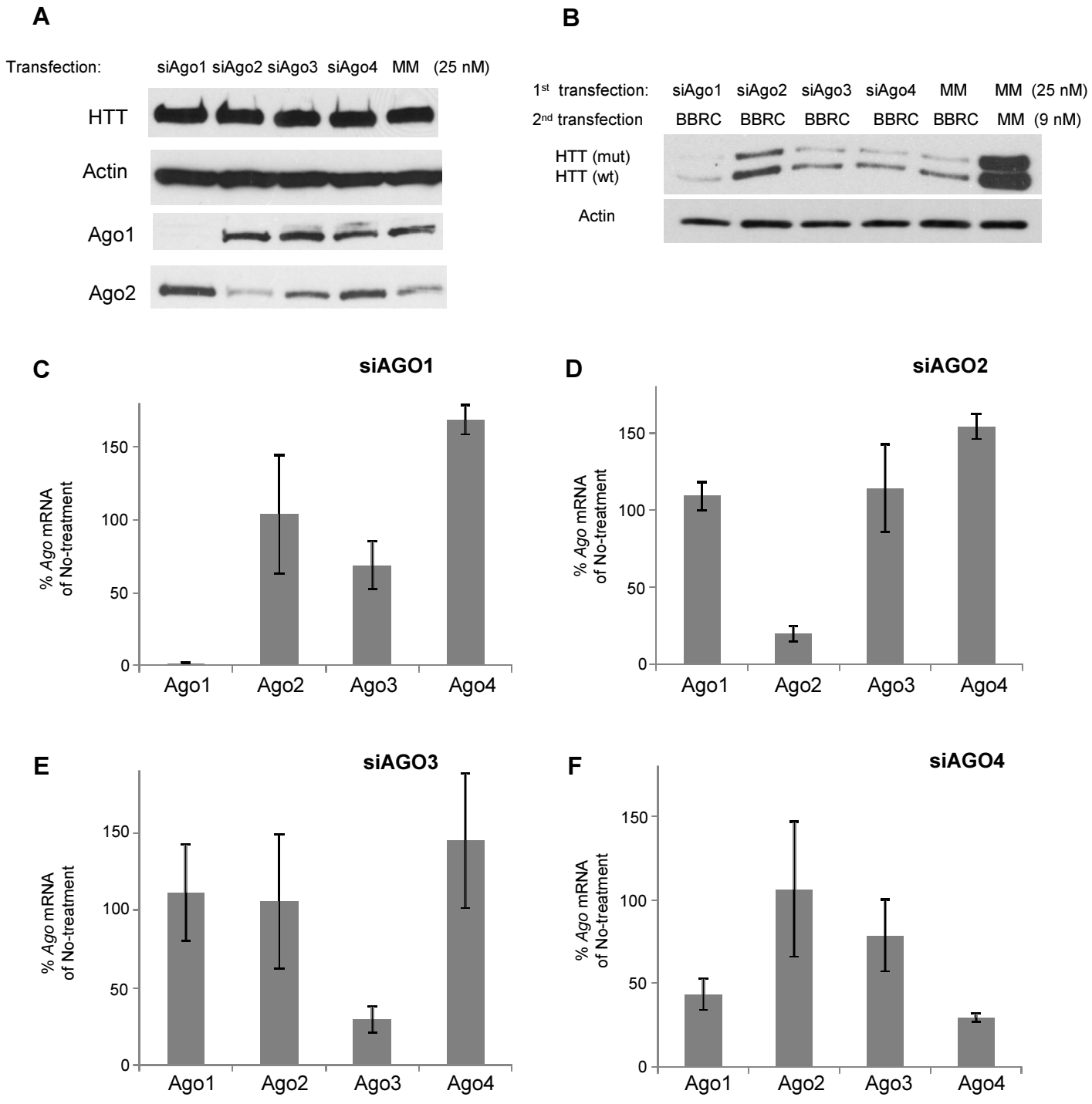

Figure 1-6. Knockdown efficiencies of AGO1-4 by siRNAs. (A) AGO1 and AGO2 knockdowns by siRNA shown by western blot. (B) AGO2 reversal was sufficient to reverse HTT knockdown by BBRC, a canonical siRNA duplex targeting HTT outside of CAG-repeat region. (C-F) AGO1-4 knockdowns by siRNAs (25nM) shown by q-PCR with relative Ago mRNA levels normalized to no treatment samples. Error bars represent standard error of the mean (SEM) from three independent experiments.

Figure 1-7

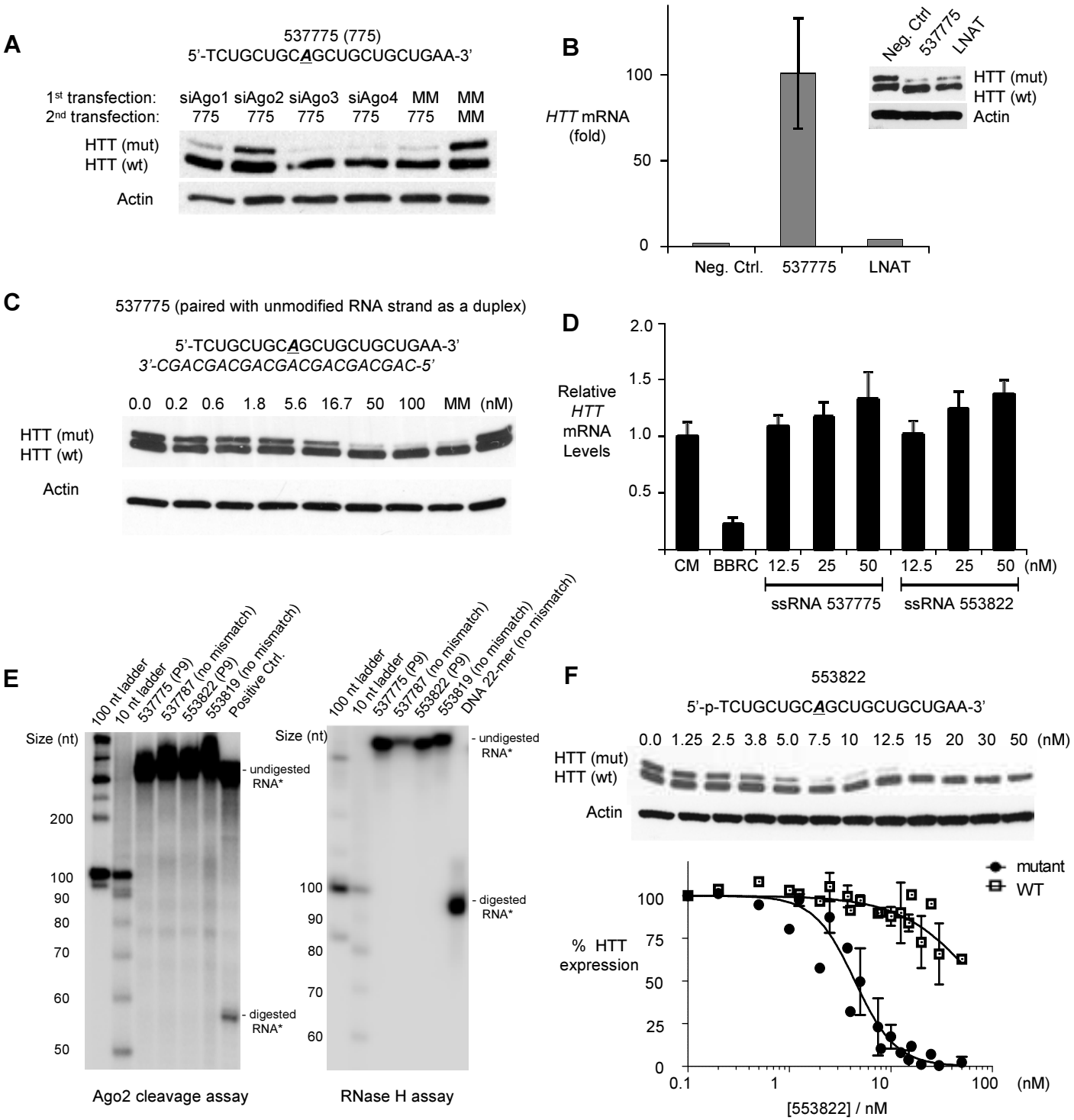
A
537775 (775)
5'-TCUGCUGCAGCUGCUGCUGAA-3'
1st transfection: siAgo1 siAgo2 siAgo3 siAgo4 MM MM
2nd transfection: 775 775 775 775 775 MM
HTT (mut)
HTT (wt)
Actin
B
Neg. Ctrl
537775
LNAT
HTT (mut)
HTT (wt)
Actin
HTT mRNA (fold)
100
50
0
Neg. Ctrl.
537775
LNAT
C
537775 (paired with unmodified RNA strand as a duplex)
5'-TCUGCUGCAGCUGCUGCUGAA-3'
3'-CGACGACGACGACGACGACGAC-5'
0.0 0.2 0.6 1.8 5.6 16.7 50 100 MM (nM)
HTT (mut)
HTT (wt)
Actin
D
Relative HTT mRNA Levels
2.0
1.5
1.0
0.5
CM BBRC 12.5 25 50 12.5 25 50 (nM)
ssRNA 537775
ssRNA 553822
E
100 nt ladder
10 nt ladder
537775 (P9)
537787 (no mismatch)
553822 (P9)
553819 (no mismatch)
Positive Ctrl.
DNA 22-mer (no mismatch)
Size (nt)
200
100
90
80
70
60
50
- undigested RNA*
- digested RNA*
Ago2 cleavage assay
RNase H assay
F
553822
5'-p-TCUGCUGCAGCUGCUGCUGAA-3'
0.0 1.25 2.5 3.8 5.0 7.5 10 12.5 15 20 30 50 (nM)
HTT (mut)
HTT (wt)
Actin
mutant
WT
% HTT expression
100
75
50
25
0
0.1
1
10
100 (nM)
[553822] / nM

Figure 1-7. Mechanism of allele-selective inhibition of HTT by ss-siRNA

(A) Western analysis of the effect siRNA-mediated reduction of AGO1-4 expression on allele-selective inhibition by ss-siRNA 553822.

(B) RNA immunoprecipitation (RIP) using anti-AGO2 antibody after transfection of ss-siRNA 537775, a control ss-siRNA 522247 not targeting HTT, or an allele-selective single-stranded ASO (LNAT) (Hu et al., 2009) at 25nM. Y-axis measures fold-enrichment of *HTT* mRNA of anti-AGO2 vs IgG pulldown.

(C) Western analysis of inhibition of HTT expression by ss-siRNA 537775 in complex with a complementary unmodified RNA.

(D) Effect of ss-siRNAs 537775 or 553822 on levels of *HTT* mRNA evaluated by q-PCR.

(E) *In vitro* assays using recombinant RNase H and Ago2 proteins do not show efficient substrate cleavage by ss-siRNA.

(F) Primary data and Hill plot used for determining cooperativity of HTT inhibition by ss-siRNA 553822. X-axis shows ss-siRNA concentration in logarithmic scale. Hill coefficient (n^h) is 2.2±0.3 for mutant HTT and 1.2±0.2 for WT HTT.

Error bars from western analysis are standard error of the mean (SEM), and error bars on *HTT* mRNA levels are standard deviations (SD) from replicate data.

Figure 1-8

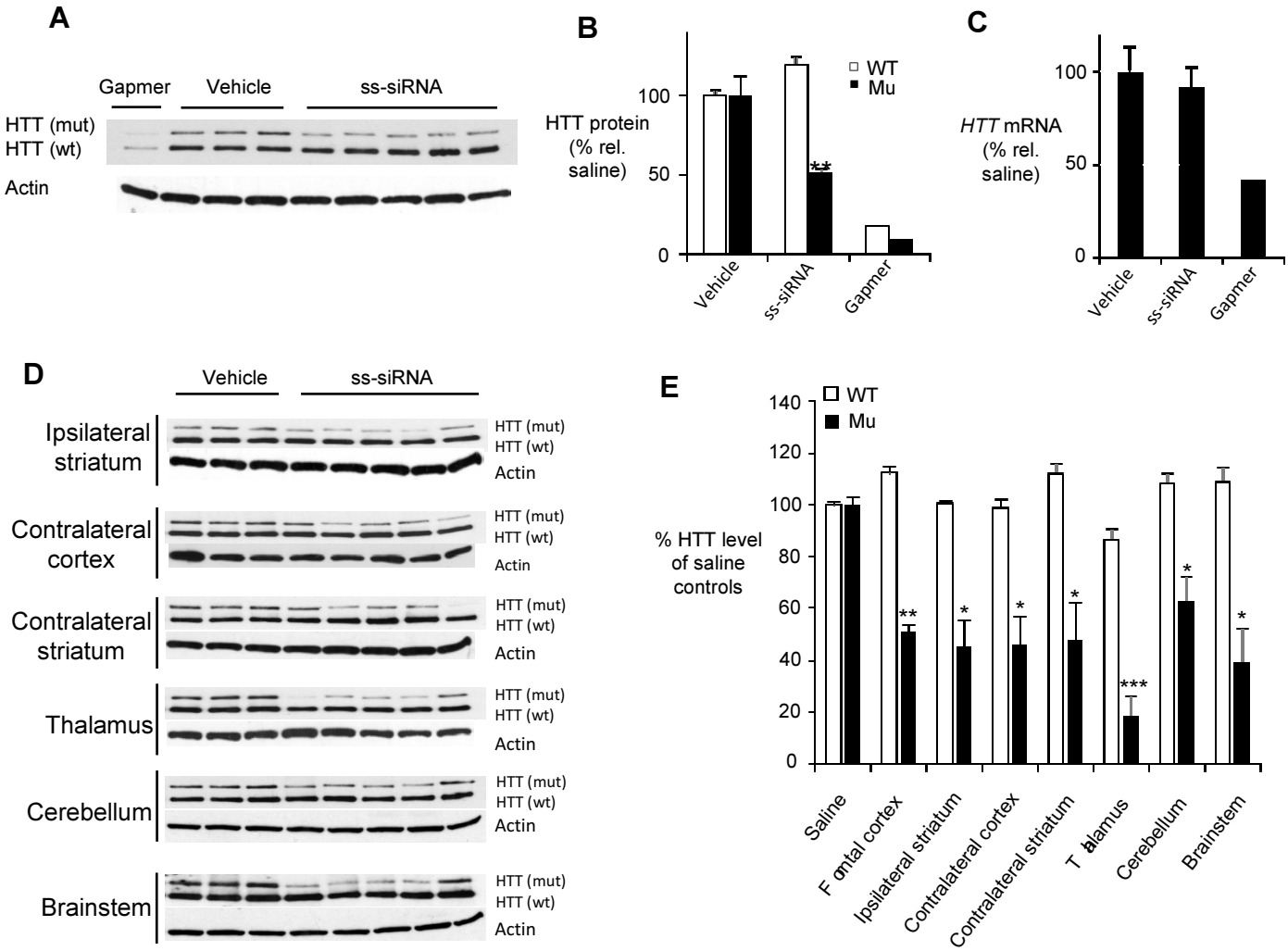

Figure 1-8. Allele-selective inhibition of HTT by ssiRNA in *Hdh*$^{Q150/Q7}$ mouse model. (A) Western analysis of HTT expression on allele-selective inhibition by ss-siRNA 537775 (n=5) in *Hdh*$^{Q150/Q7}$ mouse frontal cortex. (B) Quantitation of data in (A). (C) qPCR analysis of *HTT* mRNA levels in mouse frontal cortex after treatment with ss-siRNA, vehicle, or control gapmer ASO. (D) Western analysis HTT expression after allele-selective inhibition by ss-siRNA 537775 (n=5) in different brain regions. (E) Quantitation of western analysis from (C). Error bars represent standard error of the mean (SEM) from images of multiple western gels. *p < 0.05; **p < 0.01; ***p < 0.001.

Figure 1-9

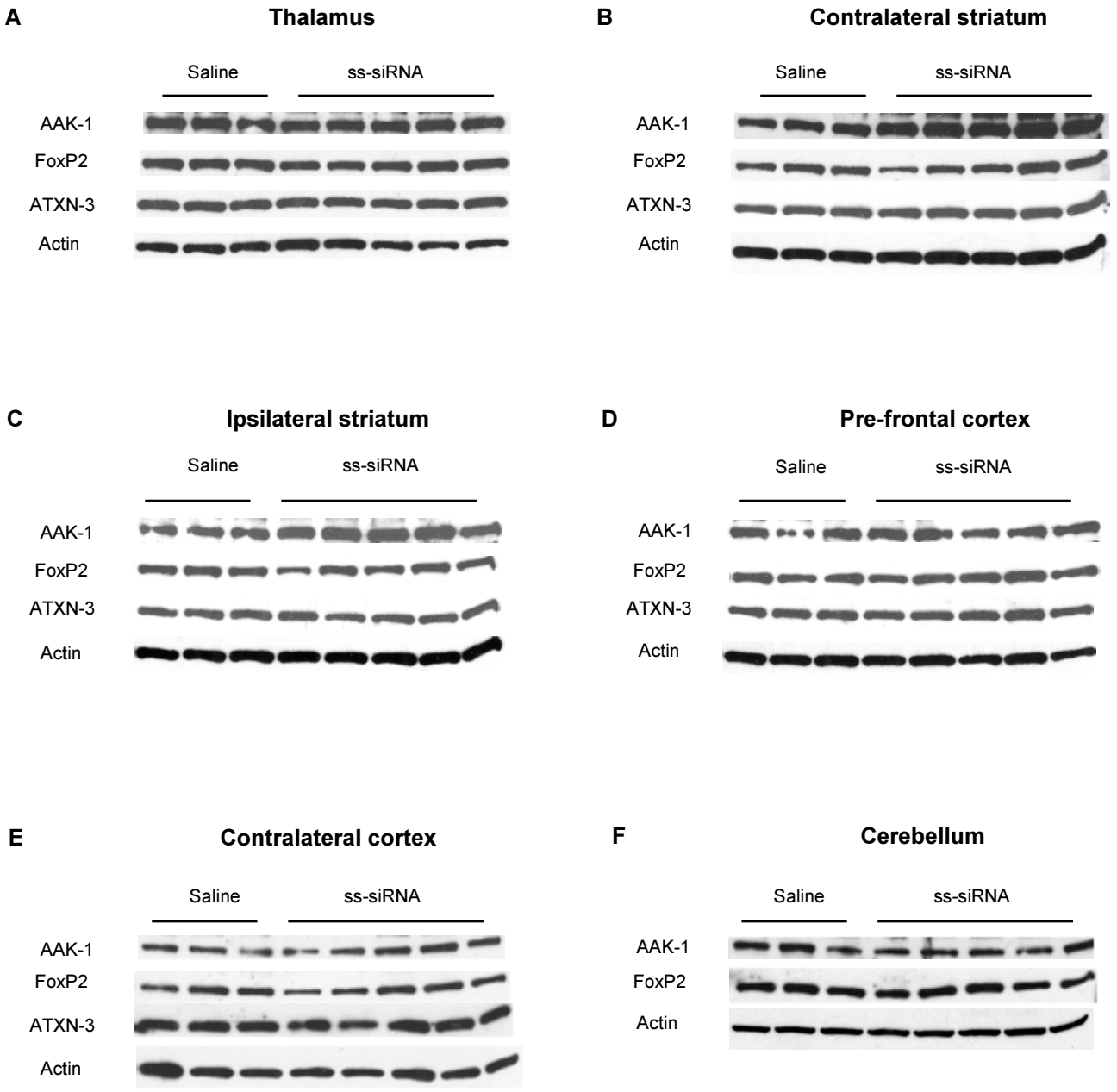

Figure 1-9. **Protein levels of several CAG-repeat-containing genes in various mouse brain tissues after ss-siRNA treatments of *Hdh*$^{Q150/Q7}$ model mice.** No significant changes are observed in the several poly-Q peptides after *in vivo* administration of ssRNA 537775 in: (A) thalamus; (B) contralateral striatum; (C) ipsilateral striatum; (D) pre-frontal cortex; (E) contralateral cortex; and (F) cerebellum.

Figure 1-10

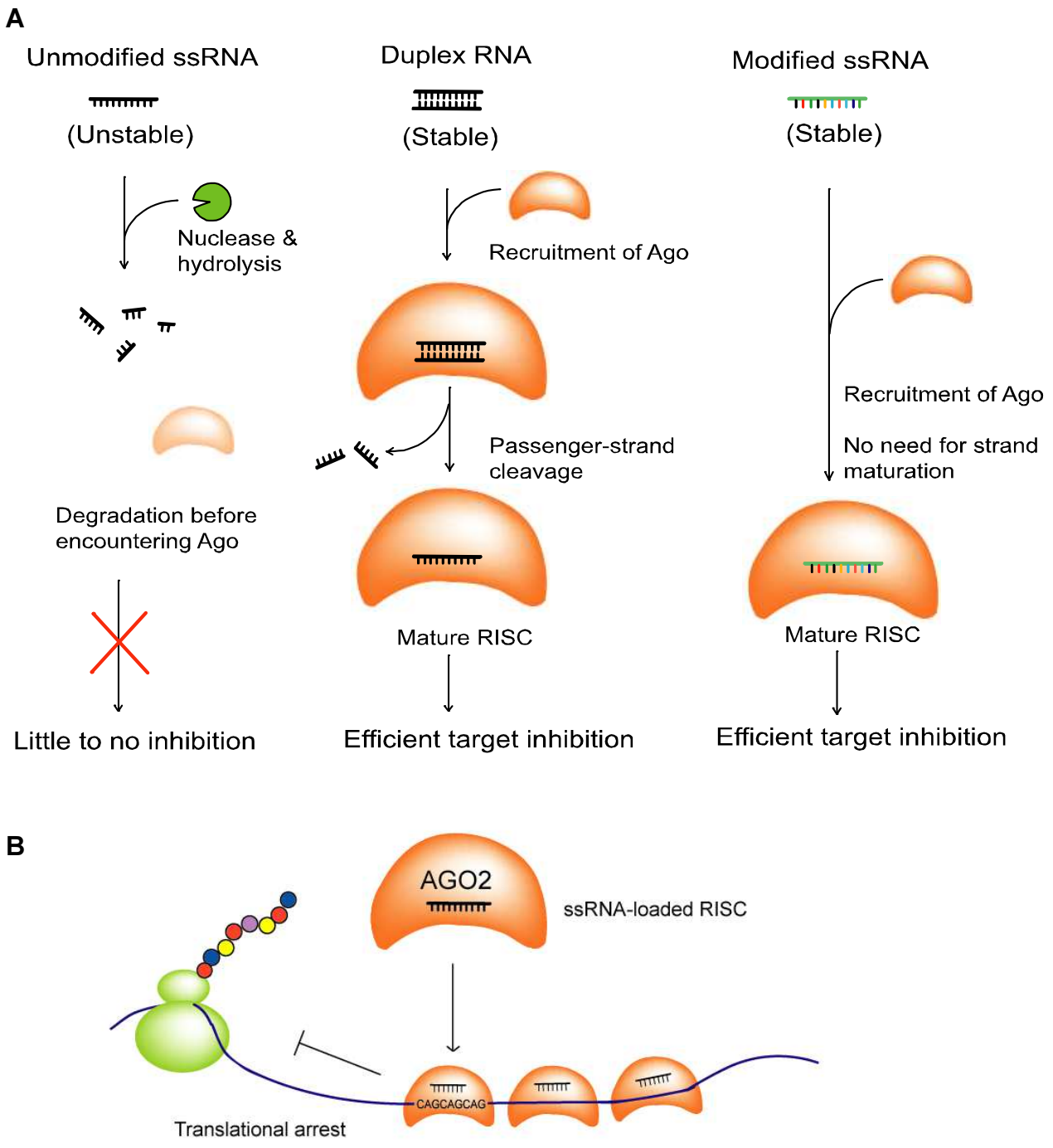

Figure 1-10. Action of chemically modified ss-siRNAs and allele-selective inhibition of HTT.

(A) Chemical modifications allow ss-siRNA to be stable and function through RNAi. (B) Binding of multiple anti-CAG ss-siRNA:AGO2 complexes to expanded trinucleotide repeat contributes to allele-selective inhibition.

CHAPTER TWO

Active ss-siRNAs Are Compatible with Multiple Sequence and Structural Modifications

ABSTRACT

During the ss-siRNA design process, chemists at ISIS Pharmaceuticals accumulated a substantial amount of structure-activity relationship (SAR) knowledge on single-stranded RNAs through testing many sequences and chemistries. This knowledge was enriched by successes and lessons learned in screening and characterizing CAG-targeting ss-siRNAs that identified a number of potent and allele-selective HTT inhibitors. Nonetheless, due to the novelty of ss-siRNA, a basic set of predicative rules for designing effective ss-siRNAs are still lacking.

To better understand ss-siRNA design rules and mechanism, we modified a number of known active ss-siRNAs by mutating their sequences or attaching lipid groups. The findings led us to formulate the following basic design guidelines: 1) mRNA cleavage is the standard mechanism by which ss-siRNAs achieve gene repression; 2) ss-siRNAs can tolerate shorter lengths down to 17 nucleotides; 3) inclusions of 3-4 but not 5 mismatches generated ss-siRNAs that retained activity; and 4) attachment of a lipid moiety at several different positions did not enable direct cellular uptake of ss-siRNA, but still maintained high potency and allele-selectivity with standard transfection protocol. Together, they suggest that while adhering to a general siRNA-guide-strand layout, ss-siRNA exhibits considerable sequence and structural flexibility

that would allow design and identification of many additional active oligomers for research and therapeutic applications.

INTRODUCTION

Iterative rounds of designs and testing by chemists at ISIS Pharmaceuticals led to the advent of single-stranded small-interfering RNA (ss-siRNA), which incorporates well-known chemical modifications such as 2'-fluoro/2'-*O*-methyl-ribonucleotides in an alternating pattern and phosphorothioate linkage at every other base (Lima et al., 2012). It is remarkable that despite heavy modifications to confer properties such as nuclease resistance (for review, see Watts et al., 2008) and the complete absence of a passenger strand, the end product can still function nearly as well as a conventional siRNA. Nonetheless, as discussed in the previous chapter, ss-siRNAs do not always behave identically to their dsRNA counterparts. For instance, siRNA duplex REP, which has full complementarity against poly-CAG, is a poorly selective compound, whereas ss-siRNA 537787, which also contains no mismatch in the sequence, possesses an allele-selectivity of greater than 13-fold. Such instances of differential behaviors imply that rules governing the design of unmodified duplex siRNA do not always apply to ss-siRNA. To gain better understanding, we synthesized and characterized additional ss-siRNAs to expand the repertoire of available active oligomers and to compile a set of guidelines for future ss-siRNA designs.

A large body of literature exists on the sequence and structural requirement for designing canonical duplex siRNAs. For instance, the first systematic analysis of siRNA structural elements showed that 21-nt with 3'-overhang of two nucleotides (preferably of TT or UU) is optimal in inducing gene knockdown, with complete tolerance of deoxyribose substitutions at the over-hangs (Elbashir et al., 2001b). Furthermore, a 5'-phosphate was required for siRNA activity (Nykänen et al., 2001), while synthetic siRNAs are rapidly phosphorylated in cells and thus do not need pre-phosphorylation at 5'-terminus (Elbashir et al., 2001b).

In parallel to dsRNA, albeit much more limited in scope, a few SAR observations were made on ss-siRNAs during their initial design steps at ISIS Pharmaceuticals and subsequent testing both at ISIS and in our laboratory: i) 5'-phosphate is sufficient for gene repression in cell cultures but is unstable *in vivo*, which can be improved by using a 5'-(*E*)-vinylphosphonate modified thymidine; ii) a 3'-dinucleotide overhang of two nucleotides (purines in particular) enhanced *in vitro* potency by several fold; iii) a hetero-duplex made by re-annealing CAG-targeting ss-siRNA with an unmodified passenger strand neither improved nor hindered HTT inhibition; iv) single-base mutations are tolerated throughout the sequence except at position 6, which abolished all activities against HTT (Lima et al., 2012; Yu et al., 2012). Taken together, these results suggest that 5'- and 3'-terminal chemistries are important in determining stability, that position 6 is particularly sensitive for RNAi engagement, and that passenger strand is dispensable to CAG-targeting ss-siRNA functions.

Although these observations provided a framework for understanding ss-siRNA mechanism, a number of outstanding questions still remain. It is unclear as to what determines cleavage- versus non-cleavage-mediated repression by ss-siRNA, how oligomeric length affects RISC-loading, and how well ss-siRNAs tolerate random mutations and additional chemical modifications. To answer these questions, we manipulated sequence and structural features of ss-siRNAs and examined their effects on ss-siRNA activity.

RESULTS

ss-siRNAs with Full Complementarity Can Degrade Target mRNA

Mechanistic studies presented in Chapter 1 suggested that CAG-targeting ss-siRNA inhibited HTT expression by RISC-mediated translational repression. On the other hand, it was demonstrated by our colleagues at ISIS Pharmaceuticals that many ss-siRNAs are fully capable of reducing mRNA levels (Lima et al, 2012). To establish what determines whether an ss-siRNA goes through a cleavage-dependent or independent process, we first tested the ability of ss-siRNA 537787, which contains no mismatch in its CAG-targeting sequence, to reduce target transcript level. Data obtained by qPCR from biological replicates showed that 537787 did not appreciably decrease *HTT* mRNA level (Figure 2-1). Consistent with its inability to induce cleavage, 537787 exhibited significant allele-selectivity at the HTT protein level (Chapter 1, Figure 1-2A), in contrast to the unmodified siRNA duplex REP that indiscriminately inhibited both mutant and wild-type HTT proteins and reduced *HTT* mRNA (Hu et al., 2010). This result suggests that the degree of sequence complementarity alone is insufficient to predict an ss-siRNA's ability as a slicer.

Using *PTEN* as an alternative target gene, we replicated and expanded findings by Lima and colleagues (Lima et al., 2012) in a HD-patient-derived fibroblast cell-line (GM04281). By qPCR and western blot, *PTEN* mRNA and protein levels were decreased by ss-siRNA 522247, which targets sequence with *PTEN* exon 9 with full complementarity (Figure 2-2). RNA immunoprecipitation (RIP) assay with primers against exon 1 of *PTEN* revealed a negligible degree of enrichment of Ago2, suggesting that most recruitment of ss-siRNA-loaded Ago2 to *PTEN* mRNA probably results in rapid substrate cleavage and turnover, therefore minimizing long-lasting association that would be captured by RIP. In contrast, CAG-targeting ss-siRNAs

(Chapter 1, Figure 1-7B) induce strong enrichment of Ago2 to the target transcript (Chapter 1, Figure 1-7B), indicating a much more stable association between RISC complexes and *HTT* mRNA that mimics an miRNA-mediated translational repression without transcript cleavage.

To test if such a non-cleavage mediated process is restricted to ss-siRNAs that target expanded triplet-repeats, we designed and tested ss-siRNA 581446 that has full sequence complementary against *HTT* exon 2 outside and downstream of the poly-CAG stretch. ss-siRNA 581446 reduced HTT protein level with IC_{50} of ~15 nM and displayed little to no allele selectivity (Figure 2-3). Importantly, qPCR data showed a dose-dependent decrease in *HTT* mRNA level that closely tracked changes at the protein level, indicating that HTT inhibition by 581446 occurred by mRNA degradation.

Compared to its corresponding unmodified duplex BBRC (IC_{50}: ~ 1nM), 581446 is >10-fold less potent (Figure 2-4A), likely due to its chemical modifications that in this particular case might impair efficient Ago-loading. At higher concentrations, ssRNA and duplex siRNA achieved similarly potent *HTT* reduction at both mRNA and protein levels (Figure 2-4B). These results indicate that like canonical siRNA duplexes, ss-siRNAs likely function through standard mRNA cleavage and degradation pathways, while triplet-repeat-targeting oligomers constitute a unique class of siRNAs that do not cleave target transcripts. This lack of "slicer" activity affords them the advantage of allele-selective gene targeting by preferential translational suppression of the CAG-expanded mutant mRNA.

ss-siRNA Needs a Minimum Length of 17-nt to Retain Activity

Double-stranded siRNA generated from long dsRNA processing in mammalian cells are 21-23 nt in length (Elbashir et al., 2001a; Zamore et al., 2000). Length has long been known to

be important in synthetic siRNA design, as earlier studies had shown that dsRNAs longer than 30 base-pairs activate mammalian interferon response and result in non-specific mRNA degradation and global arrest in protein synthesis (Stark et al., 1998), an outcome that can be bypassed with using 21-nt-long dsRNA (Elbashir et al., 2001a).

Previous work in our lab with CAG-targeting antisense oligonucleotide (ASO) analogs such as peptide nucleic acid (PNA) demonstrated that considerable variations in oligomer length were tolerated, as PNAs ranging from 13- to 19-nt long displayed similar potencies and allele-selectivities against mutant HTT (Hu et al., 2009). However, the degree of CAG-targeting ss-siRNA to accommodate length variations is unknown, as longer or shorter ssRNA could potentially perturb Ago loading and RISC assembly. One study showed that asymmetric shorter-duplex siRNAs (generated by shortening the passenger strand by up to six nucleotides) were able to efficiently trigger gene silencing (Chang et al., 2009); however, the guide-strand was kept constant at 21-nt-long and thus it remained unclear whether Ago proteins could load shorter guide strand. Another group reported that 27-mer duplexes could silence EGFP reporter genes more efficiently than traditional 21-mers, but first through substrate-processing by Dicer into 21-mer siRNAs (Kim et al., 2005). More recently, Salomon and colleagues showed that dsRNAs ≥ 25nt with limited 2'-*O*-Me modifications were resistant to Dicer processing and were able to directly load into Ago2/RISC and induce mRNA cleavage (Salomon et al., 2010), thus providing preliminary evidence that increased siRNA length can be tolerated beyond the classical "19nt + 2" model.

To systematically study whether oligomer length constitutes a stringent requirement for ss-siRNA design, we obtained CAG-targeting, P9-mismatched ss-siRNAs that are progressively trimmed at the 3'-end, yielding a series of 15-20 nt long oligomers while keeping all other chemical modifications intact. The new ss-siRNAs were then tested for their abilities to inhibit

HTT expressions (Figure 2-5 and Table 2-1). Good potencies and selectivities were observed for 20-, 19-, 18- and 17-mers but with a trend of progressively decreasing activity with length (15-, 11-, 9- and 6-fold selectivity, respectively, compared to 29-fold for the "full-length", 21-mer 537775). Still shorter oligomers (16- and 15-mers) were largely inactive, likely resulting from their inability to load into Ago proteins. In agreement with this observation, unpublished data from our lab had shown that 15-bp dsRNA targeting CAG-repeats did not inhibit HTT.

These results also argue against direct mRNA binding by ss-siRNAs as a primary mechanism. Such ASO-like property, if it were to exist, would not be so dramatically affected by length constraints, as was shown from PNA studies where 13-mer remained highly active (Hu et al., 2010). This conclusion is further supported by noting that certain ss-siRNAs (e.g., 557426) are very potent HTT inhibitors despite having up to three central mismatches. Compared to ss-siRNA 537787 of full complementarity, 557426's melting temperature (after pairing with an unmodified passenger strand) is reduced by up to 20°C (Chapter 1, Table 1-1), which implied much weaker binding and annealing to the target mRNA and therefore significantly compromised potency if direct association were a major mechanistic contributor.

ss-siRNAs with Three to Four But Not Five Random Mismatched Bases Are Active

Several studies had reported that single- and double-base-pair mismatches can be tolerated within siRNA sequences without appreciable loss of activity (Amarzguioui et al., 2003; Du et al., 2005; Huang et al., 2009; Dua et al., 2011). At the same time, it is well-known that miRNAs only require limited target complementarity (except in the 2-8 nt "seed sequence", Lewis et al, 2005; Xie et al, 2005) to achieve effective reduction of their endogenous targets.

Data from screening over 20 CAG-targeting ss-siRNAs showed that many different sets of mismatches were tolerated without noticeable loss of activity (Chapter 1, Table 1-1), thus pointing to a large potential design space for additional HTT inhibitors. Four ss-siRNAs were designed and synthesized that contained between three and five mismatches outside of the predicted "seed region" but otherwise scattered throughout the sequence. Two of the four oligomers, 577138 and 577139 that contain three and four mismatched bases, respectively, were active compounds, with IC_{50} values around 20nM and selectivities greater than 4-6 fold (Figure 2-6 A-C). The other two ss-siRNAs, 577140 and 577141, contained five mismatches each and did not show any activity (Figure 2-6D and E).

While these values are less impressive compared to benchmark siRNAs such as P9 and 537775, it should be noted that even such a random set of sequences yielded a 50% hit-rate in terms of identifying new allele-selective inhibitors of HTT. Given that > 10,000 different sequences can be generated by allowing up to three mismatched bases throughout the sequence without altering the seed region (a caution that may not be necessary, as we saw from Chapter 1 that only P6 abolished all activity), a sizeable number of candidate active inhibitors likely exist. This expanded repertoire may become important as we search for sequences with minimal off-target effects and cytotoxicity.

Lipid-Modified ss-siRNAs Retained High Potency But Did Not Enable Direct Cellular Uptake

In our cell-culture-based experiments, ss-siRNAs have been introduced using lipid-based transfection reagents. When added alone without formulation, ss-siRNA treatment did not inhibit HTT expression even at extremely high concentrations (unpublished data), indicating poor

cellular uptake. When complexed with PepMute^{TM} (SignaGen Laboratories), a non-lipid based transfection reagent mimicking a viral cell-penetrating peptide (CPP), three active ss-siRNAs displayed no HTT inhibition, suggesting little to no CCP-mediated ss-siRNA uptake (Figure 2-7). Interestingly, unmodified duplex siRNAs P910 (which targets CAG repeats) and BBRC (which targets HTT outside of poly-CAG) both showed good inhibition under the same experimental conditions (Figure 2-7D). These data suggest that alternative transfection techniques such as PepMute have differential effects on duplex versus modified ss-siRNAs, further highlighting differences between the two classes of nucleic acids.

When infused as simple saline formulation *in vivo*, ss-siRNA 537775 displayed good inhibitory activity against HTT across many parts of the CNS (Yu et al, 2012). It has been known for some time that *in vivo* administered siRNAs can be efficiently taken up both locally and systemically in organs such as the liver to achieve gene knockdown through a yet uncharacterized process (Kordasiewicz et al., 2012). Thus, *in vitro* cell uptake may be achieved while *in vivo* uptake may be enhanced in the absence of formulations if ss-siRNAs are modified with certain chemistries.

To test this theory, we treated HD fibroblasts with lipid-modified ss-siRNAs that are identical to 537775 (i.e., with mismatched base at position 9) except for having a palmitic acid (C16:0) attached at nucleotide position 6, 8, or 12. When added to cells with regular transfection reagent, all three oligomers are active and allele-selective inhibitors of HTT (Figure 2-8), with 573309 (mismatch at P9, lipid at P6) displaying a mutant IC_{50} at 1.4 nM and selectivity > 30-fold, equaling the values of benchmark siRNAs P9 and 537775. The ss-siRNA 573312 (mismatch at P9, lipid at P8) exhibited a mutant IC_{50} of 2.8 nM and selectivity > 13-fold, and 573310 (mismatch at P9, lipid at P12) had the least optimal profile of the three, with mutant IC_{50} at 6.2 nM and selectivity of ~ 4-fold. These data indicate that attaching a bulky lipophilic group

at positions P6 and P8 is highly tolerated while some loss of potency is seen when attachment is made at P12. Of note, P6 and P8 are both within the predicted seed sequence of the oligomer, yet they exhibit no ill effect on ss-siRNAs' activity, suggesting that rules for regular miRNA design cannot be blindly applied to CAG-targeting ss-siRNAs.

To determine if lipid-modification alone was sufficient to confer cellular uptake, 573309, 573312, and 573310 were added to cells in the absence of transfection formulations. Little to no inhibition was seen, even at concentrations up to 4 uM (Figure 2-9). These data suggest that at least under the cell-culture conditions, palmitatoylation is insufficient to enable ss-siRNA delivery and cellular uptake. Nonetheless, it does not rule out the possibility that other lipid modifiers could achieve autonomous, transfection-free delivery or that palmitatoylation could enhance cellular uptake *in vivo*. Collectively, the results demonstrate that bulky chemical groups can be tolerated at multiple positions without compromising RNAi efficiency and help open new possibilities to attachment of additional chemical groups.

DISCUSSION AND FUTURE DIRECTIONS

Data from targeting multiple gene sequences suggest that most ss-siRNAs achieve gene inhibition by the canonical mRNA cleavage and degradation pathway, and that CAG-targeting ss-siRNAs seem to be an exception to the rule. Nonetheless, it is far from certain whether CAG-targeted ss-siRNAs are the only ss-siRNAs to exert translational repression. In fact, the chemical modifications of ss-siRNA could in theory enable more stable association of RISC to the mRNA transcript and induce translational arrest prior to or in conjunction with mRNA decay, especially if mismatches are present that interfere with Ago2-cleavage but not with transcript binding. It would be interesting to introduce mismatches within the sequences of 522247 (targets PTEN) and 557426 (BBRC equivalent that targets HTT) to see if there is loss of mRNA reduction with persistent protein reduction, which could then be explained by a new or enhanced contribution from translational repression in the context of compromised mRNA cleavage.

In screening CAG-targeting ss-siRNAs for active HTT inhibitors, it was discovered that a single-mismatch at position 6 destroyed all activity. Whether this nucleotide position is uniquely sensitive in poly-CAG recognition or whether it serves as a general requirement for ss-siRNAs is unknown. Mutating position 6 on the available active ss-siRNAs would determine if their activities are similarly abolished. On the other hand, the seed sequence (nt 2-8) complementarity, a well-known determinant of natural miRNA efficiency (Lewis et al, 2005; Xie et al, 2005), did not seem to matter significantly other than at position 6. Testing for the seed sequence requirement in non-CAG-targeting oligomers would clarify whether it plays the same important role in ss-siRNA functions as it does for miRNAs.

Data on lipid-modified oligomers demonstrated that the ss-siRNA chemistry template is sufficiently robust and flexible to tolerate chemical group attachments at various positions. As a

result, many potential applications are possible. For example, attaching a biotin tag would enable biochemical identification and study of ss-siRNAs' interacting partners (see Chapter 3). Cell-type specific delivery may also be achievable by attaching established moieties such as peptide ligands that are recognized by cell-lineage-specific surface receptors. Alternative approaches to lipid-free cellular uptake may be achieved with other appendages such as spermine-conjugate (Gagnon et al, 2011). Finally, if coupled to a nuclear-localization signal, ss-siRNA may be targeted to the nucleus for nuclear-specific events such as splicing (Liu et al, 2012).

The particular chemistry adopted for ss-siRNA is the result of testing permutations and combinations of many known modifications until both RNAi efficiency and metabolic stability are achieved. However, there is no reason to believe that this is the only viable chemistry for ss-siRNA design. Future SAR studies should examine additional chemical modification patterns to try and identify alternative designs that may be simpler, cheaper, less toxic, and more potent in cellular uptake and/or gene inhibition.

MATERIALS AND METHODS

ss-siRNA, antibodies, cell culture and transfection, analysis of HTT expression, IC_{50} and selectivity calculations, q-PCR, RNA immunoprecipitation

Most materials and protocols are identical to those used for Chapter 1 and may be referenced accordingly. Additional ss-siRNAs were synthesized by Isis Pharmaceuticals Inc. (Carlsbad, CA, USA) (Lima et al., 2012) and reconstituted in nuclease-free water. 100 μM stocks were maintained for long-term storage and 20 μM stocks are used for transfections. All concentrations were verified by UV spectrometry. An additional antibody not described before is the mouse monoclonal anti-PTEN antibody sc-7974 (clone A2B1), purchased from Santa Cruz and diluted 1:1000 for western studies. For *PTEN* q-PCR studies, the primer pair has the following sequences: 5'- CAGCCATCATCAAAGAGATCG -3' (forward primer) and 5'-TTGTTCCTGTATACGCCTTCAA-3' (reverse primer) (Agrawal and Eng, 2006). Non-lipid-mediated transfection with PepMute™ (SignaGen Laboratories) was performed per manufacturer instructions and otherwise using the same serial dilution scheme as RNAiMax-mediated transfection. Lipid-free ss-siRNA treatment of HD fibroblast was identical to the standard transfection protocol described in Chapter 1 except that no RNAiMax or other transfection reagent was added to the final reaction mixture prior to serial dilution.

REFERENCES

Agrawal, S. and Eng, C. (2006) Differential expression of novel naturally occurring splice variants of PTEN and their functional consequences in Cowden syndrome and sporadic breast cancer. Hum Mol Genet. *15*, 777-87

Amarzguioui, M., Holen, T., Babaie, E., and Prydz, H. (2003). Tolerance for mutations and chemical modifications in a siRNA. Nucleic Acids Res. *15*, 589-95.

Chang, C.I., Yoo, J.W., Hong, S.W., Lee, S.E., Kang, H.S., Sun, X., Rogoff, H.A., Ban, C., Kim, S., Li, C.J., and Lee, D. (2009) Asymmetric shorter-duplex siRNA structures trigger efficient gene silencing with reduced non-specific effects. Molecular Therapy. *17*, 725-732.

Dua, P., Yoo, J.W., Kim, S., and Lee, D.K. (2011). Modified siRNA structure with a single nucleotide bulge overcomes conventional siRNA-mediated off-target silencing. Mol. Ther. *19*, 1676-87.

Du, Q., Thonberg, H., Wang, J., Wahlestedt, C., and Liang, Z. (2005). A systematic analysis of the silencing effects of an active siRNA at all single-nucleotide mismatched target sites. Nucleic Acids Res. *33*, 1671-7.

Elbashir, S.M., Harborth, J., Lendeckel, W., Yalcin, A., Weber, K., and Tuschl, T. (2001a). Duplexes of 21-nucleotide RNAs mediate RNA interference in mammalian cell culture. Nature *411*, 494–498.

Elbashir, S.M., Martinez, J., Patkaniowska, A., Lendeckel, W., and Tuschl, T. (2001b). Functional anatomy of siRNAs for mediating efficient RNAi in *Drosophila melanogaster* embryo lysate. EMBO J. *20*, 6877–6888.

Gagnon, K.T., Watts, J.K., Pendergraff, H.M., Montaillier, C., Thai, D., Potier, P., and Corey, D.R. (2011) Antisense and antigene inhibition of gene expression by cell-permeable oligonucleotide-oligospermine conjugates. J Am Chem Soc. *133*, 8404-7

Hu, J., Matsui, M., Gagnon, K.T., Schwartz, J.C., Gabillet, S., Arar, K., Wu, J., Bezprozvanny, I., and Corey, D.R. (2009). Allele-specific silencing of mutant huntingtin and ataxin-3 genes by targeting expanded CAG repeats in mRNAs. Nat. Biotech. *27*, 478-84.

Huang, H., Qiao, R., Zhao, D., Zhang, T., Li, Y., Yi, F., Lai, F., Hong, J., Ding, X., Yang, Z., Zhang, L., Du, Q., and Liang, Z. (2009). Profiling of mismatch discrimination in RNAi enabled rational design of allele-specific siRNAs. Nucleic Acids Res. *37*, 7560-9.

Kim, D.H., Behlke, M.A., Rose, S.D., Chang, M.S., Choi, S., and Rossi, J.J. (2005). Synthetic dsRNA Dicer substrates enhance RNAi potency and efficacy. Nature Biotech. *23*, 222-226.

Kordasiewicz, H.B., Stanek, L.M., Wancewicz, E.V., Mazur, C., McAlonis, M.M., Pytel, K.A., Artates, J.W., Weiss, A., Cheng, S.H., Shihabuddin, L.S., Hung, G., Bennett, C.F., and

Cleveland, D.W. (2012). Sustained Therapeutic Reversal of Huntington's Disease by Transient Repression of Huntingtin Synthesis. Neuron. *74*, 1031-44.

Lewis, B.P., Burge, C.B., and Bartel, D.P. (2005) Conserved seed pairing, often flanked by adenosines, indicates that thousands of human genes are microRNA targets. Cell. *120*, 15-20.

Lima, W.F., Prakash, T.P., Murray, H.M., Kinberger, G.A., Li, W., Chappell, A.E., Li C.S., Murray, S.F., Gaus, H., Seth, P.P., Swayze, E.E., and Crooke, S.T. (2012) Single-stranded siRNAs Activate RNAi in Animals. Cell, *150,* 883-94

Liu, J., Hu, J., and Corey, D.R. (2012). Expanding the action of duplex RNAs into the nucleus: redirecting alternative splicing. Nucleic Acids Res. *40,* 1240-50.

Nykänen, A., Haley, B., and Zamore, P.D. (2001). ATP requirements and small interfering RNA structure in the RNA interference pathway. Cell. *107*, 309–321.

Salomon, W., Bulock, K., Lapierre, ., Pavco, P., Woolf, T., and Kamens, J. (2010). Modified dsRNAs that are not processed by Dicer maintain potency and are incorporated into the RISC. Nucleic Acids Res. *38*, 3771-3779.

Stark, G.R., Kerr, I.M., Williams, B.R., Silverman, R.H., and Schreiber, R.D. (1998) How cells respond to interferons. Annu Rev Biochem.*67*, 227-64

Watts, J.K., Deleavey, G.F., and Damha, M.J. (2008). Chemically modified siRNA: tools and applications. Durg Discov Today. *13*, 842-55

Xie, X., Lu, J., Kulbokas, E.J., Golub, T.R., Mootha, V., Lindblad-Toh, K., Lander, E.S., and Kellis., M. (2005) Systematic discovery of regulatory motifs in human promoters and 3' UTRs by comparison of several mammals. Nature. *434*, 338-45.

Yu, D., Pendergraff, H., Liu, J., Kordasiewicz, H., Cleveland, D.W., Swayze, E.E., Lima, W.F., Crooke, S.T., Prakash, T.P., and Corey, D.R. (2012) Single-Stranded RNAs Use RNAi to Potently and Allele-Selectively Inhibit Mutant Huntingtin Expression. Cell. *150,* 895-908

Zamore, P. D., Tuschl, T., Sharp, P. A., and Bartel, D. P. (2000) RNAi: Double-stranded RNA directs the ATP-dependent cleavage of mRNA at 21 to 23 nucleotide intervals. Cell. *101*, 25-33

Figure 2-1

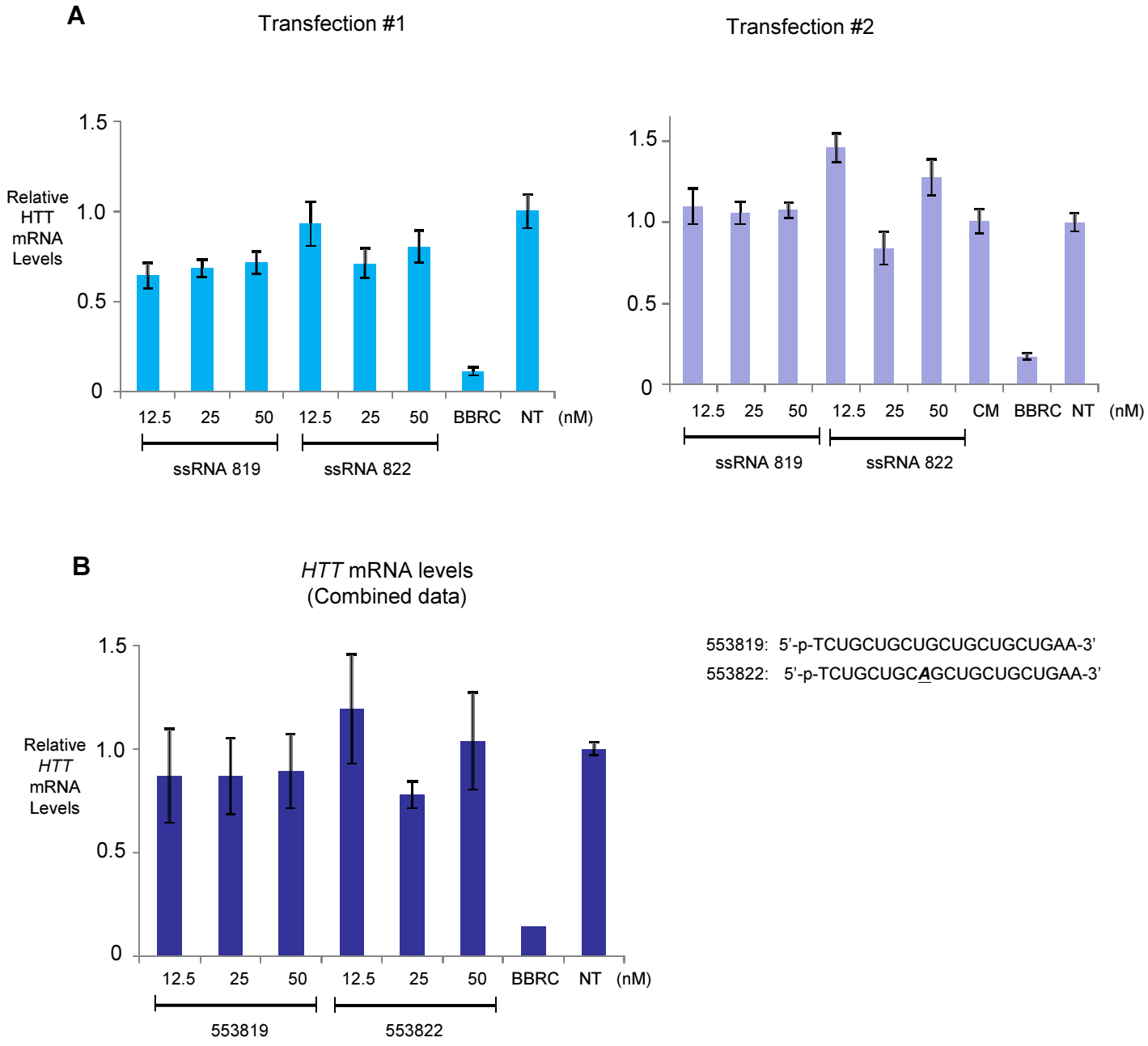
A
Transfection #1
Transfection #2
Relative HTT mRNA Levels
1.5
1.0
0.5
0
12.5 25 50 12.5 25 50 BBRC NT (nM)
ssRNA 819
ssRNA 822
12.5 25 50 12.5 25 50 CM BBRC NT (nM)
ssRNA 819
ssRNA 822
B
HTT mRNA levels
(Combined data)
Relative HTT mRNA Levels
12.5 25 50 12.5 25 50 BBRC NT (nM)
553819
553822
553819: 5'-p-TCUGCUGCUGCUGCUGCUGAA-3'
553822: 5'-p-TCUGCUGCAGCUGCUGCUGAA-3'

Figure 2-1 . ***HTT* mRNA is not reduced by ss-siRNA in HD fibroblasts:** No reduction is seen in *HTT* mRNA despite robust knockdown at protein level upon ss-siRNA treatment. (A) and (B) are results from two independent experiments; (C) is the combined data.

553819: ssRNA with no mismatch; 553822: ssRNA with P9 mismatch; CM: mismatched control; BBRC: positive siRNA control; NT: no treatment. Error bars in (A) are standard deviation (SD) from technical replicates. Error bars in (B) are standard error of the mean (SEM) from biological replicates. All CM treatments in this chapter were done at 50nM unless otherwise described.

Figure 2-2

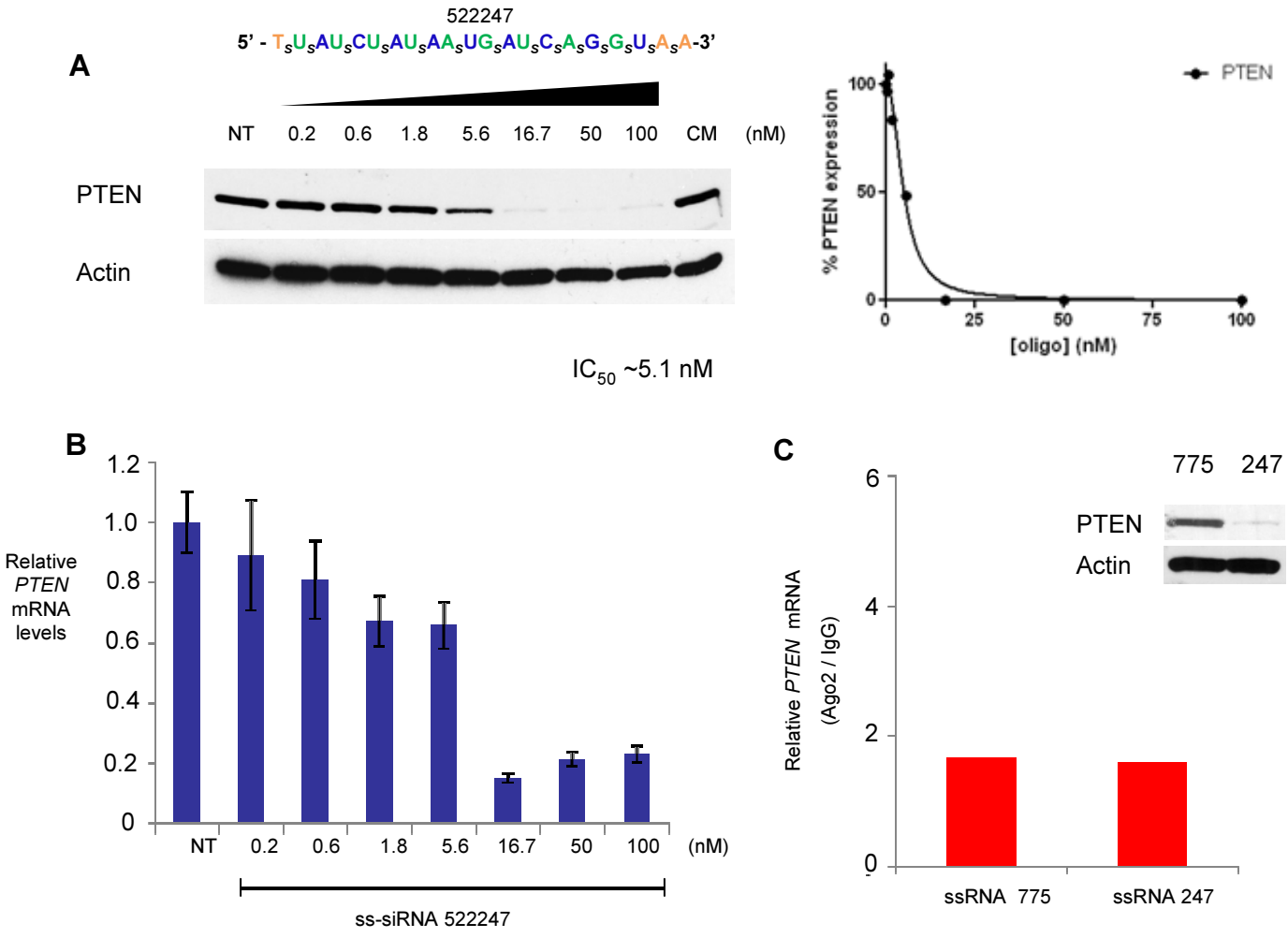

Figure 2-2. ***PTEN* protein and mRNA levels were concomitantly reduced upon ss-siRNA 522247 treatments in 69-repeat fibroblasts:** (A) Levels of PTEN protein by western blotting (left) and its quantification (right); (B) Levels of *PTEN* mRNA by qPCR with primers targeting within exon 1 of *PTEN*; (C) RNA immunoprecipitation (RIP) with anti-Ago2 antibody revealed no enrichment of Ago2 on *PTEN* mRNA.

522247: ssRNA targeting *PTEN*; CM: mismatched control; NT: no treatment. Error bars are standard deviation (SD) from technical replicates.

Figure 2-3

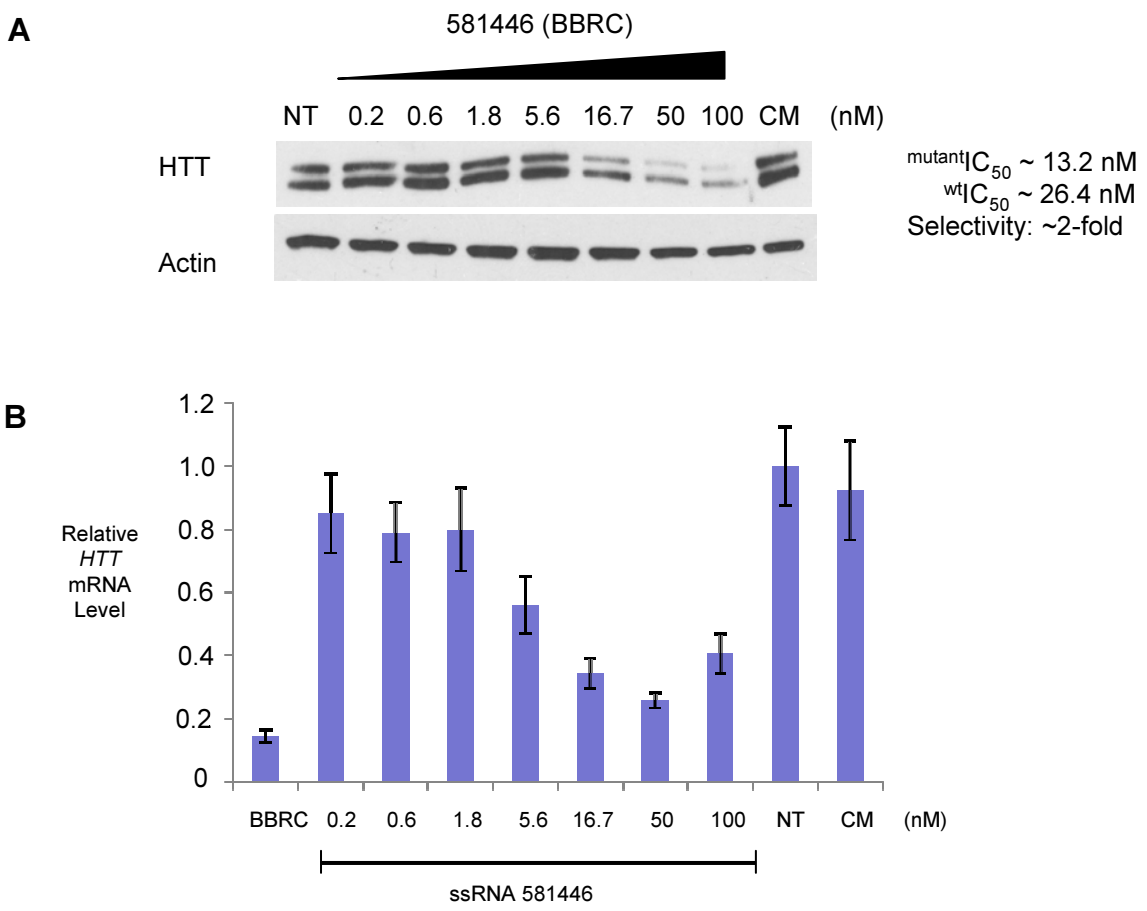

Figure 2-3. **ss-siRNA 581446 reduced *HTT* at both protein and mRNA levels:** Concomitant reductions are seen in *HTT* mRNA and protein levels upon ss-siRNA treatment. 581446: ssRNA targeting *HTT*'s coding region outside of CAG repeats; CM: mismatched control; NT: no treatment. qPCR was performed with primers targeting within exons 64/65 of *HTT*. Error bars are standard deviation from technical replicates.

Figure 2-4

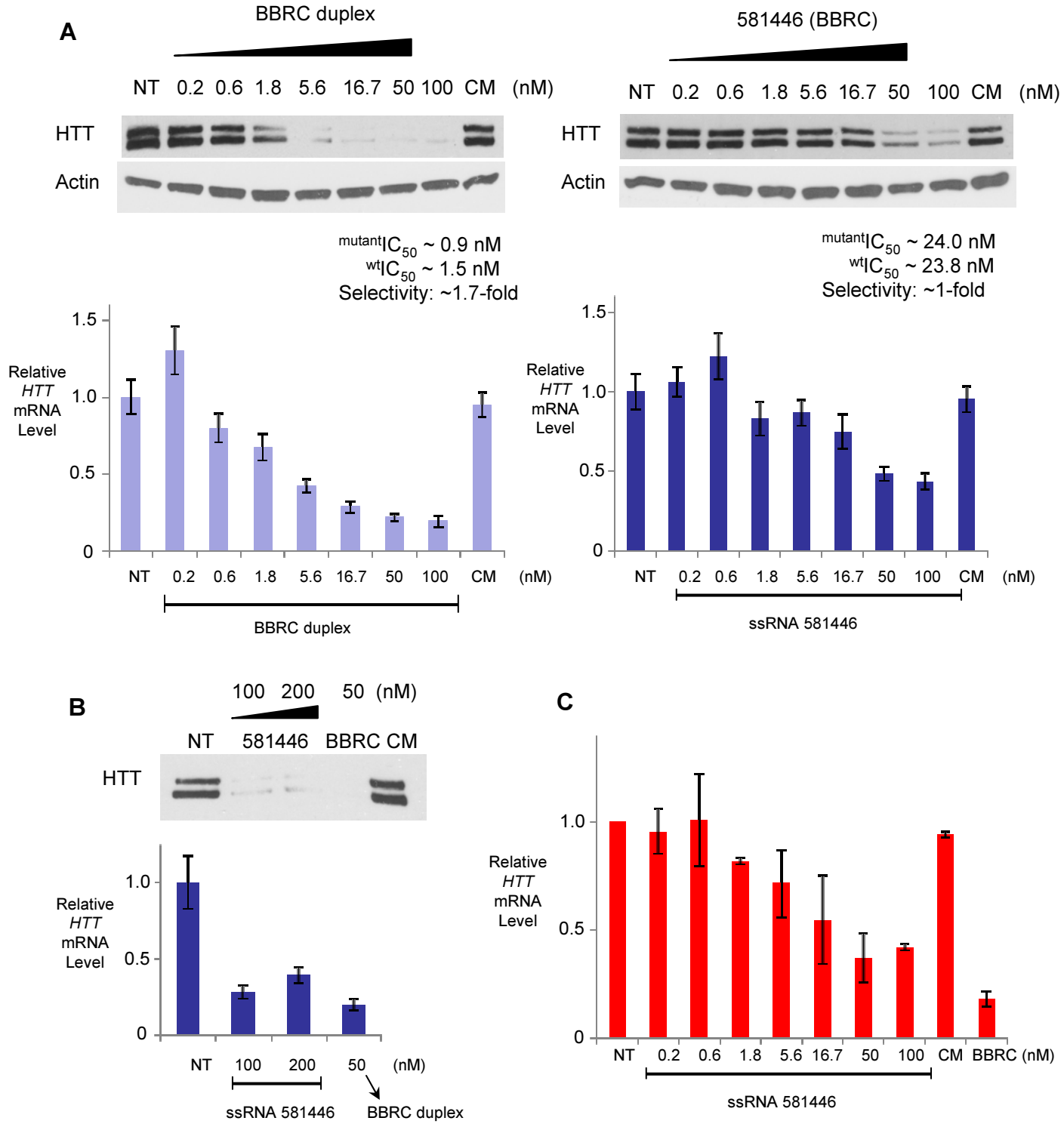
A
BBRC duplex
NT 0.2 0.6 1.8 5.6 16.7 50 100 CM (nM)
HTT
Actin
mutantIC50 ~ 0.9 nM
wtIC50 ~ 1.5 nM
Selectivity: ~1.7-fold
Relative HTT mRNA Level
1.5
1.0
0.5
0
NT 0.2 0.6 1.8 5.6 16.7 50 100 CM (nM)
BBRC duplex
581446 (BBRC)
NT 0.2 0.6 1.8 5.6 16.7 50 100 CM (nM)
HTT
Actin
mutantIC50 ~ 24.0 nM
wtIC50 ~ 23.8 nM
Selectivity: ~1-fold
Relative HTT mRNA Level
1.5
1.0
0.5
0
NT 0.2 0.6 1.8 5.6 16.7 50 100 CM (nM)
ssRNA 581446
B
100 200 50 (nM)
NT 581446 BBRC CM
HTT
Relative HTT mRNA Level
1.0
0.5
0
NT 100 200 50 (nM)
ssRNA 581446
BBRC duplex
C
Relative HTT mRNA Level
1.0
0.5
0
NT 0.2 0.6 1.8 5.6 16.7 50 100 CM BBRC (nM)
ssRNA 581446

Figure 2-4. **ss-siRNA 581446 is less potent than the unmodified BBRC duplex:**

(A) At the same concentrations, BBRC duplex is more potent than ss-siRNA 581446 in reducing *HTT* mRNA.

(B) At maximum dosages, both are able to potently reduce *HTT* mRNA.

(C) Combined data of two independent transfections by ss-siRNA 581446.

Error bars in (A-B) are standard deviation (SD) from technical replicates. Error bars in (C) are standard error of the mean (SEM) from biological replicates.

Figure 2-5

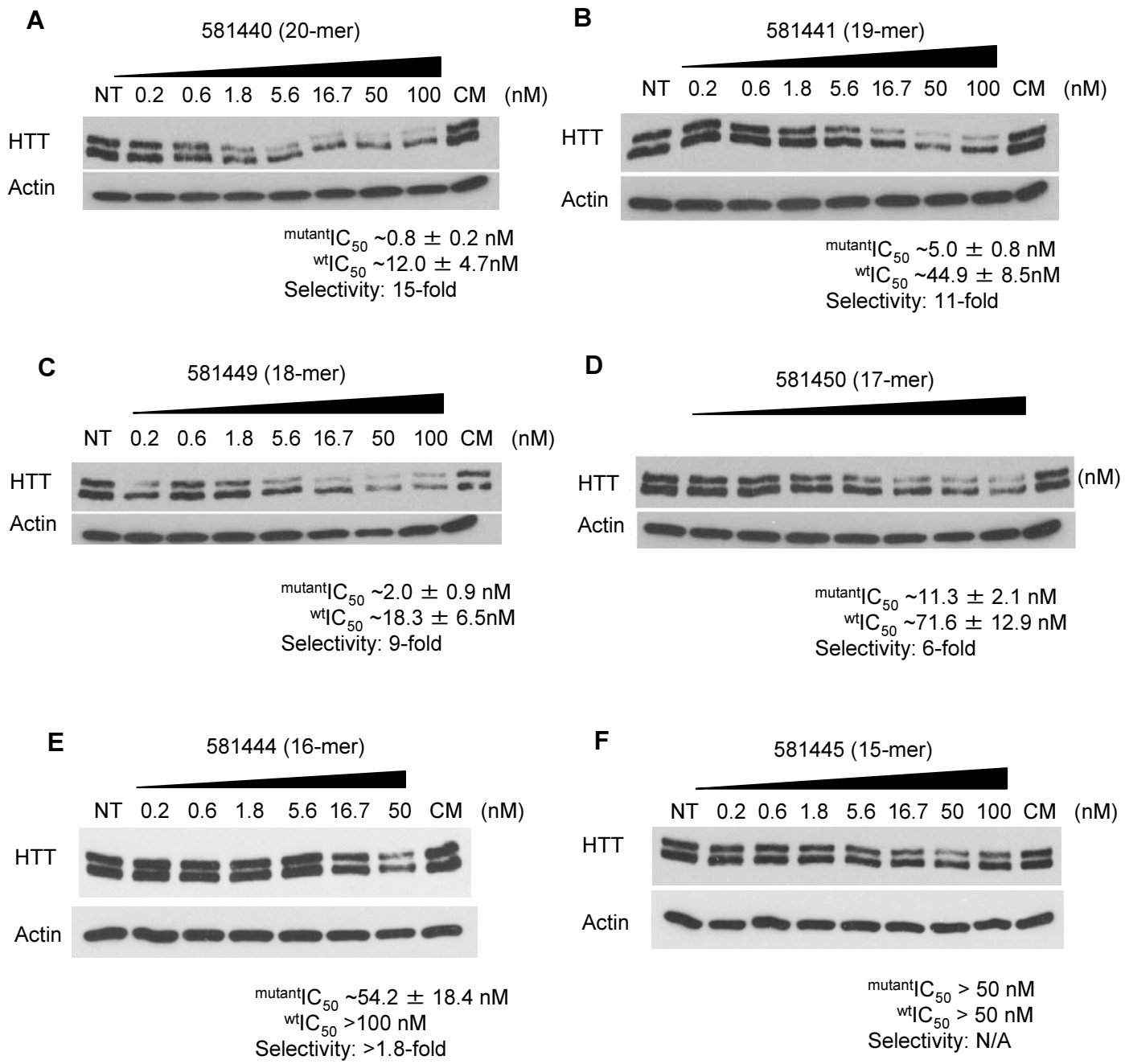

Figure 2-5. **Shorter ss-si-RNAs above 16-nt in length are active:** A panel of 15 to 20 nt long ss-si-RNAs were tested in HD-patient fibroblast cell-lines. All are active to some extent except 15- and 16-mer. CM: mismatched control; NT: no treatment. Error measurements are standard error of the mean (SEM) from biological replicates.

Table 2-1: Effects of ss-si-RNAs of progressively shorter length on HTT levels

ISIS No.	Length	Sequence	mut IC50 (nM)	WT IC50 (nM)	Selectivity (fold)	Tm* (in duplex)
553822	21	**5' - P-$T_sC_sUG_sCU_sGC_sA$G$_sCU_sGC_sU_sG_sC_sU_sG_sA_sA$-3'**	4.9 ± 0.8	90.4 ± 9.7	18	85
581440	20	**5' - P-$T_sC_sUG_sCU_sGC_sA$G$_sCU_sGC_sU_sG_sC_sU_sA_sA$-3'**	0.8 ± 0.2	12.0 ± 4.7	15	80-83
581441	19	**5' - P-$T_sC_sUG_sCU_sGC_sA$G$_sCU_sGC_sU_sG_sC_sA_sA$-3'**	5.0 ± 0.8	44.9 ± 8.5	11	79-82
581449	18	**5' - P-$T_sC_sUG_sCU_sGC_sA$G$_sCU_sGC_sU_sG_sA_sA$-3'**	2.0 ± 0.9	18.3 ± 6.5	9	75-78
581450	17	**5' - P-$T_sC_sUG_sCU_sGC_sA$G$_sCU_sGC_sU_sA_sA$-3'**	11.3 ± 2.1	71.6 ± 12.9	6	72-75
581444	16	**5' - P-$T_sC_sUG_sCU_sGC_sA$G$_sCU_sGC_sA_sA$-3'**	54.2 ± 18.4	> 100	> 1.8	70-74
581445	15	**5' - P-$T_sC_sUG_sCU_sGC_sA$G$_sCU_sGA_sA$-3'**	> 50	> 50	N/A	67-68

Error measurements are standard error of the mean (SEM) from biological replicates.

* Tm is measured on the heteroduplex formed by annealing ss-siRNA to an unmodified 21-mer RNA passenger strand.

Figure 2-6

A

ISIS No.	Mismatch position	Sequence	mut IC50 (nM)	WT IC50 (nM)	Selectivity (fold)	Tm (in duplex)
553822	9	**5' - P-$T_sC_sUG_sCU_sGC_sAG_sCU_sGC_sU_sG_sC_sU_sG_sA_sA$-3'**	4.9 ± 0.8	90.4 ± 9.7	18	85
577138	9, 10, 13	**5' - P-$T_sC_sUG_sCU_sGC_sAC_sCU_sCC_sU_sG_sC_sU_sG_sA_sA$-3'**	17.5	> 100	> 5.7	65-67
577139	9, 10, 13, 19	**5' - P-$T_sC_sUG_sCU_sGC_sAC_sCU_sCC_sU_sG_sC_sU_sC_sA_sA$-3'**	26.3	> 100	> 4	57-60
577140	9, 10, 13, 16, 19	**5' - P-$T_sC_sUG_sCU_sGC_sAC_sCU_sCC_sU_sC_sC_sU_sC_sA_sA$-3'**	65.6	> 100	> 1.5	59-63
577141	9, 10, 13, 16, 19	**5' - P-$T_sC_sUG_sCU_sGC_sAC_sCU_sCC_sU_sU_sC_sU_sU_sA_sA$-3'**	>100	> 100	N/A	63-64

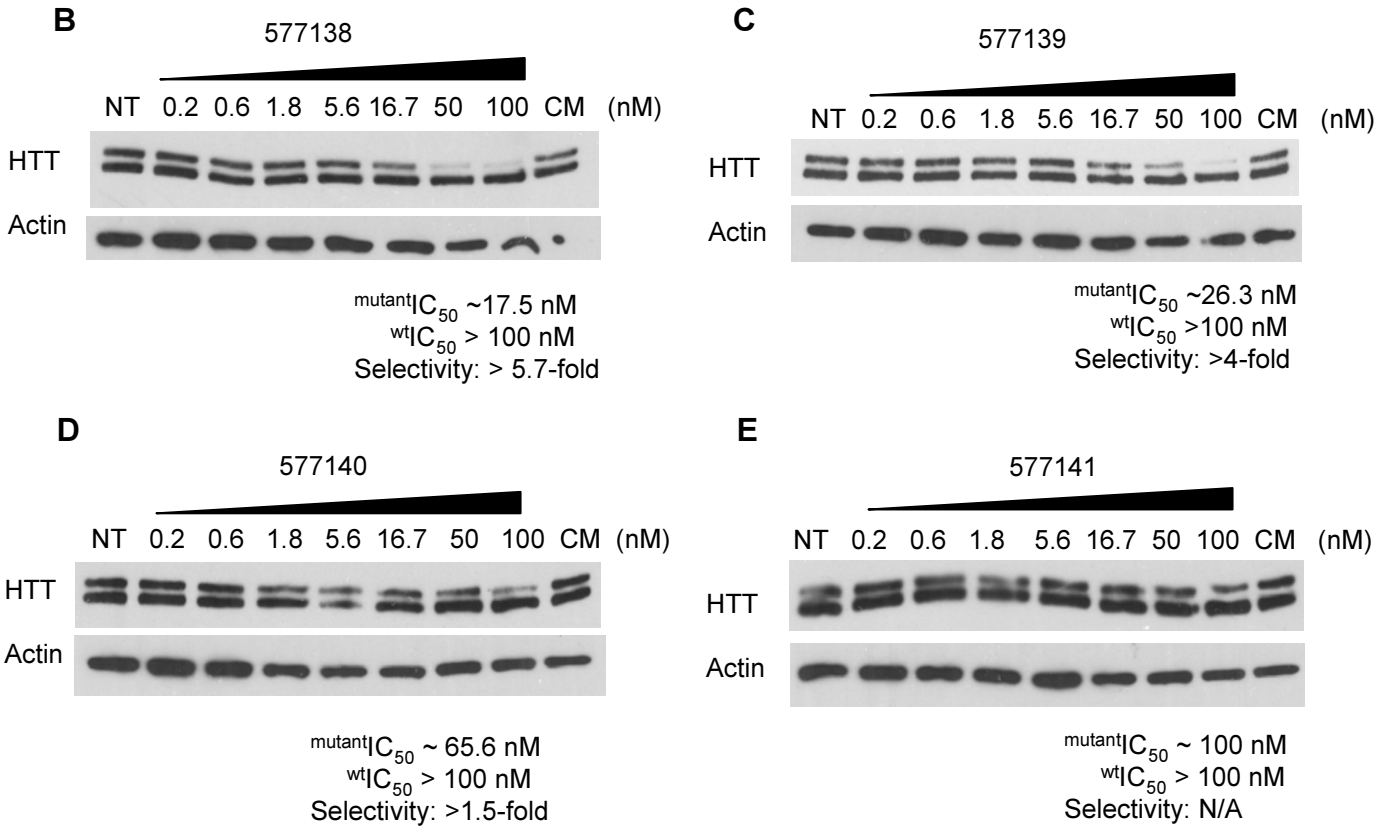

Figure 2-6. ss-si-RNAs of up to four but not five random mismatches combinations were active HTT inhibitors: (A) Sequence, Tm and IC_{50} information of the four ss-siRNAs tested; (B-E) Gel images of full-dose studies by western blot and quantitations. CM: a mismatched control RNA; NT: no treatment.

Figure 2-7

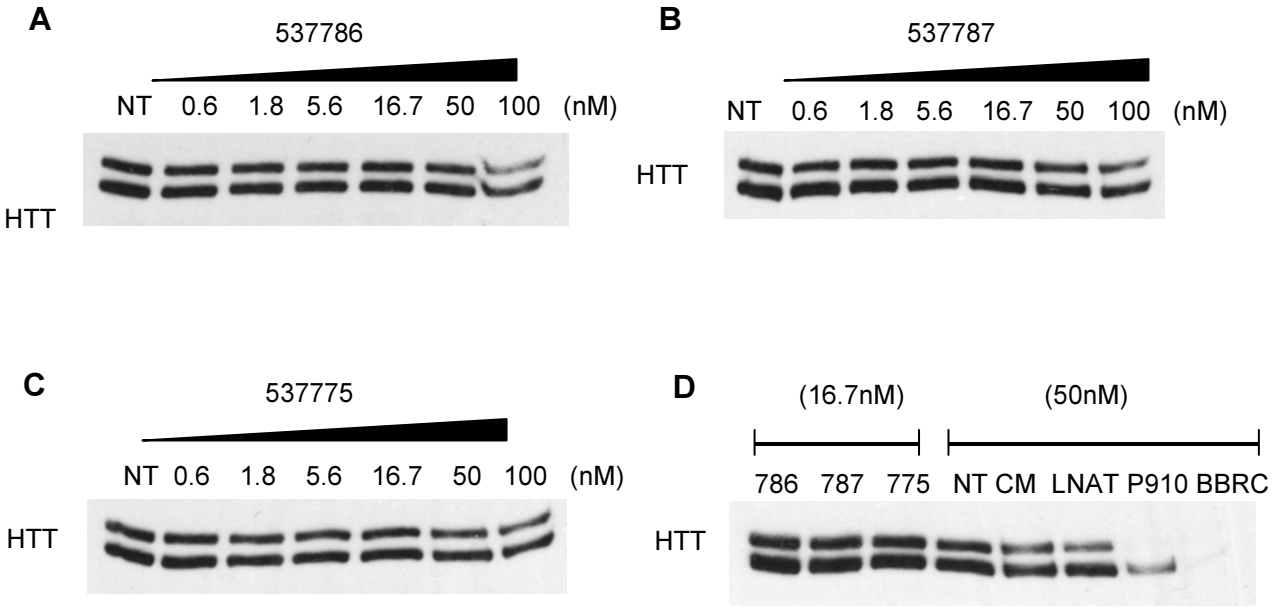

Figure 2-7. **ss-siRNAs formulated with PepMute™ reagents were inactive when added to HD-patient-derived fibroblasts.** PepMute™ (Invitrogen): a viral-peptide mimic transfection reagent; 537787: CAG-targeting ssRNA targeting with no mismatched base; 537775: CAG-targeting ssRNA targeting with mismatch at position 9; 537786: CAG-targeting ssRNA targeting with mismatch at position 10; LNAT: locked-nucleic acid-based ASO that targets CAG repeats; P910: unmodified duplex siRNA that targets CAG and has mismatches at positions 9 and 10; BBRC: unmodified duplex siRNA that targets outside of CAG repeat region; CM: mismatched control; NT: no treatment.

Figure 2-8

A

Isis # VinylP	AS -Sequence (5' to 3')
537775	5'-T_SC$_S$U$_S$G$_S$C$_S$U$_S$G$_S$C$_S$A$_S$G$_S$C$_S$U$_S$G$_S$C$_S$U$_S$G$_S$C$_S$U$_S$G$_S$A$_S$A-3'
573309	5'-T_SC$_S$U$_S$G$_S$C$_S$U$_{Sc16}$G$_S$C$_S$A$_S$G$_S$C$_S$U$_S$G$_S$C$_S$U$_S$G$_S$C$_S$U$_S$G$_S$A$_S$A-3'
573312	5'-T_SC$_S$U$_S$G$_S$C$_S$U$_S$G$_S$U$_{SC16}$A$_S$G$_S$C$_S$U$_S$G$_S$C$_S$U$_S$G$_S$C$_S$U$_S$G$_S$A$_S$A-3'
573310	5'-T_SC$_S$U$_S$G$_S$C$_S$U$_S$G$_S$C$_S$A$_S$G$_S$C$_S$U$_{SC16}$G$_S$C$_S$U$_S$G$_S$C$_S$U$_S$G$_S$A$_S$A-3'

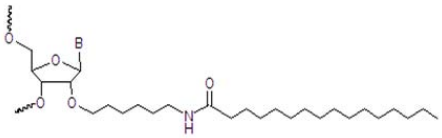

2'-F, 2'-*O*-Me, s = PS, 2'MOE, *T* = 5'-(*E*)-VinylP-2'-O-MOE

B

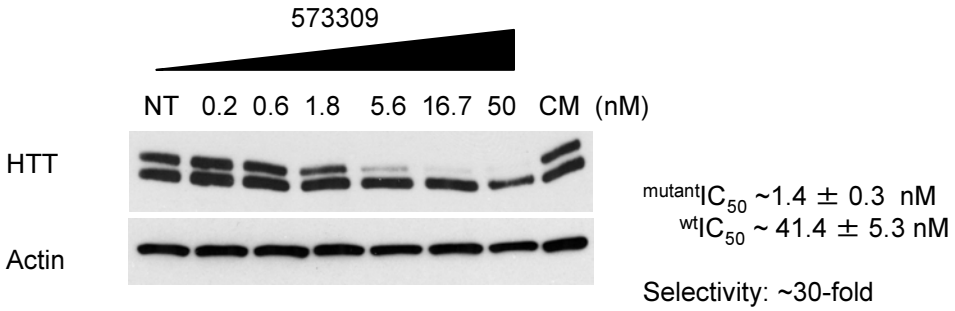

C

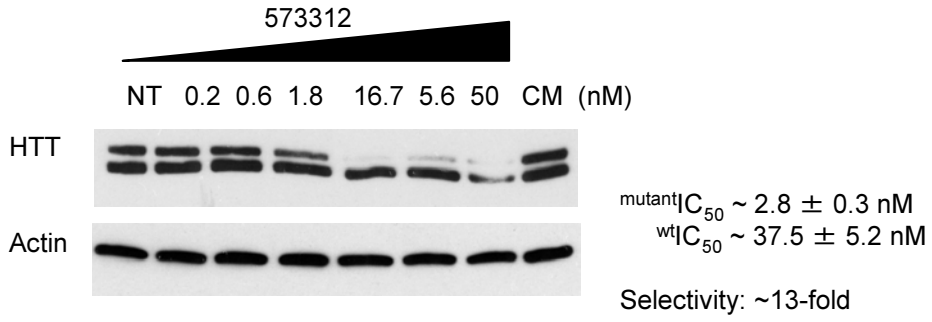

D

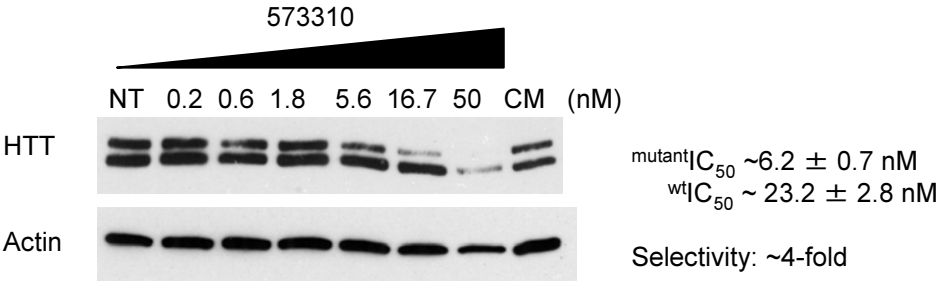

Figure 2-8. **Lipid-modified ss-siRNAs retained activity against HTT when conjugated with lipid-based transfection reagent:** (A) Sequences of the three lipid-conjugated ss-siRNAs tested; (B-D) Representative western gel images of each oligomer. CM: mismatched control; NT: no treatment. Transfections were performed with Lipofectamine™ RNAiMAX reagents. Error bars are standard error of the mean (SEM) from biological replicates.

Figure 2-9

A

Isis # VinvIP	AS -Sequence (5' to 3')
537775	5'-T_SC$_S$UG_SCU_SG$C_S$$\underline{A}$$G_SCU_SGC_SU_SGC_SU_SG_SA_S$A-3'
573309	5'–T_SC$_S$UG_SCU_{Sc16}G$C_S$$\underline{A}$$G_SCU_SGC_SU_SGC_SU_SG_SA_S$A-3'
573312	5'–T_SC$_S$UG_SCU_SG$U_{SC16}$$\underline{A}$$G_SCU_SGC_SU_SGC_SU_SG_SA_S$A-3'
573310	5'–T_SC$_S$UG_SCU_SG$C_S$$\underline{A}$$G_SCU_{SC16}GC_SU_SGC_SU_SG_SA_S$A-3'

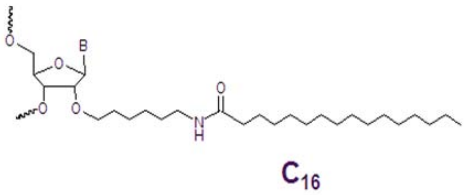

2'-F, 2'-*O*-Me, s = PS, 2'MOE, *T* = 5'-(*E*)-VinylP-2'-O-MOE T

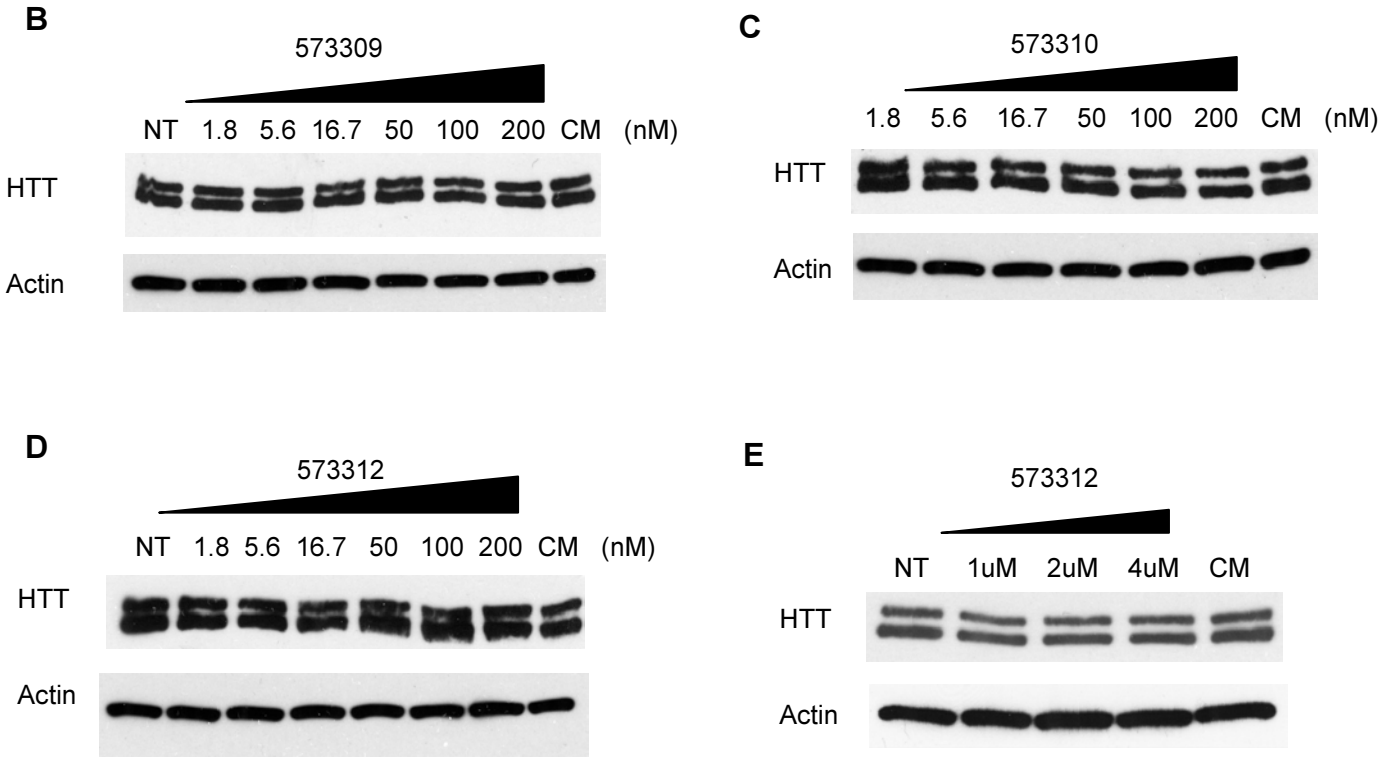

Figure 2-9. **Lipid-modified ss-siRNAs are inactive against HTT when added directly without transfecting reagents:** (A) Sequences of the three lipid-conjugated ss-siRNAs; (B-D) Representative western gel images of each oligomer. CM: mismatched control; NT: no treatment. All experiments were performed without transfecting reagents.

CHAPTER THREE

TNRC6/GW182 Family Proteins Are Required for HTT Inhibition by CAG-Targeting Single-Stranded and Duplex siRNAs

ABSTRACT

Both duplex CAG-targeting siRNAs and single-stranded siRNAs (ss-siRNAs) have been shown to be potent and allele-selective inhibitors of huntingtin (HTT). However, the mechanism by which they achieve inhibition is not well understood. Previous studies have established Ago2 as a central mediator in the process. To probe the involvement of other RNAi factors, we first performed pull-down assays with a biotinylated ss-siRNA and showed it to directly interact with Ago2 and GW182 inside cells and to efficiently load into Ago2 *in vitro*. Knock-down of RNAi factors Dicer and C3PO did not significantly affect HTT inhibition by either single-stranded or double-stranded siRNAs, suggesting that neither Dicer-assisted RISC-loading nor passenger-strand maturation is the rate-limiting step. In contrast, TNRC6/GW182 family proteins were required for HTT inhibition by CAG-targeting ss-siRNAs and duplex RNAs but dispensable for a cleavage-inducing siRNA. RNA immunoprecipitation (RIP) confirmed physical association between GW182 and *HTT* mRNAs upon treatment of active ss-siRNA and duplex siRNA. These results suggest a model in which TNRC6/GW182 family proteins function downstream of Ago2 to engage CAG-targeting duplex siRNAs and ss-siRNAs in a miRNA-like pathway and achieve translational inhibition of HTT.

INTRODUCTION

Since the discovery of RNA interference (RNAi) in *C. elegans* (Fire et al., 1998), tremendous progress has been made in characterizing the molecular players and mechanisms involved. RNAi in *C. elegans* was shown by northern blot to center on mRNA reduction (Montgomery et al., 1998; Ngo et al., 1998), and genetic screening for RNAi defective strains identified the PIWI-Argonaute-family gene *rde-1* as an essential gene (Tabara et al., 1999). Biochemical studies identified a class of short dsRNAs, ~25 nt long in plants (Hamilton and Baulcombe, 1999) and 21-23 nt long in *Drosophila* (Zamore et al., 2000) to be closely associated with silencing by RNAi. Aided by biochemical fractionation, these siRNAs were shown to be generated by the enzyme Dicer from longer dsRNA precursors (Bernstein et al., 2001), while the central engine of RNAi was revealed to be a nuclease complex termed RNA-induced silencing complex (RISC) (Hammond et al., 2000) with identification of its core factor Argonaute-2 (Ago2) shortly after (Hammond et al., 2001; Liu et al., 2004). While four Ago proteins exist in mammalian genome, only Ago2 catalyzes cleavage of mRNA, and homozygous Ago2-knockout mice were embryonically lethal (Liu et al., 2004). Parallel work using *in vitro* reconstitution assays revealed that active RISC contains only the guide strand (Martinez et al., 2002).

In parallel to studies centered on siRNA, the discovery of microRNAs also generated intense interest. MicroRNAs (miRNAs) are a large set of RNAs 20- to 22-nt in length made endogenously from processing of longer duplex pri- and pre-miRNAs by Drosha and Dicer (for reviews, see Bartel, 2004; Bartel, 2009). miRNAs are evolutionarily conserved and biologically important in regulating up to 30% of human genes (Lewis et al., 2005; Xie et al., 2005) and in controlling vital functions such as cell proliferation, differentiation, and organism development.

Unlike siRNAs, mammalian miRNAs typically exhibit only partial sequence complementarity to target mRNAs, with highest degree of complementarity in the 2-8 nt "seed" region.

Due to the fact that CAG-targeting siRNAs (both single-stranded and duplex) share certain key characteristics with common generic miRNAs such as imperfect sequence complementarity and target protein knockdown without decreasing mRNA, we hypothesized that they function as miRNA-mimics and inhibit HTT expression by translational repression. However, the underlying molecular mechanism is poorly understood. Work in our lab implicated Ago2 as an essential factor by observing that reducing Ago2 level partially reversed HTT-inhibition by CAG-targeting siRNAs, and Ago2 is recruited to *HTT* mRNA with siRNA treatment (Yu et al., 2012; Hu, Liu et al., 2012; see Chapter 1). *In vitro* Ago2 cleavage assays showed that CAG-targeting siRNAs are poor inducers of substrate cleavage, further supporting a model for cleavage-independent translational inhibition (Yu et al., 2012; Hu, Liu et al., 2012). However, it remains to be investigated which additional proteins are involved.

To answer this question, we took a candidate approach to examine the association and functional importance of three major RNAi factors: Dicer, C3PO, and GW182/TNRC6A family proteins. Dicer is an RNAse III family ribonuclease best known for its role in processing longer pre-miRNAs (Bernstein et al., 2001). In addition to generating 21-22nt dsRNA, Dicer has been proposed to mediate siRNA-loading onto Ago proteins (Sakurai et al., 2010) as well as determining guide-strand selection by sensing 5'-end thermal instability (Tomari et al., 2004; Noland et al., 2011). C3PO is a Mg^{2+}-dependent endonucleolytic protein complex involved in facilitating passenger strand degradation after it is nicked by Ago2 (Liu et al., 2009). TNRC6A (also known as GW182) is a central component of intracellular RNA-processing foci known as P-bodies and has been shown to co-localize with endogenous Ago proteins and transfected siRNAs (Jakymiw et al., 2005; Liu et al., 2005a). Multiple lines of evidence have suggested

TNRC6A/GW182 to be an important mediator of miRNA-induced translational repression (Liu et al., 2005a; Behm-Asmant 2006; Li et al., 2008; Lazzaretti et al., 2009).

RESULTS

Biotin Pull-down Identified Ago2 and GW182 as Binding Factors of ss-siRNAs

While RNA immunoprecipitation (RIP) experiments provided evidence of recruitment and association between Ago2 and *HTT* mRNA upon ss-siRNA treatment (Chapter 1, Figure 1-8B), we are interested in both obtaining direct evidence of ss-siRNA association with Ago2 as well as identifying additional binding partners inside cells. To this end, we generated ss-siRNA 580940 by tagging a biotin to the 3'-terminus of P9-mismatched ss-siRNA 537775 in order to directly co-purify proteins stably bound to the oligomer (Figure 3-1A). 537775 is a chemically modified ss-siRNA with a mismatched base at position 9 of an otherwise pure poly-CUG sequence; it was shown to target CAG repeats and achieve allele-selective HTT inhibition in cell culture and *in vivo* (Chapter 1, Chapter 2, and Yu et al., 2012).

580940 was first tested for its ability to inhibit mutant HTT in HD-patient cells (GM04281 with 69 CAG repeats/mutant allele, 17 CAG repeats/wild-type allele). It displayed $^{mut}IC_{50}$ of 1.6 nM and allele-selectivity of over 31-fold, indicating that biotinylation did not affect ss-siRNA's ability to inhibit HTT (Figure 3-1A). Next, ss-siRNA 580940 was transfected into large dishes of fibroblasts; whole cell extract was harvested 4 days later and biotin pull-down was performed using streptavidin-coated paramagnetic Dynabeads (Invitrogen). After several rounds of washes, ss-siRNA bound proteins were eluted and assayed by western blot. When probed with Ago2 antibody, strong bands were seen in elutants from 580940- and biotinylated siLuc (positive control)-treated cell extracts but not in no-treatment cell extract (Figure 3-1B).

Although Ago proteins are the commonly known mediators of RNAi, many other proteins have been shown to be parts of the miRNA-induced silencing complex (miRISC, i.e., miRNA ribonucleoparticles or miRNP). Therefore, we probed for the presence of other major RNAi

factors. Like Ago2, clear bands were seen when we blotted with TNRC6A/GW182 antibody. Little to no signals were observed after probing with Dicer or C3PO antibody, while antibodies against additional RNAi factors such as TRBP failed to produce specific bands (Figure 3-1C). Together, these results demonstrate that ss-siRNAs physically associate with some known RNAi factors. More importantly, we have validated biotin-tagged ss-siRNA as an important tool to search for intracellular binding partners.

Biotinylated ss-siRNAs Efficiently Load into and Pull Down Ago2 from Cell Extract *in vitro*

To more directly assay the ability of ss-siRNA to engage RNAi machinery, we performed *in vitro* loading assays, in which extract from untreated cells was mixed in the presence of 1mM ATP with either ss-siRNA 580940 or biotinylated siLuc guide-strand at a final concentration of 100nM. After one hour of rotation at room temperature, we performed streptavidin-bead pull-down on the oligomer-extract mixture and probe for the presence of Ago2 in the elutant by western blot. 580940 pulled down much more Ago2 than siLuc guide strand, indicating that modified ss-siRNA can efficiently load onto Ago (Figure 3-1D) even in a cell-free system.

Dicer Is Not Required for Efficient Gene Knock-down by CAG-targeting siRNAs

While Dicer is shown to be essential for miRNA biogenesis, its requirement for effective RNAi by exogenously introduced siRNAs has been under debate, as some studies showed diminished reporter silencing upon Dicer-TRBP depletion (Chendrimada et al., 2005) while others reported that Dicer-deficient murine embryonic stem (ES) cells still supported RNAi despite growth defects (Murchison et al., 2005). It is also important to note that Dicer-TRBP

complex interacts closely with Ago2 (Chendrimada et al., 2005) and that recombinant Dicer was shown to be able to bind single-stranded RNA *in vitro* (Kini and Walton, 2007).

Given the potential involvement of Dicer in efficient RISC loading and RNAi, we are interested in whether Dicer is necessary for RISC loading by either single-stranded or double-stranded CAG-targeting siRNAs. To this end, we performed double-transfection experiment in GM04281 HD-patient fibroblasts. First, we used duplex siRNA to reduce Dicer expression. The knockdown efficiency was verified by qPCR and western blot at > 60% reduction at both mRNA and protein level (Figure 3-2A and 2B). Cells were then treated with unmodified duplex P9, chemically modified ss-siRNA 537775, or unmodified, non-selective siRNA duplex BBRC.

Western blotting against HTT showed that Dicer-knockdown had no effect in reversing either allele-selective inhibitions by P9 or 537775 or non-allele-selective inhibition by BBRC (Figure 3-2, C to E). Our results suggest that Dicer is not important for efficient silencing by traditional siRNA BBRC, consistent with observations from some studies (Chendrimada et al., 2005) but disputing others (Murchison et al., 2005). In the case of CAG-targeting P9 duplex, Dicer appears dispensable for strand separation and loading. As for ss-siRNA 537775, it seems to load into Ago/RISC without assistance from Dicer. It should be cautioned that the lack of observed phenotypic reversal could be due to the residual pool of Dicer, and can be examined more rigorously (especially for BBRC) by using mesenchymal embryonic stem cells (MES) and/or embryonic fibroblasts (MEF) derived from Dicer-null mouse embryos (Harfe et al., 2005; Murchison et al., 2005; Tan et al., 2009).

C3PO Is Not Required for Efficient Gene Knock-down by CAG-targeting siRNAs

C3PO is a hetero-hexameric complex made of subunits Trax and translin (Tian et al., 2011) and has been shown to be important in promoting efficient RNAi *in vitro* and *in vivo* (Liu

et al., 2009). Since ss-siRNA does not have a passenger strand, C3PO is predicted to be dispensable. Unmodified siRNA duplexes such as P9 and BBRC, on the other hand, may depend on the presence of C3PO to undergo efficient strand maturation.

To probe for this possible differential requirement of C3PO, we conducted double-transfection experiments in HD-patient-derived GM04281 cells in which Trax and translin were first knocked down by siRNA either separately or in combination. In the second transfection, we then measured the ability by P9 duplex, BBRC duplex, or ss-siRNA 537775 to inhibit HTT expression after C3PO depletion. C3PO knockdown efficiency was confirmed by qPCR, which showed potent mRNA reduction either specific to *Trax* or *translin* or in combination (Figure 3-3A and B). Similarly, western blot showed effective reduction in protein level when Trax and translin were targeted either separately or together (Figure 3-3C), confirming previous reports that Trax needs translin to be stable (Clausen et al., 2006). When HTT expression is measured by western blot, we observed no reversal of HTT inhibition by duplex P9, ss-siRNA 537775, or siRNA BBRC (Figure 3-3, D-F).

The results confirm our prediction that C3PO function is dispensable for gene knockdown by ss-siRNA, which neither contains nor requires passenger strands. The lack of effect on P9-mediated HTT repression is somewhat surprising, but may be explained by the fact that its loading into catalytically inactive Ago-1, -3, -4 would remain unaffected. Alternatively, its miRNA-mimic nature may preclude the necessity for assistance from C3PO in Ago2-loading.

BBRC is a canonical siRNA that mediates transcript cleavage, and therefore should require C3PO for optimal process of passenger strand removal and RISC maturation. Nonetheless, it has been speculated that by-pass mechanisms exist independent of Ago2's catalytic activity (Matranga et al., 2005). Therefore, the slower kinetics of passenger strand processing may not be visible after new steady states of HTT protein are established that reflect

the thermodynamics rather than kinetics of RNAi. Like the Dicer knockdown studies, it should be cautioned that the lack of reversal in HTT inhibition may also be due to incomplete depletion of endogenous C3PO complex, which may be better addressed using translin-knockout mouse embryonic fibroblasts.

TNRC6/GW182 Family Proteins Are Required for Efficient Gene Knockdown by CAG-targeting siRNAs

In addition to miRISC assembly on the target mRNA transcripts, they are also observed to undergo translocation to cellular compartments known as P-bodies or GW bodies (Liu et al., 2005b; Sen and Blau, 2005). GW182 (also known as TNRC6A) is a central component of P-bodies and is structurally comprised of multiple glycine/tryptophan (GW) repeats as well as a RNA recognition motif (Estathioy et al., 2002). Knockdown of GW182 by siRNA dispersed intracellular P-bodies and abolished silencing abilities of transfected siRNAs.

It was known that tethering Ago2 to the 3'-UTR of transcript via fusing with a viral RNA binding domain resulted in translational repression, a process that required GW182 (Liu et al., 2005a). Strikingly, tethering GW182 directly to 3'-UTR led to even stronger repression that persisted after Ago2 knockdown (Behm-Asmant et al., 2006, Li et al., 2008). Studies using truncated and domain-swapped GW182/TNRC6A showed that Ago-interaction and translation inhibition were mediated by independent domains, and that the C-terminal RNA-binding domain is sufficient to silence bound transcripts independent of Ago interaction and/or P-body localization (Lazzaretti et al., 2009).

GW182/TNRC6A has two other paralogs in the human genome: TNRC6B and TNRC6C. Mass spectrometry and sucrose gradient fractionation showed that all three TNRC6 family

proteins associate with Ago1-4 in complexes that co-peaked with ribosomes and miRNAs (Landthaler et al., 2008). In addition, mRNA microarray analysis revealed that Ago 1-4 and TNRC-6A to -6C bound to and co-purified with strikingly similar sets of transcripts (Landthaler et al., 2008), and direct biochemical purification of TNRC-6B and -6C- showed them to be complexed with Ago 1-4 already loaded with miRNAs (Baillat and Shiekhattar, 2009). These and other reports (Takimoto et al., 2009; Zipprich et al., 2009) suggest that Argonaute and TNRC6 family proteins interact to form miRNP complexes and mediate translational inhibition.

We performed double-transfection experiments to test whether TNRC6 family proteins play a role in mediating HTT inhibition by CAG-targeting siRNAs. TNRC6A, 6B, or 6C expressions were reduced by siRNAs in HD-patient-derived cell-line GM04281. The knockdown efficiency was verified at both mRNA level by paralog-specific qPCR and at protein level by western blot (Figure 3-4). Knockdown of individual TNRC6 proteins did not reverse allele-selective HTT inhibition by either P9 duplex or ss-siRNA 775 (with mismatch at position 9). However, when all three TNRC6 family proteins are reduced simultaneously, we observed significant reversal of HTT inhibition by P9 and 775 (Figure 3-5A and 5B). Knockdown of two TNRC6 proteins in pair-wise fashion did not yield similar reversal (Figure 3-6 and 3-7), suggesting the three proteins compensate for each other, and full expression of any one paralog is sufficient to sustain HTT inhibition.

Western blot showed that HTT and Ago2 protein levels were not altered by the combined treatment of all three TNRC6-targeting siRNAs, demonstrating that the observed loss of HTT inhibition was unlikely to be from off-target effects (Figure 3-4D). It is interesting to observe that siRNA-mediated depletion of TNRC6 family proteins did not reverse HTT inhibition by BBRC, a traditional siRNA duplex targeting HTT for cleavage, suggesting that GW182 is selectively

important for translation- but not cleavage-mediated RNAi (Figure 3-5C). It remains possible that no reversal is observed simply because BBRC was too potent at these concentrations (5nM).

To probe whether the functional involvement of TNRC6 family proteins is accompanied by physical interactions with *HTT* transcripts, we performed RNA immunoprecipitation (RIP) to measure enrichment of *HTT* mRNA that co-purifies with GW182 proteins. Both P9 and ssRNA 537775 treatments resulted in strong (15-fold and 25-70-fold, respectively and depending on the q-PCR primers used) enrichment of *HTT* mRNA levels after immunoprecipitation by anti-GW182 antibody over those of IgG controls (Figure 3-8). In particular, no transcript enrichment is observed with either negative control oligomer treatments (CM duplex and/or ss-siRNA522247 that do not target HTT) or an LNA-based antisense oligonucleotide (ASO) treatment (Figure 3-8A), demonstrating that GW182 recruitment is an RNAi-dependent process. In conclusion, TNRC6A/GW182 and its two paralogs are required for both single-stranded and duplex CAG-targeting siRNAs to achieve potent, allele-selective HTT inhibition.

DISCUSSION

Collectively, our data indicate that Ago2 and TNRC6A/GW182 associate with chemically modified ss-siRNAs inside the cell, and efficient Ago2-loading of ss-siRNA can occur *in vitro* when mixed with native cell extract. In agreement with intracellular association between ss-siRNA and GW182/TNRC6A, simultaneously knocking down TNRC6A and its two paralogs reversed HTT inhibition by both single-stranded and duplex siRNAs. Together, we propose that siRNA-loaded Ago protein physically interacts with GW182 to form a repressive complex and block *HTT* mRNA translation.

In contrast to Ago2 and GW182, two other major RNAi factors, Dicer and C3PO, did not consistently co-purify with biotin-tagged ss-siRNA, suggesting their lack of stable association with ss-siRNA inside cells. Functionally, Dicer and C3PO also appear dispensable for CAG-targeting siRNAs HTT inhibition, as shown by the persistence of strong HTT repression after Dicer and C3PO depletions. Curiously, cleavage-inducing siRNA duplex BBRC continues to function after Dicer or C3PO reductions, presumably due to either incomplete Dicer/C3PO knockdown or them being truly dispensable in RISC-loading and maturation under the experimental setups.

In summary, we propose that single-stranded and duplex CAG-targeting siRNAs load into Ago without assistance from Dicer; thus formed miRISC bind to mutant *HTT* mRNA and recruit of TNRC6A, 6B, or 6C for translational inhibition. The latter process likely requires binding of multiple miRISCs and is possible only on the CAG-expanded mutant *HTT* mRNA versus non-expanded wild-type mRNA (Yu et al., 2012; Hu, Liu et al, 2012). Once bound, TNRC6 proteins form a stable transcript-associated complex, which is resistant against dislodgement by translating ribosomes and thereby induces potent, long-lasting HTT repression.

FUTURE DIRECTIONS

Further Examining Translational Inhibition by Polysome Profiling

Polysome profiling, which examines the movement of ribosome-bound mRNA transcript across sucrose gradient, is a powerful technique that could provide unambiguous proof that HTT inhibition by ss-siRNA occurs translationally. RNA transcripts bound by different number of ribosomes sediment under ultracentrifugation to different fractions in sucrose gradient, and can be directly visualized and fractionated by pump-coupled UV spectrometer. At 260nM wavelength, monosome and polysome peaks can be observed and separated. q-PCR of each fraction can then quantify the relative amounts of particular mRNA species that are bound to one, two, three, four or more ribosomes. A significant shift by *HTT* mRNA to the lighter fractions in siRNA-treated versus non-treated cell extract would indicate a decrease in the number of bound ribosomes per transcript and thus a reduction in translational activity.

Since CAG repeats are located within exon 2 and less than 300 nt from the translational start site (2% out of >13,000 nt in total *HTT* mRNA length), a translational block by CAG-targeting siRNAs is expected to occur very early in the transcript and bring about substantial reduction on the number of bound ribosomes. Preliminary effort in lab so far has been hampered by a lack of clear poly-ribosome peaks on UV tracing; however, the polysome bump itself is clearly and very reproducibly identified, as it disappears with EDTA treatment known to disassemble the ribosomal subunits (Figure 3-9A and B). This would enable monitoring *HTT* mRNA movement within the gradient even in the absence of visualizing the individual poly-ribosome peaks, though it might lower the publication quality. It should be noted that Dr. Keith Gagnon in the lab had previously succeeded in obtaining high-quality UV-trace showing

individual polyribosome peaks (Figure 3-9C), implying that optimal results may be achieved with further trouble-shooting.

Using Biotinylated ss-siRNA to Identify Novel Binding Partners by Mass Spectrometry

We validated the use of biotinylated ss-siRNA 580940 for identifying stable interacting partners by demonstrating its strong intracellular binding of Ago2. 580940's predictive value was further established when GW182 (which was co-purified in the biotin pulldown) but not Dicer or C3PO (which did not co-purify) was shown to be functionally required in HTT inhibition. To comprehensively identify all binding partners, we have harvested large number of dishes of HD fibroblasts treated with ss-siRNA 580940 and hope to pull down enough materials for mass spectrometry. Novel interactors identified this way can be validated by western blotting and their functional requirement tested by double-transfections. Information thus obtained would offer valuable insight in further elucidating molecular players and pathways involved in CAG-targeting HTT inhibition.

Using ss-siRNA to Further Dissect Endogenous RNAi Mechanism

With its ability to achieve gene-knockdown with only one strand, ss-siRNA offers us a unique tool to answer many mechanistic questions about endogenous RNA interference. We already saw such an instance in Chapter 2 where ss-siRNA helped us determine that the minimal length of guide strand allowed for RISC-loading is about 17 nt. Another interesting topic is the asymmetric loading of the two strands in an siRNA duplex, which can be more directly examined by designing ss-siRNAs with sequences of the guide versus passenger strand and comparing their relative RISC loading efficiencies. Furthermore, it would be interesting and therapeutically

relevant to study whether ss-siRNA would eliminate certain reported off-target effects of conventional duplex siRNAs that were presumed to result from undesired loading of the passenger strand.

Characterizing the Individual Roles of Ago1-4 in ss-siRNA Function

Four Ago variants exist in the mammalian genome: Ago1, Ago2, Ago3, and Ago4, with Ago2 being the only one with endonuclease activity that is essential for siRNA's "slicing" activity (Liu et al., 2004). Interestingly, the catalytically inactive Ago variants (Ago1, Ago3, and Ago4) are found in tandem on the same chromosome, suggesting that they arise evolutionarily by gene multiplication and may play redundant roles distinct from that of Ago2. Several studies have examined the individual roles of the four Ago variants (Azuma-Mukai et al., 2008). Of note, two studies reported that while all four variants appear equally capable of utilizing bulged miRNA duplexes, Ago2 (and in one study, also Ago1) is more effective in utilizing perfectly matched siRNAs and the process may be independent of Ago2's catalytic activity (Su et al., 2009; Broderick et al., 2011).

Work in our lab had shown that Ago2, but not Ago1, 3, or 4, appeared important for functions of either promoter-targeted agRNAs (Janowski et al., 2006; Chu et al., 2010) or CAG-targeting siRNAs (Yu et al., 2012; Hu, Liu et al., 2012). Since neither process involves mRNA cleavage, it is curious as to why Ago2 is the preferred variant and whether its catalytic activity is essential. In addition, many of the previous findings were made by using either Ago-variant-specific siRNA or antibody, which may confound interpretation due to incomplete gene inhibition, cross-targeting and cross-reactivity, and functional redundancy by the remaining Ago variants.

To clearly and unambiguously establish the (lack of) involvement of each Ago variant, I propose obtaining and testing HTT inhibition in Ago2 knockout mouse embryonic fibroblast (MEF) cell-line as well as pan-Ago mouse embryonic stem (ES) cells with individually re-introduced Ago (Liu et al., 2004; Su et al., 2009). Since these cell-lines only contain wild-type mouse *HTT* alleles (7 interrupted CAG/CAA repeats), expression of a reporter plasmid with human *HTT* exon 1 is necessary. Dr. Keith Gagnon and Hannah Pendergraff of our laboratory have already generated Renilla luciferase reporter plasmid containing poly-CAG sequences of different lengths that mimic mutant or wild-type *HTT* alleles, which in combination with the Ago knockout cell-lines may help define CAG-targeting siRNA and their exact functional relationship to each Ago variant.

MATERIALS AND METHODS

ss-siRNA, antibodies, cell culture and transfection, analysis of HTT expression, IC_{50} and selectivity calculations, q-PCR, RNA immunoprecipitation

Most materials and protocols are identical to those used for Chapters 1 and 2 and may be referenced accordingly. Additional antibodies not described before are listed as follows: mouse monoclonal Dicer antibody was purchased from Abcam and diluted 1:1000 for western studies; rabbit polyclonal GW182 antibody was purchased from Bethyl Laboratories and diluted 1:3000 for western and RIP studies; another rabbit polyclonal GW182 antibody was a gift from Bing Yao of Edward Chan's lab at University of Florida and was diluted 1:2000 for western studies; rabbit polyclonal C3PO antibody was a generous gift from Qinghua Liu's lab and diluted 1:2000 for western studies.

Double Transfection Experiment

The experimental protocol and timeline for double-transfection experiments are identical to that described before and may be referenced accordingly. Additional sets of siRNA and qPCR primers are listed below. With the exception of siDicer, all were designed by Dr. Keith Gagnon in the lab.

siRNA duplex against GW182/TNRC6A has the following sequences: 5'-GCCAGAUGCCUAACAAUCA-3' (sense strand) and 5'-UGAUUGUUAGGCAUCUGGCTT-3' (antisense strand). siRNA duplex against TNRC6B has the following sequence: 5'-GGACAAGCGAGCGAUGAAU-3' (sense strand) and 5'-AUUCAUCGCUCGCUUGUCCTT-3' (antisense strand). siRNA duplex against TNRC6C has the following sequences: 5'-GAACCACAAACGUCCACUU-3' (sense strand) and 5'-AAGUGGACGUUUGUGGUUCTT-

3’ (antisense strand). siRNA duplex against Dicer has the following sequences: 5’-UGCUUGAAGCAGCUCUGGA-3’ (sense strand) and 5’-UCCAGAGCUGCUUCAAGCATT-3’ (antisense strand). siRNA duplex against Trax has the following sequences: 5’-GAGAAGGGAAGGAUGUUAA-3’ (sense strand) and 5’-UUAACAUCCUUCCCUUCUCTT-3’ (antisense strand). siRNA duplex against translin has the following sequences: 5’-GACUCGAGAAGCAGUUACA-3’ (sense strand) and 5’-UGUAACUGCUUCUCGAGUCTT-3’ (antisense strand).

q-PCR primer pair that measures Dicer mRNA level has the following sequences: 5’-TGCATCTTGGACAAAAGAGAGA-3’ (forward primer) and 5’-CATTCAAGGCGACATAGCAA-3’ (reverse primer). q-PCR primer pair that measures Trax mRNA level has the following sequences: 5’-ATCAGTTCCATCGAGCCATT-3’ (forward primer) and 5’-CTTTCCCATTGTCTTCAGTCG-3’ (reverse primer). q-PCR primer pair that measures translin mRNA level has the following sequences: 5’-CAGGGTGCTGGGTTTCAG-3’ (forward primer) and 5’-ACACAAACCTCCAGTGCTCA-3’ (reverse primer). q-PCR primer pair that measures GW182/TNRC6A mRNA level targets junction of exon 5 and 6 and has the following sequences: 5’-AACGGAGAGGTGCAGAACAG-3’ (forward primer) and 5’-CCCGCTGGGAATTTTCATA-3’ (reverse primer); q-PCR primer pair that measures TNRC6B mRNA level targets the junction of exon 23 and 24 has the following sequences: 5’-CGATACAGCACCAAACAGGA-3’ (forward primer) and 5’-TCATCAGTGGCAAACTCAGC-3’ (reverse primer). q-PCR primer pair that measures TNRC6C mRNA level targets the junction of exon 5 and 6 and has the following sequences: 5’-GTGGCATTTGGAAGAGCTG-3’ (forward primer) and 5’-GTTCATTTCATCCCCACCAC-3’ (reverse primer).

Biotin Pull-down and *In Vitro* Ago2-loading Assays

HD-patient derived GM04281 (69 CAG repeat) fibroblasts were grown in 150 cm^2 dishes and transfected at 20nM with biotinylated ss-siRNA 580940 or unmodified siLuc antisense strand using lipid RNAiMAX (Invitrogen) and Optimem (Invitrogen). Media were changed 24 and 72 hr after transfection, and cells ($\sim 4 \times 10^7$) were harvested by trypsin 96 hr after transfection. Typically, 2-4 dishes of cells were seeded and transfected per treatment.

A small quantity of cells are saved and harvested for protein to check knockdown efficiency by western blot. Cells were pelleted by gentle centrifugation at 500g and resuspended in cold PBS washing solution. After a second round centrifugation at 500g and aspirating off PBS, total cell lysate was isolated by adding to the cell pellet 1mL/dish of lysis buffer of the following formula: 150 mM NaCl, 20 mM Tris–HCl pH 4, 2 mM $MgCl_2$, 0.5% NP-40, with 1 × Roche protease inhibitors cocktail and RNAse in (50 U/mL final) supplemented just prior to usage The mixture was left on ice for 10 min, and insoluble material was removed by centrifugation at maximum speed for 15 min at 4°C. Materials may be stored at -80°C at this point.

40 µL of streptavidin-coated paramagnetic Dynabeads (Invitrogen) were pre-equilibrated in lysis buffer and incubated with 250 µL of cell lysate supplemented with Roche protease inhibitor and SuperaseIn (50U/mL final) on rotator at 4°C for 3 h. 5 µL of lysate was set aside for input control. At the end of incubation, Dynabeads were separated with DynaMag^{TM}-2 magnetic stand (Invitrogen) and the supernatant was removed. Four washes were performed by adding 500 µL of IP wash buffer (250 mM NaCl, 20 mM Tris-HCl, 2 mM $MgCl_2$, 0.01% SDS) and consisting of 3-min-long rotation followed by separation on magnetic stand. Complexes were then eluted with 30 µL 1× SDS buffer and the elutants may be run on SDS-PAGE gels followed

by standard western blot procedures. *In vitro* Ago2-loading assay was identical to biotin pull-down assay, except that ss-siRNA 580940 was mixed with non-treatment cell exact with 1mM ATP supplement and then complexed with Dynabeads on rotator. Subsequent washing and eluting steps were identical.

REFERENCES

Azuma-Mukai, A., Oguri, H., Mituyama, T., Qian, Z.R., Asai, K., Siomi, H., and Siomi, M.C. (2008). Characterization of endogenous human Argonautes and their miRNA partners in RNA silencing. Proc Natl Acad Sci U S A. *105*, 7964-9

Baillat, D., and Shiekhattar, R. (2009) Functional dissection of the human TNRC6 (GW182-related) family of proteins. Mol. Cell. Biol. *29*, 4144-55

Bartel, D.P. (2004) MicroRNAs: genomics, biogenesis, mechanism, and function. Cell, *116*, 281-97.

Bartel, D.P. (2009) MicroRNAs: target recognition and regulatory functions. Cell, *136*, 215-33.

Bazzini, A.A., Lee, M.T., and Giraldez, A.J. (2012) Ribosome profiling shows that miR-430 reduces translation before causing mRNA decay in zebrafish. Science, *336*, 233-7.

Behm-Ansmant, I., Rehwinkel, J., Doerks, T., Stark, A., Bork, P., and Izaurralde, E. (2006). mRNA degradation by miRNAs and GW182 requires both CCR4:NOT deadenylase and DCP1:DCP2 decapping complexes. Genes & Dev. *20*, 1885-98

Bernstein, E., Caudy, A. A., Hammond, S. M. and Hannon, G. J. (2001) Role for a bidentate ribonuclease in the initiation step of RNA interference. Nature, *409*, 363-366.

Broderick, J.A., Salomon, W.E., Ryder, S.P., Aronin, N., and Zamore, P.D. (2011) Argonaute protein identity and pairing geometry determine cooperativity in mammalian RNA silencing. RNA. *17*, 1858-69

Chendrimada, T.P., Gregory, R.I., Kumaraswamy, E., Norman, J., Cooch, N., Nishikura, K., and Shiekhattar, R. (2005). TRBP recruits the Dicer complex to Ago2 for microRNA processing and gene silencing. Nature, *436*, 740-4.

Chu, Y., Yue, X., Younger, S.T., Janowski, B.A., and Corey, D.R. (2010) Involvement of argonaute proteins in gene silencing and activation by RNAs complementary to a non-coding transcript at the progesterone receptor promoter. Nucleic Acids Res. *38*, 7736-48

Claussen, M., Koch, R., Jin, Z.Y., and Suter, B. (2006). Functional characterization of Drosophila Translin and Trax. Genetics. *174*, 1337-47.

Eystathioy, T., Chan, E.K., Tenenbaum, S.A., Keene, J.D., Griffith, K., and Fritzler, M.J. (2002) A phosphorylated cytoplasmic autoantigen, GW182, associates with a unique population of human mRNAs within novel cytoplasmic speckles. Mol. Biol. Cell. *13*, 1338-51

Fire, A., Xu, S., Montgomery, M.K., Kostas, S.A., Driver, S.E., and Mello, C.C. (1998). Potent and specific genetic interference by double-stranded RNA in *Caenorhabditis elegans*. Nature *391*, 806–811.

Gu, S., Jin, L., Zhang, F., Sarnow, P., and Kay, M.A. (2009) Biological basis for restriction of microRNA targets to the 3' untranslated region in mammalian mRNAs. Nat. Struc. Mol. Biol. *16*, 144-150.

Hamilton, A.J., and Baulcombe, D.C. (1999). A species of small antisense RNA in posttranscriptional gene silencing in plants. Science *286*, 950–952.

Hammond, S.M., Bernstein, E., Beach, D., and Hannon, G.J. (2000) An RNA-directed nuclease mediates posttranscriptional gene silencing in Drosophila cells. Nature, *404*, 293-296

Hammond, S.M., Boettcher, S., Caudy, A.A., Kobayashi, R., and Hannon, G.J. (2001). Argonaute2, a link between genetic and biochemical analyses of RNAi. Science *293*, 1146–1150.

Harfe, B.D., McManus, M.T., Mansfield, J.H., Hornstein, E., and Tabin, C.J. (2005) The RNaseIII enzyme Dicer is required for morphogenesis but not patterning of the vertebrate limb. Proc Natl Acad Sci U S A. 102, 10898-903.

Hu, J.‡, Liu, J.‡, Yu, D., Chu, Y., and David R. Corey (2012) Mechanism of allele-selective inhibition of huntingtin expression by duplex RNAs that target CAG repeats. Nucleic Acids Res. *40,* 11270-80

Jakymiw, A., Lian, S., Eystathioy, T., Li, S., Satoh, M., Hamel, J.C., Fritzler, M.J., and Chan, E.K. (2005) Disruption of GW bodies impairs mammalian RNA interference. Nat. Cell. Biol. *7*, 1267-74

Janowski, B.A., Huffman, K.E., Schwartz, J.C., Ram, R., Nordsell, R., Shames, D.S., Minna, J.D., and Corey, D.R. (2006) Involvement of AGO1 and AGO2 in mammalian transcriptional silencing. Nat Struct Mol Biol. *9*, 787-92

Kini, H.K., and Walton, S.P. (2007). In vitro binding of single-stranded RNA by human Dicer. FEBS Lett. *581*, 5611-6.

Landthaler, M., Gaidatzis, D., Rothballer, A., Chen, P.Y., Soll, S.J., Dinic, L., Ojo, T., Hafner, M., Zavolan, M., and Tuschl, T. (2008) Molecular characterization of human Argonaute-containing ribonucleoprotein complexes and their bound target mRNAs. RNA. *14*, 2580-96

Lazzaretti, D., Tournier, I., and Izaurralde, E. (2009) The C-terminal domains of human TNRC6A, TNRC6B, and TNRC6C silence bound transcripts independently of Argonaute proteins. RNA. *15*, 1059-66

Lewis, B.P., Burge, C.B., and Bartel, D.P. Conserved seed pairing, often flanked by adenosines, indicates that thousands of human genes are microRNA targets (2005). Cell. *120*, 15-20.

Li, S., Lian, S.L., Moser, J.J., Fritzler, M.L., Fritzler, M.J., Satoh, M., and Chan, E.K. (2008) Identification of GW182 and its novel isoform TNGW1 as translational repressors in Ago2-mediated silencing. J Cell. Sci. *121*, 4134-44

Lima, W.F., Prakash, T.P., Murray, H.M., Kinberger, G.A., Li, W., Chappell, A.E., Li, C.S., Murray, S.F., Gaus, H., Seth, P.P., Swayze, E.E., and Crooke, S.T. (2012) Single-stranded siRNAs Activate RNAi in Animals. Cell, *150,* 883-94

Liu, J., Hu, J., and Corey, D.R. (2012). Expanding the action of duplex RNAs into the nucleus: redirecting alternative splicing. Nucleic Acids Res. *40,* 1240-50.

Liu, J., Rivas, F.V., Wohlschlegel, J., Yates, J.R. 3rd, Parker, R., and Hannon, G.J. (2005) A role for the P-body component GW182 in microRNA function. Nat. Cell. Biol. *7*, 1261-6

Liu, J., Valencia-Sanchez, M.A., Hannon, G.J., and Parker, R. (2005) MicroRNA-dependent localization of targeted mRNAs to mammalian P-bodies. Nat. Cell. Biol. *7*, 719-23

Liu, J., Carmell, M.A., Rivas, F.V., Marsden, C.G., Thomson, J.M., Song, J.J., Hammond, S.M., Joshua-Tor, L., and Hannon, G.J. (2004) Argonaute2 is the catalytic engine of mammalian RNAi. Science *305*,1437–1441

Liu, Y., Ye, X., Jiang, F., Liang, C., Chen, D., Peng, J., Kinch, L.N., Grishin, N.V., and Liu, Q. (2009). C3PO, an endoribonuclease that promotes RNAi by facilitating RISC activation. Science, *325*, 750-3.

Martinez, J., Patkaniowska, A., Urlaub, H., Lührmann, R., and Tuschl, T. (2002) Single-stranded antisense siRNAs guide target RNA cleavage in RNAi. Cell. *110*, 563-74.

Matranga, C., Tomari, Y., Shin, C., Bartel, D.P., and Zamore, P.D. (2005). Passenger-strand cleavage facilitates assembly of siRNA into Ago2-containing RNAi enzyme complexes. Cell, *123*, 607-20.

Murchison, E.P., Partridge, J.F., Tam, O.H., Cheloufi, S., and Hannon, G.J. (2005). Characterization of Dicer-deficient murine embryonic stem cells. Proc Natl Acad Sci U S A. *102*, 12135-40.

Noland, C.L., Ma, E., and Doudna, J.A. (2011). siRNA repositioning for guide strand selection by human Dicer complexes. Mol. Cell. *43*, 110-21

Ngo, H., Tschudi, C., Gull, K., and Ullu, E. (1998). Double-stranded RNA induces mRNA degradation in *Trypanosoma brucei*. Proc. Natl. Acad. Sci. USA *95*, 14687–14692.

Sakurai, K., Amarzguioui, M,, Kim, D.H., Alluin, J., Heale, B., Song, M.S., Gatignol, A., Behlke, M.A., and Rossi, J.J. (2011). A role for human Dicer in pre-RISC loading of siRNAs. Nucleic Acids Res. *39*, 1510-25.

Sen, G.L., and Blau, H.M. (2005). Argonaute 2/RISC resides in sites of mammalian mRNA decay known as cytoplasmic bodies. Nat. Cell. Biol. *7*, 633-6

Su, H., Trombly, M.I., Chen, J., and Wang, X. (2009) Essential and overlapping functions for mammalian Argonautes in microRNA silencing. Genes Dev. *23*, 304-17

Tabara, H., Sarkissian, M., Kelly, W.G., Fleenor, J., Grishok, A., Timmons, L., Fire, A., and Mello, C.C. (1999). The rde-1 gene, RNA interference, and transposon silencing in *C. elegans*. Cell *99*,
123–132

Takimoto, K., Wakiyama, M., and Yokoyama, S. (2009). Mammalian GW182 contains multiple Argonaute-binding sites and functions in microRNA-mediated translational repression. RNA, *15*, 1078-89.

Tan, G.S., Garchow, B.G., Liu, X., Yeung, J., Morris, J.P. 4th, Cuellar, T.L., McManus, M.T., and Kiriakidou, M. (2009) Expanded RNA-binding activities of mammalian Argonaute 2. Nucleic Acids Res. *37*, 7533-45

Tian, Y., Simanshu, D.K., Ascano, M., Diaz-Avalos, R., Park, A.Y., Juranek, S.A., Rice, W.J., Yin, Q., Robinson, C.V., Tuschl, T., and Patel, D.J. (2011). Multimeric assembly and biochemical characterization of the Trax-translin endonuclease complex. Nat. Struct. Mol. Biol. *18*, 658-64.

Tomari, Y., Matranga, C., Haley, B., Martinez, N., and Zamore, P.D. (2004). A protein sensor for siRNA asymmetry. Science, *306*, 1377-80

Xie, X., Lu, J., Kulbokas, E.J., Golub, T.R., Mootha, V., Lindblad-Toh, K., Lander, E.S., and Kellis, M. (2005) Systematic discovery of regulatory motifs in human promoters and 3' UTRs by comparison of several mammals. Nature. *434*, 338-45.

Yu, D., Pendergraff, H., Liu, J., Kordasiewicz, H., Cleveland, D.W., Swayze, E.E., Lima, W.F., Crooke, S.T., Prakash, T.P., and Corey DR. (2012) Single-Stranded RNAs Use RNAi to Potently and Allele-Selectively Inhibit Mutant Huntingtin Expression. Cell, *150,* 895-908

Zamore, P.D., Tuschl, T., Sharp, P.A., and Bartel, D.P. (2000) RNAi: Double-stranded RNA directs the ATP-dependent cleavage of mRNA at 21 to 23 nucleotide intervals. Cell *101*, 25-33.

Zipprich, J.T., Bhattacharyya, S., Mathys, H., and Filipowicz, W. (2009) Importance of the C-terminal domain of the human GW182 protein TNRC6C for translational repression. RNA. *15*, 781-93

Figure 3-1

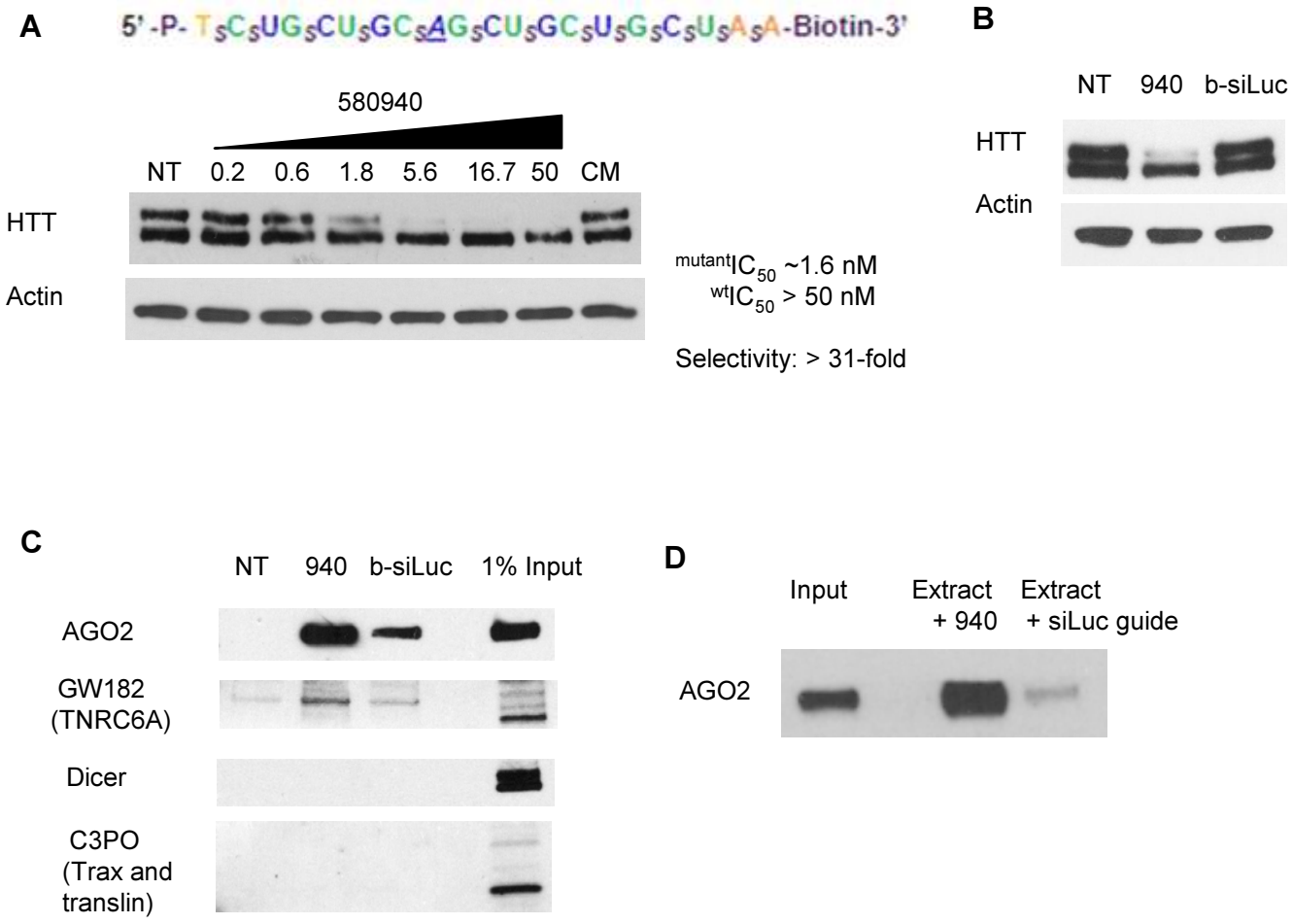
A
5'-P- TsCsUGsCUsGCsAGsCUsGCsUsGsCsUsAsA-Biotin-3'
580940
NT 0.2 0.6 1.8 5.6 16.7 50 CM
HTT
Actin
mutantIC50 ~1.6 nM
wtIC50 > 50 nM
Selectivity: > 31-fold
B
NT 940 b-siLuc
HTT
Actin
C
NT 940 b-siLuc 1% Input
AGO2
GW182 (TNRC6A)
Dicer
C3PO (Trax and translin)
D
Input
Extract + 940
Extract + siLuc guide
AGO2

Figure 3-1. **Identification of major associating RNAi factors by biotinylated ss-siRNA:**

(A) ss-siRNA 580940 is identifical to 537775 with P9 mismatch except with an additional biotin-tag at the 3'-end. 580940 is similar in potency and allele-selectivity to 537775 in targeting HTT.

(B) Selective HTT inhibition is seen with large-scale transfection of 580940 for biotin pull-down studies.

(C) Streptavidin pull-down followed by western blot showed that 580940 stably associates with Ago2 and GW182, but not Dicer or C3PO.

(D) *In vitro* Ago2 loading assay: 580940 and unmodified, biotinylated siLuc-guide were mixed with no-treatment cell extract *in vitro* for 1hr at 0.1uM, and the mixtures were precipitated by strepavidin-coated beads to probe for ssRNAs' ability to load into and pull down Ago2.

NT: no treatment; 940: ss-siRNA 580940; b-siLuc: an unmodified si-luciferease guide strand with a 3'-biotin tag. Images are representative data from two independent transfections and multiple pull-down assays.

Figure 3-2

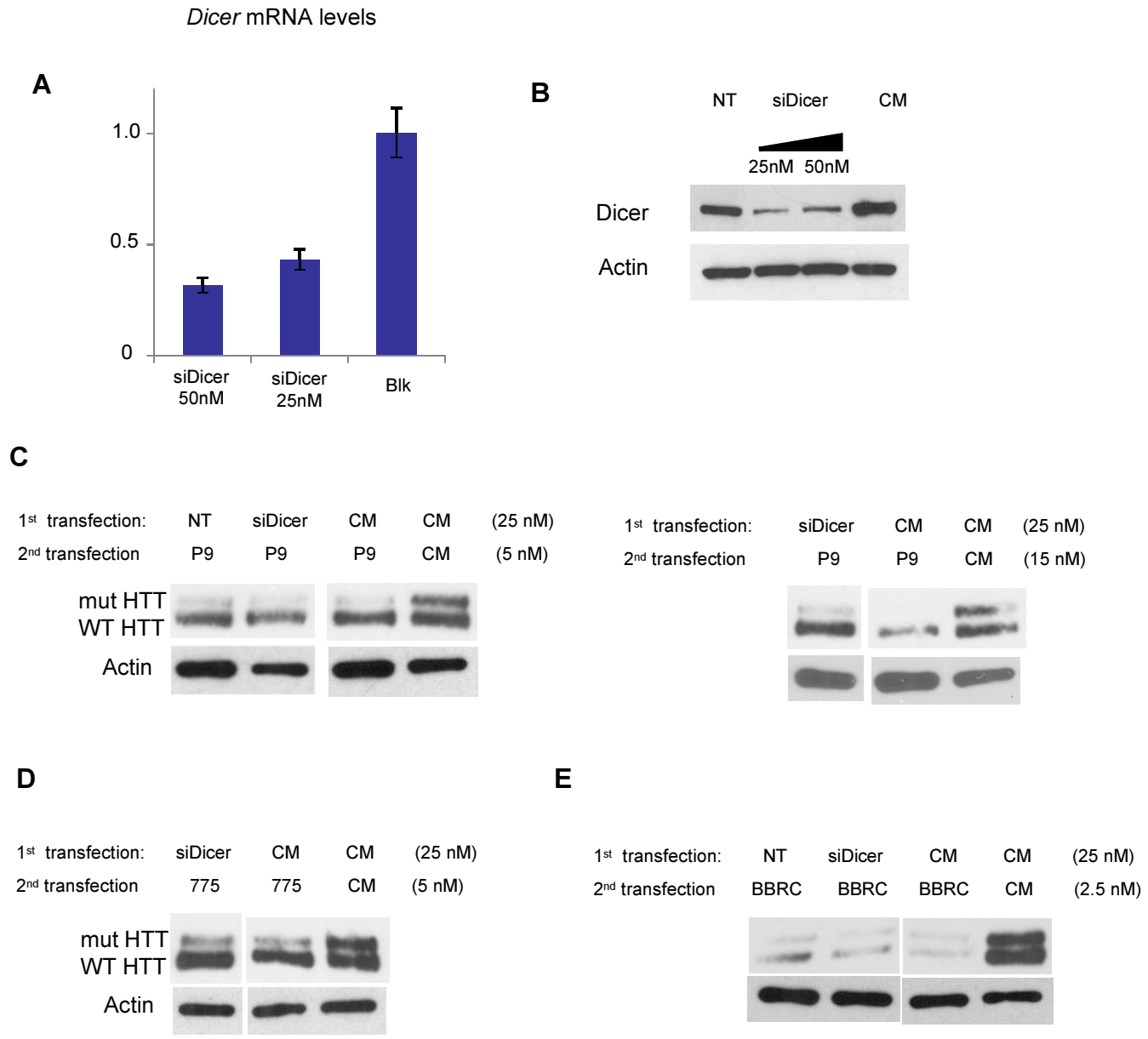

Figure 3-2. **Dicer knockdown did not reverse HTT inhibition by CAG-targeting or canonical siRNAs:** (A) q-PCR showing reductions in *Dicer* mRNA after treatment with Dicer-targeting siRNA at 25nM and 50nM; (B) western showing reductions in Dicer protein after treatment with Dicer-targeting siRNA at 25nM and 50nM; (C) No reversal of HTT inhibition is seen despite effective Dicer reductions.

P9: unmodified CAG-targeting duplex siRNA with mismatch at P9; 775: ss-si-RNA 537775 with mismatch at P9; CM: mismatched control; BBRC: siRNA targeting *HTT* mRNA outside of CAG-repeats; NT: no treatment.

Figure 3-3

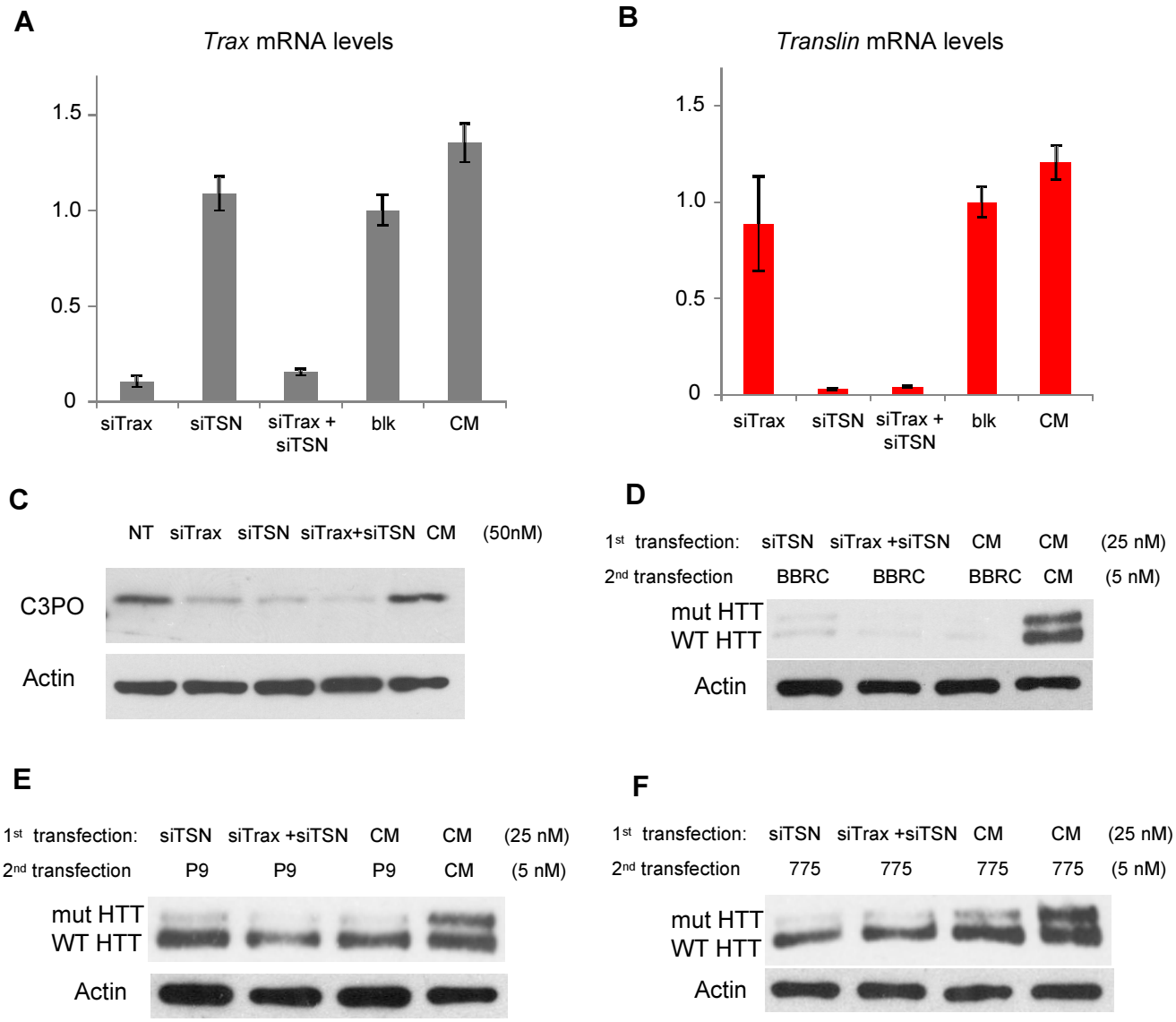

Figure 3-3. **C3PO knockdown did not reverse HTT inhibition by CAG-targeting or canonical siRNAs:** (A, B) q-PCR showing reductions in *Trax* or *translin* (*TSN*) mRNAs after treatment with siRNA targeting Trax and translin either separately or in combination at 25nM each; (C) western showing reductions in C3PO complex after treatment with Trax and/or translin-targeting siRNA at 25nM each; (D-F) No reversal of HTT inhibition is seen by BBRC, P9, or 537775 despite effective C3PO reductions.

P9: unmodified CAG-targeting duplex siRNA with mismatch at P9; 775: ss-si-RNA 537775 with mismatch at P9; CM: mismatched control; BBRC: siRNA targeting HTT outside of CAG-repeats; NT/Blk: no treatment/blank.

Figure 3-4

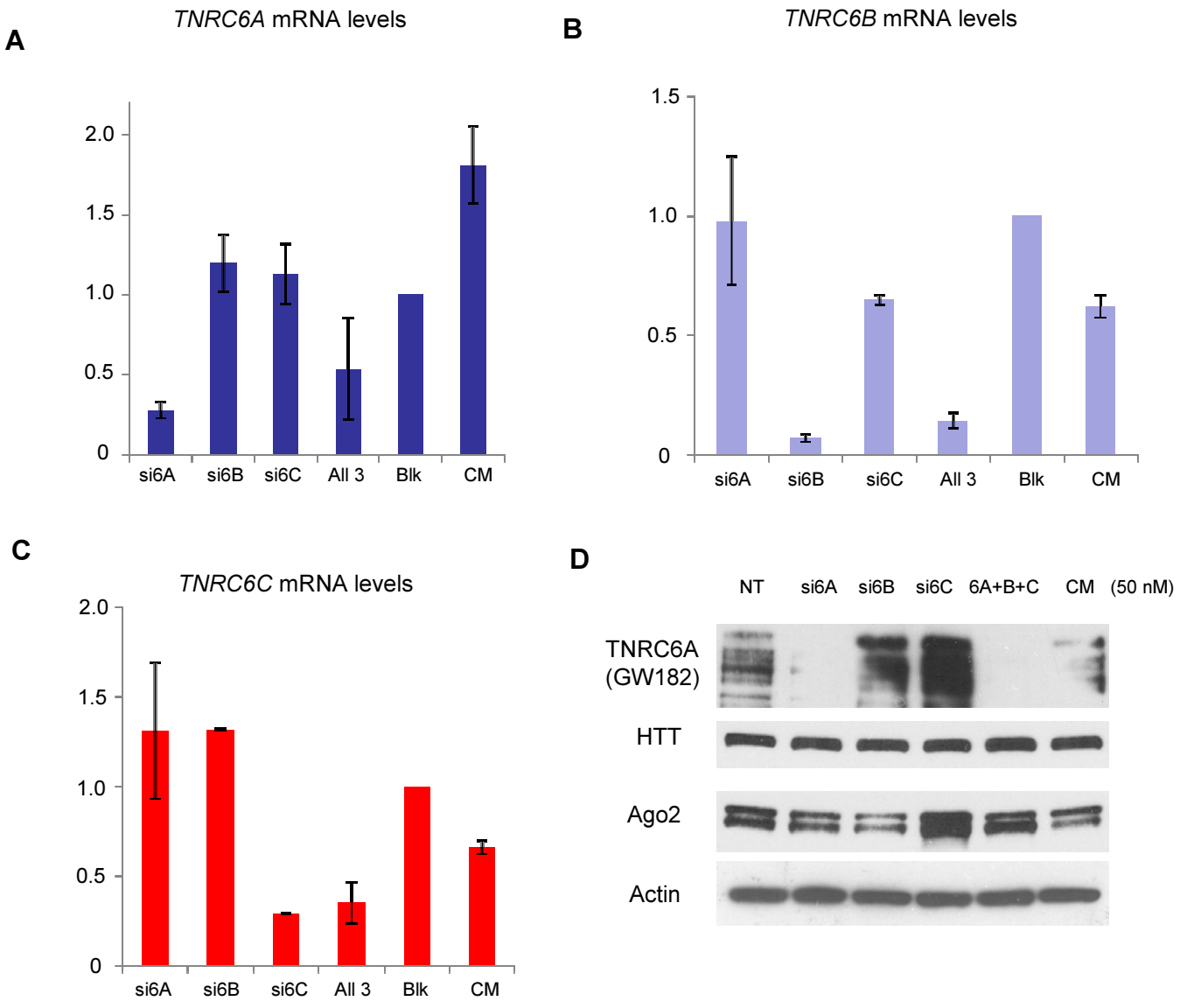

Figure 3-4. **TNRC6A, 6B, and 6C knockdowns by siRNA were efficient and specific :** (A-C) q-PCR showing reductions in *TNRC6A*, *6B*, and *6C* mRNA levels after treatment with siRNAs targeting each paralog separately or in combination at 25nM each; (D) western showing reductions in TNRC6A/GW182 protein after treatment with various siRNAs at 25nM each.

si6A: siRNA targeting TNRC6A/GW182; si6B: siRNA targeting TNRC6B; si6C: siRNA targeting TNRC6C; NT/blk: no treatment/blank; CM: mismatched control.

Figure 3-5

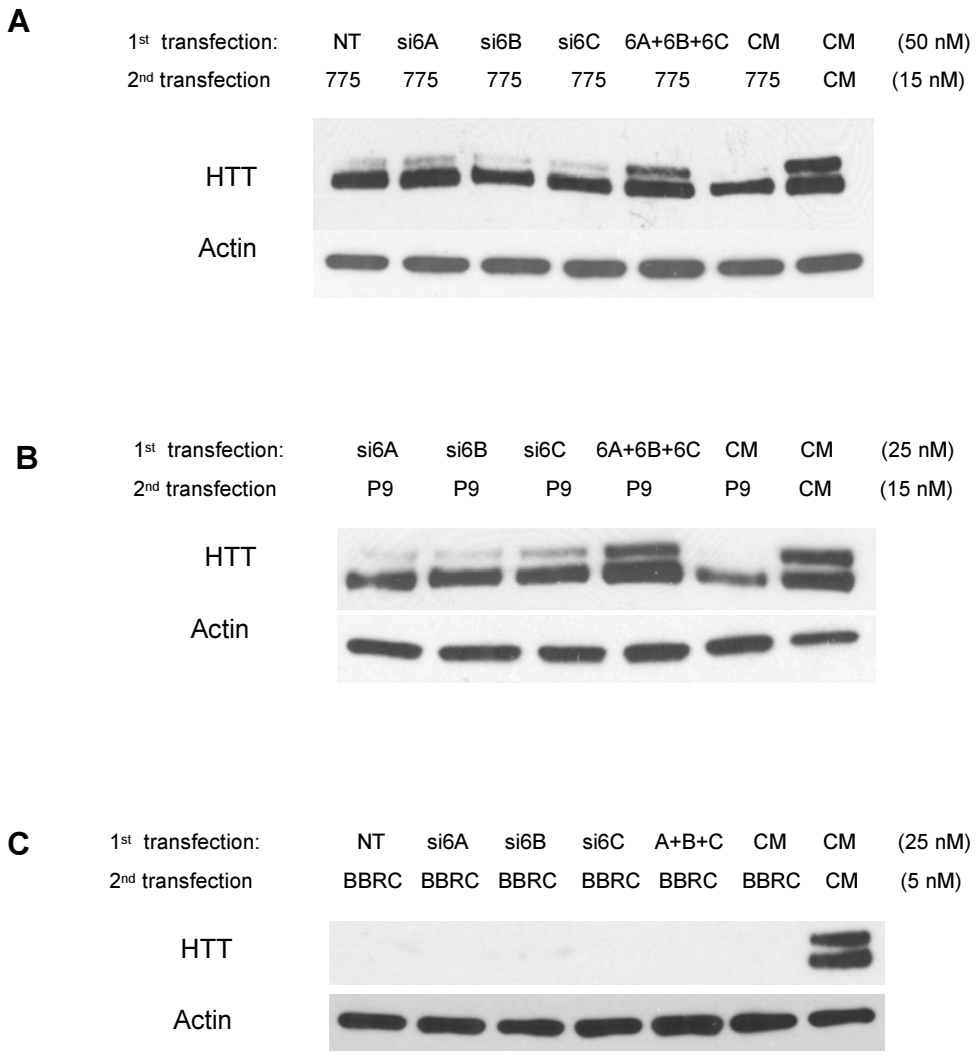

Figure 3-5. **TNRC6A-C knockdown in combination reversed HTT inhibition by CAG-targeting but not canonical siRNAs :** (A-B) Significant reversal of ss-si-RNA 537775 and P9 duplex-mediated HTT inhibition is observed when all three TNRC6 family proteins are reduced; (C) No reversal of BBRC-mediated HTT inhibition is seen when TNRC6A-6C levels are reduced.

P9: unmodified CAG-targeting duplex siRNA with mismatch at P9; 775: ss-si-RNA 537775 with mismatch at P9; CM: mismatched control; BBRC: siRNA targeting HTT outside of CAG-repeats; si6A: siRNA targeting TNRC6A/GW182; si6B: siRNA targeting TNRC6B; si6C: siRNA targeting TNRC6C; NT: no treatment.

Figure 3-6

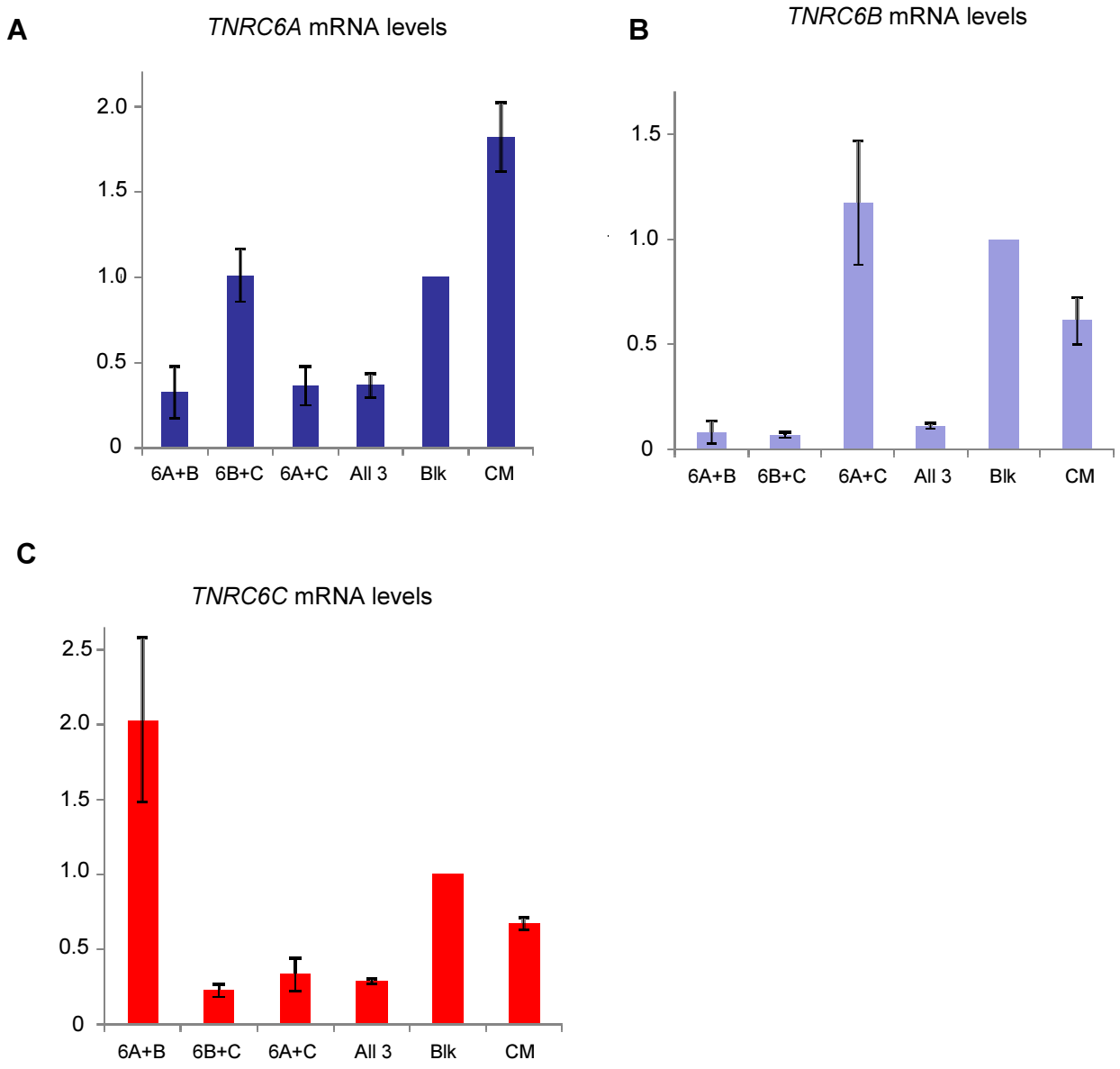

Figure 3-6. **TNRC6A, 6B, and 6C knockdowns in pairs by siRNA were efficient and specific:** (A-C) q-PCR showing reductions in *TNRC6A*, *6B*, and *6C* mRNA levels after treatment with siRNAs targeting each variant in pairs or all together at 25nM each.

si6A: siRNA targeting TNRC6A/GW182; si6B: siRNA targeting TNRC6B; si6C: siRNA targeting TNRC6C; NT/blk: no treatment/blank; CM: a mismatched control RNA.

Figure 3-7

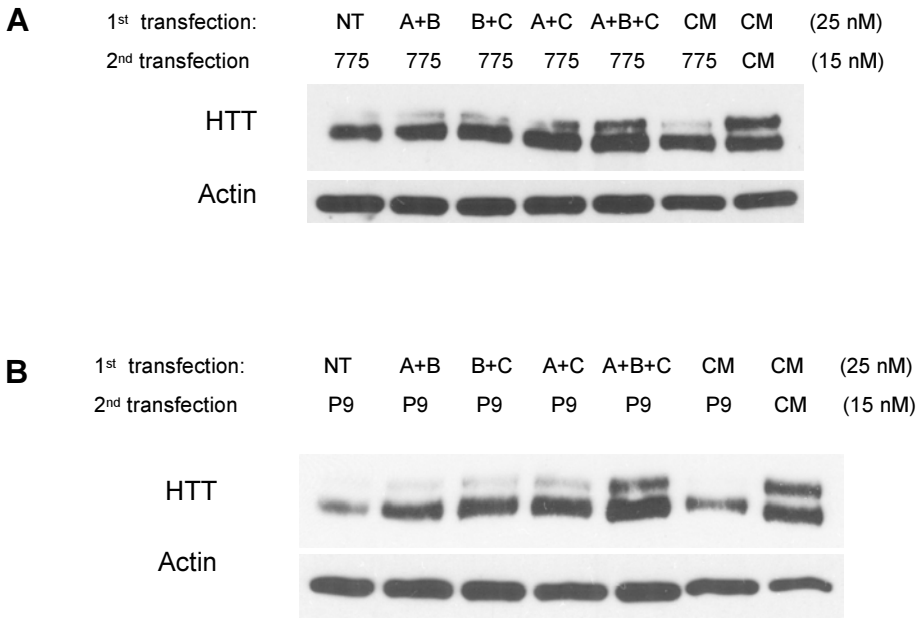

Figure 3-7. **Knockdown of all three TNRC6 paralogs but not two at a time reversed HTT inhibition by CAG-targeting siRNAs:** (A) Significant reversal of ss-si-RNA 775 and P9 duplex-mediated HTT inhibition is observed when all three TNRC6 family proteins are reduced but not from pair-wise knockdowns; (B) Similar observations were seen with P9-mediated HTT inhibition.

P9: unmodified CAG-targeting duplex siRNA with mismatch at P9; 775: ss-si-RNA 537775 with mismatch at P9; si6A: siRNA targeting TNRC6A/GW182; si6B: siRNA targeting TNRC6B; si6C: siRNA targeting TNRC6C; CM: mismatched control; NT: no treatment.

Figure 3-8

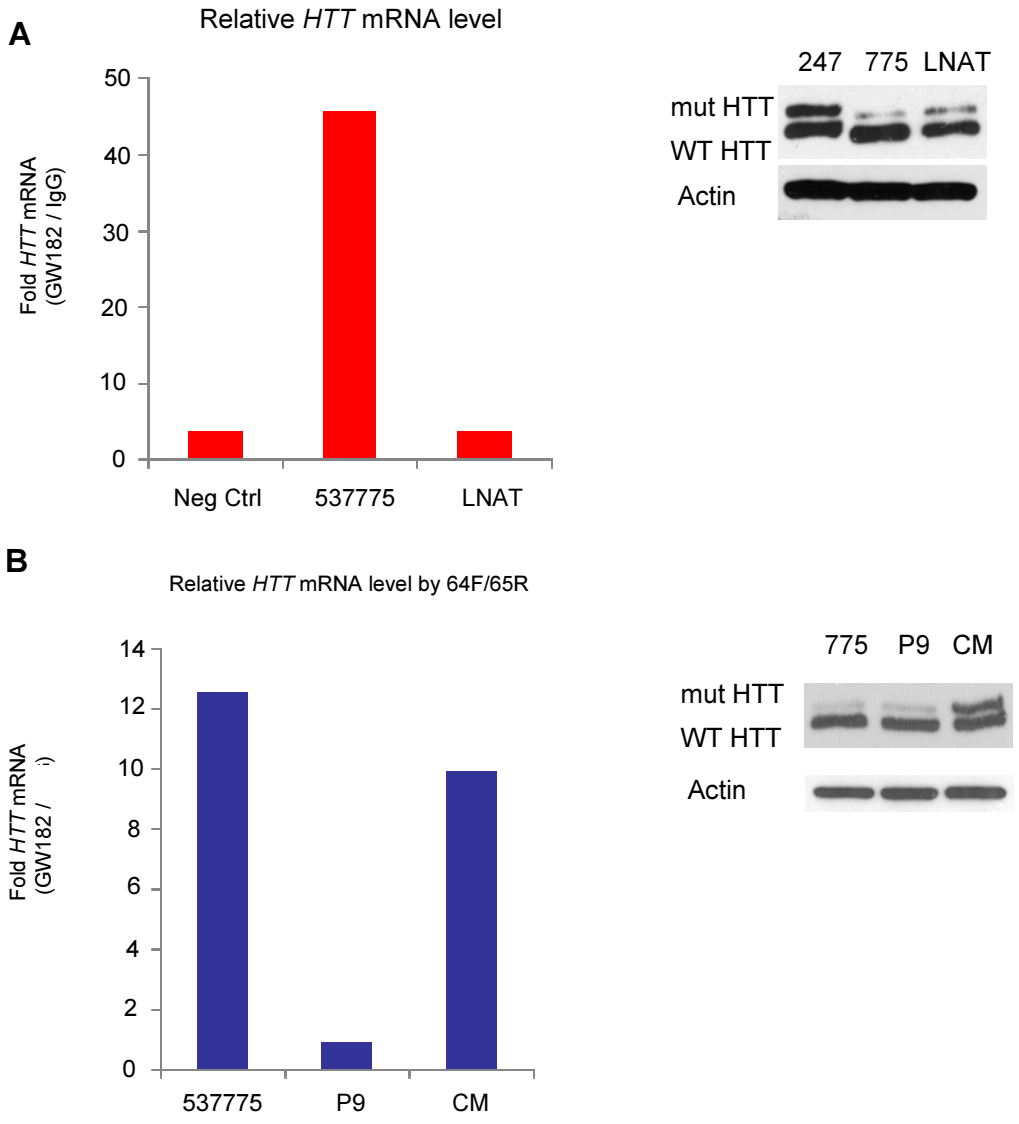

Figure 3-8. **TNRC6A/GW182 is strongly recruited to *HTT* mRNA by CAG-targeting single-stranded or duplex siRNA treatment:** (A) One experimental data set with 775, 247, and LNAT compared side-by side; (B) A second transfection with P9, CM, and 775 compared side-by side. Y-axis values correspond to fold-enrichment of *HTT* mRNA co-purifying with anti-GW182 versus IgG.

P9: unmodified CAG-targeting duplex siRNA with mismatch at P9; 775: ss-si-RNA 537775 with mismatch at P9; CM: mismatched dsRNA negative control; 247: ss-si-RNA 522247 that serves as negative control; LNAT: locked-nucleic acid-based ASO targeting CAG-repeat region.

Figure 3-8 (cont'd)

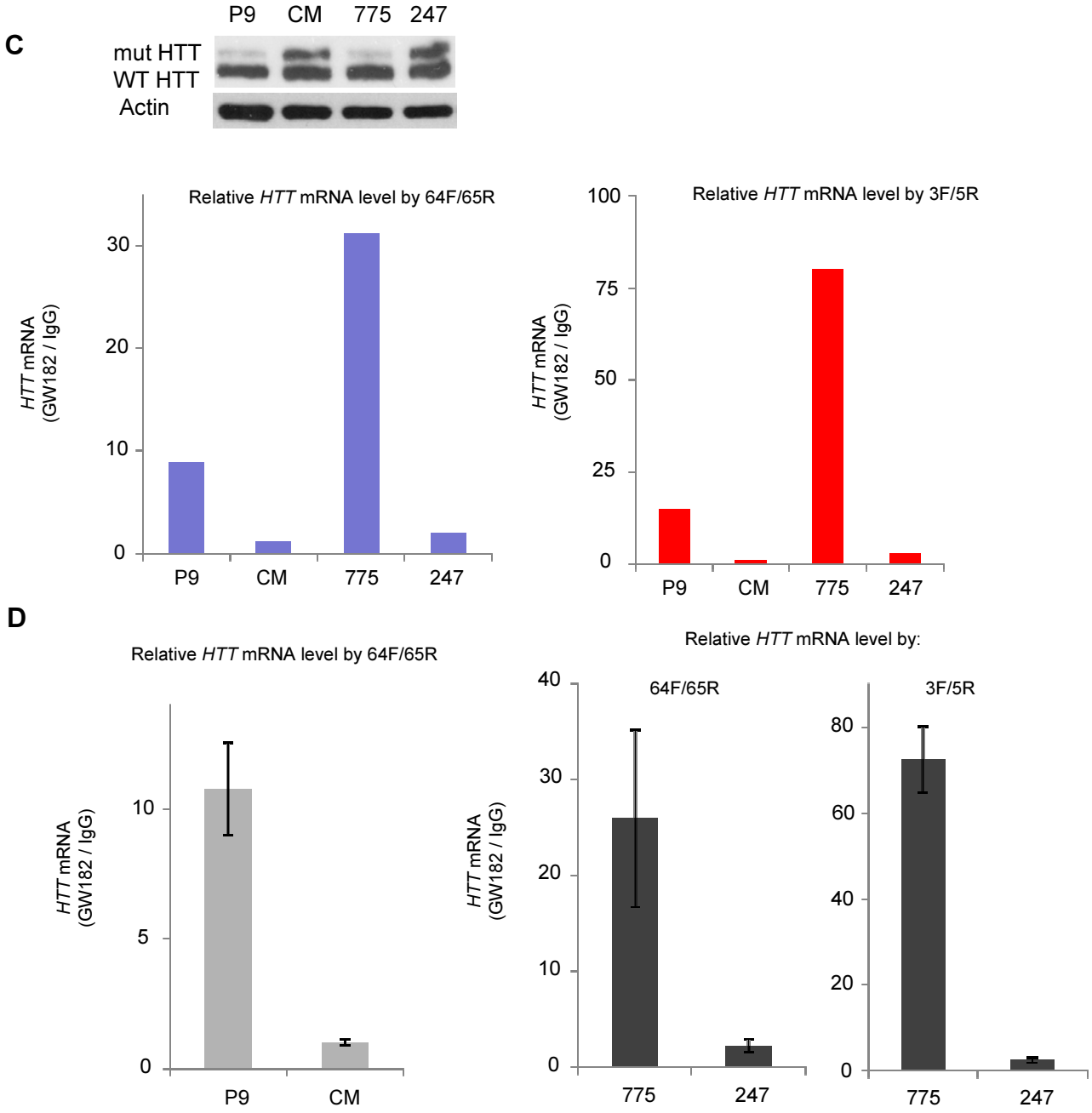

Figure 3-8 (cont'd). **TNRC6A/GW182 is strongly recruited to *HTT* mRNA by CAG-targeting single-stranded or duplex siRNA treatment:** (C) A third transfection with P9, CM, 775, and 247 compared side-by side. (D) Combined data showing relative enrichment of *HTT* mRNA by either P9 or 775 when compared to the ds- or ss-RNA controls.

Error bars represent standard error of the mean from two or more independent experiments. Y-axis values correspond to fold-enrichment of *HTT* mRNA co-purifying with anti-GW182 versus IgG. P9, 775, 247 and CM were explained on the previous page.

Figure 3-9

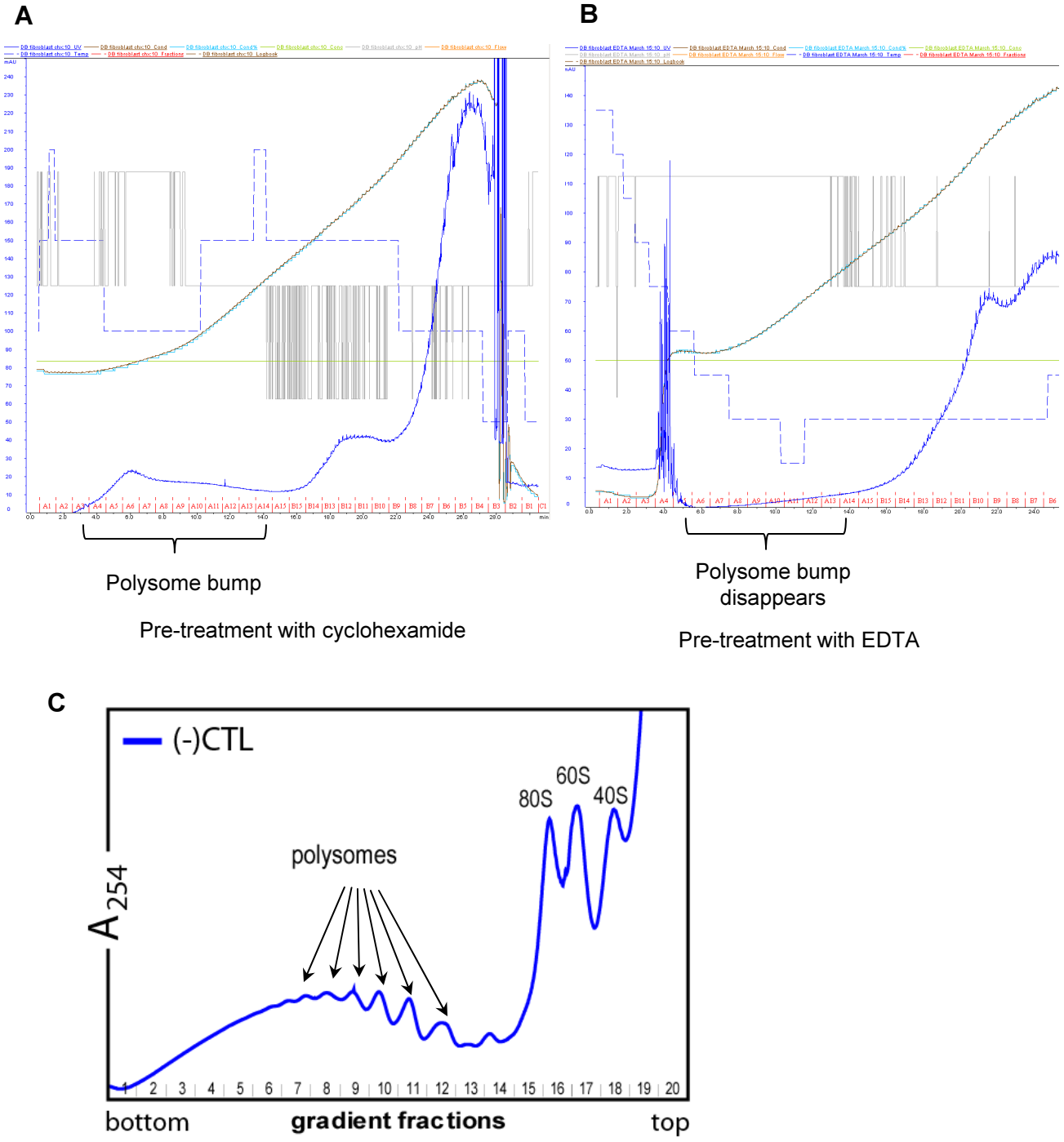

Figure 3-9. **Identification of polysome fraction on sucrose gradient as preliminary work to setting up polysome profiling:** (A) Treatment with cyclohexamide "fixes" the ribosomes on mRNAs and allow visualization and fractionation of the polysome fraction; (B) Treatment with EDTA, which chelates Ca^{2+} and disassembles ribosomes, makes the polysome bump vanish. (C) UV tracing plot by Dr. Keith Gagnon showing the polyribosome peaks

CHAPTER FOUR

Potent and Allele-selective Inhibition of Ataxin-3 by Chemically Modified Single-stranded RNAs That Target CAG Repeats

ABSTRACT

Spinocerebellar ataxia type 3 (SCA3) is an incurable neurological disorder caused by CAG-expansion in exon 10 of the gene *ATAXIN-3* (*ATXN3*/*MJD1*). Studies in animal models have shown that eliminating the mutant, glutamine-expanded ataxin-3 protein could cure the disease. Chemically modified, single-stranded small-interfering RNAs (ss-siRNA) that target CAG repeats have been previously demonstrated to potently and selectively inhibit expression of the mutant allele of *HUNTINGTIN* (*HTT*). Here, we show that a subset of CAG-targeting ss-siRNAs are also potent and allele-selective inhibitors of mutant ataxin-3. As anti-HTT agents, they do not adversely reduce the level of wild-type ataxin-3 in HD-patient-derived cells. As novel anti-ATXN3 agents, they inhibit expression of mutant ataxin-3 with low nM IC_{50} and an allele-selectivity up to 8-fold in SCA3-patient-derived cells. ATXN3-inhibition by ss-siRNAs appears to occur at the translational level; it proceeds through RNA interference (RNAi) in the absence of a passenger strand and involves Ago2 and GW182 proteins. Interestingly, unlike duplex siRNAs, a number of CAG-targeting ss-siRNAs that are good selective HTT inhibitors turn out to lack selectivity against ATXN3. This observation suggests that sequences flanking CAG-repeats are important determinants of gene-specific susceptibility to inhibition, and it highlights potential mechanistic differences between regular siRNAs and modified ss-siRNAs.

INTRODUCTION

Spinocerebellar ataxia type 3 (SCA3), commonly known as Machado-Joseph's Disease (MJD), is a dominantly inherited, incurable neurological disorder. It is one of at least 24 spinocerebellar ataxia syndromes and has the highest prevalence worldwide (Schöls et al, 2004). The disease itself is characterized by a number of symptoms, including cerebellar ataxia, pyramidal and extrapyramidal signs, peripheral neuropathy, and ophthalmoplegia. Like Huntington's disease (HD), SCA3 is a trinucleotide repeat expansion disorder, caused by expanded CAG in the gene *MJD1* (also known as *ATAXIN-3*) that encodes ataxin-3 protein. Wild-type *ataxin-3* allele contains 13-36 copies of CAG, while this number increases to 62-84 in MJD patients (Kawaguchi et al, 1994). The resulting glutamine-expanded peptide forms intranuclear inclusions inside neurons and induces cellular toxicity (Paulson et al, 1997).

Transgenic mice that overexpress expanded ATXN3 recapitulate MJD phenotype (Ikeda et al, 1996; Cemal et al, 2002). Importantly, disease progression can be reversed in a conditional mouse model by turning off mutant ataxin-3 even after symptomatic onset (Boy et al, 2009), suggesting that targeting ataxin-3 could lead to curative therapy. One powerful tool for achieving gene-specific repression is siRNA, which has seen considerable progress in drug development against neurodegenerative disorders such as Huntington's disease (HD) and amyotrophic lateral sclerosis (ALS) (Boudreau et al, 2009; Ding et al, 2003; Drouet al, 2009).

The vast majority of MJD patients are heterozygous at the *ATXN3* locus, and the need to maintain wild-type ataxin-3 expression for potential SCA3 therapeutics has been debated. On one hand, rare cases of homozygous individuals have been reported, who developed SCA3 at earlier onset with more severe disease progression (Lang et al, 1994; Carvalho et al, 2008), and one study using a *Drosophila* SCA3 model showed that wild-type ataxin-3 helped suppress

polyglutamine toxicity (Warrick et al, 2006). On the other hand, *ATXN3* knockout mice appeared healthy and fertile with normal life-span (Schmitt et al, 2007; Switonski et al, 2011), and work using a SCA3 rat model showed that the disease phenotype was neither exacerbated by WT ataxin-3 depletion nor improved by WT ataxin-3 overexpression (Alves et al, 2010).

Two groups designed allele-selective siRNA/shRNAs against mutant *ATXN3* mRNA by taking advantage of a strong G/C SNP linkage disequilibrium at 3' end of the CAG repeat tract (Miller et al, 2003; Alves et al, 2008). Both allele-selective and non-allele-selective reductions of ataxin-3 by lentiviral transduced shRNAs were shown to significantly improve neuropathology in SCA3 mouse models (Alves et al, 2008; Alves et al, 2010). While these results suggest that wild-type ataxin-3 is dispensable for normal functions, it is unknown whether a lack of overt defects from wild-type ataxin-3 depletion in rodent models necessarily translates into clinical safety in human patients, especially if long-term, high-dosage treatment is needed. Therefore, allele-selective inhibitors of ataxin-3 may prove to be important in SCA3 drug development.

The aforementioned SNP site covers about 70% of MJD patients in some populations, leaving a third of the patients in need of alternative drugs. To identify a comprehensive allele-selective inhibitor, we have exploited a universal difference between normal and diseased individuals, the difference in CAG repeat expansion length, by developing siRNAs that directly target the poly-CAG tract. While an siRNA duplex fully complementary to the CAG repeats was non-selective, additional siRNA duplexes with central mismatched bases exhibited potent and highly selective inhibition of mutant ataxin-3 (Hu et al, 2009; Hu et al, 2011). Similarly high potency and allele-selectivity had previously been observed and validated with the same set of siRNAs in targeting the mutant *Huntingtin* (*HTT*) allele (Hu et al, 2009; Hu et al, 2011), making these oligomers potentially multi-functional agents against several polyglutamine diseases.

One persistent challenge in the RNAi therapeutics field is that of *in vivo* delivery, as RNA duplexes are often unstable and have sub-optimal tissue uptake and distribution. Two recent studies demonstrated that a class of chemically modified, single-stranded small-interfering RNAs (ss-siRNAs) can efficiently engage endogenous RNAi pathway and achieve robust gene inhibition without passenger strands (Lima et al, 2012; Yu et al, 2012). ss-siRNAs that target CAG repeats were shown to be potent and allele-selective inhibitors of HTT both in cell-culture and *in vivo*, where ventricular infusion by osmotic pump without formulation led to mutant HTT reduction throughout the mouse brain (Yu et al, 2012).

In addition to Argonaute proteins, one other factor that has been implicated in mediating miRNA-induced translational inhibition is GW182 (also known as TNRC6A). GW182 contains multiple glycine/tryptophan (GW) repeats (Estathioy et al, 2002) and co-localizes with endogenous Ago proteins loaded with miRNAs (Jakymiw et al, 2005; Liu et al, 2005; Landthaler et al, 2008). Structural studies have shown that the N- and C-terminal domains of GW182 independently mediate Ago-interaction and translation inhibition (Lazzaretti et al, 2009).

Here, we show that some CAG-targeting ss-siRNAs are potent and selective inhibitors of mutant ataxin-3. ss-siRNA associates with Ago2 and recruits it to *ATXN3* mRNA, and the mechanism of inhibition appears to occur at the translational inhibition that may involve GW182 protein. The selectivity against *ATXN3* depends on the individual ss-siRNA sequence. A number of ss-siRNAs were found to be poorly allele-selective compared to duplex siRNAs of identical sequences. Along with the observation that ss-siRNAs but not dsRNAs produce a faster migrating ataxin-3 band, these results underlie potential mechanistic differences between the two classes of siRNAs despite sharing key players of a common pathway.

RESULTS

CAG-targeting ss-siRNAs Can Allele-selectively Inhibit Mutant Ataxin-3 in SCA3 cells

We had previously shown that siRNA duplexes and chemically modified ss-siRNAs of sequences complementary to poly-CAG repeats were highly selective inhibitors against mutant HTT (Hu et al, 2009; Yu et al, 2012). We started by testing ss-siRNA 537775, which has mismatch at P9 in its $(CUG)_7$ sequence, in the GM06151 SCA3-patient-derived fibroblasts. This cell line has a 74-CAG-repeat mutant *ATXN3* allele and a 24-CAG-repeat wild-type *ATXN3* allele, making it an ideal model for assaying selective inhibition. By separating mutant and wild-type ataxin-3 bands on SDS-PAGE based on molecular weight difference from poly-glutamine expansion, we observed that 537775 inhibited mutant ataxin-3 expression with high potency (IC_{50} ~ 2.9 nM) and good allele-selectivity (8-fold; Figure 4-1A). Another ss-siRNA 580940, which is identical to 53775 except with a 3'-biotin tag, also robustly and selectively inhibited mutant ataxin-3 (IC_{50} ~5.1 nM and selectivity ~ 5-fold, Figure 4-1B), confirming that CAG-targeting ss-siRNAs with P9 mismatch are potent and selective ataxin-3 inhibitors.

Our work in targeting HD patient-derived fibroblasts had shown that 537775 possessed better allele-selectivity in discriminating between mutant and wild-type HTT alleles (>30-fold) than what we observed for ATXN-3 (~8-fold). One concern in the application of CAG-targeting ss-siRNAs in HD treatments is that they might inadvertently diminish the expression of other poly-glutamine containing genes such as *ATXN3*. To test whether CAG-targeting ss-siRNAs are sufficiently selective against ATXN3 at doses needed for efficient HTT inhibition, we measured the expression of ataxin-3 by western blot in a HD-patient cell-line GM04281 (heterozygous at *HTT* locus but containing two wild-type *ATXN3* alleles) after treatment with ss-siRNA 537775 or 580940. Neither ss-siRNA reduced ataxin-3 expression at concentrations up to 50nM (Figure 4-

1C and D), while only 2-5nM was needed to eliminate the majority of the mutant HTT (Yu et al, 2012; see also Chapter 1, Figure 1-1B and Chapter 3, Figure 3-1A). Therefore, 537775 and its P9-mismatched homologues do not appear to affect the levels of ataxin-3 or other polyglutamine-containing genes at concentrations needed for efficient HTT inhibition (Yu et al, 2012; see also Chapter 1, Figure 1-3E and Figure 1-9).

ss-siRNAs Exhibited Reduced Selectivity against ATXN3 Compared to HTT

To more thoroughly test whether CAG-targeting ss-siRNAs are allele-selective inhibitors of ataxin-3, we transfected ss-siRNA 537787 (no mismatch) and 537786 (a single mismatched base at position 10) into SCA3 patient cells. Unlike 537775, these two ss-siRNAs strongly inhibited both alleles (Figure 4-2A and B). We also measured ataxin-3 protein expression in HD fibroblasts treated with 537787 and 537786. In agreement with results from SCA3 fibroblasts, there is noticeable reduction of ataxin-3 in HD fibroblasts (which have two copies of wild-type *ATXN3*) at concentrations ≥ 16.7nM (Figure 4-2C and D).

In addition to the lack of selectivity by 537787 and 537786, we observed the appearance of a faster migrating third band around 37kD, and its intensity correlates proportionally to the degree of ataxin-3 knockdown. Investigation into the identity of this faster migrating third band will be discussed in greater details in Chapter 5. In a simplified view, this band serves as a sensitive indication of non-selective ataxin-3 reduction, since its presence is much weaker when cells are treated with more selective ss-siRNAs like 537775.

Our previous work had shown that 537787 and 537786 were both selective ss-siRNAs against HTT, with allele-selectivity of >13-fold and >4-fold, respectively (Chapter 1, Table 1-1). These results suggest that depending on the oligomer sequence, some ss-siRNAs may be

selective against HTT but not ATXN3. Another striking example is the ss-siRNA 557426, which contains three central mismatches. While it possesses an IC_{50} of 3.3nM and >30-fold allele-selectivity against HTT (Figure 4-3B, also Yu et al, 2012), it is a much weaker inhibitor against ataxin-3 (IC_{50} > 20nM) and has no selectivity (Figure 4-3A). Such gene-dependent behavior could arise from different local folding between *HTT* and *ATXN3* mRNAs. The poly-CAG stretch of the transcript has been reported to form higher-order structures such as stem loops (de Mezer et al, 2011). It is conceivable that differences in sequences flanking the repeats leads to differential mRNA conformations and susceptibility towards ss-siRNA-mediated inhibition, the degree of which may depend on the exact position of the mismatched base(s) on the ss-siRNA.

Chemical Modifications May Affect ss-siRNA Potency Compared to Unmodified Duplex siRNA

The differential behavior of some ss-siRNAs in inhibiting HTT versus ATXN3 is somewhat surprising, as unmodified CAG-targeting dsRNAs tended to maintain similarly high selectivities against both genes (Hu et al, 2009; Hu et al, 2011). While 537775 does not greatly differ from the P9 duplex in repressing ATXN3 (Figure 4-2A and E), 537787 (no mismatch) contrasts starkly with that of unmodified REP duplex (no mismatch, Figure 4-3B). As another example, ss-siRNA 557409 (mismatched bases at positions 9 and 10), which only has 3-fold selectivity (Figure 4-3C) against ATXN3, differs significantly from P910 duplex (>16-fold allele-selectivity; Figure 4-3D). Of note, the high mobility third band only appears with ss-siRNA treatment; no unmodified dsRNA has ever produced this band (Figure 4-2E, 4-3C and D). These differences suggest that chemical modifications associated with ss-siRNAs may alter their

functional profiles away from their unmodified dsRNA counterparts; the degree of deviation seems to depend on the exact sequence as well as the identity of each individual gene target.

Ataxin-3 Inhibition by ss-siRNAs Involves Ago2 and Proceeds through RNAi

Canonical siRNAs are 21-22 nt double-stranded duplexes comprising of a guide strand and a passenger strand. Our previous work demonstrated that ss-siRNAs (which resemble chemically modified guide strands) achieved HTT inhibition by loading into Ago2/RISC and engaging endogenous RNAi pathway (Yu et al, 2012). To determine whether ATXN3-inhibition by ss-siRNA goes through a similar pathway, we used siRNAs to knock down expression of each one of the four human Ago proteins (Ago1–4) and then treated SCA3 fibroblasts with either ss-siRNA 537775 or unmodified duplex P910. Ago2 reduction had the greatest effect, as *ATXN3* inhibition was mitigated and allele-selectivity was lost (Figure 4-4A and B). These data suggest that Ago proteins, in particular Ago2, are required for ATXN3-inhibition by CAG-targeting duplex and ss-siRNAs.

To test whether there is physical association between ss-siRNA and Ago2, we transfected SCA3 cells with 3'-biotinylated ss-siRNA 580940 (mismatched at position 9). Western blots showed clear selective inhibition of ataxin-3 by 580940 (Figure 4-4C), and biotin pull-down was performed using streptavidin-coated beads. Western blots showed that Ago2 co-purified with ss-siRNA from elutants of 580940-treated cell extract but not in non-treated samples (Figure 4C), demonstrating a stable association between ss-siRNA and Ago2 inside cells. On the other hand, another known RNAi factor, C3PO, was not detected by immunoblotting after streptavidin pulldown of 580940-treated fibroblasts (see also Chapter 3, Figure 3-1 and 3-3).

To test whether Ago2 is recruited to *ATXN3* mRNA upon ss-siRNA treatment, we performed RNA-immunoprecipitation (RIP). ss-siRNA-treated SCA3 cells were harvested and cellular extract precipitated with either anti-Ago2 antibody or normal mouse IgG. The eluted RNA was reverse-transcribed into cDNA and the relative amount of *ATXN3* transcript was determined by q-PCR. Significant enrichment of *ATXN3* mRNA was found in RNA co-purifying with anti-Ago2 over IgG background after treatment with 537775, but not with a control ss-siRNA that does not target either CAG repeats or *ATXN3* (Figure 4-4D). These results suggest that Ago2 is recruited to target transcript upon transfection of active ss-siRNA, further supporting an RNAi-based mechanism of ATXN3 inhibition.

ATXN3-inhibition by ss-siRNAs Appears to Occur at the Translational Level and May Involve GW182

To test whether *ATXN3* mRNA itself is targeted for degradation, we performed q-PCR on RNA extracted from ss-siRNA-treated SCA3 fibroblasts. While a non-selective siRNA duplex (siAX2) that targets outside of CAG repeats reduced *ATXN3* mRNA by >80% relative to non-treated sample, ss-siRNA 537775 did not reduce *ATXN3* mRNA at concentrations up to 50nM (Figure 4-4E), a dose where most mutant ATXN3 protein is gone (Figure 4-1A and 4-1E). These results suggest that ss-siRNA does not cause cleavage of *ATXN3* mRNA, and gene repression occurs at the translational level without transcript degradation. This observation is in agreement with our previous work that showed CAG-targeting ss-siRNAs inhibited HTT expression by translational block (Yu et al, 2012; Hu, Liu et al, 2012).

Work in our lab showed that GW182 likely plays an essential role in mediating HTT inhibition by CAG-targeting siRNAs (Hu, Liu et al, 2012; also see Chapter 3). To test whether

GW182 is involved in ATXN3 inhibition by ss-siRNA, we performed RIP using rabbit polyclonal antibody against GW182 and measured the amount of recovered *ATXN3* mRNA by q-PCR. We saw a significant enrichment of *ATXN3* mRNA after immunoprecipitation by anti-GW182 over that of IgG control in extract of cells treated with 537775 but not with a control ss-siRNA (Figure 4-5A). These results demonstrate that like Ago2, GW182 is recruited to *ATXN3* target transcript by ss-siRNA and is a potential mediator of inhibition.

Depletion of GW182/TNRC6 Family Proteins Reversed ATXN3-inhibition by CAG-targeting Duplex siRNA but Not ss-siRNA

To examine the functional requirement for GW182/TNRC6A and its two mammalian paralogs TNRC-6B and -6C in ATXN3 inhibition, we used siRNA to knock down expression of the three variants either individually or in combination. Knockdown efficiency and specificity were verified by western blot and q-PCR (Figure 4-5B and C), and blotting with Ago2 and ataxin-3 antibodies showed no loss of expression. When SCA3 cells were treated with siRNAs after TNRC6 depletions, we observed a reversal in ATXN3-inhibition by unmodified P9 duplex but not by ss-siRNA 537775 (Figure 4-6A and B). The reversal occurred only after all three TNRC6 paralogs were depleted and not with knocking down any two of the three (Figure 4-6C and D). In agreement with previous findings that TNRC6 paralogs are specifically involvement in translation- but not cleavage-based inhibition, depleting TNRC6 proteins did not reverse ATXN3 inhibition by a canonical duplex siRNA targeting ATXN3 outside of poly-CAG region (Figure 4-6E).

DISCUSSION

There are at least nine polyglutamine neurodegenerative diseases whose shared genetic cause is expansion of CAG repeats within coding genes, and in many cases the wild-type proteins are known to play important functions. In theory, CAG-targeting siRNAs could be a universal treatment to all of them if their proven potency and allele-selectivity against HTT were transposable to all other disease-inducing genes. While a number of unmodified dsRNAs displayed excellent allele-selectivity in both HTT and ATXN3, the picture is starkly different with chemically modified ss-siRNAs. We observe a much more diminished repertoire of ss-siRNAs that can satisfy selectivity requirement for both genes, and the degree of functional similarity between the two may depend on the local structure and topology of the mRNA targets, some of which may be more sensitive to the chemical modifications present on ss-siRNAs. Nonetheless, a subset of ss-siRNAs appeared to retain sufficient allele-selectivity in SCA3 cells to merit consideration as novel SCA3 therapeutic candidates, and future work is needed to explore whether changing or removing certain chemical modifications, coupled with additional sequence permutations, could identify more selective *ATXN3* ss-siRNA inhibitors.

While the functional differences between ss-siRNA and dsRNA pose special challenges to their therapeutic applications, they also present several exciting mechanistic puzzles. What is the magic switch that renders an siRNA duplex highly selective, while its modified "half-brother" ss-siRNA has no selectivity at all? What molecular players are at stake and what modifications (if any) are responsible? For instance, it is surprising that no change was seen for ss-siRNA-mediated ATXN3 inhibition after TNRC6 depletion while a significant reversal was observed for unmodified duplex CAG-targeting siRNA. This result appears at odd with prior findings that GW182 is recruited to *ATXN3* mRNA with ss-siRNA treatment (Figure 4-4E) and

that it is required for HTT-inhibition by CAG-targeting ss-siRNA and duplex siRNA alike (see Chapter 3). Furthermore, the appearance of a faster migrating band specific to ss-siRNA- but not dsRNA-treatment points to a fundamental mechanistic difference between the two classes of homologous oligomers. The identification of this unknown peptide and its genesis would provide valuable insight into the mechanism of ss-siRNA-mediated inhibition (see Chapter 5 for details) and help guide future ss-siRNA designs and development.

.

FUTURE DIRECTIONS

Altering Chemical Modifications on ss-siRNA to Improve Allele-selectivity in ATXN3

While the chemical make-up of ss-siRNA has proven effective in designing inhibitors against *HTT* and *PTEN* both in cell culture and *in vivo* (Lima et al, 2012; Yu et al, 2012), it appears sub-optimal for targeting *ATXN3*. Since many combinations of chemical modifications are possible, it would be worthwhile re-designing and testing other patterns of modifications on ss-siRNA and identify new ones that more closely recapitulate duplex siRNA function in a broader range of gene targets. This direction is currently being pursued jointly by our collaborators at ISIS Pharmaceuticals and our lab.

Characterizing Functional Differences between ss-siRNA and dsRNA in SCA3 Cells

From a basic science point of view, the functional difference between ss-siRNA and dsRNA is fascinating and may shed light on yet unknown aspects of RNAi mechanism. The reduced allele-selectivity by ss-siRNA (2-8 fold) mirrors the value from antisense oligonucleotide (ASO), arguing that the modifications on ss-siRNA confer some degree of residual ASO-like properties. Supporting this notion is the observation that CAG-targeting PNAs could also induce the faster-migrating band, albeit much less efficiently (Dr. Jiaxin Hu, unpublished data). Yet at the same time, previous structure-relationship studies argued against ss-siRNA as ASO mimics (Chapter 2). In addition, several lines of mechanistic data in ATXN3 (Figures 4-4 and 4-5) suggest that Ago2 and RNAi are involved by ss-siRNA, although the picture is complicated by the inconclusive requirement for TNRC6 family proteins.

To elucidate the interplay between RNAi and direct oligomer binding, *in vitro* binding studies may need to be performed to characterize ss-siRNA's ability to bind *ATXN3* mRNA outside the context of RNAi. Loading and competition assays can help determine the preference of ss-siRNA as Ago2-bound versus as unbound species, as well as the relative affinities of *ATXN3* mRNA for ss-siRNA-loaded RISC versus ss-siRNA by itself. It may also be worthwhile to test CAG-targeting ss-siRNAs in cell lines of various CAG repeat lengths to explore whether selectivity depends on the number of repeats.

Characterizing Differences in mRNA Folding between *HTT* and *ATXN3* Transcripts

One possible explanation for different inhibitory outcomes of ss-siRNA in HTT versus ATXN3 is the mRNA folding determined by gene-specific flanking sequences. Preliminary data from our collaborators using selective 2'-hydroxyl acylation analyzed by primer extension (SHAPE) technology has shown that the surface accessibility of *HTT* mRNA drops dramatically around the CAG-repeat stretch (unpublished data from the laboratory of Dr. Kevin Weeks, UNC Chapel Hill). It would be interesting to see *ATXN3* mRNA behaves similarly around its CAG repeats. To examine how *HTT* and *ATXN3* transcripts give divergent functional profiles for ss-siRNA but not dsRNA, *in vitro* binding assays may need to be performed using pre-loaded recombinant hAgo2 proteins. Circular dichroism and NMR may also be employed to study binding characteristics between mRNA substrate and Ago2 loaded with ss-siRNA versus unmodified siRNA. A crystal structure of such a complex could be key in ultimately solving the puzzle.

Expanding ss-si-RNAs to Additional Applications

The stability and loading efficiency of chemically modified ss-siRNA make it a powerful tool in many areas beyond targeting triplet-expansion-disease genes. One obvious extension would be to design single-stranded RNAs of the same chemical modifications with known miRNA sequences that target 3'-UTR and see if they are active oligomers. Also, our lab had shown that promoter-targeted antigene RNA duplexes (agRNAs) can efficient inhibit or activate transcription of several genes. Work from our lab (Matsui et al, 2012) found that similar inhibition can be achieved using chemically modified ssRNAs without a passenger strand, therefore establishing the utility of ssRNAs in nuclear processes. For instance, we could use modified ssRNAs to target long-noncoding RNAs (lincRNAs) such as Xist and HotAir to modulate transcription, X-inactivation and embryonic development, target pri-miRNA to modulate miRNA maturation by Drosha, and target centromeric and telomeric regions of the chromosome to modulate cell division and ageing. As another set of examples, duplex miRNAs have been implicated in additional biological processes such as DNA methylation (Gagnon and Corey, 2012) and splicing (Liu et al, 2012), some of which have urgently unmet therapeutic needs such as in Duchenne muscular dystrophy (Goemans et al, 2009; Kinali et al, 2009). Recapitulating these processes using modified ssRNAs would not only introduce a novel class of oligomers with more drug-like properties, but also offer a new tool to dissect the mechanisms from angles unattainable in the past, such as RNAi in the absence of passenger strands. ss-siRNAs could also be explored as novel antagomirs that more efficiently target and degrade endogenous miRNAs due to its ability to recruit Ago proteins, with a wide range of research and clinical purposes such as regulating oncogene expression for cancer therapy (Krützfeldt et al, 2005).

MATERIALS AND METHODS

ss-siRNA, antibodies, cell culture and transfection, analysis of HTT/ATXN3 expression, IC_{50} and selectivity calculations, q-PCR, and RNA immunoprecipitation

The materials and protocols for the above experiments are identical to those used for the Huntingtin projects (Chapters 1-3) and may be referenced accordingly. One additional cell-line is SCA3/MJD patient derived fibroblast cell-line GM06151, which is maintained under the same conditions as HD-patient-derived fibroblasts. One additional siRNA not described before is siAX2 that targets *ATXN3* outside of CAG repeat region for cleavage-mediated gene inhibition. Its sequence is as follows: 5'-GGACAGUUCACAUCCAUTT-3' (sense strand) and 5'-AUGGAUGUGAACUCUGUCCTT-3' (antisense strand).

Two pairs of qPCR primers were used to measure *ATXN3* mRNA level. Primer pair 3F/4R targets the junction of exon 3 and 4 and has the following sequences: 5'-GGAAATATGGATGACAGTGG-3' (forward primer) and 5'-ATCCTGAGCCTCTGATACTC-3' (reverse primer). Primer pair 7F/8R targets the junction of exon 7 and 8 and has the following sequences: 5'-AGATGATTAGGGTCCAACAG-3' (forward primer) and 5'-TAACACTCGTTCCAGGTCTG-3' (reverse primer).

REFERENCES

Alves, S., Nascimento-Ferreira, I., Auregan, G., Hassig, R., Dufour, N., Brouillet, E., Pedroso de Lima, M.C., Hantraye, P., Pereira de Almeida, L., and Déglon, N. (2008) Allele-specific RNA silencing of mutant ataxin-3 mediates neuroprotection in a rat model of Machado-Joseph disease. PLoS One. *3*, e3341

Alves, S., Nascimento-Ferreira, I., Dufour, N., Hassig, R., Auregan, G., Nóbrega, C., Brouillet, E., Hantraye, P., Pedroso de Lima, M.C., Déglon, N., and de Almeida, L.P. (2010) Silencing ataxin-3 mitigates degeneration in a rat model of Machado-Joseph disease: no role for wild-type ataxin-3? Hum Mol Genet. *19*, 2380-9

Boy, J., Schmidt, T., Wolburg, H., Mack, A., Nuber, S., Böttcher, M., Schmitt, I., Holzmann, C., Zimmermann, F., Servadio, A., and Riess, O. (2009) Reversibility of symptoms in a conditional mouse model of spinocerebellar ataxia type 3. Hum Mol Genet., *18*, 4282-95

Boudreau, R.L., McBride. J.L., Martins, I., Shen, S., Xing, Y., Carter, B.J., and Davidson, B.L. (2009) Nonallele-specific silencing of mutant and wild-type huntingtin demonstrates therapeutic efficacy in Huntington's disease mice. Mol Ther. *17*, 1053-63

Butland, S.L., Devon, R.S., Huang, Y., Mead, C.L., Meynert, A.M., Neal, S.J., Lee, S.S., Wilkinson, A., Yang, G.S., Yuen, M.M., Hayden, M.R., Holt, R.A., Leavitt, B.R., and Ouellette, B.F. (2007) CAG-encoded polyglutamine length polymorphism in the human genome. BMC Genomics.*8*, 126.

Carvalho, D.R., La Rocque-Ferreira, A., Rizzo, I.M., Imamura, E.U., and Speck-Martins, C.E. (2008) Homozygosity enhances severity in spinocerebellar ataxia type 3. Pediatr Neurol. *38*, 296-9.

Cemal, C.K., Carroll, C.J., Lawrence, L., Lowrie, M.B., Ruddle, P., Al-Mahdawi, S., King, R.H., Pook, M.A., Huxley, C., and Chamberlain, S. (2002) YAC transgenic mice carrying pathological alleles of the MJD1 locus exhibit a mild and slowly progressive cerebellar deficit. Hum Mol Genet. *11*, 1075-94.

de Mezer, M., Wojciechowska, M, Napierala M, Sobczak K, Krzyzosiak WJ. (2011) Mutant CAG repeats of Huntingtin transcript fold into hairpins, form nuclear foci and are targets for RNA interference. Nucleic Acids Res. *39*, 3852-63

Ding, H., Schwarz, D.S., Keene, A., Affar, el B., Fenton, L., Xia, X., Shi, Y., Zamore, P.D., and Xu, Z. (2003) Selective silencing by RNAi of a dominant allele that causes amyotrophic lateral sclerosis. Aging Cell. *2*, 209-17

Drouet, V., Perrin, V., Hassig, R., Dufour, N., Auregan, G., Alves, S., Bonvento, G., Brouillet, E., Luthi-Carter, R., Hantraye, P., and Déglon, N. (2009) Sustained effects of nonallele-specific Huntingtin silencing. Ann Neurol. *65*, 276-85

Eystathioy, T., Chan, E.K., Tenenbaum, S.A., Keene, J.D., Griffith, K., and Fritzler, M.J. (2002) A phosphorylated cytoplasmic autoantigen, GW182, associates with a unique population of human mRNAs within novel cytoplasmic speckles. Mol. Biol. Cell. *13*, 1338-51

Gagnon, K.T. and Corey, D.R. (2012). Argonaute and the nuclear RNAs: new pathways for RNA-mediated control of gene expression. Nucleic Acids Res. *22*, 3-16.

Goemans, N.M., Tulinius, M., van den Akker, J.T., Burm, B.E., Ekhart, P.F., Heuvelmans, N., Holling, T., Janson, A.A., Platenburg, G.J., Sipkens, J.A., Sitsen, J.M., Aartsma-Rus, A., van Ommen, G.J., Buyse, G., Darin, N., Verschuuren, J.J., Campion, G.V., de Kimpe, S.J., and van Deutekom, J.C. (2011). Systemic administration of PRO051 in Duchenne's muscular dystrophy. N. Engl. J. Med. *364*, 1513-22

Hu, J., Gagnon, K.T., Liu, J., Watts, J.K., Syeda-Nawaz, J., Bennett, C.F., Swayze, E.E., Randolph, J., Chattopadhyaya, J., and Corey, D.R. (2011) Allele-selective inhibition of ataxin-3 (ATXN3) expression by antisense oligomers and duplex RNAs. Biol Chem. *392*, 315-25

Hu, J., Liu, J., and Corey, D.R. (2010) Allele-selective inhibition of huntingtin expression by switching to an miRNA-like RNAi mechanism. Chem Biol. *17*, 1183-8

Hu, J.‡, Liu, J.‡, Yu, D., Chu, Y., and David R. Corey (2012) Mechanism of allele-selective inhibition of huntingtin expression by duplex RNAs that target CAG repeats. Nucleic Acids Res. *40,* 11270-80

Hu, J., Matsui, M., Gagnon, K.T., Schwartz, J.C., Gabillet, S., Arar, K., Wu, J., Bezprozvanny, I., and Corey, D.R. (2009) Allele-specific silencing of mutant huntingtin and ataxin-3 genes by targeting expanded CAG repeats in mRNAs. Nat Biotechnol. *27*, 478-84

Ikeda, H., Yamaguchi, M., Sugai, S., Aze, Y., Narumiya, S., and Kakizuka, A. (1996) Expanded polyglutamine in the Machado-Joseph disease protein induces cell death in vitro and in vivo. Nat Genet. *13*, 196-202

Jakymiw, A., Lian, S., Eystathioy, T., Li, S., Satoh, M., Hamel, J.C., Fritzler, M.J., and Chan, E.K. (2005) Disruption of GW bodies impairs mammalian RNA interference. Nat. Cell. Biol. *7*, 1267-74

Kawaguchi, Y., Okamoto, T., Taniwaki, M., et al. (1994) CAG expansions in a novel gene for Machado-Joseph disease at chromosome14q32.1. Nat Genet, *8*, 221–228.

Kinali, M., Arechavala-Gomeza, V., Feng, L., Cirak, S., Hunt, D., Adkin, C., Guglieri, M., Ashton, E., Abbs, S., Nihoyannopoulos, P., Garralda, M.E., Rutherford, M., McCulley, C., Popplewell, L., Graham, I.R., Dickson, G., Wood, M.J., Wells, D.J., Wilton, S.D., Kole, R., Straub, V., Bushby, K., Sewry, C., Morgan, J.E., and Muntoni, F. (2009). Local restoration of dystrophin expression with the morpholino oligomer AVI-4658 in Duchenne muscular

dystrophy: a single-blind, placebo-controlled, dose-escalation, proof-of-concept study. Lancet Neurol. *8*, 918-28

Krützfeldt, J., Rajewsky, N., Braich, R., Rajeev, K.G., Tuschl, T., Manoharan, M., and Stoffel, M. (2005) Silencing of microRNAs in vivo with 'antagomirs'. Nature, *438*, 685-9.

Landthaler, M., Gaidatzis, D., Rothballer, A., Chen, PY., Soll, S.J., Dinic, L., Ojo, T., Hafner, M., Zavolan, M., and Tuschl, T. (2008) Molecular characterization of human Argonaute-containing ribonucleoprotein complexes and their bound target mRNAs. RNA. *14*, 2580-96

Lang, A.E., Rogaeva, E.A., Tsuda, T., Hutterer, J., and St George-Hyslop. P. (1994) Homozygous inheritance of the Machado-Joseph disease gene. Ann Neurol. *36*, 443-7

Lazzaretti, D., Tournier, I., and Izaurralde, E. (2009) The C-terminal domains of human TNRC6A, TNRC6B, and TNRC6C silence bound transcripts independently of Argonaute proteins. RNA. *15*, 1059-66

Lima, W.F., Prakash, T.P., Murray, H.M., Kinberger, G.A., Li, W., Chappell, A.E., Li C.S., Murray, S.F., Gaus, H., Seth, P.P., Swayze, E.E., and Crooke, S.T. (2012) Single-stranded siRNAs Activate RNAi in Animals. Cell, *150,* 883-94

Liu, J., Hu, J., and Corey, D.R. (2012). Expanding the action of duplex RNAs into the nucleus: redirecting alternative splicing. Nucleic Acids Res. *40,* 1240-50.

Liu, J., Rivas, F.V., Wohlschlegel, J., Yates, J.R 3rd, Parker, R., and Hannon, G.J. (2005) A role for the P-body component GW182 in microRNA function. Nat. Cell. Biol. *7*, 1261-6

Matsui, M., Prakash, T.P., and Corey, D.R. (2012). Transcriptional silencing by single-stranded RNAs targeting a noncoding RNA that overlaps a gene promoter. ACS Chem. Biol. Epub ahead of print.

Miller, V.M., Xia, H., Marrs, G.L., Gouvion, C.M., Lee, G., Davidson, B.L., and Paulson, H.L. (2003) Allele-specific silencing of dominant disease genes. Proc Natl Acad Sci U S A. *100*, 7195-200

Paulson, H.L., Perez, M.K., Trottier, Y., Trojanowski, J.Q., Subramony, S.H., Das, S.S., Vig, P., Mandel, J.L., Fischbeck, K.H., and Pittman, R.N. (1997) Intranuclear inclusions of expanded polyglutamine protein in spinocerebellar ataxia type 3. Neuron. *19*, 333-44

Schöls, L., Bauer, P., Schmidt, T., Schulte, T., and Riess, O. (2004). Autosomal dominant cerebellar ataxias: clinical features, genetics, and pathogenesis. Lancet Neurol. *3*, 291-304.

Schmitt, I., Linden, M., Khazneh, H., Evert, B.O., Breuer, P., Klockgether, T., and Wuellner, U. (2007) Inactivation of the mouse Atxn3 (ataxin-3) gene increases protein ubiquitination. Biochem Biophys Res Commun. 362, 734-9

Switonski, P.M., Fiszer, A., Kazmierska, K., Kurpisz, M., Krzyzosiak, W.J., and Figiel, M. (2011) Mouse ataxin-3 functional knock-out model. Neuromolecular Med. *13*, 54-65.

Warrick, J.M., Morabito, L.M., Bilen, J., Gordesky-Gold, B., Faust, L.Z., Paulson, H.L., aqnd Bonini, N.M. (2005). Ataxin-3 suppresses polyglutamine neurodegeneration in Drosophila by a ubiquitin-associated mechanism. Mol Cell. *18*, 37-48.

Yu, D., Pendergraff, H., Liu, J., Kordasiewicz, H., Cleveland, D.W., Swayze, E.E., Lima, W.F., Crooke, S.T., Prakash, T.P., and Corey, D.R. (2012) Single-Stranded RNAs Use RNAi to Potently and Allele-Selectively Inhibit Mutant Huntingtin Expression. Cell, *150,* 895-908

Figure 4-1

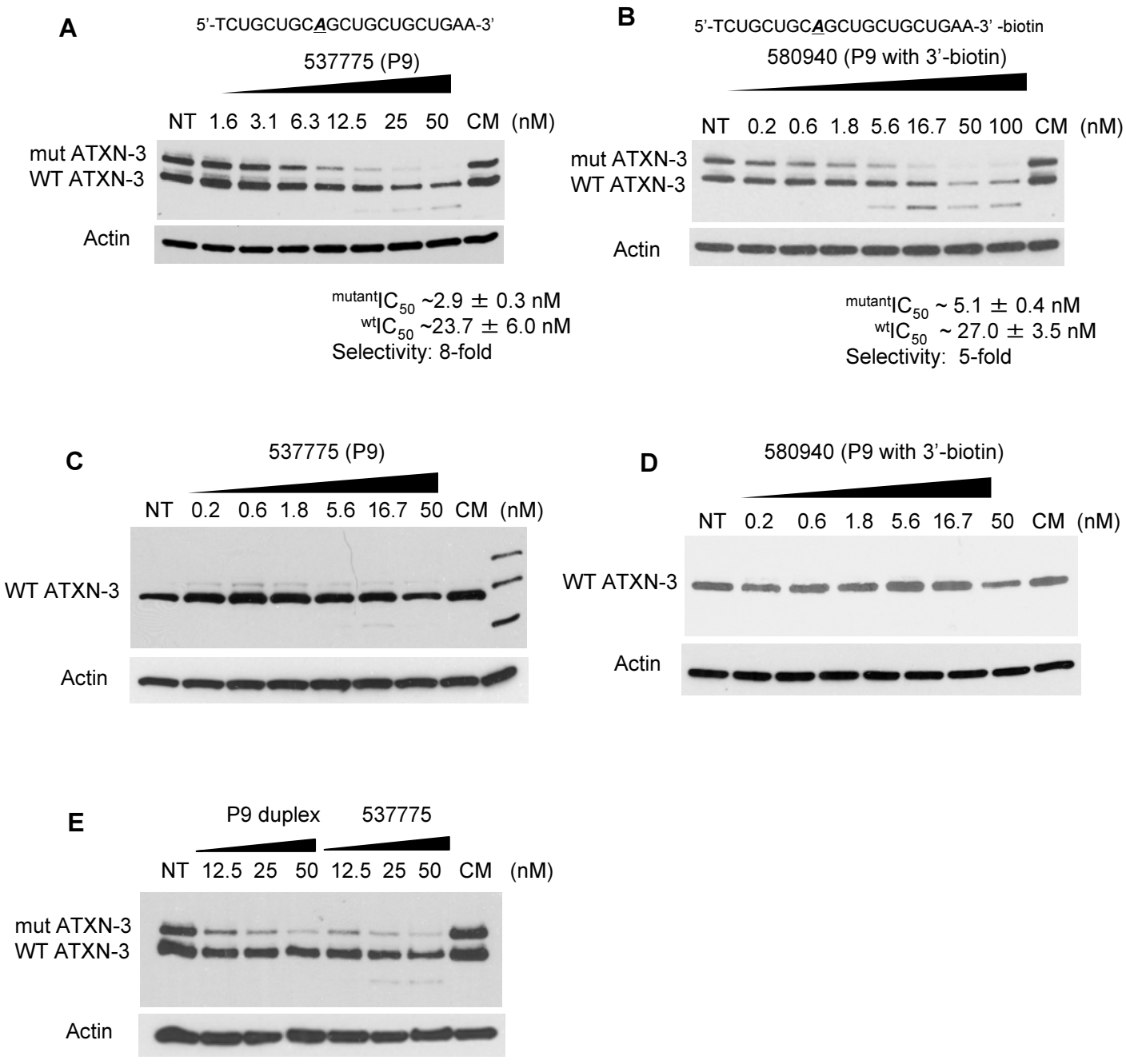
A
5'-TCUGCUGCAGCUGCUGCUGAA-3'
537775 (P9)
NT 1.6 3.1 6.3 12.5 25 50 CM (nM)
mut ATXN-3
WT ATXN-3
Actin
mutantIC50 ~2.9 ± 0.3 nM
wtIC50 ~23.7 ± 6.0 nM
Selectivity: 8-fold
B
5'-TCUGCUGCAGCUGCUGCUGAA-3' -biotin
580940 (P9 with 3'-biotin)
NT 0.2 0.6 1.8 5.6 16.7 50 100 CM (nM)
mut ATXN-3
WT ATXN-3
Actin
mutantIC50 ~ 5.1 ± 0.4 nM
wtIC50 ~ 27.0 ± 3.5 nM
Selectivity: 5-fold
C
537775 (P9)
NT 0.2 0.6 1.8 5.6 16.7 50 CM (nM)
WT ATXN-3
Actin
D
580940 (P9 with 3'-biotin)
NT 0.2 0.6 1.8 5.6 16.7 50 CM (nM)
WT ATXN-3
Actin
E
P9 duplex
537775
NT 12.5 25 50 12.5 25 50 CM (nM)
mut ATXN-3
WT ATXN-3
Actin

Figure 4-1. **CAG-targeting ss-siRNAs with P9 mismatch are potent and allele-selective inhibitors of ataxin-3:**

(A) ss-siRNA 537775 selectively reduces mutant ataxin-3 protein levels in a SCA3-patient fibroblast cell-line (mutant allele: 74 CAG repeats; wild-type allele: 24-CAG repeats);
(B) ss-siRNA 580940 selectively reduces mutant ataxin-3 protein levels in SCA3 fibroblasts;
(C) ss-siRNA 537775 does not affect wild-type ataxin-3 protein levels in a HD-patient fibroblast cell-line;
(D) ss-siRNA 580940 does not affect wild-type ataxin-3 protein levels in a HD-patient fibroblast cell-line;
(E) ss-siRNA 537775 inhibits ataxin-3 similarly to unmodified P9 duplex in SCA3 fibroblasts.

537775: CAG-targeting ss-siRNA with a single mismatched base at P9; 580940: same as 537775 except with a 3'-biotin tag; CM: a mismatched control RNA; NT: no treatment. All CM treatments in the full-dose response studies of this chapter were at 50nM unless otherwise indicated.

Figure 4-2

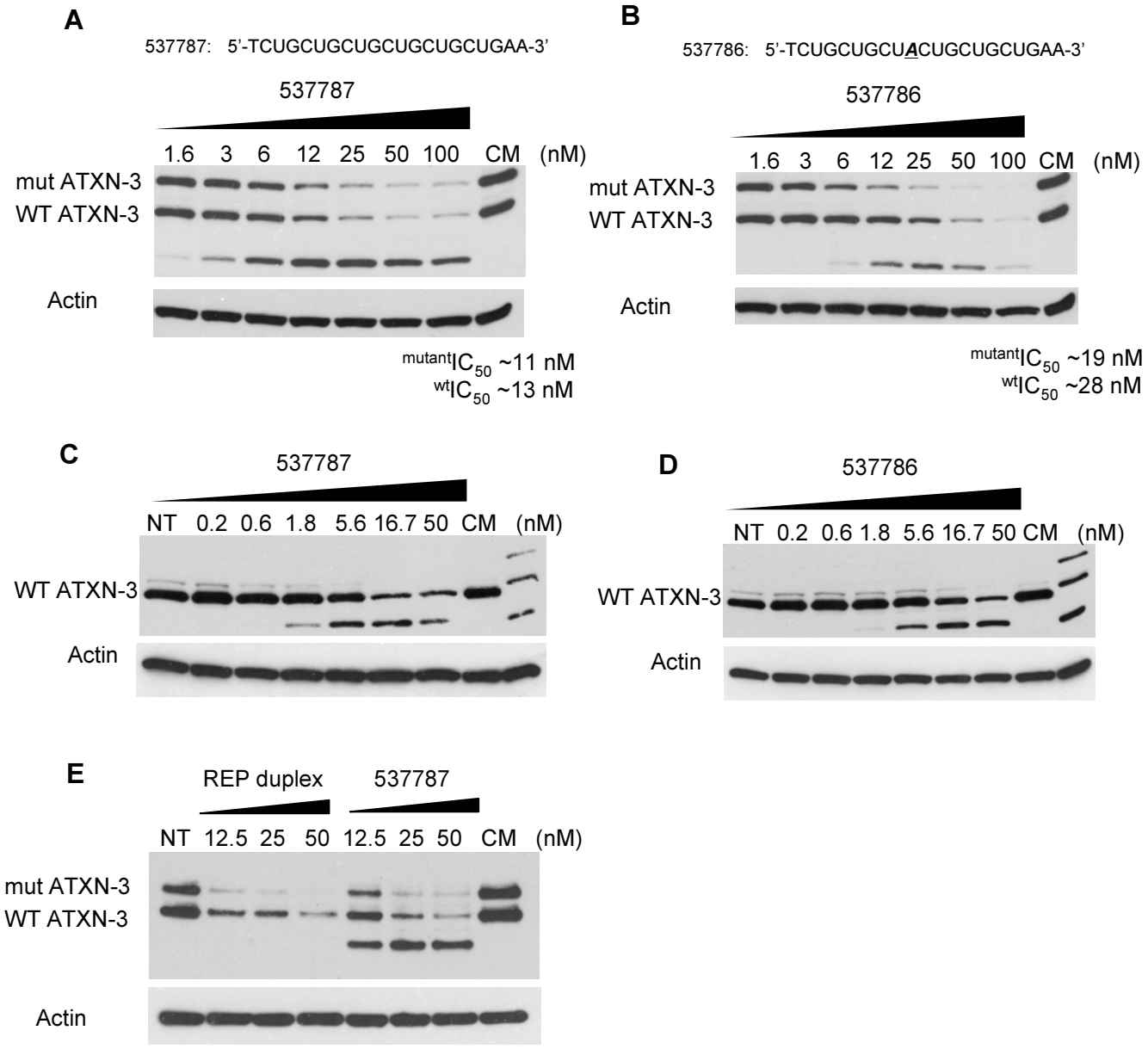

Figure 4-2. **Additional CAG-targeting ss-siRNAs are less potent and allele-selective inhibitors of ataxin-3:** (A-B) Effects of ss-siRNA treatment on ataxin-3 protein levels in a SCA3-patient fibroblast cell-line (mutant allele: 74 CAG repeats; wild-type allele: 24-CAG repeats). (C-D) Effects of ss-siRNA treatment on ataxin-3 protein levels in a HD-patient fibroblast cell-line (two copies of wild-type *ATX3* alleles).

537787: ss-siRNA with no mismatch; 537786: ss-siRNA with a single mismatched base at P10.; CM: a mismatched control RNA; NT: no treatment.

Figure 4-3

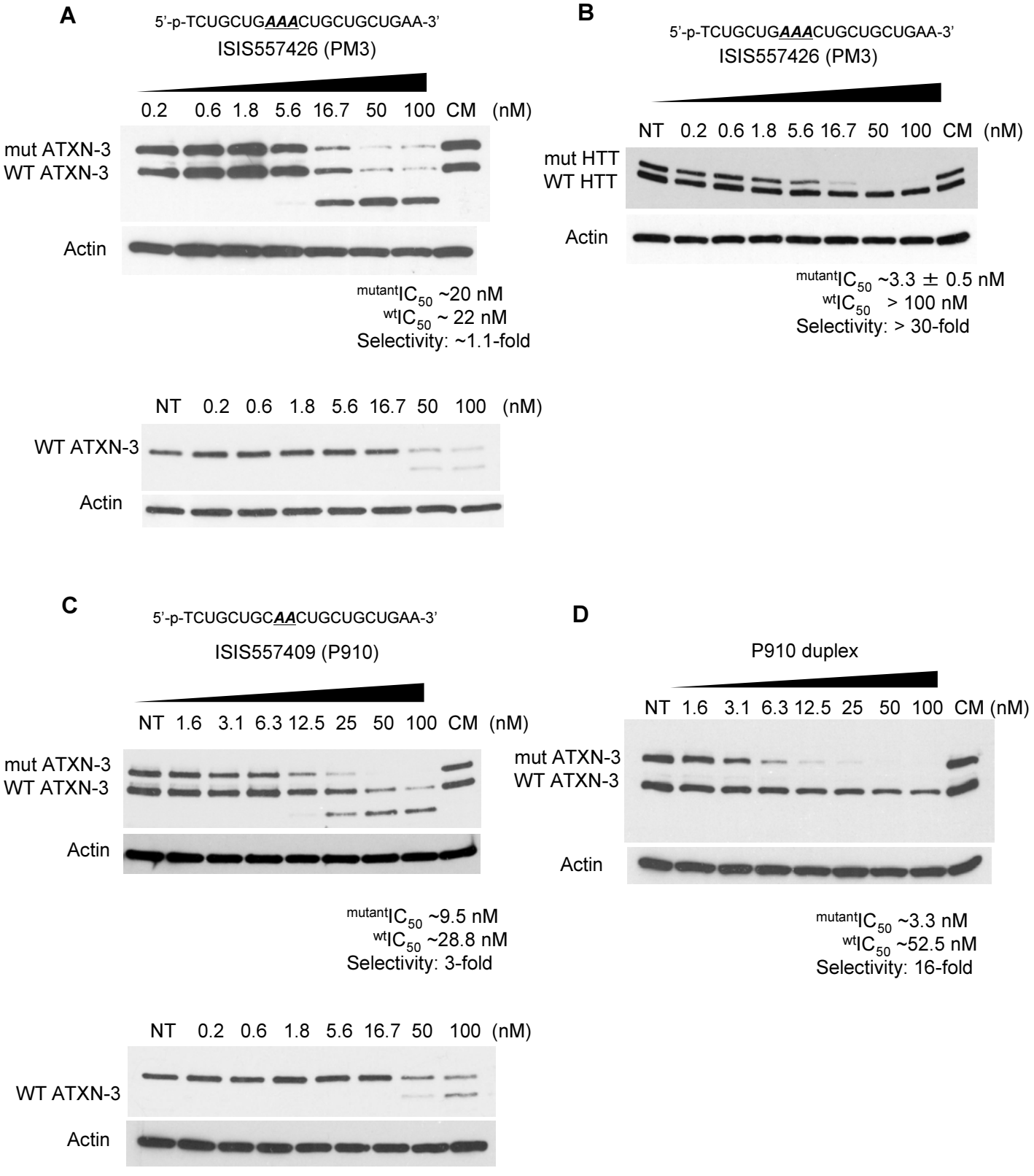
A
5'-p-TCUGCUGAAACUGCUGCUGAA-3'
ISIS557426 (PM3)
0.2 0.6 1.8 5.6 16.7 50 100 CM (nM)
mut ATXN-3
WT ATXN-3
Actin
mutantIC50 ~20 nM
wtIC50 ~ 22 nM
Selectivity: ~1.1-fold
B
5'-p-TCUGCUGAAACUGCUGCUGAA-3'
ISIS557426 (PM3)
NT 0.2 0.6 1.8 5.6 16.7 50 100 CM (nM)
mut HTT
WT HTT
Actin
mutantIC50 ~3.3 ± 0.5 nM
wtIC50 > 100 nM
Selectivity: > 30-fold
NT 0.2 0.6 1.8 5.6 16.7 50 100 (nM)
WT ATXN-3
Actin
C
5'-p-TCUGCUGCAACUGCUGCUGAA-3'
ISIS557409 (P910)
NT 1.6 3.1 6.3 12.5 25 50 100 CM (nM)
mut ATXN-3
WT ATXN-3
Actin
mutantIC50 ~9.5 nM
wtIC50 ~28.8 nM
Selectivity: 3-fold
NT 0.2 0.6 1.8 5.6 16.7 50 100 (nM)
WT ATXN-3
Actin
D
P910 duplex
NT 1.6 3.1 6.3 12.5 25 50 100 CM (nM)
mut ATXN-3
WT ATXN-3
Actin
mutantIC50 ~3.3 nM
wtIC50 ~52.5 nM
Selectivity: 16-fold

Figure 4-3. **ss-siRNA and dsRNA of identical guide-strand sequence can behave differently:**

(A) ss-siRNA 557426 is non-selective against ATXN3 both in SCA3 cells (upper image) and HD cells (lower image);
(B) ss-siRNA 557426 is highly allele-selective against HTT in HD cells;
(C) ss-siRNA 557409 (mismatches at P9 and P10) is poorly selectively against ATXN3 both in SCA3 cells (upper image) and HD cells (lower image);
(D) Unmodified P910 duplex (mismatches at P9 and P10) displays high selectivity against ATXN3 in SCA3 cells;

537775: ss-siRNA with a single mismatched base at position 9; P9: unmodified RNA duplex with mismatch at position 9; 537787: ss-siRNA with no mismatch; REP: unmodified RNA duplex without mismatch; 557409: ss-siRNA with mismatches at positions 9 and 10; P910: unmodified RNA duplex with mismatches at positions 9 and 10; CM: a mismatched control RNA; NT: no treatment.

Figure 4-4

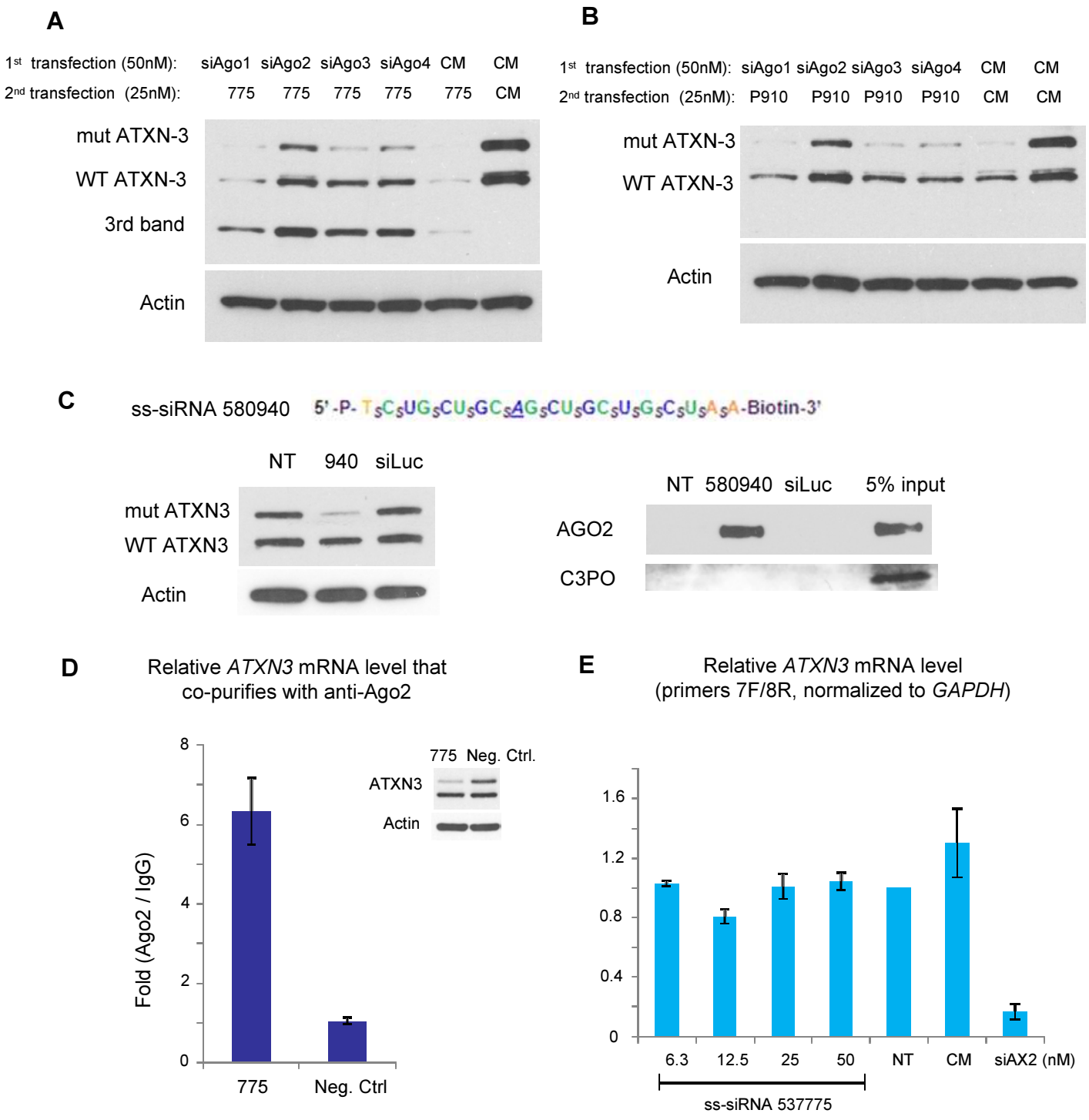
A
1st transfection (50nM): siAgo1 siAgo2 siAgo3 siAgo4 CM CM
2nd transfection (25nM): 775 775 775 775 775 CM
mut ATXN-3
WT ATXN-3
3rd band
Actin
B
1st transfection (50nM): siAgo1 siAgo2 siAgo3 siAgo4 CM CM
2nd transfection (25nM): P910 P910 P910 P910 CM CM
mut ATXN-3
WT ATXN-3
Actin
C
ss-siRNA 580940 5'-P- TsCsUGsCUsGCsAGsCUsGCsUsGsCsUsAsA-Biotin-3'
NT 940 siLuc
mut ATXN3
WT ATXN3
Actin
NT 580940 siLuc 5% input
AGO2
C3PO
D
Relative ATXN3 mRNA level that co-purifies with anti-Ago2
Fold (Ago2 / IgG)
8
6
4
2
0
775 Neg. Ctrl.
ATXN3
Actin
775
Neg. Ctrl
E
Relative ATXN3 mRNA level (primers 7F/8R, normalized to GAPDH)
1.6
1.2
0.8
0.4
0
6.3 12.5 25 50 NT CM siAX2 (nM)
ss-siRNA 537775

Figure 4-4. **Mechanism of ss-siRNA-mediated *ATXN3* inhibition:**

(A) Double-transfection experiment shows Ago2 to be required for ataxin-3 inhibition by ss-siRNA 537775;

(B) Double-transfection experiment shows Ago2 to be required for ataxin-3 inhibition by siRNA duplex P910;

(C) Biotinylated ss-siRNA 580940 immunoprecipitated Ago2 but not C3PO from treated cell extract;

(D) Ago2 is recruited to *ATXN3* mRNA upon 537775 treatment, as seen by >6-fold enrichment of *ATXN3* transcript when immunoprecipitated with anti-Ago2 antibody,

(E) qPCR with primer pair targeting exon 7/8 of *ATXN3* shows no reduction of *ATX3* mRNA when SCA3 fibroblasts are treated with ss-siRNA 537775.

775: ss-siRNA 537775 with a single mismatched base at position 9; P910: unmodified RNA duplex with mismatches at position 9 and 10; 580940: ss-siRNA with mismatch at positions 9 and a 3'-biotin tag; CM: a mismatched control RNA; NT: no treatment. siAX2: a canonical siRNA duplex targeting *ATXN3* outside of repeats; siAgo1-4: siRNAs targeting Ago1-4; Neg. Ctrl: ss-siRNA 522247 with sequence unrelated to ATXN3.

Figure 4-5

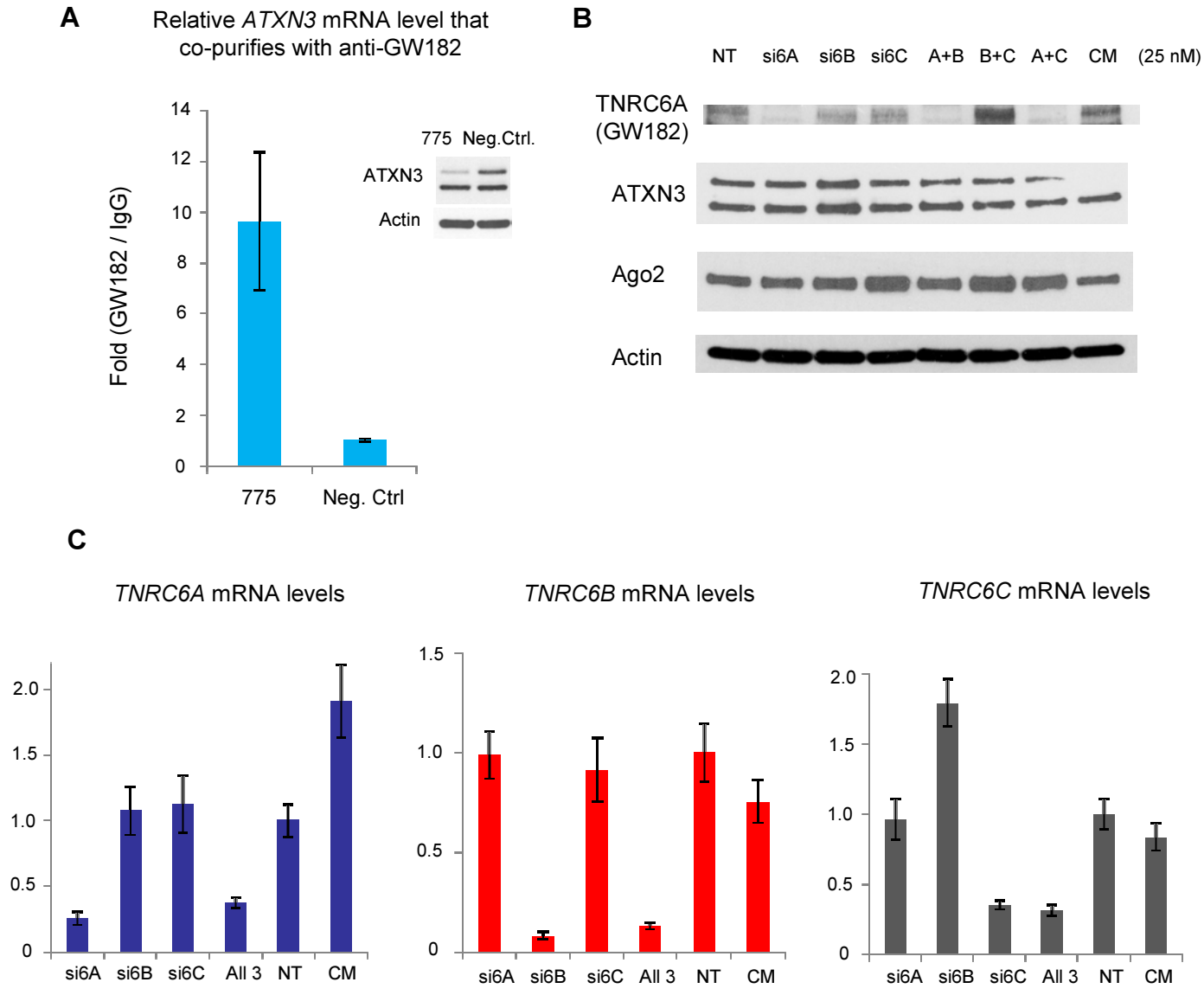

Figure 4-5. **GW182 is recruited to *ATXN3* mRNA upon ss-siRNA treatment:** (A) qPCR with primer pair targeting exon 7/8 of *ATXN3* shows no reduction of *ATXN3* mRNA when SCA3 fibroblasts are treated with ss-siRNA 537775; (B) western blot shows specific knockdown of TNRC6A upon siRNA treatment (mutant ATXN3 band on the last lane was accidentally cut off prior to blotting); (C) q-PCR confirms variant-specific knockdown of the three TNRC6 paralogs by siRNA.

537775: ss-siRNA with a single mismatched base at position 9; CM: mismatched control; NT: no treatment. Neg. Ctrl: negative control ss-siRNA 522247 not targeting *ATXN3*.

Figure 4-6

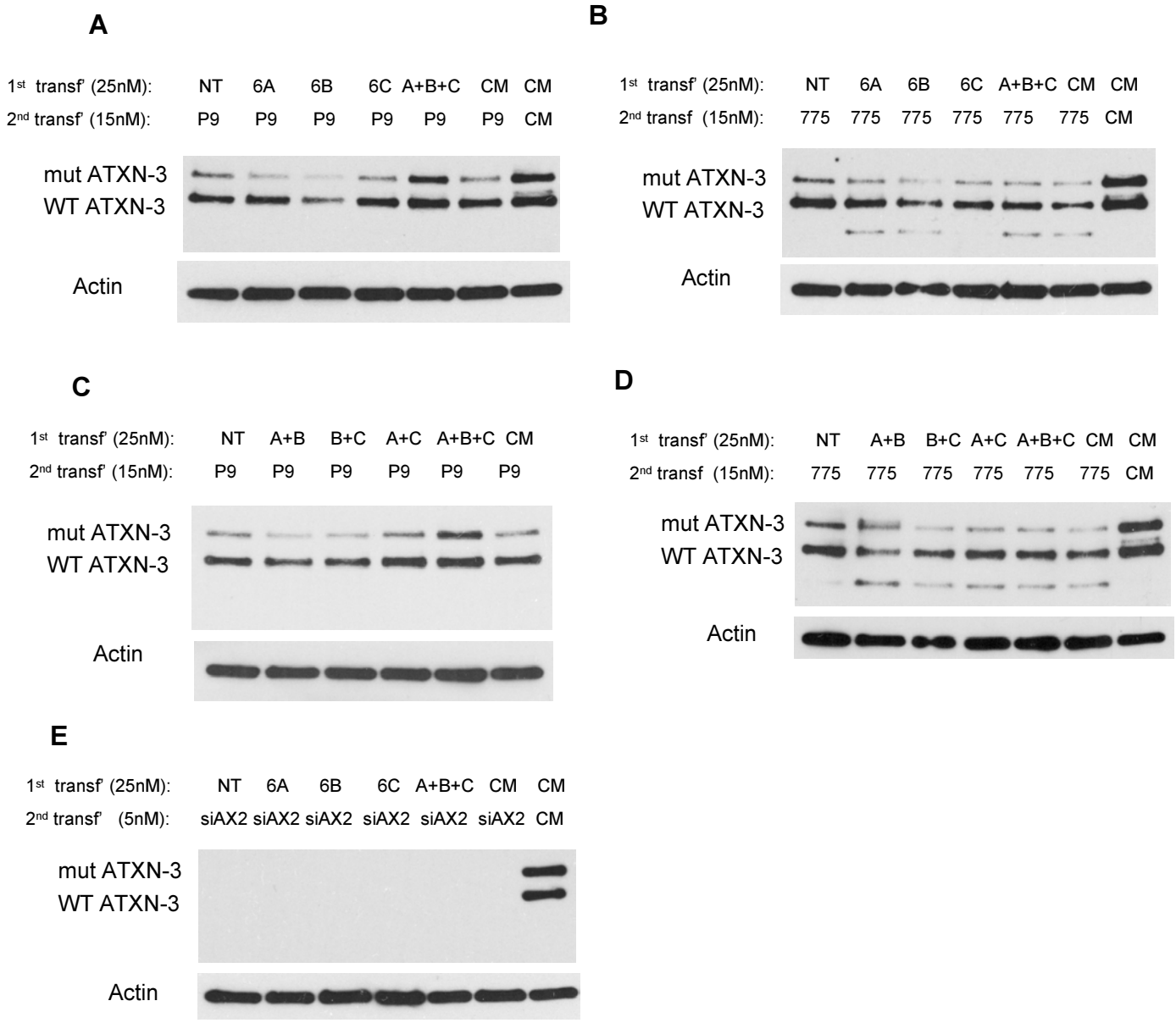

Figure 4-6. **GW182/TNRC6 family proteins may play different roles in ss-siRNA vs dsRNA-mediated ATXN3 inhibition:** (A and C) Depleting all three TNRC6 paralogs reversed P9-mediated ATXN3 inhibition; (B and D) Depleting any or all three TNRC6 paralogs had no effect on 537775-mediated ATXN3 inhibition; (E) Depleting any or all three TNRC6 paralogs had no effect on siAX2-mediated ATXN3 inhibition;

537775: ss-siRNA with a single mismatched base at position 9; P9: unmodified duplex siRNA with a single mismatched base at position 9; siAX2: a canonical siRNA targeting *ATXN3* outside of CAG repeats; CM: mismatched control; NT: no treatment.

CHAPTER FIVE

Exploring Repeat Expansion-containing Genes as a Model for Translational Inhibition by ORF-targeting miRNAs

ABSTRACT

The vast majority of mammalian miRNAs target the 3'-untranslated region (3'-UTR) to achieve gene repression. Rare miRNA sites within open reading frames (ORFs) have been previously identified and found to be enriched for repetitive sequences, though their mechanism of inhibition remains uncharacterized. Trinucleotide repeat expansion in mRNAs associated with disease genes such as *ATAXIN-3* (*ATXN3*) may offer a unique system to study the mechanism of ORF-targeted miRNAs. We have shown that chemically modified ss-siRNAs complementary to poly-CAG inhibit ataxin-3 at the protein level without reducing its mRNA abundance, suggesting a translational block. Interestingly, a higher mobility band appears with ss-siRNA treatment, and additional western blots with different antibodies suggested that it corresponds to a shorter ATXN3 peptide species that contains few, if any, polyglutamine repeats. Pre-treatment with either pan-caspase inhibitor z-vad-fmk or calpain inhibitor calpeptin did not diminish the intensity of the novel band, making it unlikely a proteolytic product. Instead, its apparent molecular weight is consistent with a truncation product resulting from early translational termination, therefore potentially shedding light on a model of cooperative binding and ribosomal blockage by ORF-targeted siRNAs.

INTRODUCTION

MicroRNAs (miRNAs) are a large set of 20- to 22 -nt short RNAs generated endogenously from processing of longer duplex pri- and pre-miRNAs by Drosha and Dicer (Bartel, 2009). They are evolutionarily conserved and may have important regulatory roles on up to 30% of human genes (Lewis et al., 2005; Xie et al., 2005) spanning vital functions such as cell proliferation, cell differentiation, and organism development. Unlike siRNAs, miRNAs in mammalian genomes are only partially complementary to their target mRNAs, with highest sequence complementarity in the 2-8 nt seed region (Lewis et al, 2005; Xie et al, 2005).

The mechanism of miRNA-mediated gene repression has been a topic of active research and intense debate. Early reports suggested that miRNAs achieve gene down-regulation at the translational level, largely from observations that protein levels but not mRNA levels of target genes were reduced by miRNAs. A number of different but not mutually exclusive models have been proposed, including interruption of ribosomal assembly at the 5'-cap (Pillai et al., 2005; Mathonnet et al., 2007) and ribosomal "drop-off" during elongation (Nottrott et al., 2006; Petersen et al., 2006).

It was also discovered that some miRNAs can down-regulate levels of multiple target mRNAs (Lim et al., 2005), and the process could be associated with transcript deadenylation and degradation (Giraldez et al., 2006; Eulalio et al., 2009). Subsequently, the use of ribosome profiling revealed that up to 84% of miRNA-targeted genes had decreased mRNA levels (Guo et al., 2010). A model proposed destabilization of mRNAs may to the predominant manner by which miRNAs achieve gene repression. However, this model does not preclude the possibility that mRNA decay is preceded by translational inhibition and thus may not be the cause but the consequence of miRNA-mediated gene inhibition (Omer et al., 2009). Indeed, two recent studies

in *Drosophila* S2 cells and zebrafish embryos with improved temporal resolution established that translational repression takes place before either mRNA deadenylation or mRNA decay, the latter processes likely only serving to consolidate rather than initiate target gene repression (Bazzini et al., 2012; Djuranovic et al., 2012).

Due to the fact that CAG-targeting small RNAs (both single-stranded and duplex) share certain properties with some generic miRNAs, including imperfect complementarity from mismatched bases and strong reduction at the protein level without decreasing target mRNA, we hypothesized that they function as miRNA-mimics and inhibit HTT expression by translational repression. However, the majority of predicted miRNA target sites are located within 3'UTR, whereas the CAG-expansion target sequences lie within the coding region of genes such as *Huntingtin* (*HTT*) and *Ataxin*-3 (*ATXN3*). Using a luciferase-based reporter construct containing 3'UTR miRNA sites, one group showed that removing the stop codon and extending ORF into 3'UTR significantly compromised miRNA's ability to exert translational inhibition. This result may be due to the traffic from actively translating and hence translocating ribosomes, which hindered stable binding of miRISC to its target sites (Gu et al., 2009). This observation explains from an evolutionary point of view the low frequency of ORF- and 5'UTR-located miRNA target sites across the human genome (since the translational machinery assembles at the 5'-cap and scans through 5'UTR until it encounters the AUG start codon).

Nonetheless, a few predicted sequences within the coding region have been verified as bona fide miRNA target sites (Duursmaet al., 2008; Tay et al., 2008; Forman et al., 2008; Shen et al., 2008). This suggests that ORF-targeted miRNAs are operable and potentially conserved methods of gene regulation. Interestingly, a recent report examined the few examples of efficient mammalian miRNA target sites within ORFs. They were found to be enriched for highly repetitive sequences such as those encoding tandem copies of C_2H_2 class zing-finger domains

(Schnall-Levin et al., 2011). This raises the intriguing possibility that repeat sequences within coding regions may be intrinsically primed for efficient miRNA repression by allowing binding of multiple RISC complexes, which then enables stable attachment to mRNA transcript and stalling of the translocating ribosomes.

Due to the paucity of ORF-located miRNA sites and the studies thereof, it is unclear what their mechanism of repression is and whether it fundamentally differs from that of the canonical 3'UTR-targeting miRNAs. The effort at its elucidation is hindered by the lack of a model system with easy readout and manipulation. During the study of extending CAG-targeting ss-siRNAs to SCA3, I was intrigued by the possibility that these siRNAs might mimic a system of translational repression for ORF-targeting miRNAs. Our data had shown that miRNAs, when directed to highly repetitive sequences within the coding region, can efficiently repress protein expression while minimally altering the mRNA abundance. Interestingly, a faster migrating band appeared when SCA3-patient-derived fibroblasts were treated with ss-siRNAs and blotted for SCA3 expression (Chapter 4). In this chapter, I set out to establish the identity of this novel peptide species and to find out whether it may be a truncated SCA3 peptide that then serves as a valuable window to view the underlying mechanism of translational repression.

RESULTS

CAG-targeting ss-siRNAs Generate a Faster Migrating Putative Ataxin-3 Peptide

We had previously shown that chemically modified, single-stranded siRNAs (ss-siRNAs) targeting poly-CAG stretch were able to potently and selectively inhibit mutant HTT expression while sparing wild-type HTT. Since no reduction was seen for *HTT* mRNA, we deduced that they function at the translational level and preferentially target the longer mutant transcript due to its higher number of target sites and stronger cooperative binding. However, when we extended the study to *ATXN3*, another CAG-expansion disease gene, in the SCA3-patient-derived fibroblast cell-line GM06151 (mutant *ATXN3* allele with 74 CAG repeats and wild-type *ATXN3* allele with 24 CAG repeats), a very different observation was made. While unmodified duplexes generally maintained good potency and allele-selectivity against both *HTT* and *ATXN3*, a number of ss-siRNAs saw a significant decrease in allele-selectivity against mutant *ATXN3*. A few (e.g., 537775 with mismatch at position 9) retained some selectivity; however, many others reduced mutant and wild-type ATXN3 proteins indiscriminately (Figure 5-1A and Chapter 4).

Interestingly, we observed the appearance of a faster migrating band detected with anti-ATXN3 antibody. Its intensity increased proportionally with increasing ss-siRNA dosage as the regular ATXN3 bands disappeared (see Chapter 4). The correlation between the intensity of the faster migrating band and the degree of ATXN3 inhibition suggests that it could correspond to a truncated peptide product. We hypothesize that ribosome stalled due to miRISC steric blockage at the CAG repeats releases its partially synthesized peptide, which can accumulate as truncated products. The start of the CAG repeat is found in exon 10, about three quarters of the way into the coding sequence from the N-terminal AUG start site (Figure 5-1C). In support of the truncated peptide hypothesis, the apparent molecular weight of the high-mobility band is about

37 kD (Figure 5-1D), also about three quarters that of the apparent molecular weight of wild-type ataxin-3 band (~50 kD).

The Faster Migrating Band Is Likely an Ataxin-3 Fragment Containing Few Glutamine Repeats

To exclude the possibility that the high-mobility band is due to non-specific signal from another protein, we performed western blot with a second anti-ATXN3 antibody (rabbit polyclonal antibody raised in Henry Paulson's lab) and obtained identical band patterns to those by the commercial mouse monoclonal antibody 1H9 (Figure 5-2A). When blotted with polyglutamine-specific antibody 5TF1-1C2 (Millipore) that recognizes expanded glutamine tracts (Trottier et al., 1995), the mutant ataxin-3 protein showed up strongly, but no signal appeared for either the WT or the high-mobility protein species. This result suggests that the high-mobility third band peptide contains few, if any, poly-glutamine units, supporting the notion that ribosomal stalling occurs early in the CAG-repeat stretch (Figure 5-2B).

The Faster Migrating Band Is Unlikely a Product of Proteolysis

Several studies had reported low molecular weight bands of ATXN3 that resulted from proteolytic cleavage either by apoptosis-inducing caspases (Berke et al., 2004; Jung et al, 2009) or the calcium-sensitive protease calpain (Haacke et al., 2007). To rule out the faster migrating band as a proteolytic product, we treated transfected cells with pan-caspase inhibitor z-Vad-fmk, or calpain inhibitor calpeptin. Neither drug was able to reduce or eliminate the appearance of the third band, even when added throughout the course of the experiments and at very high

concentrations (Figure 5-2C and D). The result suggests that neither caspase nor calpain plays a significant role in generating the third band.

Effort at Identification of the Fast Migrating Band by Mass Spectrometry

To establish identity of this high mobility peptide species, we pursued immunoprecipitation followed by mass spectrometry. Multiple large dishes of SCA3-patient-derived fibroblasts were grown up and treated with CAG-targeting ss-siRNA 537786 (mismatch at P10). Total cell lysate was subsequently obtained and then mixed with resin that had been pre-coated with anti-ATXN3 antibody to minimize non-specific binding. After incubation on rotator for several hours followed by washing, resin-bound proteins were eluted and a small amount of eluent was run on SDS-PAGE gels, which confirmed the presence of the faster migrating peptide (Figure 5-3C). The remaining eluent was run separately, and the gel of the expected size was excised with sterile techniques for mass spectrometry analysis. Unfortunately, low protein amount coupled with high background noise made sequence identification difficult, and two attempts at peptide identification by mass spectrometry were unsuccessful.

FUTURE DIRECTIONS

Identification of the Fast Migrating Band Using Epitope-tagged-ATXN3 Cell-lines

Given the technical difficulty associated with immunoprecipitating native ATXN3 peptides, an alternative approach may be taken by using transgenic HEK293 cells that stably express N-terminal-FLAG-tagged ATXN3 (available in Henry Paulson's lab at University of Michigan). When probed with anti-Flag antibody, ss-siRNA 537787 may induce the appearance of a high-mobility band of almost identical molecular weight as the untagged third band if it indeed represents a truncated peptide (as illustrated in Figure 5-3B). This observation would support the proposed mechanism, since no other endogenous protein expresses FLAG tag. It should be cautioned that the absence of such a band may also be due to the alterations in genetic sequence and mRNA processing, since the FLAG-tagged *ATXN3* transgene contains no intron and represents only one of the several possible fully spliced isoforms.

If a FLAG-tagged faster migrating band were to be observed, the next step would be to grow up large amount of HEK293 stable cells and harvest cell extract. The presence of the FLAG-tag would allow us to perform column-phase chromatography and many rounds of rigorous washes to minimize background signals. The final eluted fraction can be resolved by SDS-PAGE and bands excised for mass spectrometry. The peptide thus identified may confirm its proposed identity as the truncation product from translational interruptions (illustrated in Figure 5-3B) or offer alternative explanation for its genesis.

Using Ribosomal Profiling to Measure Ribosomal Densities on *ATXN3* mRNA

Ribosomal profiling is an advanced technique that allows visualization of the exact localization of ribosomes on a given mRNA, and could be ideal for direct visualization of

whether ribosomal stalling and drop-off occurs. If ribosome stalling were the primary mechanism of inhibition, we would expect substantial clearance of ribosomes downstream of the CAG repeats on *ATXN3* mRNA and/or a concomitant build-up of ribosomes immediate upstream where "road blockade" occurs in extracts from ss-siRNA-treated cells.

Specifically, after treatment with cyclohexamide to immobilize all translating ribosomes, the harvested cell extract would be incubated with monococcal nuclease to digest RNA fragments unbound unprotected by ribosomes. Monosome fraction can then be obtained (Ingolia et al., 2004) after centrifugation on 10-50% sucrose gradient and UV-monitored fractionation on HPLC. The ensuing RNA fragments can be sent off for deep sequencing. While untreated samples should yield mostly uniform ribosomal density across the *ATXN3* mRNA, we expect samples treated with ss-siRNA to have a sharp drop in ribosomal density across the CAG-repeat region (illustrated in Figure 5-4). We may also observe a slight but significant increase in ribosomal density immediately 5' to the CAG stretch, indicating that a congestion event may be taking place as ribosomes attempting to cross the miRISC-bound CAG region get stalled.

Exploring Alternative Splicing as a Cause of the Novel Band

Isoform-specific PCR primers can be designed and purchased to test whether alternative splicing is responsible for generating the faster migrating band. It is conceivable that inhibiting endogenous ataxin-3 production forces cells to up-regulate expression of an alternatively spliced mRNA isoform that skips poly-CAG-containing exon 10 and bypasses ss-siRNA repression (although it does not explain why unmodified dsRNAs do not induce the same phenomenon). To test this alternative hypothesis, PCR primers can be designed that either amplify the entire *ATXN3* transcript (6-7kb in length) or specific exon-exon junctions. The amplified products would be run on agarose gels and monitored for bands that only show up in extract from ss-

siRNA-treated cells. If a clear correlation can be established between particular PCR products and the faster migrating ATXN3 peptide band, the PCR products can be purified and sequenced and possibly unveil a splicing-dependent mechanism.

Using EGFP and Luciferase Reporter Constructs to Test the Generality of Ribosomal Stalling at Repetitive Sequences

While ATXN3 targeting by ss-siRNA offers us a unique model system to study translational repression by ORF-targeting miRNA, it has the limitation of being just one example of one particular sequence. To expand this model to additional systems, I propose generating libraries of EGFP and luciferase-based reporter plasmids and engineer different sets of tandem/repetitive sequences within their coding regions. We can then co-transfect of such reporters with modified or unmodified miRNA mimics that their repetitive sequences and monitor the efficiency of gene knockdown by fluorescence-activated cell sorting (FACS) and/or luciferase readout. The high-throughput nature of these readout methods would enable screening through a large library of reporter sequences and find out whether efficient ORF-targeting by miRNAs is a general phenomenon beyond expanded CAG repeats in *ATXN3* and *HTT*. If positive hits are identified, further characterization can be carried out with afore-described ribosome profiling to look for ribosomal density drop-off both within the reporter constructs and at endogenous ORF miRNA sites to examine the generality of this phenomenon.

DISCUSSIONS

CAG-targeting ss-siRNAs constitute one of the few validated instances where miRNA or miRNA mimics target sites within the ORF. So far, almost all the studies on miRNA's mechanism in inducing translational inhibition have shown one of the two following scenarios: i) no changes in ribosomal density upon miRNA treatment was seen, which suggested either mRNA decay or defects in peptide synthesis (Petersen et al., 2006), or ii) uniform decrease in ribosomal density was seen, which suggested interruptions at the translational initiation step (Pillai et al., 2006; Mathonnet et al., 2007), possibly through looping of 3'UTR to the 5'-cap. If the observed faster migrating band indeed represents a truncated ataxin-3 peptide, we could demonstrate for the first time that efficient miRNA targeting within the coding region leads to ribosomal stalling and drop-off and accumulation of immature peptide products.

Recent studies have suggested that ORF-targeting miRNAs are more widespread than previously thought in many organisms, for instance in *Drosophila* (Schnall-Levin et al., 2010). Plant miRNAs, which usually have near-perfect complementarity with their mRNA targets and were thought to achieve inhibition by siRNA-like cleavage events, have recently been shown to also display widespread translational repression (Brodersen et al., 2008). Since many plant miRNAs target within coding sequences, it would be of broad scientific and economic interest to explore whether the ribosomal stalling model is used as a general mechanism miRNA regulation in plants.

MATERIALS AND METHODS

ss-siRNA, antibodies, cell culture and transfection, analysis of HTT/ATXN3 expression, IC_{50} and selectivity calculations, q-PCR, and RNA immunoprecipitation

Most materials and protocols for the above experiments are identical to those described in Chapters 1-4 and may be referenced accordingly. Two major antibodies used in this study are mouse monoclonal anti-ataxin-3 antibody MAB5360 (clone 1H9 from Millipore, diluted 1:10,000 for western analysis) and mouse monoclonal anti-polyglutamine/TATA-box binding protein (TBP) antibody MAB1574 (clone 5TF1-1C2 from Millipore and diluted 1:10,000 for western analysis). One additional antibody not described before is a rabbit polyclonal anti-ataxin-3 antibody raised in Henry Paulson's lab at University of Michigan (1:3000 primary).

Establishing the molecular weight of the ataxin-3 bands

To determine the molecular weight of the mutant, the wild-type and the faster migrating ataxin-3 bands, western blot samples were run 4-15% Ready Gel Tris-HCl pre-cast gels (BioRad) for 1 hour with Precision Plus Protein™ Standards Dual Color (BioRad) to maximize separation of the lower MW bands. Edge lanes were avoided to minimize "smiling" of the bands and maximally allow proper alignments. Transferred western strips were taped firmly to the cassette along with a fluorescent ruler, which left clean marks on the film after exposure. The film was then overlaid on top of the strips, and the fluorescent ruler's exposed marks were aligned with that of the original, immobilized ruler in order to recreate the exact positioning under which the film was taken. The individual reference bands of the protein ladder were then carefully labeled on the film to determine the molecular weight of the captured ataxin-3 bands.

Caspase and calpain inhibitors information and dosing

Pan-caspase inhibitor z-vad-fmk was available as 20mM working stock in DMSA and obtained as a generous gift from Dr. Greg Kunkel of Xiaodong Wang's lab. Transfection with ss-siRNA 537786 was performed as described in Chapters 1-4 at 25nM, and z-vad-femk or DMSO control was added drop-wise by pipetting to each well at either 1:1000 or 1:200 dilution. The plates were then rocked multiple times in orthogonal directions to ensure proper mixing. Media change was made 24 hours after transfection with addition of a second round of z-vad-fmk or DMSO followed by rocking and mixing, and cells were harvested 48 hours after transfection. In total, two rounds of calpeptin treatments were performed at and after ss-siRNA transfection.

Calpain inhibitor calpeptin was stored as 10mM stock in DMSA and provided as a generous gift from Dr. Tingwan Sun of Marc Mumby's lab. Transfection with ss-siRNA 537787 was performed as described in Chapters 1-4 at 12.5nM, with the exception that calpeptin was pre-mixed with Optimem (Invitrogen) media at 1:1000, 1:500 or 1:200 dilution in Falcon tubes through several inversions and added to individual wells. Two media changes were performed at 24 and 48 hours after transfection, respectively, each using fresh media that had been added and pre-mixed with calpeptin at the designated concentrations. Cells were harvested 72 hours after transfection for western analysis. In total, three rounds of calpeptin treatments were performed at and after ss-siRNA transfection.

Sample Preparation for Mass Spectrometry

SCA3-patient derived GM06151 fibroblasts were grown in $150\,cm^2$ dishes and transfected with chemically modified ss-siRNA 537786 at 17.5nM using lipid RNAiMAX (Invitrogen) and Optimem (Invitrogen). Media were changed 24 hr after transfection, and cells ($\sim 4 \times 10^7$) were harvested by trypsinization 96 hr after transfection. A small quantity of cells are

saved and harvested for protein to check knockdown efficiency by western blot and confirm the presence of the fast-migrating band. Whole-cell lysate was prepared with protocols identical to that of the RNA-immunoprecipitation (see Materials and Methods of Chapter 1).

To minimize background signals from the antibodies themselves, we first prepared antibody-coated resin by disuccinimidyl suberate (DSS) cross-linking. 20× coupling buffer (0.2M sodium phosphate at pH 7, 1.5M NaCl), IP_{500} buffer (50mM Tris-HCl pH 7.4, 2mM $MgCl_2$, 500mL NaCl, 0.05% NP-40), and IP-EQ buffer (50mM Tris-HCl pH 7.4, 2mM $MgCl_2$, 150mL NaCl, 0.05% NP-40) were made in DNase-free water. 1mL of Protein G Plus/Protein A agarose resin (Calbiochem) was washed twice with 1mL coupling buffer and incubated with 1mL coupling buffer and 65μg of anti-ataxin-3 antibody (clone 1H9, Millipore) or normal mouse IgG (Millipore) at room temperature on rotator for 1-2 hr. The antibody-coated resin was then washed three times with 1mL coupling buffer and re-suspended in 3.6mL coupling buffer added with 80μL of 25mM DSS solution. Crosslinking was allowed to occur by 30-minute incubation on rotator at room temperature. Reaction was quenched with 0.5mL of 1M Tris-HCl (pH 8), and the pelleted resin was reconstituted in 1mL of IP_{500} buffer, washed three times with IP_{500} buffer, and re-suspended in 1mL of IP-EQ buffer.

150 μL of antibody-crosslinked resin, 750 μL of cell lysate, 200 μL of IP dilution buffer and 10μg protease inhibitor (Roche) were mixed and incubated overnight on rotator at 4ºC. Four reaction mixtures were made: ss-siRNA-treated or non-treated whole-cell lysate added resin linked with anti-ataxin-3 antibody or normal mouse IgG. After pelleting and aspiration of the supernatant, elution was performed three times by adding 15μL of 1× SDS and incubation at 95ºC for 5 min and combing all three elutants. The elutants were run on 4-15% gradient gels (BioRad) and the bands of the appropriate molecular weight were excised individually by flame-sterilized razor blades and sent to proteomics core for analysis by mass spectrometry.

REFERENCES

Bartel, D.P. (2009) MicroRNAs: target recognition and regulatory functions. Cell, *136*, 215-33

Bazzini, A.A., Lee, M.T., and Giraldez, A.J. (2012) Ribosome profiling shows that miR-430 reduces translation before causing mRNA decay in zebrafish. Science, *336*, 233-7.

Berke, S.J., Schmied, F.A., Brunt, E.R., Ellerby, L.M., and Paulson, H.L. (2004) Caspase-mediated proteolysis of the polyglutamine disease protein ataxin-3. J Neurochem. *89*, 908-18.

Djuranovic, S., Nahvi, A., and Green, R. (2012). miRNA-mediated gene silencing by translational repression followed by mRNA deadenylation and decay. Science, *336*, 237-40

Duursma, A.M., Kedde, M., Schrier, M., le Sage, C., and Agami, R. (2008). miR-148 targets human DNMT3b protein coding region. RNA, 14(5):872-7

Eulalio, A., Huntzinger, E., Nishihara, T., Rehwinkel, J., Fauser, M., and Izaurralde, E. (2009) Deadenylation is a widespread effect of miRNA regulation. RNA. *15*, 21-32.

Forman, J.J., Legesse-Miller, A., and Coller, H.A. (2008). A search for conserved sequences in coding regions reveals that the let-7 microRNA targets Dicer within its coding sequence. Proc Natl Acad Sci U S A. 2008 Sep 30;105(39):14879-84

Giraldez, A.J., Mishima, Y., Rihel, J., Grocock, R.J., Van Dongen, S., Inoue, K., Enright, A.J., and Schier, A.F. (2006). Zebrafish MiR-430 promotes deadenylation and clearance of maternal mRNAs. *312*, 75-9.

Gu, S., Jin, L., Zhang, F., Sarnow, P., and Kay, M.A. (2009) Biological basis for restriction of microRNA targets to the 3' untranslated region in mammalian mRNAs. Nat. Struc. Mol. Biol. *16*, 144-150.

Guo, H., Ingolia, N.T., Weissman, J.S., and Bartel, D.P. (2010) Mammalian microRNAs predominantly act to decrease target mRNA levels. Nature. *466*, 835-40

Haacke, A., Hartl, F.U., and Breuer, P. (2007). Calpain inhibition is sufficient to suppress aggregation of polyglutamine-expanded ataxin-3. J Biol Chem. *282*, 18851-6

Ingolia, N.T., Ghaemmaghami, S., Newman, J.R., and Weissman, J.S. (2004) Genome-wide analysis in vivo of translation with nucleotide resolution using ribosome profiling. *324*, 218-23

Jung, J., Xu, K., Lessing, D., and Bonini, N.M. (2009) Preventing Ataxin-3 protein cleavage mitigates degeneration in a Drosophila model of SCA3. Hum Mol Genet. *18*, 4843-52

Lewis, B.P., Burge, C.B., and Bartel, D.P. (2005). Conserved seed pairing, often flanked by adenosines, indicates that thousands of human genes are microRNA targets. Cell. *120*, 15-20.

Lim, L.P., Lau, N.C., Garrett-Engele, P., Grimson, A., Schelter, J.M., Castle, J., Bartel, D.P., Linsley, P.S., and Johnson, J.M. (2005) Microarray analysis shows that some microRNAs downregulate large numbers of target mRNAs. Nature. *433*, 769-73

Mathonnet, G., Fabian, M.R., Svitkin, Y.V., Parsyan, A., Huck, L., Murata, T., Biffo, S., Merrick, W.C., Darzynkiewicz, E., Pillai, R.S., Filipowicz, W., Duchaine, T.F., and Sonenberg, N. (2007). MicroRNA inhibition of translation initiation in vitro by targeting the cap-binding complex eIF4F. Science, *317*, 1764-7

Nottrott, S., Simard, M.J., and Richter, J.D. (2006). Human let-7a miRNA blocks protein production on actively translating polyribosomes. Nat. Struct. Biol. *13*, 1108-14

Omer, A.D., Janas, M.M., and Novina, C.D. (2009) The chicken or the egg: microRNA-mediated regulation of mRNA translation or mRNA stability. Mol. Cell. *35*, 739-40

Petersen, C.P., Bordeleau, M.E., Pelletier, J., and Sharp, P.A. (2006) Short RNAs repress translation after initiation in mammalian cells. Mol Cell. *21*, 533-42.

Pillai, R.S., Bhattacharyya, S.N., Artus, C.G., Zoller, T., Cougot, N., Basyuk, E., Bertrand, E., and Filipowicz, W. (2005) Inhibition of translational initiation by Let-7 MicroRNA in human cells. Science, *309*, 1573-6

Schnall-Levin, M., Rissland, O.S., Johnston, W.K., Perrimon, N., Bartel, D.P., and Berger, B. (2011) Unusually effective microRNA targeting within repeat-rich coding regions of mammalian mRNAs. Genome Res. *21*, 1395-403.

Schnall-Levin, M., Zhao, Y., Perrimon, N., and Berger, B. (2010). Conserved microRNA targeting in Drosophila is as widespread in coding regions as in 3'UTRs. Proc Natl Acad Sci USA. *107*, 15751-6.

Shen, W.F., Hu, Y.L., Uttarwar, L., Passegue, E., and Largman, C. (2008) MicroRNA-126 regulates HOXA9 by binding to the homeobox. Mol Cell Biol. *28*, 4609-19

Tay, Y., Zhang, J., Thomson, A.M., Lim, B., and Rigoutsos, I. (2008). MicroRNAs to Nanog, Oct4 and Sox2 coding regions modulate embryonic stem cell differentiation. Nature. *455*:1124-8

Trottier, Y., Lutz, Y., Stevanin, G., Imbert, G., Devys, D., Cancel, G., Saudou, F., Weber, C., David, G., Tora, L., et al.. (1995). Polyglutamine expansion as a pathological epitope in Huntington's disease and four dominant cerebellar ataxias. Nature. *378*, 403-6

Xie, X., Lu, J., Kulbokas, E.J., Golub, T.R., Mootha, V., Lindblad-Toh, K., Lander, E.S., and Kellis, M. (2005) Systematic discovery of regulatory motifs in human promoters and 3' UTRs by comparison of several mammals. Nature. *434*, 338-45

Yu, D., Pendergraff, H., Liu, J., Kordasiewicz, H., Cleveland, D.W., Swayze, E.E., Lima, W.F., Crooke, S.T., Prakash, T.P., and Corey, D.R. (2012) Single-Stranded RNAs Use RNAi to Potently and Allele-Selectively Inhibit Mutant Huntingtin Expression. Cell, *150,* 895-908

Figure 5-1

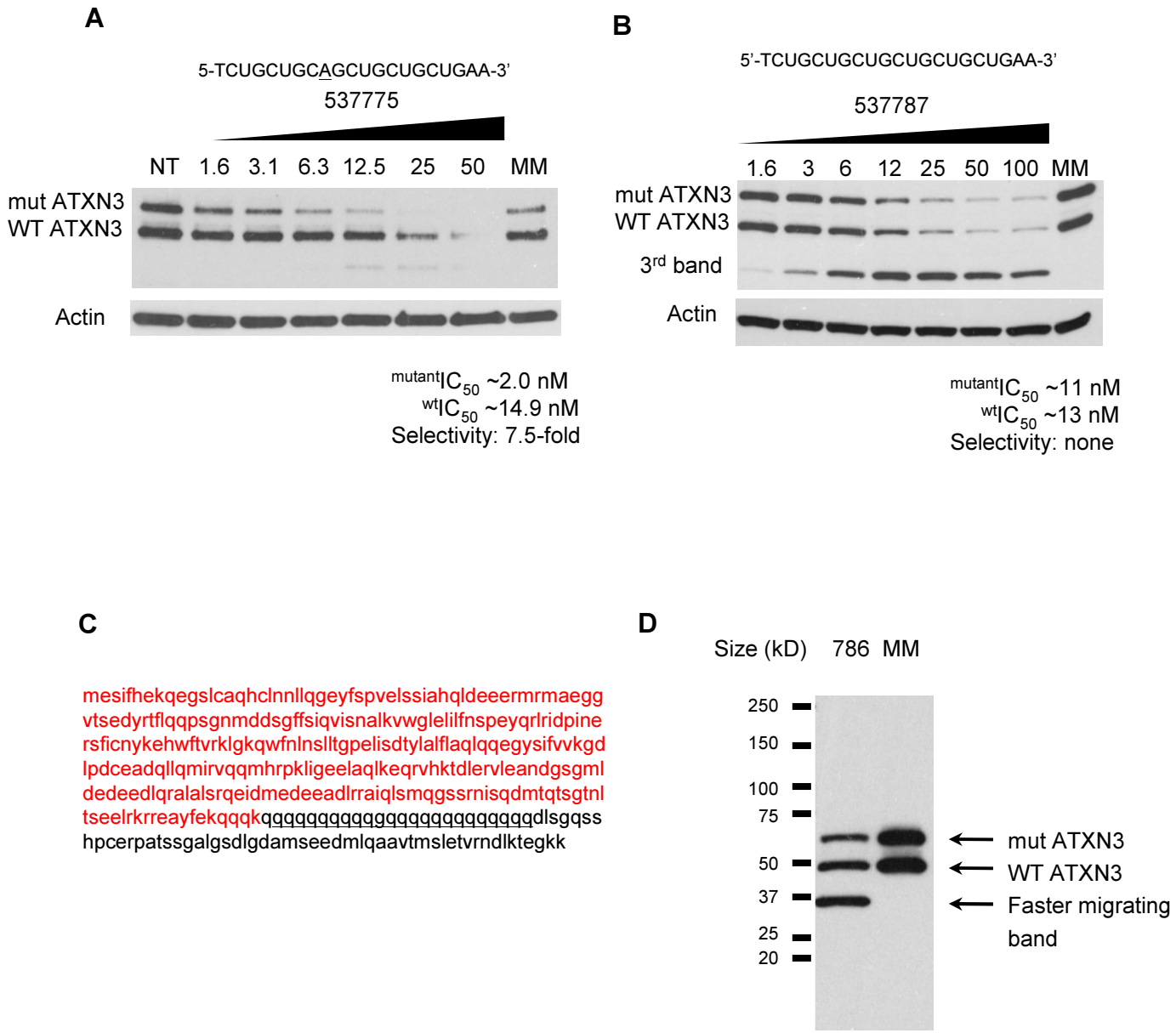

Figure 5-1. **Treating SCA3-patient-derived fibroblasts with CAG-targeting ss-siRNA leads to reduction of ATXN3 and appearance of a faster migrating band:** 537775: ss-siRNA with mismatch at position 9; 537787: ss-siRNA with no mismatch; MM: mismatched control; NT: no treatment. In (C), amino acid sequence of ATXN-3 protein, with red highlighting those before the polyglutamine tract (underlined). (D) The apparent molecular weight of the faster migrating band is ~ 37kD. 537786: ss-siRNA with mismatch at position 10.

Figure 5-2

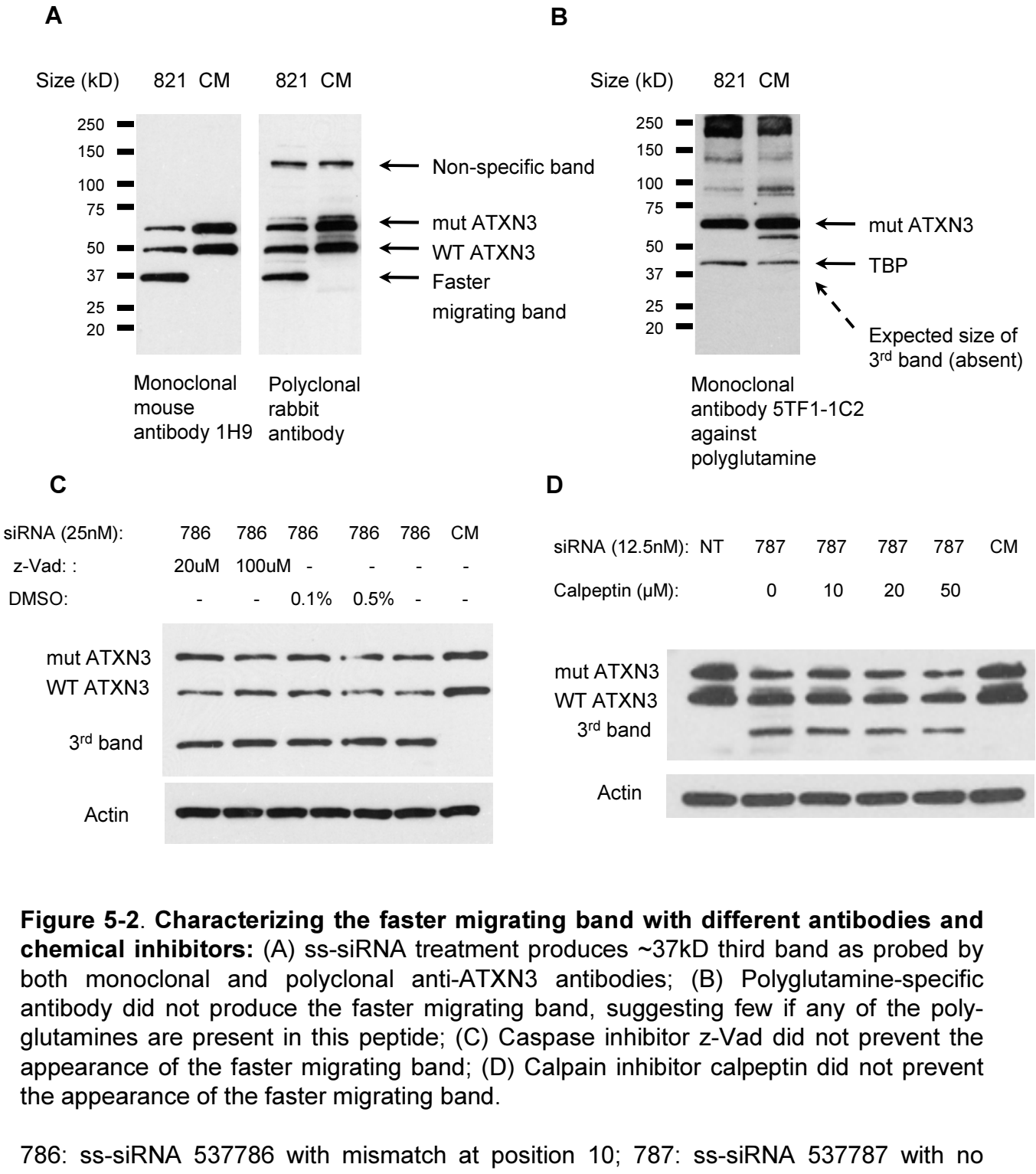

Figure 5-2. **Characterizing the faster migrating band with different antibodies and chemical inhibitors:** (A) ss-siRNA treatment produces ~37kD third band as probed by both monoclonal and polyclonal anti-ATXN3 antibodies; (B) Polyglutamine-specific antibody did not produce the faster migrating band, suggesting few if any of the poly-glutamines are present in this peptide; (C) Caspase inhibitor z-Vad did not prevent the appearance of the faster migrating band; (D) Calpain inhibitor calpeptin did not prevent the appearance of the faster migrating band.

786: ss-siRNA 537786 with mismatch at position 10; 787: ss-siRNA 537787 with no mismatch; 821: ss-siRNA 553821 with mismatch at position 10 with 5'-phosphate chemistry; CM: mismatched control; NT: no treatment.

Figure 5-3

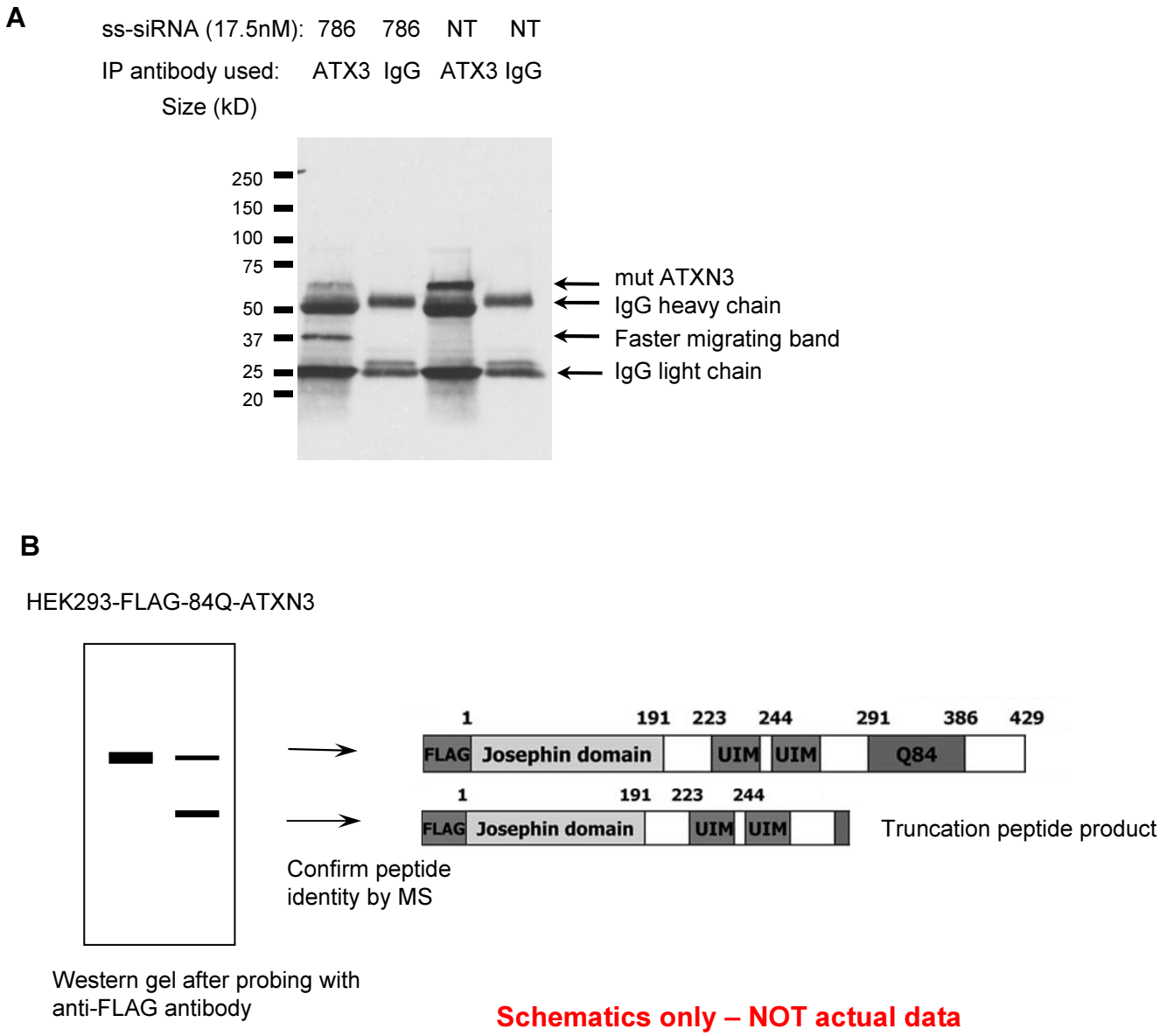

Figure 5-3. **Mass spectrometry to confirm the faster migrating band as a truncation product from early translational termination:** (A) 537786: ss-siRNA with mismatch at position 10; NT: no treatment. (B) Schematic that illustrates using FLAG-tagged ATXN3 transgenic cell-lines to look for faster migrating band when probed with anti-FLAG antibody. The graphics are partially made by reformatting figures from Jung et al, *Hum. Mol. Genet.* 2009.

Figure 5-4

A Ribosomal density map in non-treated SCA3 fibroblast extract

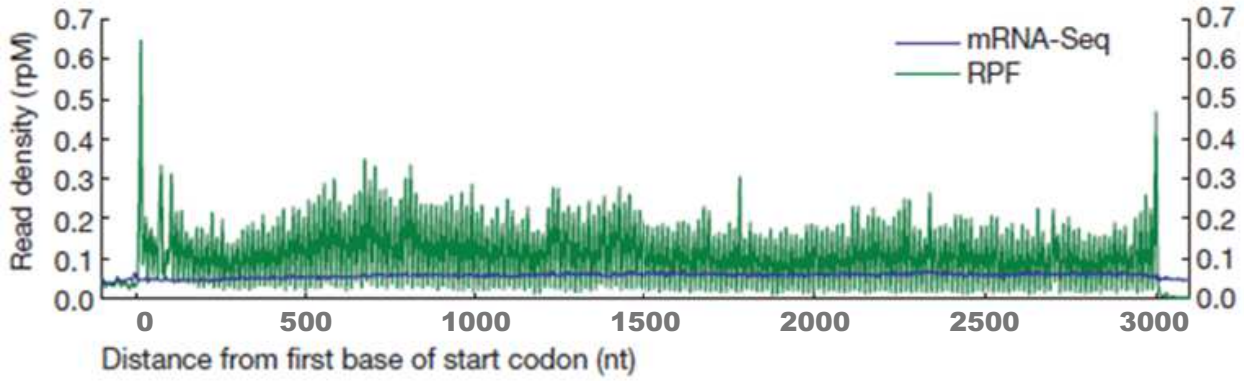

Schematics only – NOT actual data

B Ribosomal density map in ss-siRNA 537787-treated SCA3 fibroblast extract

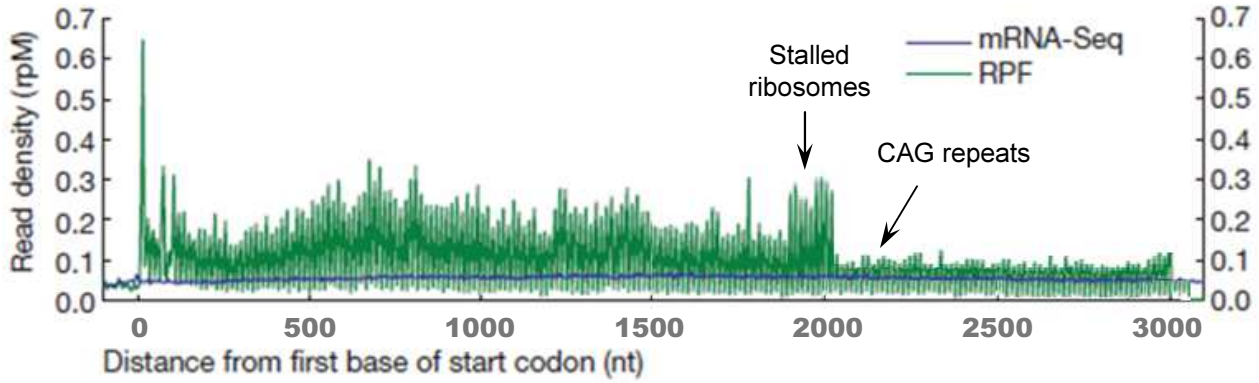

Schematics only – NOT actual data

Figure 5-4. Schematic of proposed ribosome profiling that may show steep drop-off of ribosomal density around CAG repeats: 537787: CAG-targeting ss-siRNA with no mismatch. These illustrations are created using Figure 1C of Guo et al, *Nature,* 2010 as a template and do NOT represent actual data from our laboratory.

Figure 5-5

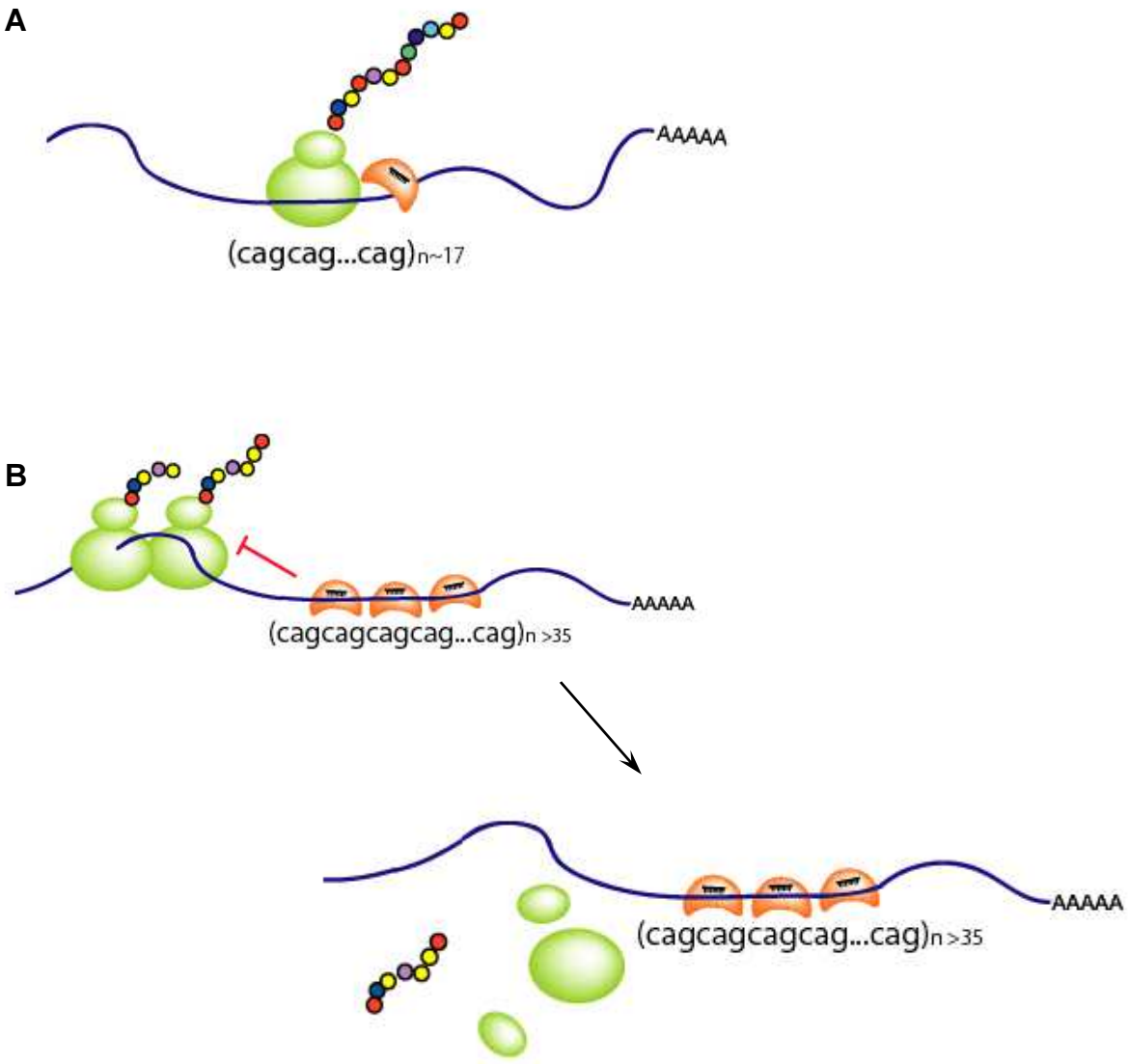

Figure 5-5. **Schematic of translational inhibition by ORF-targeting ss-siRNAs and miRNAs:** (A) ss-siRNA/miRNA with a single ORF binding site is insufficient to halt actively translating ribosomes and gets dislodged from the mRNA; (B) Multiple binding of ss-siRNA/miRNAs at repetitive ORF sequences establishes a strong inhibitory complex, which stalls and disassembles in-coming ribosomes, leading to early translation termination and release of truncated peptide product.

CHAPTER SIX

Establishment and Usage of Clonal Rett-syndrome Cell-lines to Test Compounds for Activation of Wild-type MeCP2 Expression

ABSTRACT:

Rett Syndrome is an X-linked progressive neurological disorder caused by inactivation of one allele of the *MECP2* gene. There are no curative treatments, and activation of wild-type *MECP2* expression is one strategy for stabilizing or reversing the disease. We isolated fibroblast clones that express exclusively either the wild-type or a 32-bp-deletion mutant form of *MECP2*. We developed a sensitive assay for measuring wild-type *MECP2* mRNA levels and tested small molecule epigenetic activators for their ability to activate gene expression. Although our pilot screen did not identify activators of *MECP2* expression, it established the value of using clonal cells and defined challenges that must be overcome.

Note: The following chapter is substantially made up of a research article published by Dongbo Yu under the guidance of Dr. David R. Corey (Yu et al, 2011).

INTRODUCTION:

Rett Syndrome (RTT) is a progressive neurological disorder that affects 1 in 10,000 girls (Hagberg and Hagberg, 1997). After a brief period of seemingly normal post-natal development, symptoms appear that include deceleration in growth, loss of acquired motor and language skills, characteristic hand-writhing movements, muscle hypotonia, and cognitive impairment (Zoghbi, 2003; Chahrour and Zoghbi, 2007). Symptoms grow progressively more severe but long-term survival can be achieved with supportive care. There are no curative treatments for RTT, and strategies for slowing, stabilizing, or reversing the disease constitute an urgent yet unmet need.

RTT is predominantly caused by mutations within a single identified gene, methyl CpG binding protein 2 (*MECP2*, Amir et al., 1999), providing us with an obvious therapeutic target. *MECP2* is an X-linked gene that modulates expression levels of large number of genes (Traynor et al., 2002; Chahrour et al., 2008), with the neuropeptide *BDNF* being a well-studied example (Chen et al., 2003; Chang et al., 2006; Larimore et al., 2009).

Since almost all patients are female and the majority are heterozygous for the *MECP2* locus, one intact copy of the wild-type *MECP2* gene exists in all cells of the body. Only a subset of these cells express wild-type *MECP2* due to the process of random X-inactivation during early development, resulting in a mosaic pattern of MeCP2 protein expression throughout the body. Some cells express wild type MeCP2, while others express the inactive mutant variant and have insufficient MeCP2 function. MeCP2 is expressed across a large number of tissue types (Shahbazian et al., 2002), and earlier work pointed to the exclusive role of MeCP2's dysfunction in neurons as the cause of RTT (Chen et al., 2001). More recent studies have implicated non-neuronal cells, in particular the astrocytes, to be significant players in the pathogenesis of RTT (Ballas et al., 2009; Maezawa et al., 2009).

Agents that activate expression of the wild-type allele on the silenced X-chromosome might overcome a lack of MeCP2 protein and benefit patients. Support for this hypothesis comes from studies in mouse models with an engineered *MECP2* gene deletion that mimics human RTT (Guy et al., 2001). Related studies demonstrated that conditional genetic reactivation of wild-type MeCP2 protein expression in mutant mice can reverse the disease phenotype even in late-stage symptomatic adult animals (Guy et al., 2007). The work has encouraged the belief that RTT can be treated by re-expression of wild-type MeCP2.

Gene therapy provides one strategy for increasing *MECP2* expression. Alternatively, pharmacological reactivation of the wild-type MeCP2 protein expression in cells where it is silenced due to X-inactivation would also be therapeutically beneficial in treating RTT. *In vitro* cell-based models are valuable tools in studying genetic diseases including RTT (Marchetto et al., 2010). Screening for small molecule gene activators, however, requires development of sensitive assays to detect enhanced expression of MeCP2. Examining activation in a heterogeneous population of patient cells will be difficult because any upregulation will need to be evaluated against a background of 50% or more expression of wild-type *MECP2*.

For example, an agent that promotes production of MeCP2 at a fraction of the wild-type level would be an excellent starting point for development. This relatively low level, however, would be difficult or impossible to discern against background MeCP2 expression in a heterogeneous cell population. Successful identification of lead compounds for gene activation would therefore benefit from possession of a clonal cell line with a silent wild-type allele.

RESULTS

Establishment Of Clonal RTT Cell-Lines

To specifically probe for the reactivation of wild-type *MECP2* in cells, we first isolated single cells and established fibroblast lines that express only the mutant copy of *MECP2* gene. We started this process with RTT patient-derived fibroblast cell-line, GM11272 (Coriell Institute). Many RTT cell lines containing different mutations in *MECP2* are available (Lee et al., 2001) and might have been used, but we chose GM11272 because it contains a 32-bp deletion (1155-1186) in exon 4 of *MECP2* (Figure 6-1) that simplifies discrimination of the wild-type and mutant alleles.

We derived single cell clones by diluting a suspension of GM11272 cells to 10 cells/mL and seeding them into 96-well plates at 100 μL/well. Cell clones with morphology and doubling time similar to the parent strain were then expanded with Minimum Essential Media Eagle (Sigma) supplemented with 15% FBS and 5% MEM non-essential amino acids (Sigma). Their RNA was then harvested and reverse-transcribed into cDNA for PCR analysis to classify each clone as "wild-type" or "mutant" with regard to the MeCP2 expression. We used primers flanking the 32-bp deletion region that yield amplification products of different sizes when run on agarose gel.

Most of the isolated clones expressed wild-type MeCP2. The few clones that expressed mutant MeCP2 and were silent for wild-type MeCP2 grew relatively slowly. These data suggest that the absence of MeCP2 is detrimental to cells, but this deficit was not sufficient to prevent isolation of several cell lines with the silent wild-type allele. Standard PCR without use reverse transcript revealed the presence of chromosomal MeCP2.

Establishment and Validation of Nested PCR as a Senstive Detection Assay

Identifying a pharmacological agent capable of reactivating a gene on a silent X-chromosome is challenging and would benefit from sensitive assays that can detect even small amounts of expression. Such low level expression might then serve as a basis for subsequent strategies to increase expression to therapeutically useful levels. For example, we have shown that duplex RNAs complementary to gene promoters can activate gene expression (Janowski et al., 2007). This activation, however, requires detectable expression of target transcripts at the gene promoter (Schwartz et al., 2008; Yue et al., 2010). One approach for achieving useful levels of MeCP2 would be to use pharmacological agents to prime low level expression, and then use duplex RNA to selectively activate MeCP2 transcription to a higher level. This approach might also reduce off-target effects by allowing minimal concentrations of synthetic epigenetic modifiers to be effective.

We developed a "nested" PCR approach to amplify the cDNA region around the 32-bp deletion in two separate rounds, with each round involving 25-40 amplification cycles (Table 6-1, Figure 6-2). In the first round, an "outer" primer pair amplifies a 285-bp long fragment with the reverse primer overlapping with the deletion region, thereby making the mutant transcript unable to serve as the template and thus affording allele selectivity. A second round of PCR was added using an "inner" primer pair with the reverse primer lying entirely within the deletion region, which provides a second layer of allele selectivity and increases the sensitivity of detection for the wild-type transcript.

Even without nested PCR, a population containing just 10% wild-type cells could be unambiguously detected (Figure 6-2b). Using nested PCR, however, we could readily detect

wild-type cells at 1:100 dilution. These data suggest that even a 1% upregulation of *MECP2* expression should be detectable.

The "nested" PCR products were run out on 2% agarose gels, and the presence or absence of a bright band around 250-bp indicates whether detectable levels of wild-type *MECP2* transcript existed in the starting RNA sample. Due to the high sensitivity of the assay, experiments lacking reverse transcriptase were run in parallel as negative controls. The PCR band was excised and cloned into PCR4-TOPO vector (Invitrogen) for sequencing, which confirmed the identity of the amplified inner *MECP2* fragment.

A Pilot Screen with Commercial Epigenetic Agents

We performed a pilot screening experiment using several compounds previously demonstrated to be epigenetic modifiers capable of reactivating expression of silenced genes in various cell-lines. The compounds were from two major categories: inhibitors of DNA methyl transferases (DNMT) and inhibitors of histone deacetylases (HDAC), the two major classes of enzymes frequently implicated and targeted in epigenetic studies (Kazantsev and Thompson, 2008; Brueckner and Lyko, 2004; Vecsler et al., 2003; Huang et al., 2007; Brueckner et al., 2005; Zhou et al., 2007; Tabolacci et al., 2008; Cheng et al., 2004; Fujii et al., 2003). Trichostatin A (TSA) and 5-aza-dC were dissolved in DMSO at 5 mM stocks; SAHA was dissolved in DMSO at 100 mM stock; LBH-589 and RG108 were dissolved in DMSO at 10 mM stocks; zebularine was dissolved in water at 100 mM stock; valproic acid was dissolved fresh in water to make 1M stock. We verified the identity of all compounds by mass spectrometry and used them at concentrations above those previously reported to be necessary for gene activation.

Mutant clonal fibroblasts were seeded at 60,000 cells per well in 6-well plates on Day -2. Drug treatment occurred 48h after seeding on Day 0, with the highest concentrations tested at levels 1000-fold greater than previously reported for gene activation (Table 6-2). The compounds were mixed in 250 μL media, old media was removed, 1 mL of warm fresh media was added, and 250 μL drug-containing media was added drop-wise in a circular motion over each well. Gentle rocking movements were used to evenly spread the drug. Media were changed at 24h. Total cellular RNA was harvested on Day 3 (72h after drug-treatment) by treating with Tri-Reagent (Sigma). Chloroform extraction of the aqueous layer followed by isopropanol and 70% ethanol washes yielded total cellular RNA, which was DNase-I treated and reverse-transcribed to produce cDNA that served as template for detection by nested PCR.

We treated RTT clonal fibroblasts with the epigenetic modifying compounds (Table 6-2). While the cDNA derived from the control wild-type clonal cells repeatedly yielded bright bands near the predicted 250 bp size, none of the mutant *MECP2* fibroblast-derived cDNA consistently produced the expected PCR band regardless of the type of drug treatment received (Figure 6-3). Occasionally, bands appeared in mutant cell-cDNA lanes of both RT and no-RT control conditions. These results, however, were not reproducible and can be explained by the high sensitivity of the assay and the potential for artifactual amplification products. It is likely that the bands are due to either genomic DNA contamination of experimental material or trace contamination from the products of previous PCR amplifications. We also tested compounds in combination. TSA/5-azaC, TSA/5-aza-dC/zebularine, RG108/5-aza-dC, RG108/TSA, TSA/5-aza-dC/zebularine/RG108 or TSA/5-aza-dC/zebularine/ RG108/LBH589 combinations were inactive. Exposure of cells to 5-aza-dC for up to six days did not activate MeCP expression. Apicidin and MS-275 were also inactive.

Careful handling of pipettes, autoclaving the Eppendorf tubes, using an isolated bench area with constant ethanol wiping, as well as more stringent DNase I treatment conditions (37°C for 30 min and 75°C for 15 min) reduced but did not eliminate the occurrence of occasional contaminant bands. To achieve meaningful results, experiments were repeated and results examined together.

DISCUSSION

Our results highlighted both the strengths and challenges of our approach. Regardless of the agent used, the experiments did not show any evidence for reactivation of *MECP2* expression. cDNA from wild-type control fibroblasts, however, consistently produced bright bands showing that *MECP2* can be routinely confirmed by the nested PCR approach. As little as one *MECP2*-expressing cell in 100 can be readily detected. While the sensitivity of the assay made these initial screening experiments more labor-intensive, the sensitivity also ensures that even a small amount of gene activation can be detected and used as a starting point for future experiments aimed at improving the potency of *MECP2* activation.

Why was activation not observed? Answering this question will require a better understanding of how the *MECP2* gene is silenced during X-chromosome inactivation and how silencing is maintained. Such understanding will facilitate rational design of therapeutic development strategies that can make use of the clonal cell lines and assays described above.

Rett Syndrome is a debilitating neurological disease with a single genetic cause yet without effective treatment. In this study, we explored a small-molecule-based approach in an effort to reverse the disease at its root cause, i.e., the absence of wild-type MeCP2 protein in affected cells. We successfully isolated a number of single cell-derived clones that selectively express only the mutant or wild-type *MECP2* transcript, and developed a nested-PCR-based method that detects low levels of wild-type *MECP2* mRNA. A pilot screen involving 7 commercially available epigenetic compounds did not find an agent that consistently reactivated wild-type MeCP2 in a mutant background. Nevertheless, the sensitivity and robustness of this *in vitro* system provides us with an important tool for future screening of effective agents against RTT.

MATERIALS AND METHODS

Isolation and Mainteinance of RTT Clonal Cells

We derived single cell clones by diluting a suspension of GM11272 cells to 10 cells/mL and seeding them into 96-well plates at 100 μL/well. Cell clones with morphology and doubling time similar to the parent strain were then expanded with Minimum Essential Media Eagle (Sigma) supplemented with 15% FBS and 5% MEM non-essential amino acids (Sigma). Their RNA was then harvested and reverse-transcribed into cDNA for PCR analysis to classify each clone as "wild-type" or "mutant" with regard to the MeCP2 expression. We used primers flanking the 32-bp deletion region that yield amplification products of different sizes when run on agarose gel.

Nested PCR

"Nested" PCR was used to amplify the cDNA region around the 32-bp deletion in two separate rounds, with each round involving 25-40 amplification cycles. In the first round, an "outer" primer pair amplifies a 285-bp long fragment with the reverse primer overlapping with the deletion region. The primer sequences are as follows: 5'-AGCGCAAGACCCGGGAGACGG-3' (forward primer) and 5'-TGGGGTCCTCGGAGCTCTCGGGCT-3' (reverse primers). A second round of PCR was added using an "inner" primer pair with the reverse primer lying entirely within the deletion region. The primer sequences are as follows: 5'-GACCCGGGAGACGGTCAGCA-3' (forward primer) and 5'-AGCTCTCGGGCTCAGGTGGAGGT-3' (reverse primer). The PCR products were run out on 2% agarose gels, and the presence or absence of a bright band around 250-bp

indicates whether detectable levels of wild-type *MECP2* transcript existed in the starting RNA sample.

Drug Treatment and RNA Isolation

Trichostatin A (TSA) and 5-aza-dC were dissolved in DMSO at 5 mM stocks; SAHA was dissolved in DMSO at 100 mM stock; LBH-589 and RG108 were dissolved in DMSO at 10 mM stocks; zebularine was dissolved in water at 100 mM stock; valproic acid was dissolved fresh in water to make 1M stock. All compounds were verified by mass spectrometry.

Mutant clonal fibroblasts were seeded at 60,000 cells per well in 6-well plates on Day -2. Drug treatment was performed 48 hr after seeding on Day 0. The compounds were mixed in 250 μL media, old growth media was removed from the wells, 1 mL of warm fresh media was added, and 250 μL drug-containing media was added drop-wise in a circular motion over each well. Gentle rocking movements were used to evenly spread the drug over the entire well. The RNA isolation technique may be referenced to HTT project section.

REFERENCES

Amir, R.E., Van den Veyver, I.B., Wan, M., Tran, C.Q., Francke, U., and Zoghbi, H.Y. (1999) Rett syndrome is caused by mutations in X-linked MECP2, encoding methyl-CpG-binding protein 2. Nat. Genet. *23*,185-8

Ballas, N., Lioy, D.T., Grunseich, C., and Mandel, G. (2009) Non-cell autonomous influence of MeCP2-deficient glia on neuronal dendritic morphology. Nat. Neurosci. *12*, 311-7

Brueckner, B., Garcia Boy, R., Siedlecki, P., Musch, T., Kliem, H.C., Zielenkiewicz, P., Suhai, S., Wiessler, M., and Lyko, F. (2005) Epigenetic reactivation of tumor suppressor genes by a novel small-molecule inhibitor of human DNA methyltransferases. Cancer Res. *65*, 6305-11

Brueckner, B., and Lyko, F. (2004) DNA methyltransferase inhibitors: old and new drugs for an epigenetic cancer therapy. Trends Pharmacol. Sci, *25*, 551-4

Chahrour, M., Jung, S.Y., Shaw, C., Zhou, X., Wong, S.T.C., Qin, J., and Zoghbi, H.Y. (2008) MeCP2, a key contributor to neurological disease, activates and represses transcription. Science. 320, 1224-9

Chahrour, M., and Zoghbi, H.Y. (2007) The story of Rett syndrome: from clinic to neurobiology. Neuron. *56*, 422-37.

Chang, Q., Khare, G., Dani, V., Nelson, S., and Jaenisch, R. (2006) The disease progression of Mecp2 mutant mice is affected by the level of BDNF expression. Neuron. *49*, 341-8.

Chen, R.Z., Akbarian, S., Tudor, M., and Jaenisch, R. (2001) Deficiency of methyl-CpG binding protein-2 in CNS neurons results in a Rett-like phenotype in mice. Nat. Genet. *27*,327-31

Chen, W.G., Chang, Q., Lin, Y., Meissner, A., West, A.E., Griffith, E.C., Jaenisch, R., and Greenberg, M.E. (2003) Derepression of BDNF transcription involves calcium-dependent phosphorylation of MeCP2. Science. *302*, 885-9.

Cheng, J.C., Weisenberger, D.J., Gonzales, F.A., Liang, G., Xu, G., Hu, Y., Marquez, V. E., and Jones, P. A. (2004) Continuous zebularine treatment effectively sustains demethylation in human bladder cancer cells. Mol. Cell. Bio. *24*, 1270-8

Fujii, S, Luo, R.Z, Yuan, J, Kadota, M, Oshimura, M, Dent, S.R, Kondo, Y, Issa, J.J., Bast Jr., R.C, and Yu, Y. (2003) Reactivation of the silenced and imprinted alleles of ARHI is associated with increased histone H3 acetylation and decreased histone H3 lysine 9 methylation. Hum. Mol. Genet. *12*, 1791-800

Guy, J., Gan, J., Selfridge, J., Cobb, S., Bird, A. (2007) Reversal of neurological defects in a mouse model of Rett syndrome. Science. *315*, 1143-7

Guy, J., Hendrich, B., Holmes, M., Martin, J. E., and Bird, A. (2001) A mouse Mecp2-null mutation causes neurological symptoms that mimic Rett syndrome. Nat Genet. *27*, 322-6

Hagberg, B., and Hagberg, G. (1997) Rett syndrome: epidemiology and geographical variability. Eur Child Adolesc Psychiatry. *6* (Suppl 1),5-7

Huang, C, Ida, H, Ito, K, Zhang, H, and Ito, Y. (2007) Contribution of reactivated RUNX3 to inhibition of gastric cancer cell growth following suberoylanilide hydroxamic acid (vorinostat) treatment. Biochem. Pharmacol. *73*, 990-1000

Janowski, B.A., Younger, S.T., Hardy, D.B., Ram, R., Huffman, K.E., and Corey, D.R. (2007) Activating gene expression in mammalian cells with promoter-targeted duplex RNAs Nat. Chem. Biol. *3*,166-73

Kazantsev, A.G., and Thompson, L.M. (2008) Therapeutic application of histone deacetylase inhibitors for central nervous system disorders. Nat. Rev. Drug. Discov. *7*, 854-68

Larimore, J. L., Chapleau, C.A., Kudo, S, Theibert, A., Percy, A.K., and Pozzo-Miller, L. (2009) Neurobiol. Dis. Bdnf overexpression in hippocampal neurons prevents dendritic atrophy caused by Rett-associated MECP2 mutations. *34*,199-211

Lee, S.S.J., Wan, M., and Francke, U. (2001) Spectrum of MECP2 mutations in Rett syndrome. Brain & Dev. *23*, S138-43

Maezawa, I., Swanberg, S., Harvey, D., LaSalle, J. M., and Jin, L.W.J. (2009) Rett syndrome astrocytes are abnormal and spread MeCP2 deficiency through gap junctions. Neurosci. *29*, 5051-61

Marchetto, M.C.N., Carromeu, C., Acab, A., Yu, D., Yeo, G. W., Mu, Y., Chen, G., Gage, F.H., and Muotri, A.R. (2010) A model for neural development and treatment of Rett syndrome using human induced pluripotent stem cells. Cell. *143*, 527-39

Schwartz, J.C., Younger, S.T., Nguyen, N.B., Hardy, D.B., Monia, B.P., Corey, D.R., and Janowski, B.A. (2008) Antisense transcripts are targets for activating small RNAs. Nat. Struct. Mol. Biol. *15*, 842.

Shahbazian, M.D., Antalffy, B., Armstrong, D.L., and Zoghbi, H.Y. Hum. (2002) Insight into Rett syndrome: MeCP2 levels display tissue- and cell-specific differences and correlate with neuronal maturation. Mol. Genet. *11*,115-24

Tabolacci, E., De Pascalis, I., Accadoa, M., Terracciano, A., Moscato, U., Chiurazzi, P., and Neri, G. (2008) Modest reactivation of the mutant FMR1 gene by valproic acid is accompanied by histone modifications but not DNA demethylation Pharmacogenet Genomics.*18*, 738-41

Traynor, J., Agarwal, P., Lazzeroni, L., and Francke, U. (2002) Gene expression patterns vary in clonal cell cultures from Rett syndrome females with eight different MECP2 mutations. BMC Med Genet. *3*, 12.

Vecsler, M., Simon, A.J., Amariglio, N., Rechavi, G., and Gak, E. 2010, MeCP2 deficiency downregulates specific nuclear proteins that could be partially recovered by valproic acid in vitro. Epigenetics. *5*, 61-7

Yue, X., Schwartz, J.C., Chu, Y., Younger, S.T., Gagnon, K.T., Elbashir, S., Janowski, B.A., and Corey, D.R. (2010) Transcriptional regulation by small RNAs at sequences downstream from 3' gene termini. Nat. Chem. Biol. *6*, 621-9

Zhou, Q., Atadja, P., and Davidson, N.E. (2007) Histone deacetylase inhibitor LBH589 reactivates silenced estrogen receptor alpha (ER) gene expression without loss of DNA hypermethylation. Cancer Biol. Ther. *6*, 64-9

Zoghbi, H.Y. (2003) Postnatal neurodevelopmental disorders: meeting at the synapse? Science., *302*, 826-30.

Figure 6-1

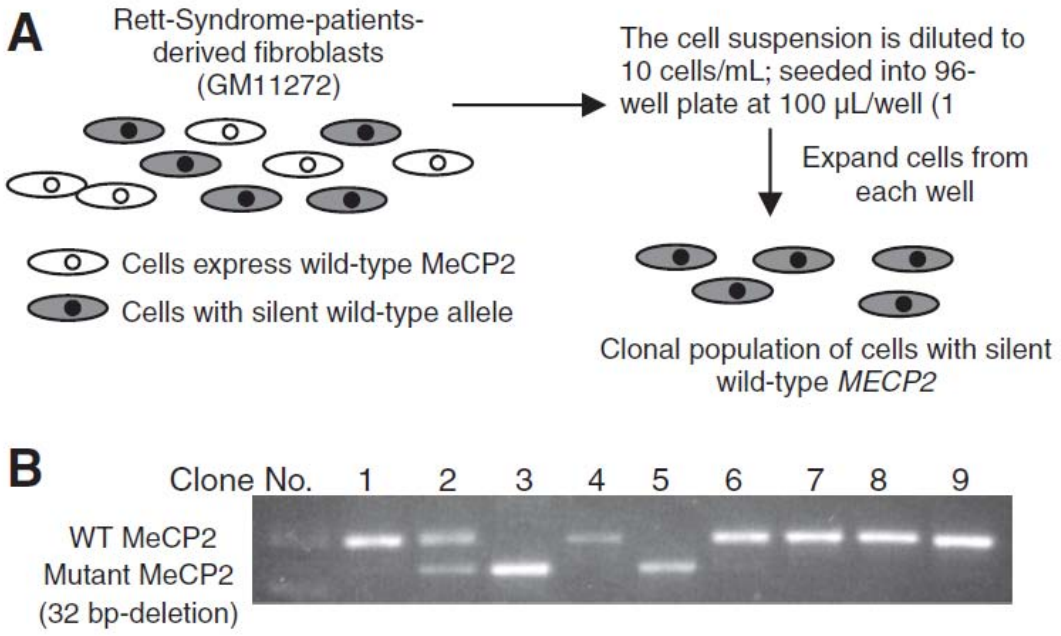

Figure 6-1. Single-cell-derived clones specifically express either mutant or wild-type *MECP2* Allele. (A) Experimental procedure employed to isolate clones that express only wild-type or mutant MeCP2; (B) Determining the expressed MeCP2 isoform of each expanded fibroblast clone by PCR. RNA is harvested from each clone, reverse-transcribed and amplified using primers flanking the 32-bp deletion. WT-MeCP2-expressing clones yielded PCR products with higher molecular weight than the shorter ones produced by the mutant-MeCP2-expressing clones. Each lane represents a different clone. 'Clone' 2 likely was the result of two parent cells, one mutant and one wild-type.

Table 6-1

Sequences of the primers used in 'nested' PCR

Name	Sequence
1st round (outer pair)	
Forward	5′-AGCGCAAGACCCGGGAGACGG-3′
Reverse	5′-TGGGGTCCTCGGAGCTCTCGGGCT-3′
2nd round (inner pair)	
Forward	5′-GACCCGGGAGACGGTCAGCA-3′
Reverse	5′-AGCTCTCGGGCTCAGGTGGAGGT-3′

Figure 6-2

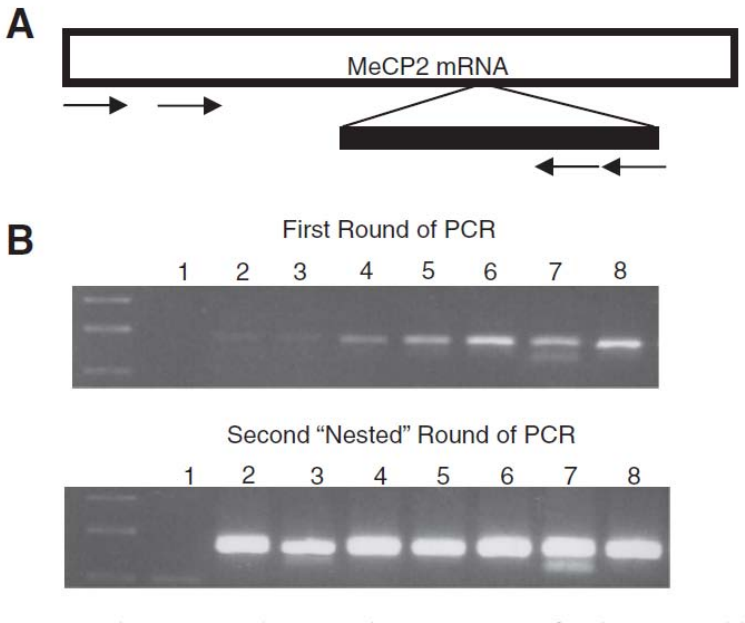

Figure 6-2. **Nested PCR is a selective and sensitive assay for detecting wild-type *MECP2* transcript.** (A) Top: schematic showing the relative positions of the nested PCR primers relative to the 32-bp deletion in *MECP2* gene locus; (B) (top) A single round of PCR with deletion-targeting primer pair achieved allele-selectivity but not sensitivity of wild-type MECP2 transcript detection; (bottom) A second 'nested' round of PCR detects wild-type transcript at as low as 1% of the total RNA mixture while maintaining selectivity in a background of mutant *MECP2* transcript. cDNA template used in each lane (from left to right starting with lane 1) is produced from mixtures of wild-type and mutant clonal fibroblasts with the following ratios: 0:100, 1:99, 5:95, 10:90, 25:75, 50:50, 75:25, 100:0.

Table 6-2

List of compounds and their maximally tested concentrations

Drug name	Published effective concentration (μM)	Maximum tested concentration (μM)
SAHA	2.5–7.5[24]	1000
RG-108	10[25]	1000
LBH-589	0.1[26]	100
Valproic acid	2000[27]	100,000
Zebularine	100[28]	1000
Trichostatin A	0.2[29]	100
5-aza-dC	0.6[29]	100

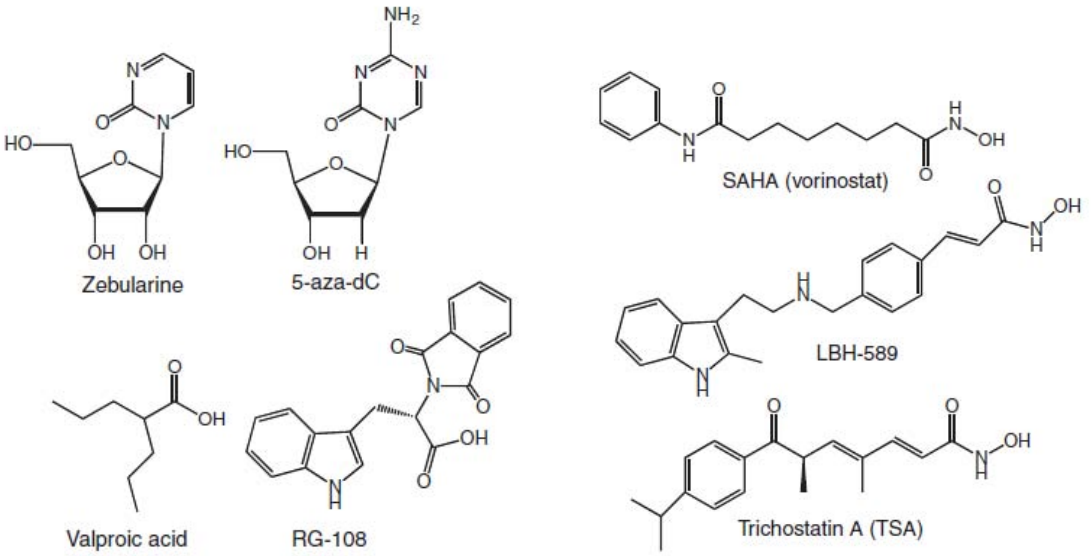

Figure 6-3

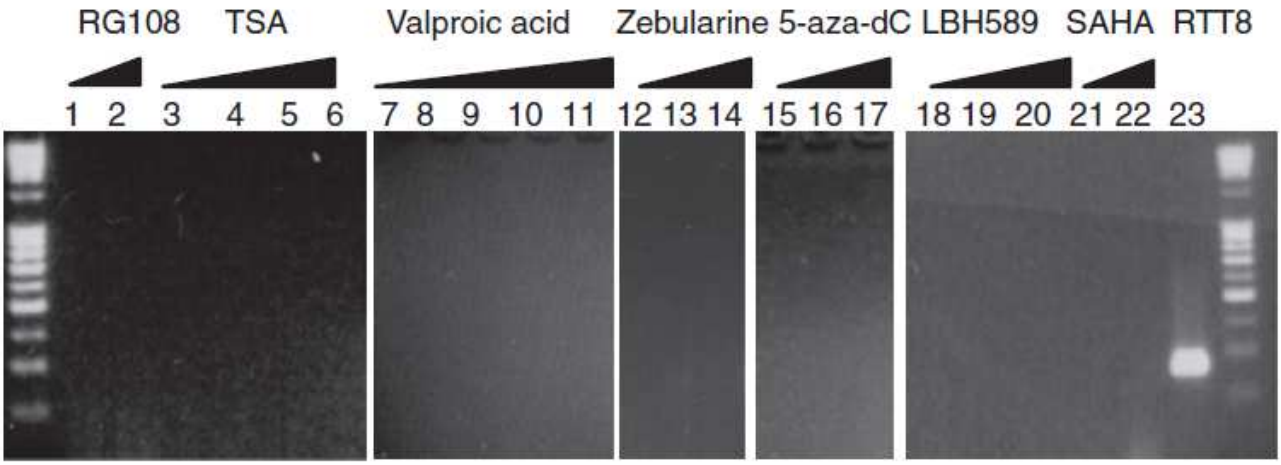

Figure 6-3. Seven commercial epigenetic reagents did not reactivate silenced WT *MECP2* in RTT3 clonal cell-line;

Lanes 1–2: RG-108 at 10 and 100 nM;
Lanes 3–6: TSA at 1, 5, 10 and 100 nM;
Lanes 7–11: valproic acid at 1, 10, 100, 1000 and 10,000 nM;
Lanes 12–14: zebularine at 1,10, 100 nM;
Lanes 15–17: 5-aza-20-deoxycytidine at 1, 10 and 100 nM;
Lanes 18–20: LBH-589 at 1, 10, 100 nM;
Lanes 21–22: SAHA at 10 and 100 nM;
Lane 23: RTT8 wild-type fibroblast-derived cDNA as template (positive control).

CHAPTER SEVEN

Effect of Chemical Modifications on Modulation of Gene Expression by agRNAs

ABSTRACT

Antigene RNAs (agRNAs) are small RNA duplexes that target sequences outside of mRNA and specifically suppress or activate gene expression in a sequence-dependent manner. For many applications *in vivo*, it is likely that agRNAs will require chemical modification. We have synthesized agRNAs that contain different classes of chemical modification and have tested their ability to modulate expression of the human progesterone receptor (PR) gene. We find that both silencing and activating agRNAs can retain activity after modification. Both guide and passenger strands can be modified, and functional agRNAs can contain 2'F-RNA, 2'OMe-RNA and LNA substitutions, or combinations of multiple modifications. The mechanism of agRNA activity appears to be maintained after chemical modification: both native and modified agRNAs modulate recruitment of RNA polymerase II, have the same effect on promoter-derived antisense transcripts, and must be double-stranded. These data demonstrate that agRNA activity is compatible with a wide range of chemical modifications and may facilitate *in vivo* applications.

Note: The following chapter is substantially made up of a research article published by Dr. Jonathan K. Watts and Dongbo Yu under the guidance of Dr. David R. Corey.

INTRODUCTION

The therapeutic potential of gene silencing by small interfering RNAs (siRNAs) is widely recognized (de Fougerolles et al, 2007). siRNA clinical candidates are commonly modified to improve their stability, specificity and potency (Manoharan, 2004; Corey, 2007; Watts et al, 2008). Modified siRNAs have been shown to reduce off-target effects resulting from the miRNA pathway (Jackson et al, 2006; Ui-Tei et al, 2008), the innate immune system (Judge and MacLachlan, 2008; Robbins et al, 2009) and loading of the wrong strand (Ui-Tei et al, 2008; Bramsen et al, 2007; Chen et al, 2008). In addition, chemically modified siRNAs have been used to deepen our understanding of the mechanism of RNAi (Parrish et al, 2000; Martinez et al, 2002; Schwarz et al, 2002; Chiu and Rana, 2002; Rand et al, 2005; Leuschner et al, 2006) and improve siRNA delivery (De Paula et al, 2007; Soutschek et al, 2004).

Antigene RNAs (agRNAs) are small duplex RNAs that target gene promoters or regions beyond the 3'-terminus of genes. Like siRNAs, they are generally 19 bp with 2-nt overhangs at the 3' ends. Depending on target sequence, cell type and basal level of expression, agRNAs can either silence (Morris et al, 2004; Janowski et al, 2005; Janowski et al, 2006) or activate (Li et al, 2006; Janowski et al, 2007) gene expression at the transcriptional level. Like gene silencing by siRNAs, modulation of gene expression by agRNAs involves argonaute (AGO) proteins (Janowski et al, 2006; Kim et al, 2006). However, instead of targeting mRNA, agRNAs target noncoding RNA transcripts (ncRNAs) overlapping gene promoters (Han et al, 2007; Schwartz et al, 2008). While agRNAs can target either sense or antisense noncoding transcripts, the agRNAs discussed in this study target an antisense transcript overlapping the promoter of the progesterone receptor (PR) gene (Schwartz et al, 2008). Thus the guide strand of these agRNA duplexes is the

sense strand, in contrast to siRNAs, for which the guide strand is by definition antisense (*i.e.*, complementary to the mRNA).

agRNAs that activate gene expression could be used to modulate expression of disease-associated genes whose upregulation might be beneficial. As with current gene silencing technology, however, it is likely that any development of agRNAs for *in vivo* use will require chemical modification to improve stability and biodistribution. In this study we examine the effects of modified nucleotides on the function of agRNAs. After examining over 120 duplexes, we identify several chemically modified compounds that retain partial or full activity.

RESULTS

Rationale Behind Selecting Target Genes and Sequences

We focused on the PR gene because it is a well-characterized target for agRNAs (Janowski et al, 2005; Janowski et al, 2006; Janowski et al, 2007; Schwartz et al, 2008). In T47D breast cancer cells, which express a high level of PR, PR expression can be dramatically reduced by agRNA PR-9 that overlaps the start site from -9 to +10 (Janowski et al, 2005; Janowski et al, 2006). In MCF7 breast cancer cells, which express PR at a lower basal level, its expression can be increased by agRNA PR-11 targeting the region from -11 to +8 (Janowski et al, 2007). PR-11 can also activate gene expression in T47D cells but activation becomes most apparent when the cells are grown under conditions that repress basal expression of PR. Whether activation or repression is observed depends primarily on the basal expression level of PR and the target sequence of the agRNA.

While PR-9 and PR-11 are benchmark agRNAs used for most experiments, we also examined other duplexes. For some modifications we tested analogues of silencing agRNA PR-26 (-26 to -8) or activating agRNA PR-22 (-22 to -4) to allow more general insights into gene modulation. To permit comparisons with an RNA that engages the post-transcriptional silencing pathway, we used modified analogues of PR2526, an siRNA that is complementary to PR mRNA from +2526 to +2544. As negative control we used MM4, a duplex containing four mismatches with respect to PR-9. Duplex and single-stranded oligomers were introduced into cells by standard transfection protocols using cationic lipid. Expression was analyzed by western analysis of PR protein and qPCR of PR mRNA.

We use descriptive compound identifiers (Table 7-1). Each type of modified duplex is assigned two uppercase letters. The first letter describes the chemical modification of the

passenger strand, while the second letter describes modification of the guide strand. A lowercase "p" indicates that the 5' end of the strand is phosphorylated. For example, a duplex labeled "NpF" has a native passenger strand and a guide strand that is phosphorylated and fully modified with 2'-fluoro (2'F-RNA) nucleotides. Passenger strands are listed above guide strands throughout.

Effects of 2'F-RNA modification on gene silencing

The structure of 2'F-RNA (Figure 7-1) is similar to that of RNA (Kawasaki et al, 1993) but confers resistance to endonucleases (Layzer et al, 2004; Morrissey et al, 2005). For siRNAs, partial modification with 2'-F RNA is tolerated throughout either strand of the duplex (Chiu and Rana, 2003; Braasch et al, 2003; Harborth et al, 2003) and there have been reports of functional siRNAs that are extensively or completely modified with 2'F-RNA (Morrissey et al, 2005; Blidner et al, 2007; Morrissey et al, 2005). 2'F-RNA has been shown to reduce the immunostimulatory activity of siRNAs (Hornung et al, 2006; Zamanian-Daryoush et al, 2008).

We tested three types of 2'F-RNA-modified strands: fully modified (**F**), modified at all of the pyrimidine units (**Y**), and modified at positions near the termini (**Z**) (Table 7-1 and Figure 7-2A). Relative to unmodified duplex PR-9, we observed reduced potency when either strand was replaced with a fully-fluorinated (PR-9 NpF, PR-9 pFN) or pyrimidine-fluorinated strand (PR-9 NpY, PR-9 pYN) (Figure 7-2B). siRNA PR2526, by contrast, retained most silencing activity after total or partial modification of its passenger strand (PR2526 pFN, PR2526 pYN) but activity was lost after modification of the guide strand (PR2526 NpF, PR2526 NpY) (Figure 7-2B). Duplexes based on either PR-9 or PR2526 containing heavy modifications in both strands were largely inactive.

Given the loss of activity after aggressive modification of PR-9, we tested more limited terminal substitutions. A PR-9 analogue containing minimal modification of the guide strand was effective when paired with an unmodified passenger strand (PR-9 NZ) but not when the passenger strand was heavily modified (PR-9 YZ and PR-9 FZ) (Figure 7-2C). Analogs of PR2526 containing a minimally modified guide strand (PR2526 NZ, PR2526 YZ, PR2526 FZ) were active regardless of the extent of modification of the passenger strand (Figure 7-2C).

We also examined the effect of 2'F-RNA modification on the activity of silencing agRNA PR-26 in an effort to determine how modification effects might vary depending on the sequence of the agRNA. When the pyrimidines of either or both strands of PR-26 were replaced with 2'F-RNA (PR-26 YN, PR-26 NY, PR-26 YY), most silencing activity was retained (Figure 7-2D). Taken together, data from PR-9 and PR-26 demonstrate that 2'F-RNA substitutions are compatible with the mechanism for agRNA activity but that the activity of individual patterns of modification can vary between duplexes.

Effect of 2'F-RNA modification on gene activation

We introduced 2'F-RNA into activating agRNA PR-11 (Figure 7-3A) and observed that the modification was broadly tolerated. Modification of the pyrimidines of the passenger strand (PR-11 pYN), total modification of the passenger strand (PR-11 pFN), or heavy modification of the guide strand (PR-11 NpF and PR11 NpY) all led to gene activation, albeit at levels below those of the unmodified PR-11 duplex (Figure 7-3B). Combining the unmodified or heavily modified passenger strands with a minimally modified guide strand showed a loss of potency as the degree of modification increased (Figure 7-3C). Nevertheless, all of these duplexes retained

significant activity (two-fold to six-fold at the RNA level). PR-11 analogues with both strands heavily modified were inactive.

To assess the generality of 2'F-RNA modification, we also tested a second activating agRNA, PR-22. For PR-22, 2'F-RNA was well-tolerated in the passenger strand and duplexes PR-22 FN and PR-22 YN were able to activate gene expression at both RNA and protein levels without loss of potency (Figure 7-3D). The guide strand of PR-22 was more sensitive to 2'F-RNA modification, with lower levels of gene activation by agRNAs PR-22 NY and PR-22 YY. Taken together with results from PR-11, these results show that 2'F-RNA substitutions can be well tolerated by activating agRNAs and that chemical modifications on the passenger strand tend to be better tolerated.

Effect of 2'-*O*-methyl-RNA on gene silencing

2'-*O*-Methyl-RNA (2'OMe) nucleotides (Figure 1) improve the thermal and nuclease stability of siRNA duplexes (Collingwood et al, 2008; Judge et al, 2006). Inclusion of 2'OMe-RNA units also reduces off-target effects mediated either through the miRNA pathway (Jackson et al, 2006) or the innate immune system (Judge et al, 2006; Robbins et al, 2007; Cekaite et al, 2007). We tested duplex RNAs containing two 2'OMe ribonucleotides at the 5'-terminus of each strand (**J**) or at all pyrimidine nucleotides (**P**) (Figure 7-4A**)**. Duplexes PR-9 JJ, containing 2'OMe nucleotides at both 5'-termini, and PR-9 PN, containing 2'OMe modification at the pyrimidine nucleotides of the passenger strand, were both effective gene silencing agents (Figure 7-4B). Duplexes containing pyrimidine modifications on the guide strand (PR-9 NP, PR-9 PP) were inactive, consistent with previous observations that 2'OMe modification is often better

tolerated in the passenger strand (Czauderna et al, 2003). Variants of PR2526, PR2526 PN, PR2526 NP, and PR2526 PP had activities similar to the PR-9 variants (Figure 7-4B).

We also examined the effects of 2'OMe modification of a second silencing agRNA, PR-26, and identified analogues that inhibited PR expression (Figure 7-4C). However, for PR-26, modification of the guide strand in PR-26 NP did not prevent gene silencing. These data demonstrate that agRNA-mediated gene silencing can tolerate the introduction of 2'OMe-RNA modifications. The influence of a specific pattern of modification, however, depends on the identity of the parent sequence and can vary between agRNAs.

Effect of 2'-*O*-methyl-RNA on gene activation

We introduced 2'-*O*-methyl modifications into two different activating agRNAs, PR-11 and PR-22 (Figure 7-5A). Substitution of 2'OMe units into PR-11 reduced activation from 8-fold to 2-3 fold (Figure 7-5B). PR-11 PP with two heavily modified strands was the least activating. By contrast, activation by modified PR-22 duplexes was relatively stable at 4-6 fold regardless of modification (Figure 7-5C). These data suggest that, as observed above for gene silencing, the impact of 2'OMe modifications on gene activation will vary depending on the parent sequence.

Effect of LNA on gene silencing

Locked nucleic acid (LNA) (Figure 7-1) is a rigid nucleotide analogue containing a constrained, bicyclic sugar. Introduction of locked nucleotides into DNA or RNA oligomers leads to substantially enhanced affinities for complementary sequences (Koshkin et al, 1998; Obika et al, 1998; Petersen and Wengel, 2003; Braasch and Corey, 2001) and enhanced resistance to digestion by nucleases (Braasch and Corey, 2001; Wahlestedt et al, 2000; Elmen et

al, 2005). Several studies have also shown that the introduction of LNA nucleotides can improve the properties of siRNAs (Bramsen et al, 2007; Braasch et al, 2003; Elmen et al, 2005; Mook et al, 2007; Hornung et al, 2005). LNA has been shown to improve loading of the desired strand, increase nuclease resistance (Elmen et al, 2005) and lower immune stimulation (Hornung et al, 2005).

We tested a series of duplexes containing four LNA nucleotides evenly distributed across either the passenger or guide strand (Figure 7-6A). PR-9 LN and PR-9 NL both retained the ability to silence gene expression, albeit to a lesser extent than PR-9 (Figure 7-6B). Significant silencing activity was maintained regardless of whether the sense or antisense strands were modified.

The high binding affinity of LNA has been used to direct loading of the appropriate strand into AGO and bias strand usage (Elmen et al, 2005). We tested a series of thermodynamically biased LNA analogues, to explore whether their activities would differ (Figure 7-6C). Strand L3 contains LNA at the second and sixth positions from its 3'-end, while strand L5 contains LNA at the second and sixth positions from its 5'-end. Modification of the 3'-end of the guide strand (PR-9 NL3), reduced activity of PR-9 (Figure 7-6C). All other RNA duplexes containing two LNA substitutions on one strand (PR-9 NL5, PR-9 L3N, PR-9 L5N) were active regardless of which strand was modified or the location of the modification. Some activity was lost when both strands were modified with LNA (PR-9 L3L5, PR-9 L5L3). Variants of PR2526 containing LNA bases yield results that were analogous to LNA-substituted variants of PR-9 (Figure 7-6B and D).

These results demonstrate that LNA modifications are compatible with gene silencing by agRNAs, but show no evidence for biased strand loading in the context of the PR-9 or PR2526 sequences. The reduction in activity upon modification of the 3' end of the guide strand ("NL3") is consistent with previous observations that LNA modification of the sixth nucleotide from the

3'-end of this strand leads to reduced potency (Elmen et al, 2005). Results were similar for each pattern of modification regardless of whether agRNA PR-9 or siRNA PR2526 was the parent duplex, emphasizing that the response of agRNAs and siRNAs to chemical modification can be similar.

Effect of LNA on gene activation

We tested LNA-modified analogs of PR-11 for gene activation in MCF7 cells (Figure 7-7A). For activating duplex PR-11, we observed activation (2-3 fold versus 6-fold for the unmodified duplex) after modification of either strand with four LNA nucleotides (PR-11 LN, PR-11 NL) (Figure 7-7B). The potency was reduced to the same extent whether the guide or passenger strand was modified. For activation by PR-11, all of the thermodynamically biased LNA analogues maintained significant activity (Figure 7-7C). Modification of either end of the guide strand (PR-11 NL3, PR-11 NL5) gave activity indistinguishable from that of the native PR-11. Passenger strand modification (PR-11 L3N, PR-11 L5N) gave a slight reduction in activation, and modification of both strands (PR-11 L3L5, PR-11 L5L3) led to a further reduction in activation. Nonetheless, even these duplexes modified in both strands gave >3-fold activation at the RNA level and clear activation at the protein level. Together with results of 2'F and 2'-OMe substitution, these data suggest that agRNA-mediated gene activation is broadly tolerant of chemical modification.

Effect of combining modifications on gene silencing

Many examples exist of potent and stable siRNAs containing multiple types of chemical modifications (Morrissey et al, 2005; Allerson et al, 2005; Koller et al, 2006; Dande et al, 2006).

In some cases, combination of multiple modifications led to potency and stability unattainable by the individual modifications alone (Allerson et al, 2005; Dande et al, 2006). We set out to explore whether combination agRNA duplexes (Figure 7-8A) would yield better gene inhibition or activation in their respective cell lines. Even if existing potency is only maintained, the combination of different chemistries could afford better stability and other desirable drug properties.

Our criteria for choosing combinations was to select modified strands from PR-9 and PR-11 analogues showing the highest activity and recombine them in new ways. For PR-9 analogues, this led to the identification of several potent new duplexes (Figure 7-8B). Duplexes including PR-9 L5L5, PR-9 JL, PR-9 JZ, and PR-9 LZ retained substantial activity. Duplexes PR-9 LL5 and PR-9 PpJ lost most activity. The effects appear complex and cannot simply be characterized by considering additive effects from the individual modifications. Nonetheless, it appears that terminal 2'F-RNA modification (**Z**) on the guide strand and LNA modification at the 5'-end of the passenger strand (**L5**) are generally well-tolerated, whereas 2'OMe modification of all pyridimines (**P**) on the passenger strand tends to disrupt the activity.

It is noteworthy that two of the most active combination duplexes also had T_m values that were too high for us to measure (PR-9 L5L5 and PR-9 JL). It is sometimes assumed that high T_m values prevent the strand separation required for siRNA/agRNA activity, but our findings confirm that the relationship between T_m and activity is more complex. This result is consistent with our previous observation that the limited number of agRNA duplexes tested to date do not rigidly adhere to published guidelines for predicting the activity of duplex RNAs (Janowski et al, 2007).

We combined modified strands from active PR-11 analogues to give a new series of activating agRNAs (Figure 7-8C). All the combination duplexes based on PR-11 lost significant

activity with respect to the unmodified control. Duplexes containing LNA in the passenger strand and 2'F-RNA at the termini of the guide strand (PR-11 LZ and PR-11 L5Z) were the best of this series, but only showed 2-3 fold activation at the RNA level (Figure 7-8D).

No evidence that single-strands mediate agRNA activity

There have been reports that single-stranded antisense RNA can lead to inhibition via the RNAi pathway (Martinez et al, 2002; Holen et al, 2003; Amarzguioui et al, 2003). In addition, previous work from our lab (Janowski et al, 2005; Beane et al, 2007; Hu and Corey, 2007) and others (Nielsen et al, 1991; Egholm et al, 1993; Giovannangeli et al, 1997; Larsen et al, 1996) has shown that single-stranded oligonucleotides including peptide nucleic acid (PNA) and LNA-DNA chimeras were able to bind chromosomal DNA and repress gene expression at the transcriptional level.

To explore whether the single-stranded RNAs contained within agRNAs can mediate such effects, we transfected T47D and MCF7 cells with various native and modified single strands from functional silencing or activating agRNA duplexes (Figure 7-9A). Transfections were carried out under the same conditions and at the same concentration (25 nM) as duplex RNAs. Results from both qPCR and western blots demonstrate that single-stranded agRNA, when transfected alone, had no effect on silencing or activation of PR gene expression (Figure 7-9B and C). Our data indicate that gene silencing or activation by the agRNA in our study is not due i) to slight excesses of one strand, ii) to degradation of one strand (prior to incorporation into AGO), or iii) to single-strand-mediated off-target effects.

These data demonstrate that potent modulation of gene expression by anti-PR agRNAs requires the presence of intact duplex RNA regardless of chemical modifications tested in this

study. However, recent studies have demonstrated that a new class of chemically modified single-stranded RNA termed single-stranded, small-interfering RNA (ss-siRNA) is able to efficiently engage RNAi machinery and mediate potent gene inhibition (Lima et al, 2012; Yu et al, 2012). Unpublished data from our lab also showed that PR-9 synthesized with the chemical backbone of ss-siRNA (see Chapter 1, Figure 1-1B for the exact chemistry) is able to silence PR expression (Matsui et al, manuscript in preparation), although the same observation did not extend to PR-11 or other agRNA sequences. These results suggest that duplex composition is not an absolute necessity for agRNA function and promoter-targeted single-stranded RNAs with the right set of modifications can be effective in modulating transcription.

Concentration Dependence of Modified Duplexes

To understand the effect of chemical modification on the potency of agRNAs we examined the dependence of gene silencing or activation on the concentration of selected RNAs. We observed that potencies of gene silencing by modified agRNAs PR-9 L5N and PR-9 NZ were similar to parent agRNA PR-9 (Figure 7-10A). Likewise, potencies of gene activation by PR-11 pYN and PR-11 pFN was similar to gene activation by parent agRNA PR-11 (Figure 7-10B). Thus it is possible to achieve potent, dose-dependent gene modulation by both activating and inhibitory chemically modified agRNAs. For silencing agRNAs based on PR-9, we calculated IC_{50} values for the native duplex and several modified analogues (Table 7-2). At both the protein and RNA levels, some of the modified analogues were of comparable potency to PR-9 itself (e.g. PR-9 NL). Others, while still active, showed reduced potency (e.g. PR-9 NZ).

Modified duplexes affect recruitment of RNA polymerase II

We have previously used chromatin immunoprecipitation (ChIP) of RNA polymerase II (RNAPII) (Schwartz et al, 2008) and nuclear run-on assays (Janowski et al, 2006) to suggest that both silencing and activating agRNAs affect PR transcription. To investigate whether chemically modified agRNAs operate through the same mechanism as their native counterparts, we carried out RNAPII ChIP using two active modified duplexes (Figure 7-11). In T47D cells, treatment with either PR-9 or its modified analogue PR-9 PN led to reduced occupancy of RNAPII at the PR promoter relative to cells treated with the luciferase control duplex siGL2 (Figure 7-11A). In MCF7 cells, treatment with either PR-11 or the modified analogue PR-11 pYN increased levels of RNAPII at the PR promoter (Figure 7-11B). The finding that native and modified duplexes behave similarly supports the suggestion that they act through similar mechanisms.

Native and modified duplexes have the same effect on antisense transcript levels

We have previously observed that both activating and inhibitory agRNAs bind to an antisense transcript that overlaps the PR promoter (Schwartz et al, 2008). This transcript originates within PR mRNA and extends 70,000 bp upstream. It is spliced, and the spliced product contains target sequences for all the agRNAs used in this study. When biotinylated agRNAs are transfected into cells they bind the antisense transcript. RNA immunoprecipitation shows that both activating and silencing agRNAs recruit argonaute protein to the antisense transcript. The antisense transcript, therefore, appears to play a central role in the mechanism of agRNAs.

We explored the effect of chemically modified agRNAs on levels of the promoter-associated antisense transcript. We previously observed that treatment of T47D cells with

silencing agRNA PR-9 led to a reduction of antisense transcript levels, while treatment of MCF7 cells with activating agRNA PR-11 led to no significant change in antisense transcript levels (Schwartz et al, 2008). We repeated these experiments using both the native duplexes and several of the most active modified analogues. We monitored expression of PR mRNA and the antisense transcripts that span the agRNA target region using qPCR.

Native and modified duplexes gave comparable results. PR-9 and modified PR analogues reduced expression of both PR mRNA and the promoter-derived antisense transcript similarly (Figure 7-11C). Conversely, PR-11 and modified analogues increased expression of PR mRNA, but caused no significant change in antisense transcript levels (Figure 7-11B). The finding that native and modified duplexes have the same effect on levels of the antisense transcript supports the conclusion that they act through similar mechanisms.

Inactive modified duplexes do not compete for target sites

It is interesting to speculate as to why some patterns of modification cause reduced activity. Inactive agRNAs could be failing at any of a number of steps: (i) loading into the RNA-induced silencing complex (RISC), (ii) cleavage or dissociation of the passenger strand, (iii) import into the nucleus, (iv) binding of the RNA target, or (v) execution of the effect (activation or silencing). We previously observed that inactive native duplexes such as PR-8 (targeting -8 to +11) and PR-12 (-12 to +7) could compete for target sites with the active duplex PR-11 (Janowski et al, 2007). Thus, treating MCF7 cells with inactive duplex PR-12 prevented gene activation by PR-11 in a subsequent transfection several days later. On the other hand, initial treatment with PR-11 followed later by PR-12 gave activation comparable to PR-11 alone (Janowski et al, 2007). This experiment showed that the order of addition is crucial and the

duplexes compete for the same target sites. Duplexes PR-8 and PR-12 failed at step (v) above – they were loaded into RISC and even bound the correct RNA target, but failed to execute an agRNA effect. Therefore, since shifting the duplex–target interaction by 1-3 bp is sufficient to eliminate activity, the geometry of interaction at the promoter may be crucial for induction of gene activation.

To test where inactive chemically modified agRNAs might be deficient we carried out a similar experiment using two inactive modified duplexes each for silencing and activation. In T47D cells we used the inactive duplexes PR-9 YY and PR-9 pFN. In both cases, levels of PR expression were identical whether the inactive duplexes were transfected before or after the active duplex PR-9 (Figure 7-12A). Similarly, treatment of MCF7 cells with PR-11 gave gene activation regardless of whether the duplexes were transfected before or after inactive modified duplexes PR-11 PL and PR-11 LP (Figure 7-12B). These data suggest that the modified duplexes did not compete for target sites with native duplexes. Since the inactive modified duplexes are not binding the target site, they must be failing at one of the first four steps in the process: RISC loading, passenger strand removal, nuclear import or target binding. Furthermore, some of the inactive modified duplexes contain native guide strands, thus it seems clear that they are failing at one of the first two steps – RISC loading or passenger strand removal – since after this point they would be identical with native duplexes. Therefore in most cases, the challenges causing modified agRNAs to fail are the same as those faced by chemically modified siRNAs that are complementary to mRNA.

DISCUSSION

Double stranded RNAs that are complementary to mRNA are currently being tested in clinical trials (de Fougerolles et al, 2007; Manoharan, 2004; Corey, 2007; Watts et al, 2008). Given the success of siRNAs in the laboratory and progress in the clinic, why would agRNAs enhance the potential for *in vivo* application of double-stranded RNA? One reason is that activating gene expression would open up a wider range of therapeutic targets and may provide new opportunities for development. For example, if more of a protein product is needed to treat a disease, upregulating expression using agRNAs might prove advantageous, especially if the protein's site of action is intracellular and cannot be accessed by systemically administered protein. Even in the case of gene silencing, where existing siRNA technology often gives superb results, it is possible that silencing at the transcriptional level may be advantageous for some targets. It is possible to envision that agRNAs may be more potent in some cases, produce longer lasting effects, or produce different modulation of isoform expression. Finally, understanding the effect of modifications will also important for future studies of agRNA function in cultured cells.

Our data have several implications for the mechanism of chemically modified agRNAs: (i) As with any structure–function analysis, the most important finding is that some designs yield active compounds whereas others do not; (ii) Two strands are necessary for efficient action of agRNAs, we observe no silencing or activation by single strands at the highest concentrations used in this study; (iii) Activation and silencing show a regular, predictable dose dependence; (iv) As with siRNAs, optimal modifications need to be determined empirically for each sequence; (v) As with siRNAs, both guide and passenger strands can be modified, but modifications are generally better tolerated on the passenger strand; (vi) IC_{50} values and maximal efficacies of modified and unmodified agRNAs are similar, consistent with the expectation that

they operate by a common mechanism; (vii) Both native and modified duplexes affect recruitment of RNAP2, also consistent with a common mechanism; (viii) Addition of modified and unmodified agRNAs leads to almost identical changes in antisense transcript levels, again consistent with a shared mechanism; and (ix) Inactive duplexes do not compete with active duplexes, suggesting that the inactive duplexes fail at a step prior to association with the antisense transcript.

The finding that agRNAs containing 2'F-RNA, 2'OMe-RNA, or LNA retain the ability to silence or activate gene expression is significant because it demonstrates that agRNAs tolerate the introduction of modifications known to be powerful tools for improving in vivo properties. For duplex RNAs that are complementary to mRNA, it is commonly observed that different sequences tolerate different chemical modifications or different patterns of the same chemical modification. The interplay of chemical modifications with each particular sequence is the ultimate determinant of duplex potency and duplexes with optimal properties must be determined empirically. No universal rules of siRNA modification have been developed because our understanding of the nature of this interplay is not yet sufficient.

Our data on agRNAs suggest the same conclusion. We have tested two different silencing agRNAs, PR-9 and PR-26, and two different activating agRNAs, PR-11 and PR-22. While both tolerate a wide range of modifications, the relative potencies of analogous modified duplexes differ. Like siRNAs, we conclude that empirical testing will be needed to identify agRNAs with the best balance of properties. While empirical testing may be necessary, we found that a wide range of modifications were compatible with gene silencing or activation by an agRNA-mediated mechanism and we predict that it will not be difficult to develop active chemically modified agRNAs for genes of interest where a parent unmodified agRNA has already been identified.

MATERIALS AND METHODS

Double-stranded RNAs

RNAs were synthesized by Alnylam Pharmaceuticals or SIGMA Custom Products using standard protocols, or were purchased from Integrated DNA Technologies. The concentrations of single strands were determined by measuring their absorbance at 260 nm (A_{260}). Complementary single strands were combined in equimolar ratios and diluted to 20 μM stock solutions in 2.5x phosphate-buffered saline. These duplexes were annealed by heating to 95 ºC and slowly cooled to room temperature on a thermal cycler. Duplex integrity was tested by a UV thermal melt experiment as described below. Duplexes were stored at -20 ºC.

Cell Culture

T47D and MCF7 cells (American Type Culture Collection) were maintained in RPMI-1640 media (Sigma) supplemented with 10% (v/v) FBS, 0.5x MEM nonessential amino acids, 0.4 units ml^{-1} bovine insulin, 10 mM HEPES and 1 mM sodium pyruvate. Cells were cultured at 37 ºC and 5% CO_2.

Lipid-mediated Transfection

Cells were plated at 110,000 to 160,000 cells per well in six-well plates (Costar) in RPMI. A higher number of cells were typically seeded for RNA analysis than for protein analysis. Transfections were performed after 1-2 d, when the cells had adhered and attained about 20-30% confluence. Lipofectamine RNAiMAX cationic lipid (1.1 μL/well, Invitrogen) and RNA (31 pmol/well) were individually diluted in Opti-MEM (Invitrogen), then combined

and allowed to incubate for 20 min (volume 250 μL/well) before pipetting into cell culture wells containing 1 mL fresh Opti-MEM (final volume 1.25 mL, 25 nM duplex RNA for all transfections except dose response experiments). The transfection solution was replaced with RPMI after 24 h, and media were changed again 2 d later. For dose response experiments, the ratio of lipid to RNA was kept constant, and the concentration of RNA was varied from 0 to 50 nM.

For competition experiments, the cells were passaged into new plates on day 2 or 3 after transfection. The second transfection was carried out on day 4 after the first transfection under identical conditions, and protein was harvested on day 7 or 8. The negative control duplex Neg1 used in these experiments consisted of oligonucleotides 5'-UCAAGAAGCCAAGGAUAAUdTdT-3' and 5'-AUUAUCCUUGGCUUCUUGAdTdT-3'.

RNA harvest, Q-PCR, and Determination of Melting Temperature (T_m)

The protocols are largely identical to those described before (reference HTT project method section for details). For analysis of PR mRNA, we used a primer-probe assay (IDT) consisting of primers 5'-CTTACCTGTGGGAGCTGTA-3' and 5'-GCACTTTCTAAGGCGACATG-3' as well as probe 5'-CTGCCCTTCCATTGCCCTCTT-3'. For analysis of promoter-derived antisense transcripts, we used SYBRgreen qPCR with primers 5'-GGAGGAGGCGTTGTTAGAAA-3' and 5'-GAAGGGTCGGACTTCTGCT-3'.

Analysis of Protein Expression

The protocols are largely identical to those described before (reference HTT project method section for details). Protein was generally harvested from treated MCF7 or T47D cells 5

d after transfection. PR monoclonal primary antibody (Cell Signaling) was diluted 1:1000 dilution in PBS-T over-night while β-actin antibody (Sigma) was diluted 1:10,000 dilution for 1 hincubation.

Chromatin Immunoprecipitation (ChIP)

Chromatin immunoprecipitation was performed essentially as described (Hardy et al., 2006). Two or three 150-mm dishes of T47D or MCF7 cells were reverse transfected with 25 nM of native agRNA, modified agRNA or luciferase control duplex siGL2 (Elbashir et al., 2001).

Media were changed on day 2 and the cells harvested on day 3. To crosslink and harvest nuclei, the cells were treated with 1% formaldehyde in PBS (10 mL) for 10 min, then the crosslinking reaction was quenched with glycine (0.125 M final concentration, at least 5 min). Cells were collected and nuclei were isolated by treatment with cold hypotonic lysis buffer (4 mL) containing 10 mM Tris (pH 7.4), 10 mM NaCl, 3 mM MgCl2 and 0.5% Nonidet P40. The pelleted nuclei were lysed with a buffer containing 1% SDS, 10 mM EDTA, 50 mM Tris-HCl (pH 8.1) and 1x complete protease inhibitor cocktail (Roche). DNA was sonicated on ice to an average fragment size of ~500 bp. The lysate was then centrifuged to remove insoluble cell debris and the supernatant precleared with Protein G Plus / Protein A Agarose suspension (Calbiochem).

An aliquot of the cleared lysate (100 µL) was diluted to 1 mL in buffer (0.01% SDS, 1.1% Triton X-100, 1.2 mM EDTA, 16.7 mM Tris pH 8.1, 167 mM NaCl and 1x complete protease inhibitor cocktail (Roche). Mouse anti-RNAPII IgG (Millipore, Catalogue #05-623, 3-6 µg) or normal mouse IgG (Millipore Catalogue #12-371, 3-6 µg) was added and the solution

rotated at 4 ºC overnight. Protein G Plus / Protein A agarose suspension (30-60 µL) was added to precipitate the antibody complexes and the beads were washed as described (Hardy et al., 2006). Complexes were eluted using 2 × 250 µL of $NaHCO_3$ (0.1 M) containing 1% SDS. NaCl was added (final concentration 200 mM) and the samples heated to 65 ºC for at least 2h to reverse crosslinks. The samples were then treated with RNase A (1 µL) at 37 ºC for 30 min, followed by Tris-HCl (pH 7.0, 20 µL), EDTA (0.5 M, 10 µL) and proteinase K (20 µg) at 42 ºC for 45 min. DNA was isolated by phenol-chloroform extraction and ethanol precipitation. Pellets were diluted to 50 µL in water and 5 µL was used per qPCR reaction. qPCR primers used at the PR promoter were Fwd 5'-CCTAGAGGAGGAGGCGTTGT and Rev 5'-ATTGAGAATGCCACCCACA. Levels of RNAPII at the GAPDH promoter were also measured with primers Fwd 5'-TACTAGCGGTTTTACGGGCG and Rev 5'-TCGAACAGGAGGAGCAGAGAGCGA and were used for normalization. Each sample was normalized to a corresponding 2% input sample.

Statistics, Dose Response Profiles, and Curve Fitting

Error bars shown on qPCR graphs correspond to standard deviations from triplicate measurements of at least two independent transfections; they include the error from the qPCR measurement as well as from differences between the transfections. For Figures 2-7 we also examined whether RNA expression levels were significantly different from the mismatch control by conducting a two-tailed unpaired Student's T-test with equal variances, and for this test we considered only biological replicates (using averages of the triplicate qPCR measurements for each). Significance levels of p-values are * ($p < 0.05$), ** ($p < 0.01$) and *** ($p < 0.005$).

Dose responses were fit to the model equation $y = 100(1-x^m/(n^m+x^m))$, where y is the percent of target (protein or mRNA) remaining, x is the concentration of agRNA in nM. The regression was fit by optimizing m and n using SigmaPlot 11, and n was taken as the IC_{50} value.

REFERENCES

Allerson, C.R., Sioufi, N., Jarres, R., Prakash, T.P., Naik, N., Berdeja, A., Wanders, L., Griffey, R.H., Swayze, E.E., and Bhat, B. (2005) Fully 2'-Modified Oligonucleotide Duplexes with Improved in Vitro Potency and Stability Compared to Unmodified Small Interfering RNA. J. Med. Chem. *48*, 901-904.

Amarzguioui, M., Holen, T., Babaie, E., and Prydz, H. (2003) Tolerance for mutations and chemical modifications in a siRNA. Nucl. Acids Res. *31*, 589-595.

Beane, R.L., Ram, R., Gabillet, S., Arar, K., Monia, B.P., and Corey, D.R. (2007) Inhibiting Gene Expression with Locked Nucleic Acids (LNAs) That Target Chromosomal DNA. Biochemistry, *46*, 7572-7580.

Blidner, R.A., Hammer, R.P., Lopez, M.J., Robinson, S.O., and Monroe, W.T. (2007) Fully 2'-deoxy-2'-fluoro substituted nucleic acids induce RNA interference in mammalian cell culture. Chem. Biol. Drug Des. *70*, 113-122.

Braasch, D.A., Jensen, S., Liu, Y., Kaur, K., Arar, K., White, M.A. and Corey, D.R. (2003) RNA Interference in Mammalian Cells by Chemically-Modified RNA. Biochemistry. *42*, 7967-7975.

Braasch, D.A., and Corey, D.R. (2001) Locked nucleic acid (LNA): Fine-tuning the recognition of DNA and RNA. Chem. Biol. *8*, 1-7.

Bramsen, J.B., Laursen, M.B., Damgaard, C.K., Lena, S.W., Ravindra Babu, B., Wengel, J., and Kjems, J. (2007) Improved silencing properties using small internally segmented interfering RNAs. Nucl. Acids Res. *35*, 5886-5897.

Cekaite, L., Furset, G., Hovig, E., and Sioud, M. (2007) Gene Expression Analysis in Blood Cells in Response to Unmodified and 2'-Modified siRNAs Reveals TLR-dependent and Independent Effects. J. Mol. Biol. *365*, 90-108.

Chen, P.Y., Weinmann, L., Gaidatzis, D., Pei, Y., Zavolan, M., Tuschl, T., and Meister, G. (2008) Strand-specific 5'-*O*-methylation of siRNA duplexes controls guide strand selection and targeting specificity. RNA *14*, 263-274.

Chiu, Y.-L., and Rana, T.M. (2002) RNAi in Human Cells: Basic Structural and Functional Features of Small Interfering RNA. Mol. Cell. *10*, 549-561.

Chiu, Y.L., and Rana, T.M. (2003) siRNA function in RNAi: A chemical modification analysis. RNA. *9*, 1034-1048.

Collingwood, M.A., Rose, S.D., Huang, L., Hillier, C., Amarzguioui, M., Wiiger, M.T., Soifer, H.S., Rossi, J.J., and Behlke, M.A. (2008) Chemical modification patterns compatible with high potency dicer-substrate small interfering RNAs. *Oligonucleotides*, **18,** 187-200.

Corey, D.R. Chemical modification: the key to clinical application of RNA interference? (2007) J. Clin. Invest. *117*, 3615-3622.

Czauderna, F., Fechtner, M., Dames, S., Aygun, H., Klippel, A., Pronk, G.J., Giese, K., and Kaufmann, J. (2003) Structural variations and stabilising modifications of synthetic siRNAs in mammalian cells. Nucl. Acids Res. *31*, 2705-2716.

Dande, P., Prakash, T.P., Sioufi, N., Gaus, H., Jarres, R., Berdeja, A., Swayze, E.E., Griffey, R.H., and Bhat, B. (2006) Improving RNA Interference in Mammalian Cells by 4'-Thio-Modified Small Interfering RNA (siRNA): Effect on siRNA Activity and Nuclease Stability When Used in Combination with 2'-*O*-Alkyl Modifications. J. Med. Chem. *49*, 1624-1634.

de Fougerolles, A., Vornlocher, H.-P., Maraganore, J., and Lieberman, J. Interfering with disease: a progress report on siRNA-based therapeutics. (2007) Nat. Rev. Drug Discov. *6*, 443-453.

De Paula, D., Bentley, M.V.L.B., and Mahato, R.I. (2007) Hydrophobization and bioconjugation for enhanced siRNA delivery and targeting. RNA. *13*, 431-456.

Egholm, M., Buchardt, O., Christensen, L., Behrens, C., Freier, S.M., Driver, D.A., Berg, R.H., Kim, S.K., Norden, B., and Nielsen, P.E. (1993) PNA Hybridizes to Complementary Oligonucleotides Obeying the Watson-Crick Hydrogen-Bonding Rules. Nature. *365*, 566-568.

Elbashir, S.M., Harborth, J., Lendeckel, W., Yalcin, A., Weber, K., and Tuschl, T. (2001) Duplexes of 21-nucleotide RNAs mediate RNA interference in cultured mammalian cells. Nature. *411*, 494-498.

Elmen, J., Thonberg, H., Ljungberg, K., Frieden, M., Westergaard, M., Xu, Y., Wahren, B., Liang, Z., Urum, H., Koch, T. *et al.* (2005) Locked nucleic acid (LNA) mediated improvements in siRNA stability and functionality. Nucl. Acids Res. *33*, 439-447.

Giovannangeli, C., Diviacco, S., Labrousse, V., Gryaznov, S., Charneau, P., and Helene, C. (1997) Accessibility of nuclear DNA to triplex-forming oligonucleotides: the integrated HIV-1 provirus as a target. Proc. Natl. Acad. Sci. U. S. A. *94*, 79-84.

Han, J., Kim, D., and Morris, K.V. (2007) Promoter-associated RNA is required for RNA-directed transcriptional gene silencing in human cells. Proc. Natl. Acad. Sci. USA. *104*, 12422-12427.

Harborth, J., Elbashir, S.M., Vandenburgh, K., Manninga, H., Scaringe, S.A., Weber, K., and Tuschl, T. (2003) Sequence, Chemical, and Structural Variation of Small Interfering RNAs and Short Hairpin RNAs and the Effect on Mammalian Gene Silencing. Antisense Nucleic Acid Drug Dev. *13,* 83-105.

Hardy, D.B., Janowski, B.A., Corey, D.R., and Mendelson, C.R. (2006) Progesterone Receptor Plays a Major Antiinflammatory Role in Human Myometrial Cells by Antagonism of Nuclear Factor-kB Activation of Cyclooxygenase 2 Expression. Mol. Endocrinol. *20,* 2724-2733.

Holen, T., Amarzguioui, M., Babaie, E., and Prydz, H. (2003) Similar behaviour of single-strand and double-strand siRNAs suggests they act through a common RNAi pathway. Nucl. Acids Res. *31,* 2401-2407.

Hornung, V., Ellegast, J., Kim, S., Brzozka, K., Jung, A., Kato, H., Poeck, H., Akira, S., Conzelmann, K.-K., Schlee, M. *et al.* (2006) 5'-Triphosphate RNA Is the Ligand for RIG-I. Science. *314,* 994-997.

Hornung, V., Guenthner-Biller, M., Bourquin, C., Ablasser, A., Schlee, M., Uematsu, S., Noronha, A., Manoharan, M., Akira, S., de Fougerolles, A. *et al.* (2005) Sequence-specific potent induction of IFN-alpha by short interfering RNA in plasmacytoid dendritic cells through TLR7. Nat. Med. *11,* 263-270.

Hu, J., and Corey, D.R. (2007) Inhibiting Gene Expression with Peptide Nucleic Acid (PNA)-Peptide Conjugates That Target Chromosomal DNA. Biochemistry. *46,* 7581-7589.

Jackson, A.L., Burchard, J., Leake, D., Reynolds, A., Schelter, J., Guo, J., Johnson, J.M., Lim, L., Karpilow, J., Nichols, K. *et al.* (2006) Position-specific chemical modification of siRNAs reduces "off-target" transcript silencing. RNA. *12,* 1197-1205.

Janowski, B.A., Huffman, K.E., Schwartz, J.C., Ram, R., Hardy, D., Shames, D.S., Minna, J.D., and Corey, D.R. (2005) Inhibiting gene expression at transcription start sites in chromosomal DNA with antigene RNAs. Nat. Chem. Biol. *1,* 216-222.

Janowski, B.A., Huffman, K.E., Schwartz, J.C., Ram, R., Nordsell, R., Shames, D.S., Minna, J.D., and Corey, D.R. (2006) Involvement of AGO1 and AGO2 in mammalian transcriptional silencing. Nat. Struct. Mol. Biol. *13,* 787-792.

Janowski, B.A., Hu, J., and Corey, D.R. (2006) Silencing gene expression by targeting chromosomal DNA with antigene peptide nucleic acids and duplex RNAs. Nat. Protocols. *1,* 436-443.

Janowski, B.A., Kaihatsu, K., Huffman, K.E., Schwartz, J.C., Ram, R., Hardy, D., Mendelson, C.R., and Corey, D.R. (2005) Inhibiting transcription of chromosomal DNA with antigene peptide nucleic acids. Nat. Chem. Biol. *1,* 210-215.

Janowski, B.A., Younger, S.T., Hardy, D.B., Ram, R., Huffman, K.E., and Corey, D.R. (2007) Activating gene expression in mammalian cells with promoter-targeted duplex RNAs. Nat. Chem. Biol. *3,* 166-173.

Judge, A.D., Bola, G., Lee, A.C.H., and MacLachlan, I. (2006) Design of Noninflammatory Synthetic siRNA Mediating Potent Gene Silencing in Vivo. Mol. Ther. *13,* 494-505.

Judge, A., and MacLachlan, I. (2008) Overcoming the innate immune response to small interfering RNA. Hum. Gene Ther. *19,* 111-124.

Kawasaki, A.M., Casper, M.D., Freier, S.M., Lesnik, E.A., Zounes, M.C., Cummins, L.L., Gonzalez, C., and Cook, P.D. (1993) Uniformly modified 2'-deoxy-2'-fluoro-phosphorothioate oligonucleotides as nuclease-resistant antisense compounds with high affinity and specificity for RNA targets. J. Med. Chem. *36,* 831-841.

Kim, D.H., Villeneuve, L.M., Morris, K.V., and Rossi, J.J. (2006) Argonaute-1 directs siRNA-mediated transcriptional gene silencing in human cells. Nat. Struct. Mol. Biol. *13,* 793-797.

Koller, E., Propp, S., Murray, H., Lima, W., Bhat, B., Prakash, T.P., Allerson, C.R., Swayze, E.E., Marcusson, E.G., and Dean, N.M. (2006) Competition for RISC binding predicts in vitro potency of siRNA. Nucl. Acids Res. *34,* 4467-4476.

Koshkin, A.A., Singh, S.K., Nielsen, P., Rajwanshi, V.K., Kumar, R., Meldgaard, M., Olsen, C.E., and Wengel, J. (1998) LNA (Locked Nucleic Acids): Synthesis of the adenine, cytosine, guanine, 5-methylcytosine, thymine and uracil bicyclonucleoside monomers, oligomerisation, and unprecedented nucleic acid recognition. Tetrahedron. *54,* 3607-3630.

Layzer, J.M., McCaffrey, A.P., Tanner, A.K., Huang, Z.A.N., Kay, M.A., and Sullenger, B.A. (2004) In vivo activity of nuclease-resistant siRNAs. RNA, *10,* 766-771.

Larsen, H.J., and Nielsen, P.E. (1996) Transcription-mediated binding of peptide nucleic acid (PNA) to double-stranded DNA: sequence-specific suicide transcription. Nucl. Acids Res. *24,* 458-463.

Leuschner, P.J.F., Ameres, S.L., Kueng, S., and Martinez, J. (2006) Cleavage of the siRNA passenger strand during RISC assembly in human cells. EMBO Rep. *7,* 314-320.

Li, L.-C., Okino, S.T., Zhao, H., Pookot, D., Place, R.F., Urakami, S., Enokida, H., and Dahiya, R. (2006) Small dsRNAs induce transcriptional activation in human cells. Proc. Natl. Acad. Sci. USA, *103,* 17337-17342.

Lima, W.F., Prakash, T.P., Murray, H.M., Kinberger, G.A., Li, W., Chappell, A.E., Li C.S., Murray, S.F., Gaus, H., Seth, P.P., Swayze, E.E., and Crooke, S.T. (2012) Single-stranded siRNAs Activate RNAi in Animals. Cell, *150,* 883-94

Manoharan, M. (2004) RNA interference and chemically modified small interfering RNAs. Curr. Opin. Chem. Biol. *8,* 570-579.

Martinez, J., Patkaniowska, A., Urlaub, H., Luhrmann, R., and Tuschl, T. (2002) Single-Stranded Antisense siRNAs Guide Target RNA Cleavage in RNAi. Cell. *110,* 563-574.

Mook, O.R., Baas, F., de Wissel, M.B., and Fluiter, K. (2007) Evaluation of locked nucleic acid-modified small interfering RNA in vitro and in vivo. Mol. Cancer Therap. *6,* 833-843.

Morris, K.V. (2009) RNA-directed transcriptional gene silencing and activation in human cells. Oligo cleotides, *19,* 299-305.*nu*

Morris, K.V., Chan, S.W.L., Jacobsen, S.E., and Looney, D.J. (2004) Small Interfering RNA-Induced Transcriptional Gene Silencing in Human Cells. Science. *305,* 1289-1292.

Morrissey, D.V., Lockridge, J.A., Shaw, L., Blanchard, K., Jensen, K., Breen, W., Hartsough, K., Machemer, L., Radka, S., Jadhav, V. *et al.* (2005) Potent and persistent in vivo anti-HBV activity of chemically modified siRNAs. Nat. Biotech. *23,* 1002-1007.

Morrissey, D.V., Blanchard, K., Shaw, L., Jensen, K., Lockridge, J.A., Dickinson, B., McSwiggen, J.A., Vargeese, C., Bowman, K., Shaffer, C.S. *et al.* (2005) Activity of stabilized short interfering RNA in a mouse model of hepatitis B virus replication. Hepatology *41,* 1349-1356.

Nielsen, P.E., Egholm, M., Berg, R.H., and Buchardt, O. (1991) Sequence-Selective Recognition of DNA by Strand Displacement with a Thymine-Substituted Polyamide. Science. *254,* 1497-1500.

Obika, S., Nanbu, D., Hari, Y., Andoh, J.-i., Morio, K.-i., Doi, T., and Imanishi, T. (1998) Stability and structural features of the duplexes containing nucleoside analogues with a fixed N-type conformation, 2'-O,4'-C-methyleneribonucleosides. Tetrahedron Lett. *39,* 5401-5404.

Parrish, S., Fleenor, J., Xu, S., Mello, C., and Fire, A. (2000) Functional Anatomy of a dsRNA Trigger: Differential Requirement for the Two Trigger Strands in RNA Interference. Mol. Cell. *6,* 1077-1087.

Petersen, M., and Wengel, J. (2003) LNA: a versatile tool for therapeutics and genomics. Trends Biotechnol. *21,* 74-81.

Rand, T.A., Petersen, S., Du, F., and Wang, X. (2005) Argonaute2 Cleaves the Anti-Guide Strand of siRNA during RISC Activation. Cell. *123,* 621-629.

Robbins, M., Judge, A., and MacLachlan, I. (2009) siRNA and Innate Immunity. Oligonucleotides. *19,* 89-102.

Robbins, M., Judge, A., Liang, L., McClintock, K., Yaworski, E., and MacLachlan, I. (2007) 2'-*O*-methyl-modified RNAs act as TLR7 antagonists. Mol. Ther. *15,* 1663-1669.

Schwarz, D.S., Hutvágner, G., Haley, B., and Zamore, P.D. (2002) Evidence that siRNAs Function as Guides, Not Primers, in the Drosophila and Human RNAi Pathways. Mol. Cell. *10,* 537-548.

Schwartz, J.C., Younger, S.T., Nguyen, N.B., Hardy, D.B., Monia, B.P., Corey, D.R., and Janowski, B.A. (2008) Antisense transcripts are targets for activating small RNAs. Nat. Struct. Mol. Biol. *15,* 842-848.

Soutschek, J., Akinc, A., Bramlage, B., Charisse, K., Constien, R., Donoghue, M., Elbashir, S., Geick, A., Hadwiger, P., Harborth, J. *et al.* (2004) Therapeutic silencing of an endogenous gene by systemic administration of modified siRNAs. Nature. *432***,** 173-178.

Ui-Tei, K., Naito, Y., Zenno, S., Nishi, K., Yamato, K., Takahashi, F., Juni, A., and Saigo, K. (2008) Functional dissection of siRNA sequence by systematic DNA substitution: modified siRNA with a DNA seed arm is a powerful tool for mammalian gene silencing with significantly reduced off-target effect. Nucl. Acids Res. *36,* 2136-2151.

Wahlestedt, C., Salmi, P., Good, L., Kela, J., Johnsson, T., Hokfelt, T., Broberger, C., Porreca, F., Lai, J., Ren, K. *et al.* (2000) Potent and nontoxic antisense oligonucleotides containing locked nucleic acids. Proc. Natl. Acad. Sci. U. S. A. *97,* 5633-5638.

Watts, J.K., Deleavey, G.F., and Damha, M.J. (2008) Chemically modified siRNA: tools and applications. Drug Discov. Today. *13,* 842-855.

Yu, D., Pendergraff, H., Liu, J., Kordasiewicz, H., Cleveland, D.W., Swayze, E.E., Lima, W.F., Crooke, S.T., Prakash, T.P., and Corey, D.R. (2012) Single-Stranded RNAs Use RNAi to Potently and Allele-Selectively Inhibit Mutant Huntingtin Expression. Cell, *150,* 895-908

Zamanian-Daryoush, M., Marques, J.T., Gantier, M.P., Behlke, M.A., John, M., Rayman, P., Finke, J., and Williams, B.R.G. (2008) Determinants of Cytokine Induction by Small Interfering RNA in Human Peripheral Blood Mononuclear Cells. J. Interferon Cytokine Res. *28,* 221-233.

Table 7-1: Descriptive strand names used throughout this chapter

Abbreviation	Chemistry
N	Native RNA strand
F	2'F-RNA, fully modified
Y	2'F-RNA, all pyrimidines
Z	2'F-RNA, contains three units near termini
P	2'-OMe-RNA, all pyrimidines
J	2'-OMe-RNA, two units at the 5'-end
L	LNA, contains four units distributed evenly
L3	LNA, contains two units toward the 3'-end
L5	LNA, contains two units toward the 5'-end
p	A lower case “p” preceding any strand abbreviation indicates a 5'-phosphate.

Table 7-2. IC_{50} values for PR-9 and modified analogues in T47D cells.

Silencing agRNA	Type of chemistry	IC_{-50} (RNA, nM)	IC_{-50} (protein, nM)
PR9	Native	5.6	12.2
PR9 NZ	2'F	18.6	19.6
PR9 JpJ	2'OMe	9.4	10.2
PR9 PN	2'OMe	12.9	12.6
PR9 NL	LNA	6.8	13.2
PR9 L5N	LNA	13.3	7.4

Figure 7-1: Chemical modifications used in this chapter.

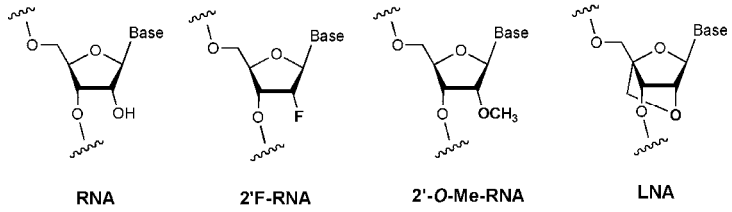

Figure 7-2

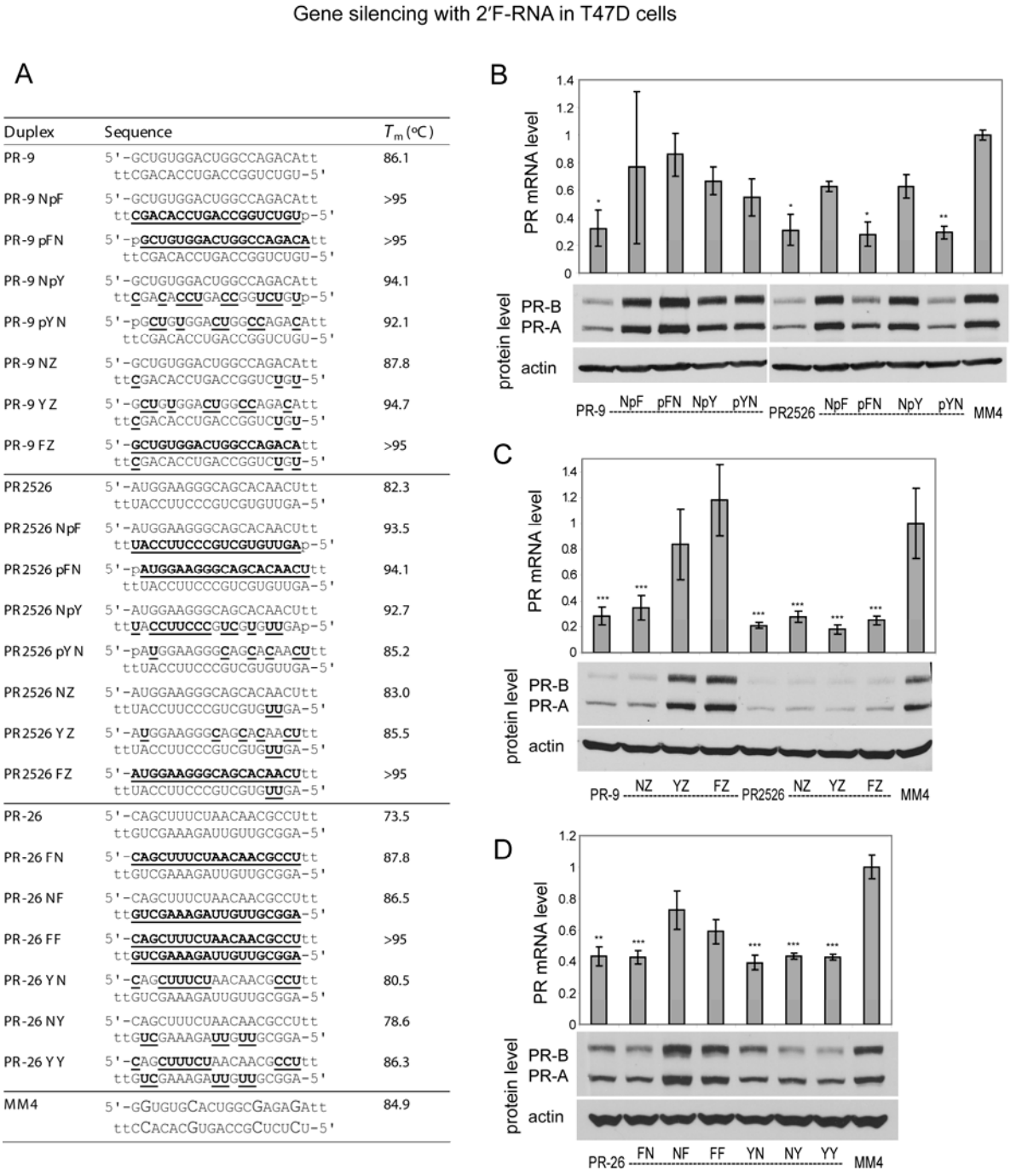

Figure 7-2. PR gene expression can be silenced by agRNAs containing 2'F-RNA. (A) Duplex sequences: passenger strands are listed on top in all cases. Modification codes: dna, RNA, **2'F-RNA**; p=phosphate. (B) PR-9 analogues and controls containing one strand modified with 2'F-RNA. (C) PR-9 analogues and controls containing a minimally 2'F-RNA-modified guide strand. (D) PR-26 analogues containing one or both strands modified with 2'F-RNA. All data are normalized to mismatch control MM4. Error bars are standard deviation (SD) from biological replicates.

Figure 7-3

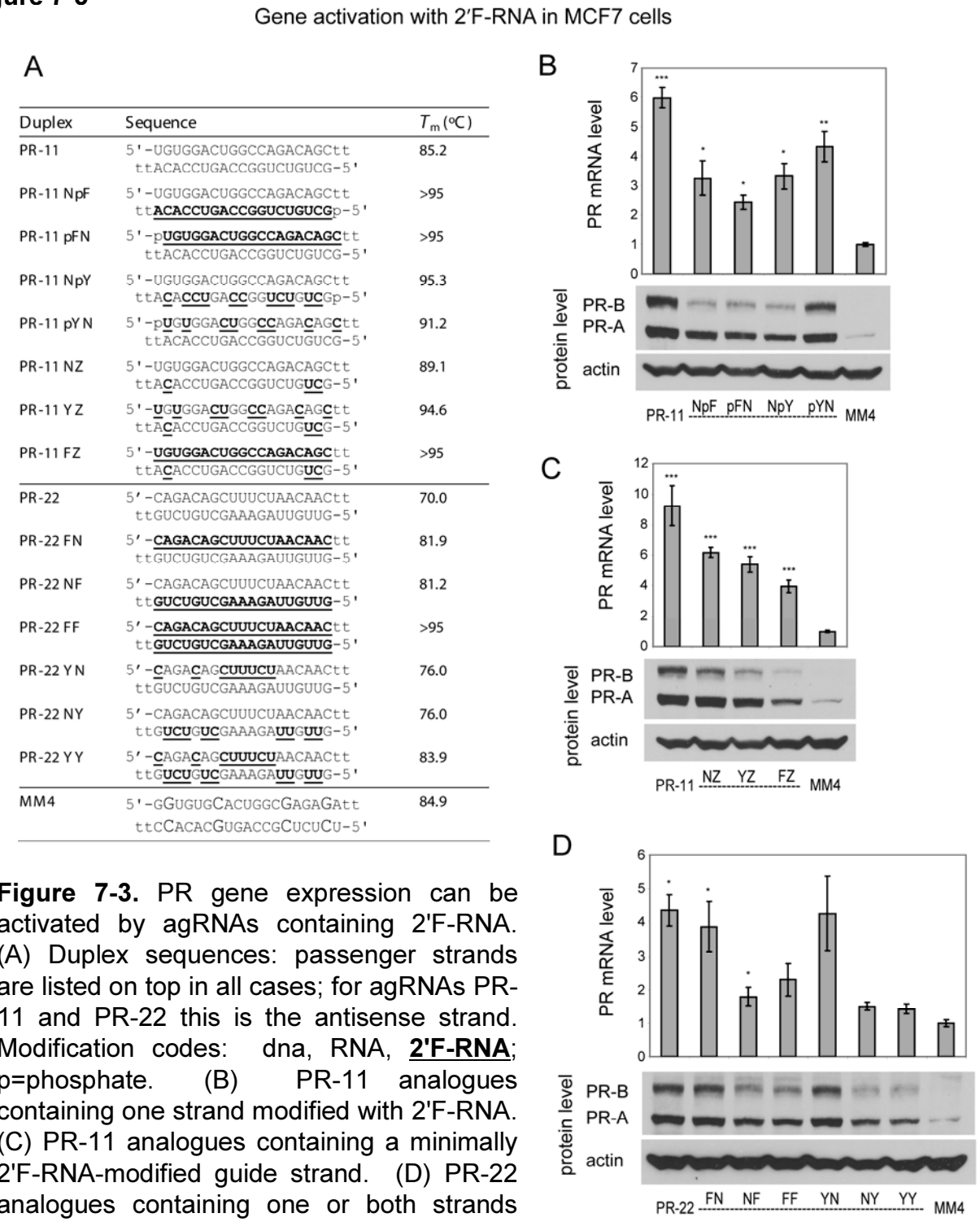

Figure 7-3. PR gene expression can be activated by agRNAs containing 2'F-RNA. (A) Duplex sequences: passenger strands are listed on top in all cases; for agRNAs PR-11 and PR-22 this is the antisense strand. Modification codes: dna, RNA, **2'F-RNA**; p=phosphate. (B) PR-11 analogues containing one strand modified with 2'F-RNA. (C) PR-11 analogues containing a minimally 2'F-RNA-modified guide strand. (D) PR-22 analogues containing one or both strands with 2'F-RNA. All data are normalized to mismatch control MM4. Error bars are standard deviation (SD) from biological replicates.

Figure 7-4

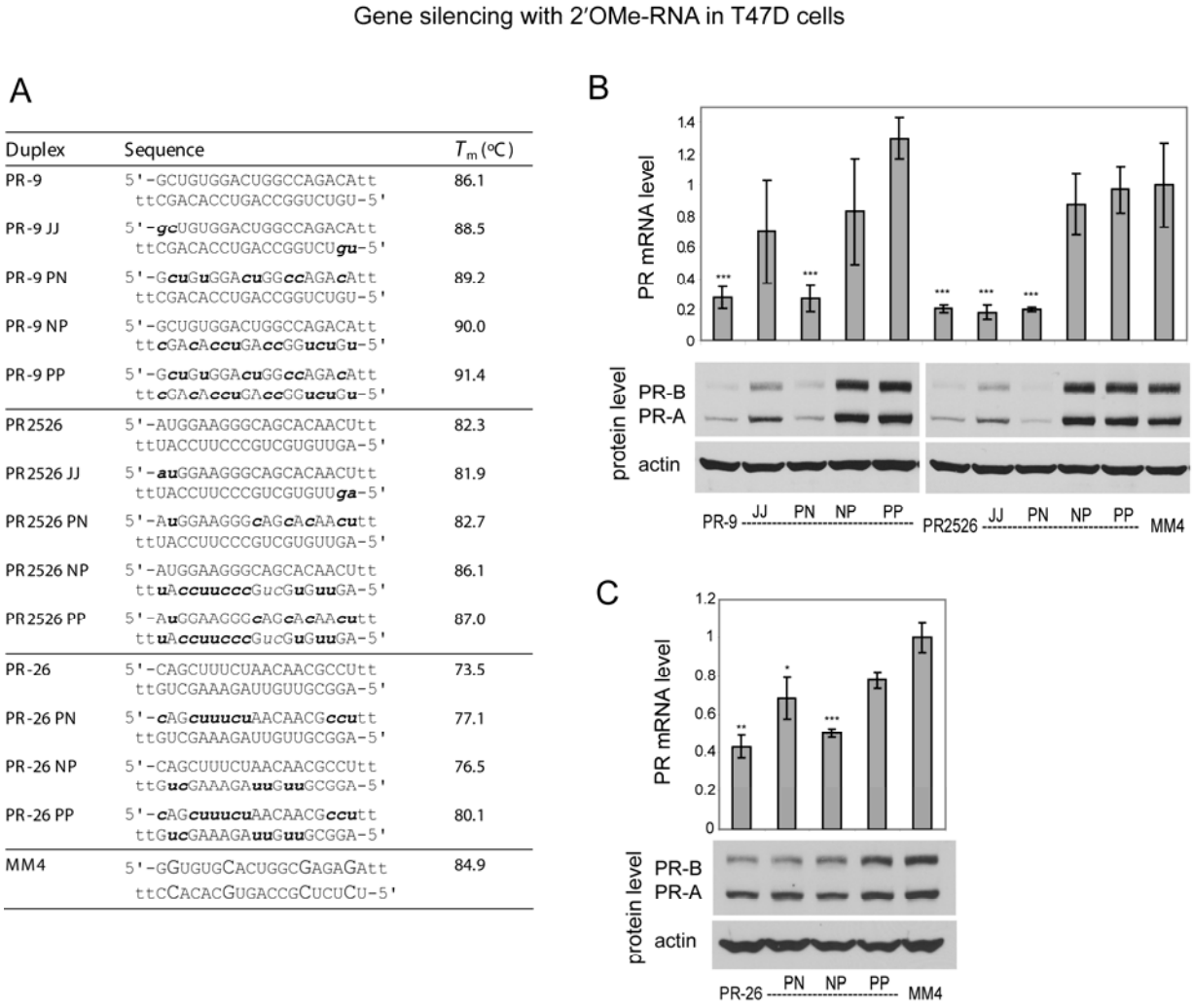

Duplex	Sequence	T_m (°C)
PR-9	5'-GCUGUGGACUGGCCAGACAtt ttCGACACCUGACCGGUCUGU-5'	86.1
PR-9 JJ	5'-***gc***UGUGGACUGGCCAGACAtt ttCGACACCUGACCGGUCU***gu***-5'	88.5
PR-9 PN	5'-G***cu***G***u***GGA***cu***GG***cc***AGA***c***Att ttCGACACCUGACCGGUCUGU-5'	89.2
PR-9 NP	5'-GCUGUGGACUGGCCAGACAtt tt***c***GA***c***A***ccu***GA***cc***GG***ucu***G***u***-5'	90.0
PR-9 PP	5'-G***cu***G***u***GGA***cu***GG***cc***AGA***c***Att tt***c***GA***c***A***ccu***GA***cc***GG***ucu***G***u***-5'	91.4
PR2526	5'-AUGGAAGGGCAGCACAACUtt ttUACCUUCCCGUCGUGUUGA-5'	82.3
PR2526 JJ	5'-***au***GGAAGGGCAGCACAACUtt ttUACCUUCCCGUCGUGUU***ga***-5'	81.9
PR2526 PN	5'-A***u***GGAAGGG***c***AG***c***A***c***AA***cu***tt ttUACCUUCCCGUCGUGUUGA-5'	82.7
PR2526 NP	5'-AUGGAAGGGCAGCACAACUtt tt***u***A***ccuuccc***G***u***C***u***G***uu***GA-5'	86.1
PR2526 PP	5'-A***u***GGAAGGG***c***AG***c***A***c***AA***cu***tt tt***u***A***ccuuccc***G***u***C***u***G***uu***GA-5'	87.0
PR-26	5'-CAGCUUUCUAACAACGCCUtt ttGUCGAAAGAUUGUUGCGGA-5'	73.5
PR-26 PN	5'-***c***AG***cuuucu***AACAACG***ccu***tt ttGUCGAAAGAUUGUUGCGGA-5'	77.1
PR-26 NP	5'-CAGCUUUCUAACAACGCCUtt ttG***uc***GAAAGA***uu***G***uu***GCGGA-5'	76.5
PR-26 PP	5'-***c***AG***cuuucu***AACAACG***ccu***tt ttG***uc***GAAAGA***uu***G***uu***GCGGA-5'	80.1
MM4	5'-GGUGUGCACUGGCGAGAGAtt ttCCACACGUGACCGCUCUCU-5'	84.9

Figure 7-4. PR gene expression can be silenced by agRNAs containing 2'OMe-RNA. (A) Duplex sequences: passenger strands are listed on top in all cases; for siRNA PR2526 this is the sense strand, but for agRNAs PR-9 and PR-26 this is the antisense strand. Modification codes: dna, RNA, ***2'O-Me-RNA***. (B) PR-9 analogues and controls containing 2'OMe-RNA. (C) PR-26 analogues containing 2'OMe-RNA. All data are normalized to mismatch control MM4. Error bars are standard deviation (SD) from biological replicates.

Figure 7-5

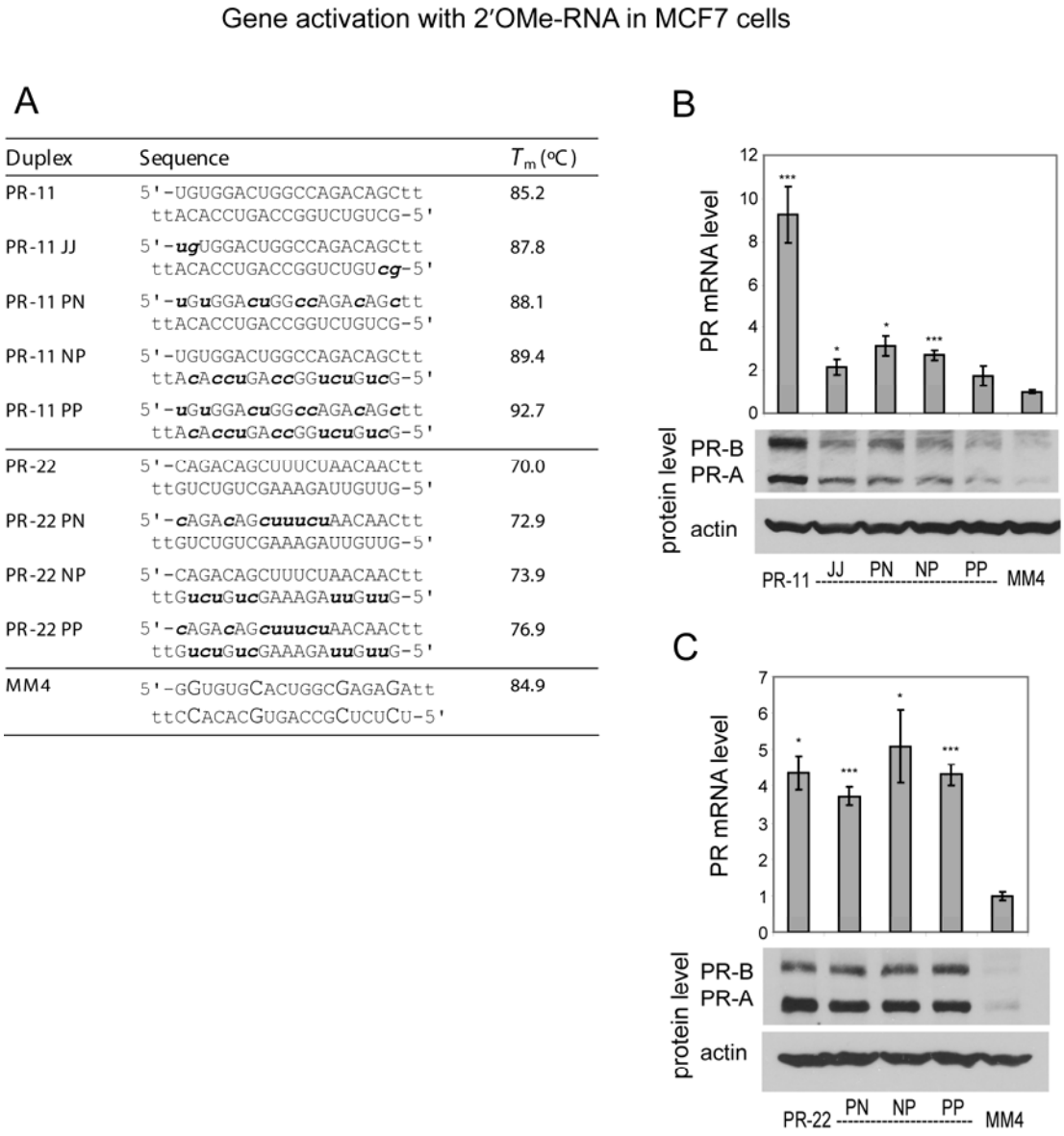

Figure 7-5. PR gene expression can be activated by agRNAs containing 2'OMe-RNA. (A) Duplex sequences: passenger strands are listed on top in all cases; for agRNAs PR-11 and PR-22 this is the antisense strand. Modification codes: dna, RNA, ***2'Ome-rna***. (B) PR-11 analogues containing 2'OMe-RNA. (C) PR-22 analogues containing 2'OMe-RNA. All data are normalized to mismatch control MM4. RNA levels are the average (+/- standard deviation) from at least two independent transfections. Protein levels were also confirmed by at least two independent transfections, from which a typical western blot is shown.

Figure 7-6

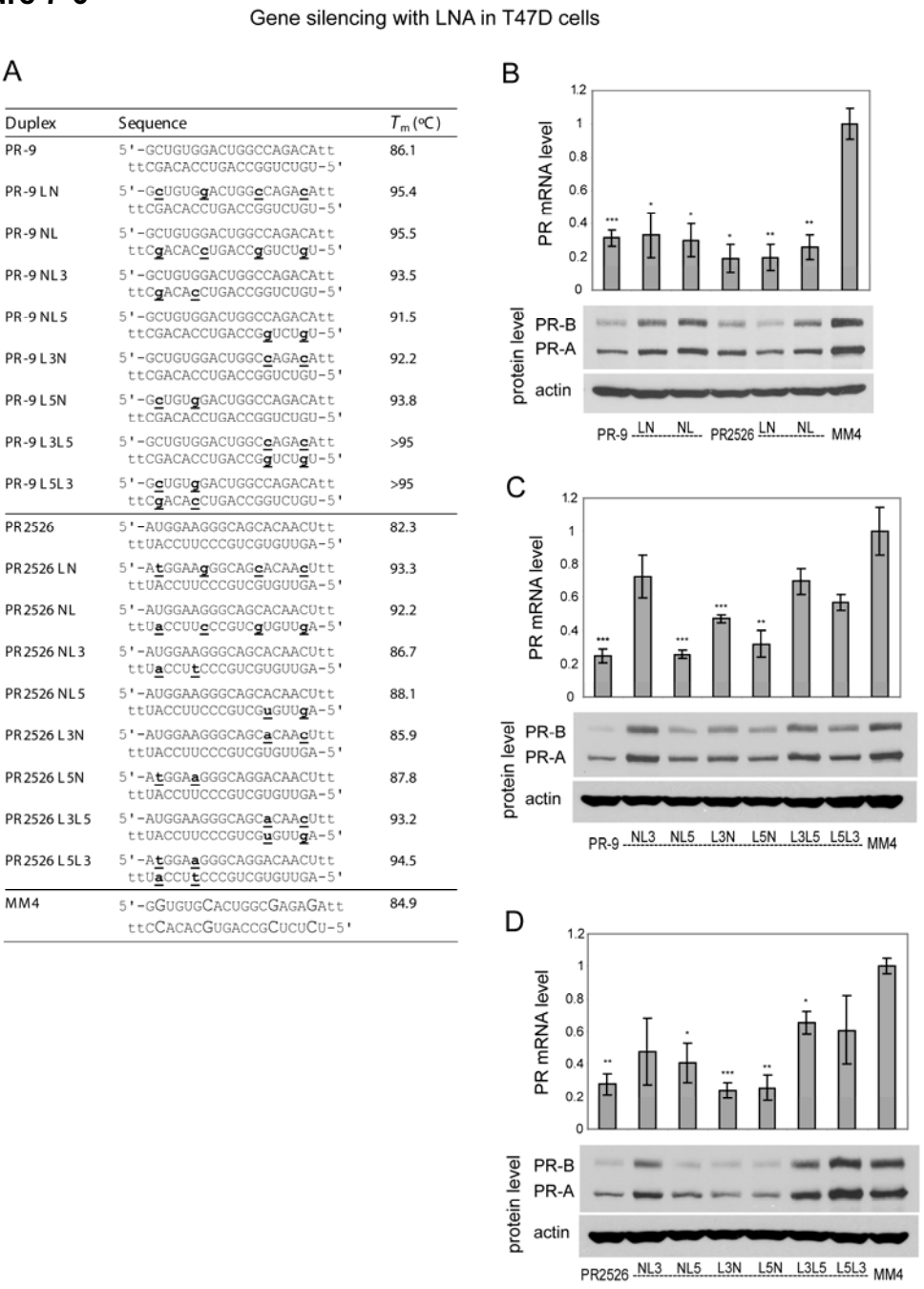

Figure 7-6. PR gene expression can be silenced by agRNAs containing LNA. (A) Duplex sequences: passenger strands are listed on top in all cases; for siRNA PR2526 this is the sense strand, but for agRNA PR-9 this is the antisense strand. LNA sequences contain 5-methylcytosine instead of cytosine. Modification codes: dna, RNA, **lna**. (B) PR-9 analogues and controls containing four evenly distributed LNA units. (C) PR-9 analogues containing LNA at strand ends. (D) PR2526 analogues containing LNA at strand ends. All data are normalized to mismatch control MM4. Error bars are standard deviation (SD) from biological replicates.

Figure 7-7

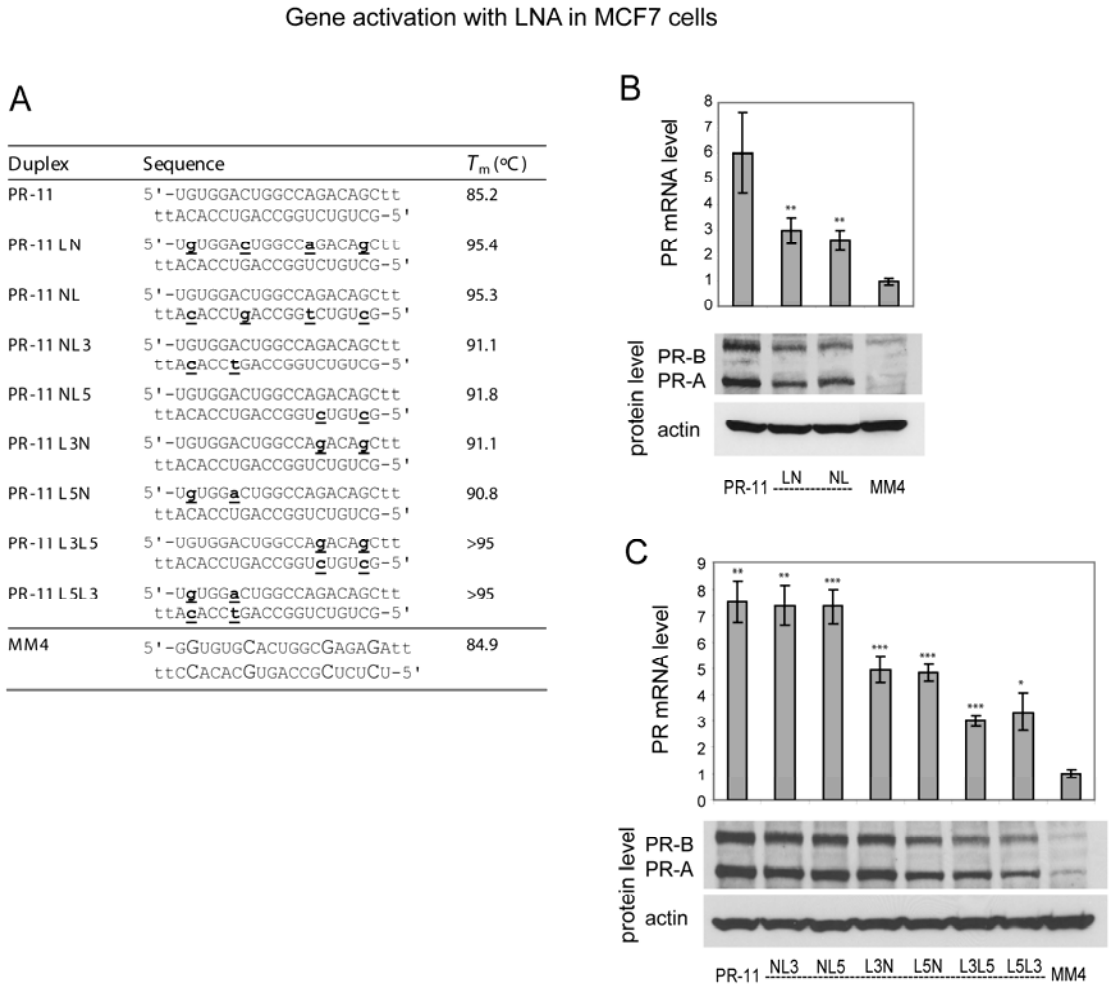

Figure 7-7. PR gene expression can be activated by agRNAs containing LNA. (A) Duplex sequences: passenger strands are listed on top in all cases; for agRNA PR-11 this is the antisense strand. LNA sequences contain 5-methylcytosine instead of cytosine. Modification codes: dna, RNA, **lna**. (B) PR-11 analogues containing four evenly distributed LNA units. (C) PR-11 analogues containing LNA at strand ends. All data are normalized to mismatch control MM4. Error bars are standard deviation (SD) from biological replicates.

Figure 7-8

Gene silencing with combination duplexes in T47D cells

A

Duplex	Sequence	T_m (°C)
PR-9	5'-GCUGUGGACUGGCCAGACAtt ttCGACACCUGACCGGUCUGU-5'	86.1
PR-9 LL5	5'-G**c**UGUG**g**ACUGG**c**CAGA**c**Att ttCGACACCUGACCG**g**UCU**g**U-5'	>95
PR-9 L5L	5'-G**c**UGUG**g**ACUGGCCAGACAtt ttC**g**ACAC**c**UGACC**g**GUCU**g**U-5'	>95
PR-9 L5L5	5'-G**c**UGUG**g**ACUGGCCAGACAtt ttCGACACCUGACCG**g**UCU**g**U-5'	>95
PR-9 LpJ	5'-G**c**UGUG**g**ACUGG**c**CAGA**c**Att ttCGACACCUGACCGGUCU***gu***p-5'	>95
PR-9 L5pJ	5'-G**c**UGUG**g**ACUGGCCAGACAtt ttCGACACCUGACCGGUCU***gu***p-5'	94.1
PR-9 PpJ	5'-G***cu***G***u***GGA***cu***GG***cc***AGA***c***Att ttCGACACCUGACCGGUCU***gu***p-5'	90.2
PR-9 JL	5'-***gc***UGUGGACUGGCCAGACAtt ttC**g**ACAC**c**UGACC**g**GUCU**g**U-5'	>95
PR-9 PZ	5'-***gc***UGUGGACUGGCCAGACAtt tt**C**GACACCUGACCGGUCU**G**U-5'	92.1
PR-9 JZ	5'-***gc***UGUGGACUGGCCAGACAtt tt**C**GACACCUGACCGGUCU**G**U-5'	88.4
PR-9 LZ	5'-G**c**UGUG**g**ACUGG**c**CAGA**c**Att tt**C**GACACCUGACCGGUCU**G**U-5'	>95
MM4	5'-GGUGUGCACUGGCGAGAGAtt ttCCACACGUGACCGCUCUCu-5'	84.9

B

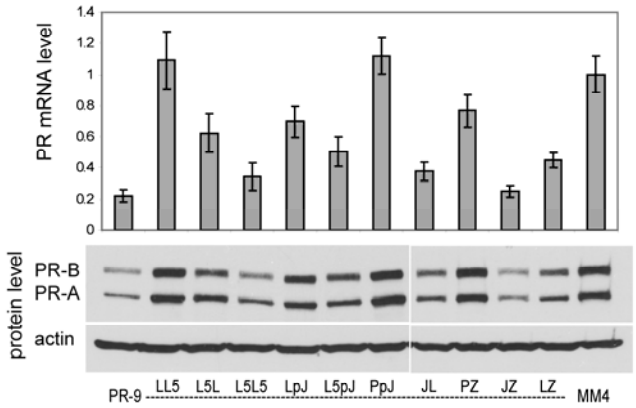

Gene activation with combination duplexes in MCF7 cells

C

Duplex	Sequence	T_m (°C)
PR-11	5'-UGUGGACUGGCCAGACAGCtt ttACACCUGACCGGUCUGUCG-5'	85.2
PR-11 LZ	5'-U**g**UGGA**c**UGGCC**a**GACA**g**Ctt ttA**C**ACCUGACCGGUCUG**UC**G-5'	>95
PR11-L5Z	5'-U**g**UGG**a**CUGGCCAGACAGCtt ttA**C**ACCUGACCGGUCUG**UC**G-5'	>95
PR11-PL3	5'-***u***G***u***GGA***cu***GG***cc***AGA***c***AG***c***tt ttA**c**ACC**t**GACCGGUCUGUCG-5'	>95
PR11-YP	5'-**U**G**U**GGA**CU**GG**CC**AGA**C**AG**C**tt ttA***c***A***ccu***GA***cc***GG***ucu***G***uc***G-5'	>95
PR11-LP	5'-U**g**UGGA**c**UGGCC**a**GACA**g**Ctt ttA***c***A***ccu***GA***cc***GG***ucu***G***uc***G-5'	>95
PR11-PL	5'-***u***G***u***GGA***cu***GG***cc***AGA***c***AG***c***tt ttA**c**ACCU**g**ACCGG**t**CUGU**c**G-5'	>95
PR11-L5P	5'-U**g**UGG**a**CUGGCCAGACAGCtt ttA***c***A***ccu***GA***cc***GG***ucu***G***uc***G-5'	>95
PR11-PL5	5'-***u***G***u***GGA***cu***GG***cc***AGA***c***AG***c***tt ttACACCUGACCGGU**c**UGU**c**G-5'	>95
MM4	5'-GGUGUGCACUGGCGAGAGAtt ttCCACACGUGACCGCUCUCu-5'	84.9

D

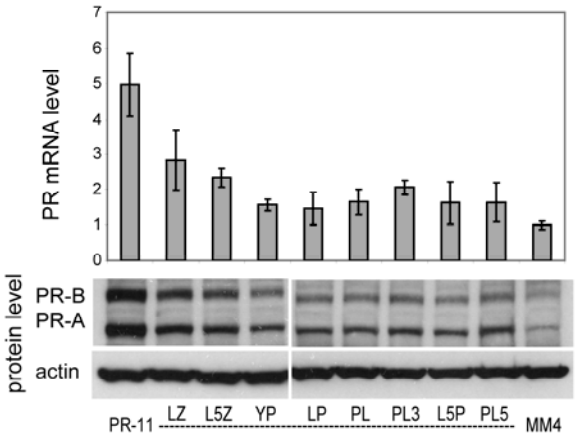

Figure 7-8. PR gene expression can be silenced or activated by agRNAs containing combinations of modifications. (A, C) Duplex sequences: passenger strands are listed on top in all cases. LNA sequences contain 5-methylcytosine instead of cytosine. Modification codes: dna, RNA, **2'F-RNA**, ***2'Ome-rna***, **lna**; p=phosphate. (B) PR−9 analogues containing combinations of previously identified active strands. (D) PR−11 analogues containing combinations of previously identified active strands. All data are normalized to mismatch control MM4. Error bars are standard deviation (SD) from biological replicates.

Figure 7-9

A

Compound	Sequence
PR-9	5'-GCUGUGGACUGGCCAGACAtt ttCGACACCUGACCGGUCUGU-5'
PR-9 N-pas	5'-GCUGUGGACUGGCCAGACAtt
PR-9 N-gui	ttCGACACCUGACCGGUCUGU-5'
PR-9 pJ-pas	5'-p***gc***UGUGGACUGGCCAGACAtt
PR-9 pJ-gui	ttCGACACCUGACCGGUCU***gu***p-5'
PR-9 J-gui	ttCGACACCUGACCGGUCU***gu***-5'
PR-9 Z-gui	tt**C**GACACCUGACCGGUC**U**G**U**-5'
PR-9 L-pas	5'-G**c**UGUG**g**ACUGG**c**CAGA**c**Att
PR-9 L-gui	ttC**g**ACAC**c**UGACC**g**GUCU**g**U-5'
PR-9 L5-gui	ttCGACACCUGACCG**g**UCU**g**U-5'
PR-11	5'-UGUGGACUGGCCAGACAGCtt ttACACCUGACCGGUCUGUCG-5'
PR-11 N-pas	5'-UGUGGACUGGCCAGACAGCtt
PR-11 N-gui	ttACACCUGACCGGUCUGUCG-5'
PR-11 Y-pas	5'-p**U**G**U**GGA**CU**GG**CC**AGA**C**AG**C**tt
PR-11 Z-gui	ttA**C**ACCUGACCGGUCUG**UC**G-5'
PR-11 L-pas	5'-U**g**UGGA**c**UGGCC**a**GACA**g**Ctt
PR-11 L-gui	ttA**c**ACCU**g**ACCGG**t**CUGU**c**G-5'
PR-11 L5-gui	ttACACCUGACCGGU**c**UGU**c**G-5'
MM4-gui	ttCACACGUGACCGCUCUCU-5'

B

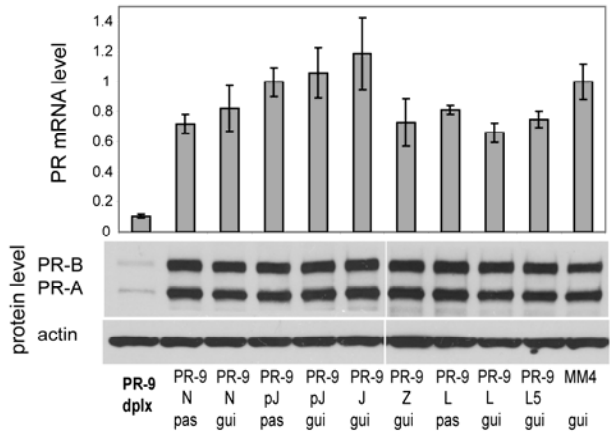

C

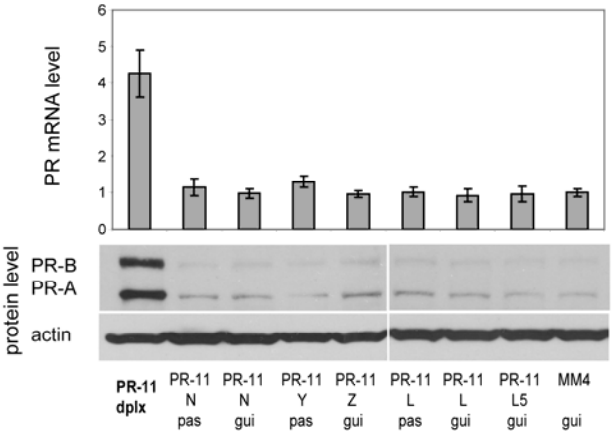

Figure 7-9. Single strands of native or modified agRNAs are inactive. (a) Sequences: passenger strands are given 5'-3', guide strands are given 3'-5' as shown. For these agRNAs the passenger strand is the antisense strand. Modification codes: dna, RNA, **2'F-RNA**, ***2'Ome-rna***, **lna**; p=phosphate. (b) PR-9 duplex and native or modified single-strands. (c) PR-11 duplex and native or modified single-strands. All data are normalized to the guide strand of mismatch control MM4. RNA levels are the average (+/- standard deviation) from at least two independent transfections. Protein levels were also confirmed by at least two independent transfections, from which a typical western blot is shown.

Figure 7-10

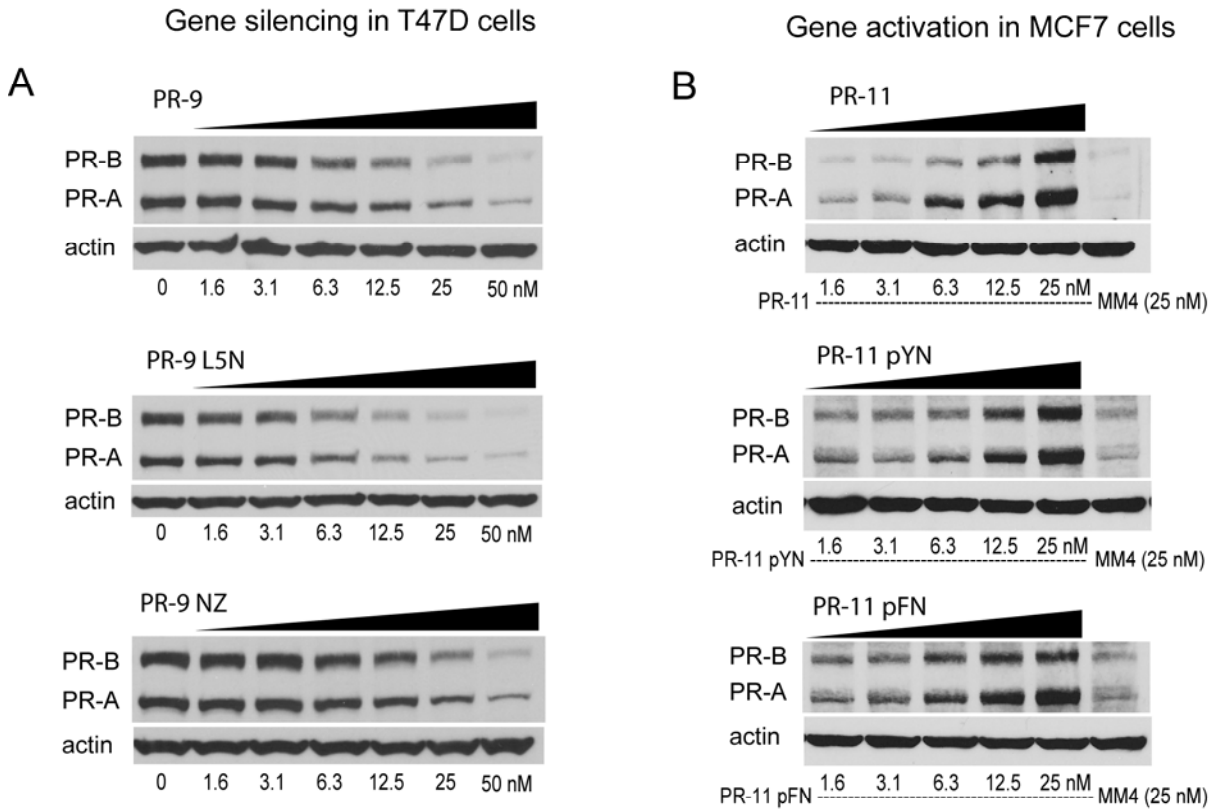

Figure 7-10. Sample dose response experiments for both silencing and activation.

Figure 7-11

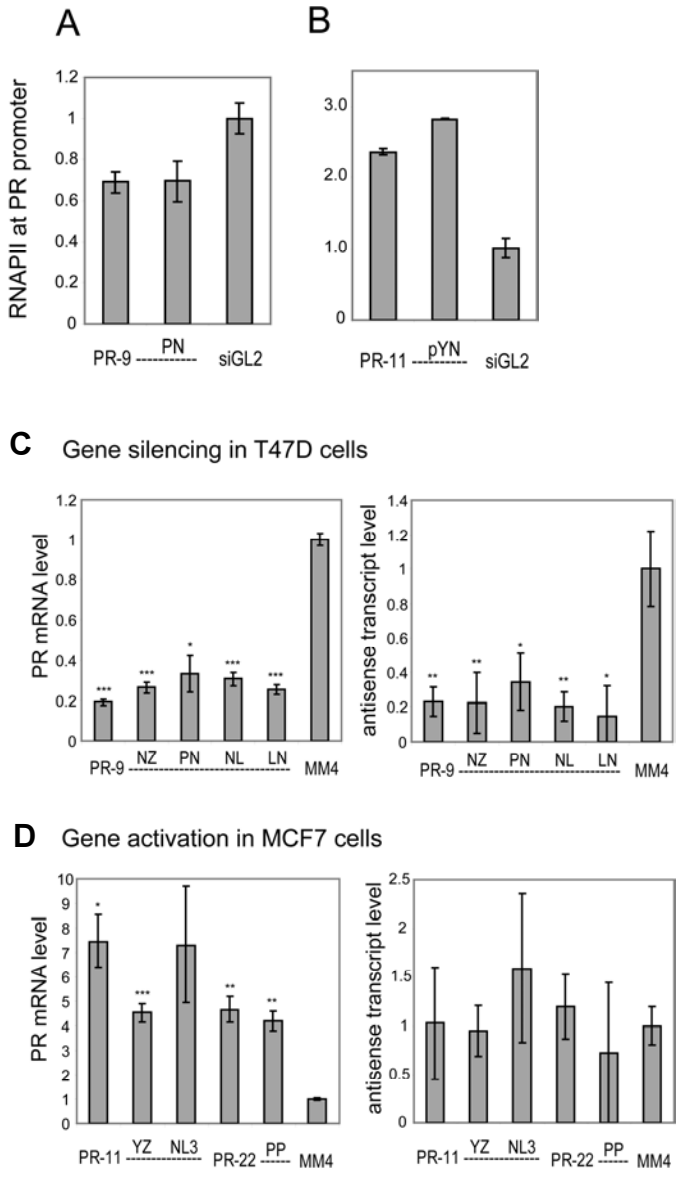

Figure 7-11. Chromatin immunoprecipitation of RNA Polymerase II (RNAPII) shows that both native and modified agRNAs operate at the transcriptional level, and native and modified duplexes have the same effect on antisense transcript levels. (A) Treatment of T47D cells with PR-9 or PR-9 PN leads to reduced occupancy of RNAPII at the PR promoter relative to cells treated with control duplex siGL2. (B) Treatment of MCF7 cells with PR-11 or PR-11 pYN leads to increased occupancy of RNAPII at the PR promoter relative to cells treated with control duplex siGL2. (C) Treatment of T47D cells with PR-9 and modified duplexes leads to a significant downregulation of both PR mRNA (left) and the promoter-associated antisense transcript (right). (D) Treatment of MCF7 cells with PR-11 and modified duplexes leads to a significant upregulation of PR mRNA (left) but no significant change in levels of the promoter-associated antisense transcript (right).

Figure 7-12

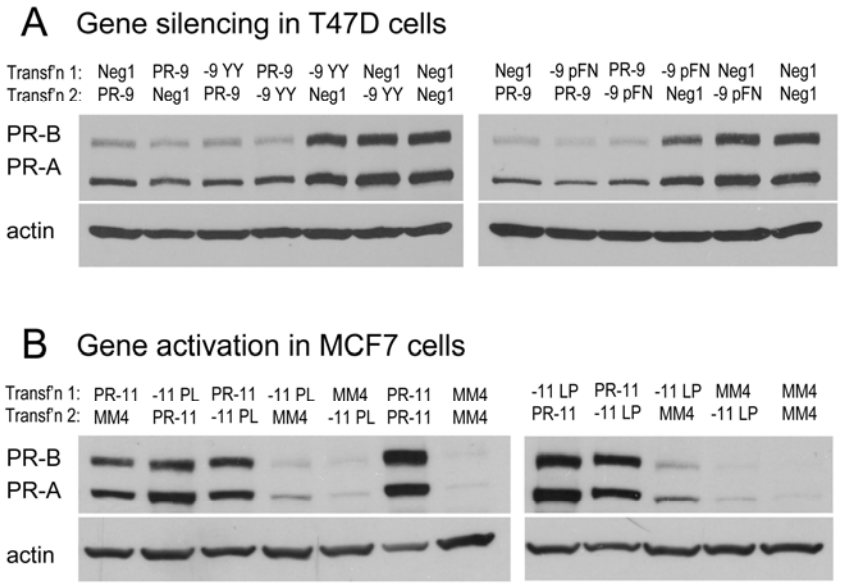

Figure 7-12. Inactive modified duplexes do not compete for target sites. Western analysis showing no competition between native agRNAs and inactive modified duplexes applied to cells in two transfections 4 days apart. (A) Native PR-9 silences gene expression equally effectively whether it is transfected before or after an inactive chemically modified duplex (or negative control). (B) Native PR-11 activates gene expression equally effectively whether it is transfected before or after an inactive chemically modified duplex.